

Carbonic Anhydrase as a Model for Biophysical and Physical-Organic Studies of Proteins and Protein–Ligand Binding

Vijay M. Krishnamurthy, George K. Kaufman, Adam R. Urbach, Irina Gitlin,
Katherine L. Gudiksen, Douglas B. Weibel, and George M. Whitesides

Chem. Rev., **2008**, 108 (3), 946-1051 • DOI: 10.1021/cr050262p

Downloaded from <http://pubs.acs.org> on December 24, 2008

More About This Article

Additional resources and features associated with this article are available within the HTML version:

- Supporting Information
- Links to the 5 articles that cite this article, as of the time of this article download
- Access to high resolution figures
- Links to articles and content related to this article
- Copyright permission to reproduce figures and/or text from this article

[View the Full Text HTML](#)



Carbonic Anhydrase as a Model for Biophysical and Physical-Organic Studies of Proteins and Protein–Ligand Binding

Vijay M. Krishnamurthy, George K. Kaufman, Adam R. Urbach, Irina Gitlin, Katherine L. Gudiksen, Douglas B. Weibel, and George M. Whitesides*

Department of Chemistry and Chemical Biology, Harvard University, 12 Oxford Street, Cambridge, Massachusetts 02138

Received December 13, 2006

Contents

I. Introduction to Carbonic Anhydrase (CA) and to the Review	948	8.3.7. Mass Spectrometry	976
1. Introduction: Overview of CA as a Model	948	8.4. Kinetic Assays for Ligand Binding	976
1.1. Value of Models	950	8.4.1. Fluorescence and Absorbance Spectroscopy	976
1.2. Objectives and Scope of the Review	950	8.4.2. Affinity Capillary Electrophoresis	976
2. Overview of Enzymatic Activity	950	8.4.3. Surface Plasmon Resonance Spectroscopy	977
3. Medical Relevance	951	8.5. Most Convenient Assays	977
II. Structure and Structure–Function Relationships of CA	953	9. Structure–Activity Relationships for Active-Site Ligands	977
4. Global and Active-Site Structure	953	9.1. Overview of Structure–Activity Relationships	977
4.1. Structure of Isoforms	953	9.2. Thermodynamic Binding Data	978
4.2. Isolation and Purification	954	9.2.1. Inhibitors with Aromatic Rings	978
4.3. Crystallization	954	9.2.2. Sulfamates and Non-aromatic Sulfonamides	978
4.4. Structures Determined by X-ray Crystallography and NMR	955	9.2.3. “Tail Approach”	987
4.4.1. Structures Determined by X-ray Crystallography	955	9.2.4. Isozyme-Specific Inhibitors	988
4.4.2. Structure Determined by NMR	955	9.2.5. Inhibition by Small Monoanions	988
4.5. Global Structural Features	963	9.2.6. Derivatives of Arylsulfonic Acids	988
4.6. Structure of the Binding Cavity	964	9.3. Kinetics of Binding	989
4.7. Zn ^{II} -Bound Water	965	9.4. Combinatorial Approaches to Ligand Design	989
5. Metalloenzyme Variants	966	9.5. Computational Approaches to Ligand Design	989
6. Structure–Function Relationships in the Catalytic Active Site of CA	968	9.6. Conclusions	990
6.1. Effects of Ligands Directly Bound to Zn ^{II}	968	10. Using CA to Study the Physical-Organic Chemistry of Protein–Ligand Interactions	990
6.2. Effects of Indirect Ligands	969	10.1. Overview	990
7. Physical-Organic Models of the Active Site of CA	969	10.2. Challenges in Rational Ligand Design	991
III. Using CA as a Model to Study Protein–Ligand Binding	970	10.2.1. General Concepts	991
8. Assays for Measuring Thermodynamic and Kinetic Parameters for Binding of Substrates and Inhibitors	970	10.2.2. Enthalpy and Entropy of Binding	991
8.1. Overview	970	10.2.3. Utility of the System of CA/ Arylsulfonamides in This Effort	992
8.2. Enzymatic Catalysis	971	10.2.4. Why Are Arylsulfonamides Such Good Ligands for CA?	993
8.3. Thermodynamic Assays for Ligand Binding	972	10.2.5. Conclusions	994
8.3.1. Fluorescence and Luminescence Spectroscopy	972	10.3. Influence of the Head Group of Arylsulfonamides on Their Binding to CA	994
8.3.2. Absorption Spectrophotometry	973	10.3.1. General Approach	994
8.3.3. Affinity Capillary Electrophoresis	974	10.3.2. pK _a Determines the Fraction of Arylsulfonamide Present in the Active, Ionized (ArSO ₂ NH ⁻) Form	994
8.3.4. Calorimetry	975	10.3.3. Selection of Standard Reaction for the Binding of Arylsulfonamides to CA	994
8.3.5. Magnetic Resonance Spectroscopy	975	10.3.4. Brønsted Relationships Reveal the Role of Basicity of the Sulfonamide Anion	995
8.3.6. Circular Dichroism Spectroscopy	975	10.3.5. What Value of pK _a for Arylsulfonamides Gives the Highest Affinity for CA?	1000
		10.3.6. Conclusions	1000

* To whom correspondence should be addressed. Tel.: (617) 495-9430. Fax: (617) 495-9857. E-mail: gwhitesides@gmwgroup.harvard.edu.

10.4. Influence of the Sulfonamide Tail Group on the Binding of Arylsulfonamides to CA	1001	11.2.3. Three-State Model with an Intermediate (Pre-equilibrium)	1018
10.4.1. General Approach	1001	11.2.4. Conclusions	1020
10.4.2. Interaction of Different Types of Tails with CA	1001	12. Protein–Ligand Interactions on Surfaces	1020
10.4.3. Conclusions	1002	12.1. Overview	1020
10.5. Bivalent Approaches to CA Binding	1002	12.2. Comparison of Thermodynamic Values for Binding Measured at Surfaces and in Solution	1020
10.5.1. General Approach: Addition of a Secondary Recognition Element to the Tail	1002	12.3. Comparison of Kinetic Values for Binding Measured at Surfaces and in Solution	1021
10.5.2. Hydrophobic Secondary Recognition Elements Close to the Phenyl Ring of the <i>para</i> -Substituted Benzenesulfonamide	1003	12.3.1. Influence of Mass Transport and Rebinding on Kinetics of Binding	1021
10.5.3. Hydrophobic Secondary Recognition Elements Separated from the Phenyl Ring of the Arylsulfonamide	1004	12.3.2. Lateral Steric Effects	1021
10.5.4. Hydrophilic or Charged Secondary Recognition Elements	1005	12.4. Conclusions	1021
10.5.5. Metal Ions as Secondary Recognition Elements	1005	13. Protein–Ligand Interactions in the Gas Phase	1021
10.5.6. Reactive Epoxides as Secondary “Recognition” Elements: Covalent Labeling of CA	1005	13.1. Overview	1021
10.5.7. Conclusions	1006	13.2. Using Mass Spectrometry to Estimate Solution-Phase Affinities	1021
10.6. Enthalpy and Entropy of Binding of Arylsulfonamides to CA	1006	13.3. Using Mass Spectrometry to Understand the Stability of Protein–Ligand Complexes in the Gas Phase	1022
10.6.1. Overview and General Approach	1006	13.4. Conclusions	1022
10.6.2. Influence of Structural Perturbations of the Head and Ring Regions of the Arylsulfonamide on the Observed Enthalpy and Entropy of Binding	1006	IV. Using CA as a Model Protein for Biophysical Studies	1023
10.6.3. Thermodynamics of Association of the Arylsulfonamide Anion (ArSO_2NH^-) with $\text{CA-Zn}^{\text{II}}-\text{OH}_2^+$	1008	14. Protein Charge Ladders as a Tool to Probe Electrostatic Interactions in Proteins	1023
10.6.4. Comparison of $\Delta H^\circ_{\text{ArSO}_2\text{NH}^-}$ from Calorimetry and van’t Hoff Analysis	1010	14.1. Protein Charge Ladders	1023
10.6.5. Influence of the Head Group: Fluorinated Benzenesulfonamides	1010	14.2. Determination of Net Charge (Z_0), Change in Charge (ΔZ) Upon Acetylation, and Hydrodynamic Radius of a Protein	1023
10.6.6. Influence of the Tail Group: Oligoethylene Glycol, Oligoglycine, and Oligosarcosine Tails	1011	14.3. Probing Long-Range Electrostatic Contributions to the Binding of Charged Sulfonamides Using Charge Ladders and ACE	1024
10.6.7. Conclusions	1011	14.4. Charge Ladders in the Gas Phase: Mass Spectrometry	1025
10.7. Overall Conclusions	1011	14.5. Protein Hydrophobic Ladders and Interactions with Sodium Dodecyl Sulfate	1025
10.7.1. Why Is CA a Good Model System for Rational Ligand Design?	1011	14.6. Perfunctionalized Proteins	1026
10.7.2. Lessons in Design of Arylsulfonamide Ligands for CA	1012	14.7. Conclusions	1027
10.7.3. General Lessons in Rational Ligand Design	1012	15. CA as a Model Protein for Studying the Denaturation and Renaturation of Proteins	1027
11. Kinetics and Mechanism of Protein–Inhibitor Binding in Solution	1013	15.1. Overview	1027
11.1. Kinetics of Interaction of Arylsulfonamides with CA	1013	15.2. Pathway for Refolding of CA after Denaturation by Guanidine	1028
11.1.1. Overview	1013	15.2.1. Seeds for Protein Folding	1028
11.1.2. Influence of the Head Group and the Ring on the Kinetics of Binding	1013	15.2.2. Metal Cofactor	1029
11.1.3. Which Are the Reactive Species of CA and Sulfonamide?	1013	15.2.3. Molten Globule	1029
11.1.4. Influence of the Tail on the Kinetics of Binding	1015	15.2.4. C-terminal Folding, the C-terminal Knot, and Refolding of the Active Site	1031
11.1.5. Conclusions	1016	15.2.5. N-terminal Folding	1032
11.2. Mechanism of the Binding of Arylsulfonamides to CA	1017	15.3. Denaturing CA with Other Denaturants	1032
11.2.1. Overview	1017	15.3.1. Urea	1032
11.2.2. Two-State Model for Binding (Assuming No Intermediate)	1017	15.3.2. Acid	1033
		15.3.3. Heat	1034
		15.3.4. Sodium Dodecyl Sulfate (SDS)	1034
		15.4. Recovery of Enzymatic Activity after Refolding	1035
		15.4.1. CA as a Model for Studying Aggregation	1035
		15.4.2. Preventing Aggregation	1036
		15.4.3. Chaperonin-Assisted Folding of CA	1037

15.5. Conclusions from Studies on the Folding and Unfolding of CA	1038
V. Why Is CA a Good Model?	1038
16. Conclusions	1038
16.1. What Are the Strengths and Weaknesses of CA as a Model Protein?	1038
16.2. What Are the Advantages of Using CA to Understand the Thermodynamics and Kinetics of Binding of Ligands to Proteins?	1039
16.3. What Are the Advantages of Using CA to Compare Binding in Solution to that at Solid Surfaces or in the Gas Phase?	1040
16.4. What Are the Advantages of Using CA to Understand the Role of Electrostatics in Protein Stability and Protein–Ligand Binding?	1040
16.5. What Are the Advantages of Using CA to Understand How Proteins Fold and Unfold?	1040
16.6. Coda	1040
17. Acknowledgments	1041
18. References	1041

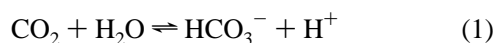


Vijay M. Krishnamurthy received a B.S. in Chemistry from the University of North Carolina at Chapel Hill in 1999. His undergraduate thesis, completed under the direction of Professor Royce W. Murray, examined the polymeric precursor to monolayer-protected gold clusters. He received a Ph.D. from Harvard University in 2006. His Ph.D. thesis, completed under the direction of Professor George M. Whitesides, explored the thermodynamic principles of rational ligand design and multivalency.

I. Introduction to Carbonic Anhydrase (CA) and to the Review

1. Introduction: Overview of CA as a Model

Carbonic anhydrase (CA, EC 4.2.1.1) is a protein that is especially well-suited to serve as a model in many types of studies in biophysics, bioanalysis, the physical-organic chemistry of inhibitor design, and medicinal chemistry. In vivo, this enzyme catalyzes the hydration of CO₂ and the dehydration of bicarbonate (eq 1).



The active site of α -CAs comprises a catalytic Zn^{II} ion coordinated by three imidazole groups of histidines and by one hydroxide ion (or water molecule), all in a distorted tetrahedral geometry. This grouping is located at the base of a cone-shaped amphiphilic depression, one wall of which is dominated by hydrophobic residues and the other of which is dominated by hydrophilic residues.¹ Unless otherwise stated, “CA” in this review refers to (i) various isozymes of α -CAs or (ii) the specific α -CAs human carbonic anhydrases I and II (HCA I and HCA II) and bovine carbonic anhydrase II (BCA II); “HCA” refers to HCA I and HCA II; and “CA II” refers to HCA II and BCA II.

CA is particularly attractive for biophysical studies of protein–ligand binding for many reasons. (i) CA is a monomeric, single-chain protein of intermediate molecular weight (~30 kDa), and it has no pendant sugar or phosphate groups and no disulfide bonds. (ii) It is inexpensive and widely available. (iii) It is relatively easy to handle and purify, due in large part to its excellent stability under standard laboratory conditions. (iv) Amino acid sequences are available for most of its known isozymes. (v) The structure of CA, and of its active site, has been defined in detail by X-ray diffraction, and the mechanism of its catalytic activity is well-understood. (vi) As an enzyme, CA behaves not only as a hydratase/anhydrase with a high turnover number but also as an esterase (a reaction that is easy to follow experimentally). (vii) The mechanism of inhibition of CA by ligands that bind to the Zn^{II} ion is fairly simple and well-characterized; it is, therefore, easy to screen



George K. Kaufman received his B.A. in Classics, B.S. in Chemical Physics, and M.S. in Chemistry in 2002 from Brown University under Prof. Matthew B. Zimmt. He is currently a Ph.D. student under George M. Whitesides at Harvard University. His research interests include magnetic and electrostatic self-assembly, electret materials, protein aggregation and multivalency, and molecular electronics using self-assembled monolayers.



Adam R. Urbach was born in Houston, Texas, and obtained his B.S. in Chemistry from the University of Texas at Austin and his Ph.D. with Peter Dervan from Caltech in 2002. Following an NIH postdoctoral fellowship under George M. Whitesides, he joined the Chemistry Department at Trinity University, where he is currently an Assistant Professor. His research interests are in the area of biomolecular recognition.



Irina Gitlin received a B.S. in Chemical Engineering from the University of Illinois at Urbana-Champaign in 2000. She has recently completed her Ph.D. in Chemistry with G. M. Whitesides. Her research in the area of protein chemistry explores the role of electrostatic interactions in protein stability, binding of ligands, and susceptibility to denaturation by surfactants. She has also worked in the area of microfluidics.



Katherine L. Gudiksen received her B.S. degree in Chemistry and Physics and her B.A. degree in Mathematics from Hope College, Holland, MI. She received her Ph.D. from Harvard University in 2006 working with Prof. G. M. Whitesides. She is currently a co-founder and Director of Technology at Nidaan, Inc., a start-up company focusing on biomarker discovery and cancer diagnostics. Her research interests include tools for proteomics and the role of hydrophobicity and electrostatics in protein folding.

inhibitors and to examine designed inhibitors that test theories of protein–ligand interactions. (viii) It is possible to prepare and study the metal-free apoenzyme and the numerous variants of CA in which the Zn^{II} ion is replaced by other divalent ions. (ix) Charge ladders of CA II—sets of derivatives in which acylation of lysine amino groups ($-\text{NH}_3^+ \rightarrow -\text{NHAc}$) changes the net charge of the protein—allow the influence of charge on properties to be examined by capillary electrophoresis. Some disadvantages of using CA include the following: (i) the presence of the Zn^{II} cofactor, which can complicate biophysical and physical-organic analyses; (ii) a structure that is more stable than a representative globular protein and, thus, slightly suspect as a model system for certain studies of stability; (iii) a function–interconversion of carbon dioxide and carbonate—that does not involve the types of enzyme/substrate interactions that are most interesting in design of drugs; (iv) a catalytic reaction that is, in a sense, *too* simple (determining the mechanism of a reaction is, in practice, usually made easier if the reactants and products have an intermediate level of complexity); and (v) the absence of a solution structure of CA (by NMR spectroscopy). The ample X-ray data, however, paint an



Douglas B. Weibel received his B.S. degree in Chemistry in 1996 from the University of Utah (with Prof. C. Dale Poulter) and his Ph.D. in Chemistry in 2002 from Cornell University (with Prof. Jerrold Meinwald). From 1996–1997, he was a Fulbright Fellow with Prof. Yoshinori Yamamoto at Tohoku University. From 2002–2006, he was a postdoctoral fellow with George M. Whitesides at Harvard University. He is currently an Assistant Professor of Biochemistry at the University of Wisconsin—Madison. His research interests include biochemistry, biophysics, chemical biology, materials science and engineering, and microbiology.



George M. Whitesides received his A.B. degree from Harvard University in 1960 and his Ph.D. degree from the California Institute of Technology in 1964. A Mallinckrodt Professor of Chemistry from 1982 to 2004, he is now a Woodford L. and Ann A. Flowers University Professor. Prior to joining the Harvard faculty in 1992, he was a member of the chemistry faculty of the Massachusetts Institute of Technology. His research interests include physical and organic chemistry, materials science, biophysics, complexity, surface science, microfluidics, self-assembly, micro- and nanotechnology, and cell-surface biochemistry.

excellent picture of the changes (which are generally small) in the structure of CA that occur on binding ligands or introducing mutations.

The most important class of inhibitors of CA, the arylsulfonamides, has several characteristics that also make it particularly suitable for physical-organic studies of inhibitor binding and in drug design: (i) arylsulfonamides are easily synthesized; (ii) they bind with high affinity to CA ($1 \mu\text{M}$ to sub-nM); (iii) they share one common structural feature; and (iv) they share a common, narrowly defined geometry of binding that exposes a part of the ligand that can be easily modified synthetically. There are also many non-sulfonamide, organic inhibitors of CA, as well as anionic, inorganic inhibitors.

We divide this review into five parts, all with the goal of using CA as a model system for biophysical studies: (I) an overview of the enzymatic activity and medical relevance of CA; (II) the structure and structure–function relationships

of CA and its engineered mutants; (III) the thermodynamics and kinetics of the binding of ligands to CA; (IV) the effect of electrostatics on the binding of ligands to and the denaturation of CA; and (V) what makes CA a good model for studying protein–ligand binding and protein stability.

1.1. Value of Models

CA serves as a good *model* system for the study of enzymes. That is, it is a protein having some characteristics representative of enzymes as a class, but with other characteristics that make it especially easy to study. It is a moderately important target in current medicinal chemistry: its inhibition is important in the treatment of glaucoma, altitude sickness, and obesity; its overexpression has recently been implicated in tumor growth; and its inhibition in pathogenic organisms might lead to further interesting drugs.^{2,3} More than its medical relevance, its tractability and simplicity are what make CA a particularly attractive model enzyme.

The importance of models in science is often underestimated. Models represent more complex classes of related systems and contribute to the study of those classes by focusing research on particular, tractable problems. The development of useful, widely accepted models is a critical function of scientific research: many of the techniques (both experimental and analytical) and concepts of science are developed in terms of models; they are thoroughly engrained in our system of research and analysis.

Examples of models abound in *successful* areas of science: in biology, *E. coli*, *S. cerevisiae*, *Drosophila melanogaster*, *C. elegans*, *Brachydanio rerio* (zebrafish), and the mouse; in chemistry, the hydrogen atom, octanol as a hydrophobic medium, benzene as an aromatic molecule, the 2-norbornyl carbocation as a nonclassical ion, substituted cyclohexanes for the study of steric effects, *p*-substituted benzoic acids for the study of electronic effects, cyclodextrins for ligand–receptor interactions; in physics, a vibrating string as an oscillator and a particle in a box as a model for electrons in orbitals.

Science needs models for many reasons:

(1) Focus: Models allow a community of researchers to study a common subject. Solving any significant problem in science requires a substantial effort, with contributions from many individuals and techniques. Models are often the systems chosen to make this productive, cooperative focus possible.

(2) Research Overhead: Development of a system to the point where many details are scientifically tractable is the product of a range of contributions: for enzymes, these contributions are protocols for preparations, development of assays, determination of structures, preparation of mutants, definition of substrate specificity, study of rates, and development of mechanistic models. In a well-developed model system, the accumulation of this information makes it relatively easy to carry out research, since before new experiments begin, much of the background work—the fundamental research in a new system—has already been carried out.

(3) Recruiting and Interdisciplinarity: The availability of good model systems makes it relatively easy for a neophyte to enter an area of research and to test ideas efficiently. This ease of entry recruits new research groups, who use, augment, and improve the model system. It is especially important to have model systems to encourage participation by researchers

in other disciplines, for whom even the elementary technical procedures in a new field may appear daunting.

(4) Comparability: A well-established model allows researchers in different laboratories to calibrate their experiments, by reproducing well-characterized experiments.

(5) Community: The most important end result of a good model system is often the generation of a scientific community—that is, a group of researchers examining a common problem from different perspectives and pooling information relevant to common objectives.

One of the goals of this review is to summarize many experimental and theoretical studies of CA that have established it as a model protein. We hope that this summary will make it easier for others to use this protein to study fundamentals of two of the most important questions in current chemistry: (i) Why do a protein and ligand associate selectively? (ii) How can one design an inhibitor to bind to a protein selectively and tightly? We believe that the summary of studies of folding and stability of CA will be useful to biophysicists who study protein folding. In addition, we hope that the compilation of data relevant to CA in one review will ease the search for information for those who are beginning to work with this protein.

1.2. Objectives and Scope of the Review

This review includes information relevant to the use of CA as a model system for physical-organic studies of protein–ligand interactions and for developing strategies for rational drug design. The problem of designing high-affinity ligands to proteins is essentially one of molecular recognition in aqueous solution and one that chemistry should, in principle, be able to solve. The problem has been intractable for 50 years, however, and one important reason seems to be deficiencies in our understanding of the underlying physical principles.^{4,5} CA is particularly valuable for approaching this problem because it allows studies of binding of molecules to regions of the active site *adjacent* to the principal binding site—that is, the arylsulfonamide binding site, with its clearly defined hydrophobic pocket centered on the (His)₃Zn^{II} group; this additional binding site localizes the –SO₂NH[–] group of an inhibitor near the Zn^{II} ion. CA is, thus, uniquely suited for studies of structural *perturbations* to binding (perturbational studies often provide the most profitable strategy for testing hypotheses in difficult fields of science, among which rational drug design is certainly one).

We also discuss the use of CA for studying the folding, unfolding, and aggregation of proteins, as well as for developing biophysical assays for the binding of substrates and ligands to proteins. This review will give only brief surveys of the biology, physiology, or catalytic activity of CA and the use of its inhibitors in medicine; these subjects are reviewed extensively and in depth elsewhere.^{2,6–15}

2. Overview of Enzymatic Activity

CA catalyzes the reversible hydration of CO₂ to bicarbonate (eq 1 and Figure 1) in a two-step “ping-pong” mechanism.¹⁴ The first step involves the direct nucleophilic attack of a Zn^{II}-bound hydroxy group on CO₂ to form a metal-bound bicarbonate, followed by displacement of bicarbonate by a molecule of water. In the second step, the Zn^{II}-bound water molecule (see section 4.7) transfers a proton to molecules of buffer in the solvent and regenerates the zinc-

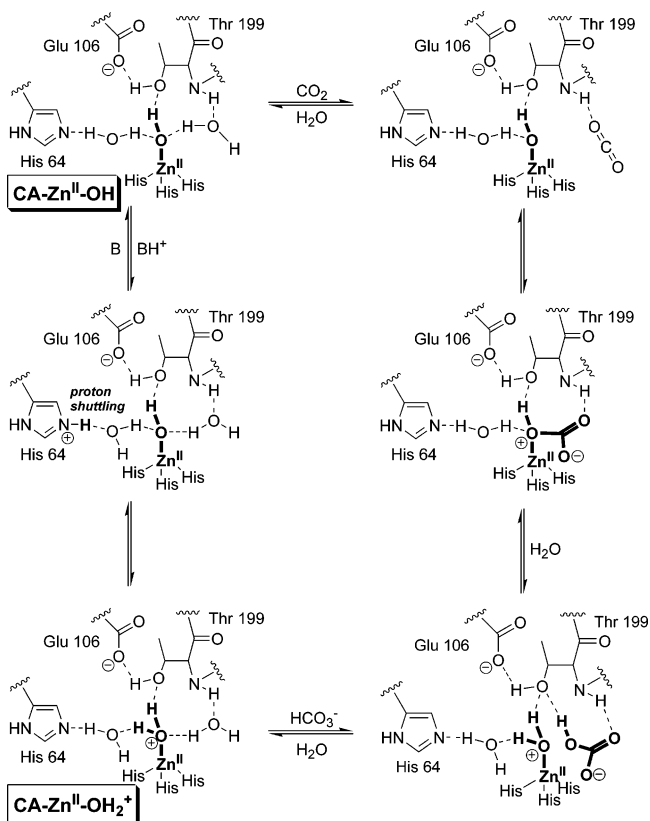
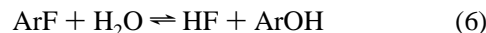


Figure 1. Mechanism of catalysis of the hydration of CO₂ by HCA II.¹⁴ The putative structures of the species CA–OH and CA–OH₂⁺, discussed in detail in the text, are indicated. We show the formal charge *only* on the zinc-bound water (and not the histidine residues) to emphasize that this water ligand is acidic (analogous to a hydronium ion being acidic) and adopt this convention throughout the remainder of the review.

hydroxide form of CA. CA is an extremely efficient catalyst: catalytic turnovers for several variants of CA are among the highest known ($k_{\text{cat}}^{\text{CO}_2} \approx 10^6 \text{ s}^{-1}$), and the second-order rate constants for these enzymes approach the limit of diffusional control ($k_{\text{cat}}/K_{\text{m}}^{\text{CO}_2} \approx 10^8 \text{ M}^{-1} \text{ s}^{-1}$).¹⁴ Snider et al. compiled a comprehensive list of values of $k_{\text{cat}}/K_{\text{m}}$ for enzymes that have second-order rate constants that approach the limit imposed by diffusion.¹⁶ Table 1 lists kinetic constants for various isozymes of CA^{17–29} and (for comparison) other highly efficient enzymes.^{30–36}

The catalytic activity of CA is not limited to the hydration of CO₂ (eqs 2–8). Although other activities may not be relevant to its principal biological role, CA can catalyze the hydration of aryl and aliphatic aldehydes^{37–39} and the hydrolysis of a wide variety of esters *in vitro*.^{40,41} Bovine CA II (BCA II) resolves mixtures of racemic *N*-acetylamino acids by selectively hydrolyzing the ester of only one enantiomer.⁴² Human CA I and CA II (HCA I and HCA II) catalyze the hydrolysis of 1-fluoro-2,4-dinitrobenzene⁴³ and sulfonyl chlorides.⁴⁴ HCA I and II also catalyze the hydration of cyanamide to urea.⁴⁵



While understanding of the mechanism of catalysis by CA is most detailed for HCA II, the available evidence suggests that all members of the α -CA family (see section 4.1) share the same ping-pong mechanism. The active site of CA contains a Zn^{II} ion with a bound hydroxyl group (Zn^{II}–OH) surrounded by three histidine residues held in a distorted tetrahedral geometry. Computational studies suggest that carbon dioxide is not coordinated to the Zn^{II} but instead binds weakly ($K_{\text{d}} \approx 100 \text{ mM}$) in a hydrophobic region 3–4 Å away from the Zn^{II} complex.^{46,47} Evidence suggests that the Zn^{II}-bound hydroxy group attacks CO₂ to initiate hydrolysis and produce bicarbonate, which is displaced from the Zn^{II} ion by a molecule of water.⁴⁸ The Zn^{II}-bound water (see section 4.8) loses a proton to generate a new Zn^{II}–OH for another round of catalysis.^{46,49} It is generally accepted that this proton is shuttled to buffers in solution by a series of intramolecular and intermolecular proton-transfer steps.^{50,51}

Perhaps unexpectedly, the transfer of a proton from Zn^{II}-bound water to buffer molecules appears to be the rate-limiting step in catalysis.⁴⁸ Proton transfer involves His64, which acts as a proton shuttle (see section 4.6).⁵² Mutation of His64 to Ala generates a protein having 6–12% of the activity of native enzyme for hydration of CO₂, depending on the buffer used in the experiment.⁵³ Increasing the concentration of buffer (from 0 to 0.5 M) enhances the rate by up to 25%. In several crystal structures, the side chain of His64 has been observed in two orientations, one pointed into the active site toward the Zn^{II} ion, and the other pointed out of the active site.⁵⁴ The dependence of these conformations on pH suggests a key role of His64 in the mechanism of proton shuttling.⁵⁵

Figure 1 outlines the details of the mechanism of hydration of CO₂ by HCA II.¹⁴ While rate constants for individual steps in the CA-catalyzed hydration of CO₂ are unknown, steady-state rate constants have been determined for many isozymes of CA (Table 1). Many groups have addressed these concepts computationally; the results of these studies will not be reviewed here.^{47,56–64}

3. Medical Relevance

Bicarbonate, a primary substrate of CA, is active in many biological processes: (i) as a counterion in sodium transport, (ii) as a carrier for CO₂, (iii) as a buffer, and (iv) as a metabolite in biosynthetic reaction pathways.⁶⁵ Although carbon dioxide reacts spontaneously with water at 37 °C to produce a proton and bicarbonate (eq 1), this reaction is not fast enough to accomplish the hydration of CO₂ and the dehydration of HCO₃[–] that are required for respiration in living organisms.⁶⁶

As far as we know, CA exists in all organisms. Its ubiquity reflects the fact that CO₂ is the terminal product of the oxidative metabolism of carbon-based molecules. In mammals, CA catalyzes the reversible hydration of CO₂ to bicarbonate (and the reverse reaction). These reactions are important to a variety of biological processes, including the following: (i) regulation of respiration and gas exchange,^{8,67,68} (ii) regulation of acid–base equilibria,^{67,69} (iii) vision,^{13,70,71} (iv) development and function of bone,^{72,73} (v) calcification,⁷³

Table 1. Steady-State Rate Constants for Hydration of CO₂ by Isozymes of CA and Kinetic Constants, for Comparison, of Other Highly Efficient Enzymes

Isozyme	Source	$k_{\text{cat}} \times 10^{-5} \text{ (s}^{-1}\text{)}$	$k_{\text{cat}}/K_m \times 10^{-7} \text{ (M}^{-1} \text{ s}^{-1}\text{)}$	Ref
CA I	human	2	5	17
CA II	human	14	15	17
CA III	human	0.1	0.03	18
CA III	bovine	0.064	0.04	19
CA IV	human	11	5	20
CA IV	murine	11	3.2	21
CA VA	murine	3	3	22
CA VB	human	9.5	9.8	27
CA VI	human	3.4	4.9	28
CA VI	rat	0.7	1.6	23
CA VII	murine	9.4	7.6	24
CA IX	human	3.8	5.5	25
CA XII	human	4	7.4	25
CA XIII	murine	0.83	4.3	26
CA XIV	human	3.12	3.9	29
acetylcholinesterase	eel electric-organ	0.14	16	30–33
catalase	human	5.5	0.7	34
catalase	horse liver	380	3.5	30, 35
β -lactamase	human	0.02	10	30
superoxide dismutase	human	0.04	800	36
triosephosphate isomerase	human	0.043	24	30

(vi) metabolism,^{7,10} (vii) signaling and memory,^{74,75} (viii) gustation,⁷⁶ (ix) production of saliva,⁷⁷ (x) production of pancreatic juices,⁷⁸ (xi) intestinal transport of ions,^{78–81} (xii) muscle function^{82–84} and the nervous system,⁸⁰ (xiii) regulation of seminal fluid,⁸⁵ (xiv) adaptation to cellular stress,^{86,87} (xv) acidification of the extracellular environment around hypoxic tumor cells,⁸⁸ and (xvi) several biosynthetic pathways.^{75,89}

CA plays an important role in the eye, where it is present in the lens, vitreous body, cornea, and retina. Within the ciliary body, the CA II-catalyzed formation of bicarbonate is the primary mechanism for the transport of sodium into the eye.⁹⁰ The influx of sodium ions into the eye is accompanied by the transport of water; both processes are important in maintaining the aqueous humor. Inhibition of carbonic anhydrase decreases the production of bicarbonate, which subsequently lowers intraocular pressure.⁹¹ Oral and topical arylsulfonamide inhibitors of CA dramatically reduce intraocular pressure; this activity has made them mainstays of the treatment of glaucoma.^{70,92,93} In addition to their use in treating glaucoma, inhibitors of CA are also used in treating both macular degeneration and macular edema, disorders that affect the central retina.^{94,95}

In the nervous system, CA serves many functions. In the choroid plexus, CA contributes to the production of cerebrospinal fluid.⁹⁶ In the brain, CA is found in oligodendrocytes and glial cells but is at the highest concentrations in sensory neurons, where it is important in signal processing, long-term synaptic transformation, and attentional gating of memory storage.^{74,97} Activation of CA rapidly increases levels of bicarbonate in memory-related neural structures.⁹⁸ Regulation of the flux of bicarbonate into synaptic receptor channels allows CA to function as a gate that regulates the transfer of signals through the neural network.⁷⁴ Inhibitors of CA can (i) impair spatial learning without affecting other behaviors—this selective effect may be important for the temporary suppression of memory;⁹⁷ (ii) act as anticonvulsant and antiepileptic agents;⁹⁹ (iii) obviate or delay the use of shunts in the brains of hydrocephalic infants and other patients;^{100,101} and (iv) effectively prevent episodic hypokalemic periodic paralysis.¹⁰²

Inhibitors of CA are important in renal pharmacology as diuretic agents. Sulfonamide inhibitors, such as acetazol-

amide (**137**, Table 10), increase the excretion of sodium and bicarbonate by preventing the reabsorption of bicarbonate and produce a diuretic effect.¹⁰³ The thiazide class of inhibitors are potent diuretics that affect intracellular pH and decrease the transport of sodium ions across the luminal membrane.¹⁰³ As a consequence of their diuretic effect, inhibitors of CA are used to treat hypertension and congestive heart failure.^{104,105} Inhibitors of CA can suppress the secretion of gastric acid, which is important in treating ulcerogenesis,^{106–108} and they can normalize severe metabolic alkalosis.

CA is involved in the extracellular acidification required for bone resorption at the osteoclast–bone interface.^{109,110} Defective bone resorption and a general failure of bone remodeling characterize osteopetrosis, a rare disease that produces dense, brittle bone and can be caused by a hereditary deficiency in HCA II.¹¹¹ Inhibition of CA has been shown to reduce bone loss in postmenopausal osteoporosis, a disease in which bones become extremely porous, are subject to fracture, and heal slowly.¹¹²

CA provides bicarbonate as a substrate for a variety of enzyme-catalyzed carboxylation reactions. Gluconeogenesis requires mitochondrial CA V to provide bicarbonate for pyruvate carboxylase, a key enzyme that replenishes intermediates in the synthesis of fatty acids, amino acids, neurotransmitters, and porphyrins. Inhibition of CA V can reduce gluconeogenesis,^{113,114} ureagenesis, and lipogenesis.^{115,116} Inhibitors of CA are used to treat acute mountain sickness,^{117,118} to improve the arterial oxygenation of patients suffering from chronic obstructive pulmonary disease (COPD),^{119,120} and as antimicrobial agents.¹²¹

Supuran, Chegwiddden, and others have recently observed that inhibitors of carbonic anhydrase inhibit the growth of several types of tumors in cell culture and in vivo.^{10,122–128} In addition, some isozymes of CA (in particular CA IX) and CA-related proteins are overexpressed in tumors.^{129–135} The exact connection between carbonic anhydrase and cancer is currently under investigation. For example, HCA IX is responsible for the hypoxia-induced acidification of the extracellular environment of hypoxic tumor cells.⁸⁸ Acidification (due to the activity of overexpressed HCA II, IX, or XII) increases the invasive behavior of cancer cells.¹³⁶ Acetazolamide decreases both the acidification around and the invasiveness of certain cancer cells.^{88,136} Several sul-

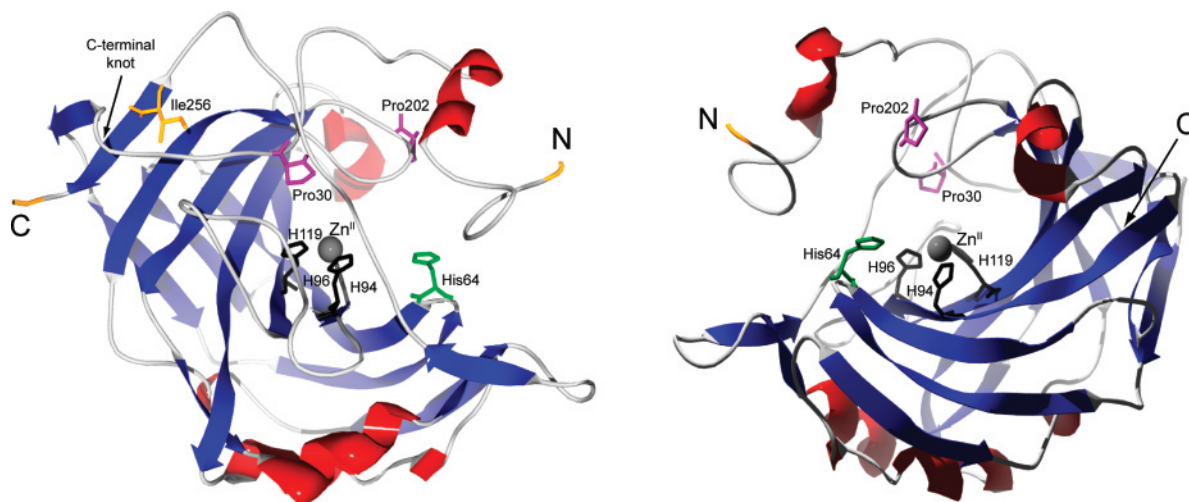


Figure 2. Ribbon rendering of HCA II from two perspectives, with α -helices in red and β -sheets in blue. The N- and C-termini, the C-terminal knot, and the primary residues involved in the initiation of folding and of coordinating the Zn^{II} cofactor are indicated.

fonamides are currently being tested clinically for their effects on tumor suppression.^{137,138}

II. Structure and Structure–Function Relationships of CA

4. Global and Active-Site Structure

4.1. Structure of Isoforms

The CAs are ubiquitous throughout nature and are expressed in eukaryotes (e.g., animals and plants), eubacteria, and archaea. CAs are divided into at least three classes based on amino acid homology: (i) α -CAs from animals (all mammalian CAs), plants, eubacteria, and viruses; (ii) β -CAs from plants, bacteria, and animals (e.g., *C. elegans*); and (iii) γ -CAs from bacteria and plants.^{139,140} There are two other possible classes of CA: (i) δ -CA TWCA1 from a marine diatom, *Thalassiosira weissflogii*, which is possibly a homolog of α -CAs,^{141,142} and (ii) ϵ -CAs from bacteria, which probably represent a subclass of β -CA that has diverged such that only one of its two domains has retained a viable active site.^{143,144} This review covers only the α -CAs because they are the most thoroughly studied and are the only class present in humans. There are at least 16 members of the α -CA family: CA I, II, III, IV, VA, VB, VI, VII, VIII, IX, X, XI, XII, XIII, XIV, and XV.^{26,145,146} They have wide-ranging cellular localizations: cytosolic (CA I, II, III, VII, and XIII), membrane-bound (CA IV, IX, XII, XIV, and XV), mitochondrial (CA VA and VB), and salivary secretions (CA VI).^{145,146}

We focus on HCA I, HCA II, and *bovine* carbonic anhydrase II (BCA II) because they are soluble, monomeric, of relatively low molecular weight (~ 30 kDa), and extremely well-characterized biophysically. There is a wealth of structural information available on HCA I and HCA II (Figure 2); this information makes them particularly well-suited for biophysical studies. While BCA II is not as well-characterized structurally as HCA I and HCA II (only two crystal structures are available for BCA II¹⁴⁷), these structures, and the high degree of sequence homology between BCA II, HCA I, and HCA II (Figure 3), suggest a very similar global and active site architecture of these isoforms. BCA II is the least expensive pure commercial variant of CA and often the one used in physical-organic studies.

HCA I	ASPDWGYDDK	NGPEQWSKLY	PIANGNNQSP	VDIKTSETKH
HCA II	-SHHWGYGKH	NGPEHWHKDF	PIAKGERQSP	VDIDTHTAKY
BCA II(R)	-SHHWGYGKH	NGPEHWHKDF	PIANGERQSP	VDIDTKAVVQ
	* .***. .:	****:* *	***:*.***	****.***
HCA I	DTSLK PISVS	YNPATAKE I I	NVGHFSHFVN	EDNDNRSVLK
HCA II	DPSLKPLSVS	YDQATSLRIL	NNGHAFNVEF	DDSQDKAVLK
BCA II(R)	DPALKPLALV	YGEATSRMV	NNGHFSFNVEY	DDSQDKAVLK
	*.:****: .:	*. ***: .:	* ***:***: .:	*.:****:***
HCA I	GGPFSDSYRL	FQFHFHWGST	NEHGSEHTVD	GVKYSALHVV
HCA II	GGPLDGTYRL	IQFHFHWGSL	DGQGSEHTVD	KKKYAAELHL
BCA II(R)	DGPLTGTYRL	VQFHFHWGSS	DDQSEHTVD	RKKYAAELHL
	..** :.***	.*****	: :*****	**:*****:
HCA I	AHWNSAKYSS	LAEAASKADG	LAVIGVLMKV	GEANPKLQKV
HCA II	VHWNT-KYGD	FGKAVQPDG	LAVLGIFLKV	GSARKPLQKV
BCA II(R)	VHWNT-KYGD	FGTAAQPDG	LAVVGVFVKV	GDANPALQKV
	..***: ***	:. *.:**	***:***:***	*.:* ****
HCA I	LDALQAIKTK	GKRAPFTNFD	PSTLLPSSLD	FWTYPGSLTH
HCA II	VDVLDSEIKTK	GKSADFNTFD	PRGLLPESLD	YWTYPGSLTT
BCA II(R)	LDALDSIKTK	GKSTDFNFD	PGSLLPNVLD	YWTYPGSLTT
	*.:***:****	** : *.***	* ***. **	:*****
HCA I	PPLYESVTWI	ICKESISVSS	EQLAQFRSLL	SNVEGDNAV
HCA II	PPLLECVTWI	VLKEPISVSS	EQVLKFRKLN	FNGEGEPEEL
BCA II(R)	PPLLESVTWI	VLKEPISVSS	QQMLKFRTLN	FNAEGEPELL
	*** *.****	: **.****	:*: :***.*	* **:
HCA I	MQHNNRPTQP	LKGRIVRASV	-	
HCA II	MVDNWRPAQP	LKNRQIKASF	K	
BCA II(R)	MLANWRPAQP	LKNRQVRGFP	K	
	* * **:*	**.*	: .:	

Figure 3. Amino acid sequences of HCA I, HCA II, and BCA II. Sequence homology is denoted by the symbols “*”, “:”, and “.”; “*” represents identical residues, “:” represents charge/polarity conserved residues, and “.” denotes polarity conserved residues. BCA II exists as two variants: an “R” form (shown here), where residue 56 exists as an Arg, and a “Q” form, where it exists as Gln. This residue is underlined above.

An overlay of crystal structures of these isoforms shows their high structural homology (Figure 4). The extensive homology in amino acid sequence between these isoforms is the basis for their similar physical properties and number and types of chemically reactive side chains (Table 2).^{148–150} Details of the active site, as well as changes in the structures of HCA I and HCA II (and by extension BCA II) upon binding of ligands, are known from many structural studies

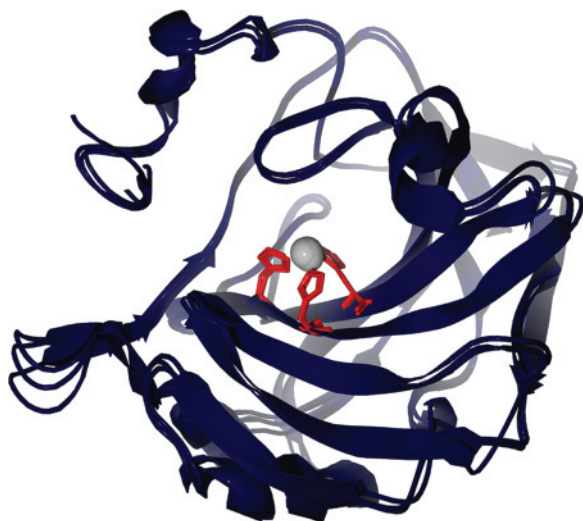


Figure 4. Overlay of X-ray structures of HCA I, HCA II, and BCA II, with His residues in the active site highlighted. This image was rendered using POV-Ray 3.5 (www.povray.org). The accession numbers from the protein data bank (PDB) for the rendered structures are 2CAB (HCA I), 2CBA (HCA II), and 1V9E (BCA II).^{147,184,239}

Table 2. Abundance of Reactive Amino Acid Side Chains in HCA I, HCA II, and BCA II

	HCA I	HCA II	BCA II (R) ^a	BCA II (Q) ^a
M^b (g mol ⁻¹)	28 846.4	29 227.9	29 089.9	29 061.9
ϵ_{280}^c (M ⁻¹ cm ⁻¹)	47 000	54 700	55 300	55 200
pI ^d	6.60	7.40	5.90	5.40
amino terminus	NHCOCH ₃	NHCOCH ₃	NHCOCH ₃	NHCOCH ₃
carboxy terminus	CO ₂ ⁻	CO ₂ ⁻	CO ₂ ⁻	CO ₂ ⁻
no. of amino acids modifiable groups: ^e	260	259	259	259
Lys	18	24	18	18
Arg	7	7	9	8
His	11	12	11	11
Asp/Glu	27	32	30	30
Cys	1	1	0	0
Tyr	8	8	8	8
Ser	30	18	16	16
Thr	14	12	14	14
Trp	6	7	7	7
Phe	11	12	11	11

^a R or Q variant at position 56. ^b Average isotopic mass calculated from the primary sequence (with Zn^{II} and with post-translational modifications) with all residues in their neutral (un-ionized) forms. ^c Nyman and Lindskog reported the extinction coefficients at 280 nm (in units of L g⁻¹ cm⁻¹) to be 1.63 for HCA I, 1.87 for HCA II, and 1.90 for BCA II (assuming that $M = 30\,000$ g mol⁻¹, ϵ_{280} would be 48 900 for HCA I, 56 100 for HCA II, and 57 000 for BCA II).¹⁴⁸ The values reported here use the extinction coefficients from Nyman and Lindskog together with the values of M in this table. ^d Values of pI were from Sigma Aldrich, Inc. (<http://www.sigmaaldrich.com>). These data agree with those of Funakoshi and Deutsch (pI = 6.57 for HCA I, pI = 7.36 for HCA II)¹⁴⁹ and Jonsson and Pettersson (pI = 5.9 for BCA II).¹⁵⁰ ^e Data from Swiss Prot (<http://au.expasy.org/sprot/>).

by X-ray crystallography. In addition, numerous complexes of CA with bound inhibitors have been characterized structurally, thermodynamically, and kinetically. We discuss these topics in sections 9–11.

4.2. Isolation and Purification

Methods for isolating and purifying CA are well-established and widely accessible. Commercial sources usually isolate isozymes HCA I, HCA II, and BCA II from red blood cells, in which CA is the second most abundant

protein after hemoglobin. Academic laboratories typically produce HCA II and BCA II by recombinant technology in *E. coli*;^{151,152} this method provides the structural flexibility and specificity of site-directed mutagenesis, which is useful for biophysical and biochemical studies. The blood protein and the wild-type recombinant construct are identical except for the N-terminus, which is a post-translationally acetylated Ser in the native CA and exists as Met-Ala or Ala in the recombinant version.¹⁵³

The laboratory procedure for the purification of HCA from red blood cells involves lysis of the cells and removal of the cellular remnants by centrifugation, followed by separation of hemoglobin from HCA on a sulfonamide-modified agarose affinity column.^{154,155} Divalent anions (e.g., sulfate in 0.1 M tris-SO₄/0.2 M Na₂SO₄, pH 9.0 buffer) do not bind appreciably in the active site of HCA, and thus, they are used to remove nonspecifically bound protein by screening ionic interactions. The two isozymes of HCA can then be eluted consecutively from the column. HCA I, which has a higher dissociation constant for sulfonamides than HCA II, is eluted with tris-SO₄ buffer containing 0.2 M KI; HCA II elutes with tris-SO₄ buffer containing 0.4 M NaN₃. Osborne and Tashian showed that CA isozymes from other species can be purified in a similar way, with only minor modifications.¹⁵⁴ Commercial suppliers do not use the chromatographic methods, but their exact procedures are proprietary.

The purification of recombinant protein proceeds in a similar manner, with cell lysis, DNA digestion by DNase, and centrifugation as the initial steps. CA can then be purified by affinity chromatography, as described above, with only one isozyme present in the lysate. Fierke and co-workers developed another procedure for purifying recombinant HCA II and its less active mutants.^{46,153,156} The procedure consists of the following: (i) agarose-based, cation-exchange column chromatography and (ii) gel filtration column chromatography. The latter procedure eliminates the need for extensive dialysis to remove the azide ions used for elution in affinity chromatography. These procedures routinely produce HCA II at >90% purity, as determined by SDS-PAGE;¹⁵⁶ these purities are high enough for crystallization for X-ray diffraction.

4.3. Crystallization

The limiting factor in the ability to solve three-dimensional structures by single-crystal X-ray diffraction analysis is the growth of protein crystals. Because of the large number of crystal structures solved for CA and its excellent stability under standard laboratory conditions, methods for growing diffraction-quality crystals of CA and complexes of CA with bound inhibitor are well-developed.

One typically uses the hanging-drop or sitting-drop method to crystallize HCA II. These methods involve combining a drop of a solution of the protein, methyl mercuric acetate (MMA), and tris-sulfate with a precipitant buffer of ammonium sulfate and tris-sulfate. The pH used in the buffer depends on the desired conditions and has been reported in the range of 4.7–10 (see Table 4). Sodium azide is sometimes added to the drop and the precipitant buffer in order to prevent microbial growth. Azide (**199**) is a weak inhibitor of CA ($K_i = 0.59$ mM with BCA II), and so interpretations of electron density cannot ignore the possibility of binding of azide or the competition of azide with other weakly bound ligands (see section 9.2.5).¹⁵⁷ The mercury from MMA coordinates to the Cys206 residue in

Table 3. X-ray Crystal Structures for CA of Non-Human Species

Species	Common name	CA isoform	CA class	PDB ID(s) ^a	Res (Å)	Ref
<i>Bos Taurus</i>	cow	II	α	1V9E , 1V9I ^{b,c}	1.95–2.95	147
		III	α	n/a	2.0	161
<i>Mus musculus</i>	mouse	IV	α	2ZNC, 3ZNC ^d	2.80	162
		V	α	1DMX, 1DMY, 1KEQ , 1URT	1.88–2.8	163–165
		V–MI ^f	α	n/a	1.88	164
		XIV ^e	α	1RJ5 , 1RJ6 ^g	2.81–2.9	166
<i>Rattus norvegicus</i>	rat	III	α	1FLJ	1.80	167
<i>Neisseria gonorrhoeae</i>	gonorrhea		α	1KOP, 1KOQ	1.90	168
<i>Dunaliella salina</i>	green alga	II	α	1Y7W	1.86	169
<i>Porphyridium purpureum</i>	red alga		β	1DDZ	2.20	170
<i>Pisum sativum</i>	pea		β	1EKJ	1.93	171
<i>Escherichia coli</i>	<i>E. Coli</i>		β	1I6O, 1I6P , 2ESF, 1T75 ^c	2.00–2.5	172, 173
<i>Mycobacterium tuberculosis</i>	<i>M. tuberculosis</i>	Rv3588c	β	1YM3 , 2A5V	1.75–2.2	174, 175
		Rv1284	β	1YLK	2.0	175
<i>Haemophilus influenzae</i>			β	2A8C, 2A8D	2.20–2.3	173
<i>Halothiobacillus neapolitanus</i>		CsoSCA	β	2FGY	2.20	144
<i>Methanobacterium thermoautotrophicum</i>			β	1G5C	2.10	176
<i>Methanosarcina thermophila</i>			γ	1QQ0, 1QRE , 1QRF, 1QRG, 1QRL, 1QRM, 1THJ	1.46–2.8	177, 178

^a The structure with the highest resolution is bold. ^b 1V9I is a site-specific mutant (Gln253Cys) of BCA II. ^c Not published: 1V9I, 1T75. ^d 3ZNC is complexed with brinzolamide (**161**). ^e Extracellular domain. ^f This isoform is a double mutant (Phe65Ala, Tyr131Cys) of MCA V in which the introduced Cys residue was modified with 4-chloromethylimidazole to introduce a methylimidazole (MI) group.¹⁶⁴ ^g 1RJ6 is complexed with acetazolamide (**137**).

HCA II,¹⁵⁸ prevents aggregation of the crystals, and facilitates the growth of diffraction-quality crystals that grow faster and to a larger size than crystals grown in the absence of MMA.¹⁵⁹ Although the mercury does not perturb the structure of the enzyme (beyond a conformational change of the side chain of Cys206), it can be removed from the sample by dialyzing the crystals against cysteine and ammonium sulfate for 3 days, or by treatment of the crystals with 2-mercaptoethanol.^{158,159} When preparing enzyme–inhibitor complexes, the CA crystals may be cross-linked by adding a solution of glutaraldehyde, ammonium sulfate, and tris-sulfate to the hanging drop, followed by solution of the inhibitor. BCA II has been crystallized simply in tris buffer, pH 7.5, with 2.4 M ammonium sulfate as precipitant, without the necessity for engineered cysteine residues and MMA.¹⁴⁷

4.4. Structures Determined by X-ray Crystallography and NMR

4.4.1. Structures Determined by X-ray Crystallography

X-ray structural analysis has established the structure of wild-type CA, with and without bound inhibitors. The environment of the catalytic Zn^{II} ion in the active site and how inhibitors interact with this ion and with the adjacent amino acid residues are well-established. X-ray crystallography has also demonstrated how site-specific mutations affect the local and global structures of CA. These mutant structures have been used to infer the mechanism of binding and catalysis for the wild-type (w.t.) enzyme.

As of December 2007, there were 279 X-ray structures of CA in the Protein Data Bank (PDB);¹⁶⁰ of these, 245 were isoforms of HCA. HCA II, with 221 structures, is by far the most commonly studied (unless otherwise stated, this review numbers residues according to the structure of HCA II). Structures for CAs from several non-human species also exist (Table 3).^{144,147,161–178} Considering the widespread usage of the relatively inexpensive BCA II, it is surprising that there exists only one high-resolution crystal structure for BCA II (PDB accession number 1V9E, at 1.95 Å resolution)¹⁴⁷ and one structure for the Gln253Cys mutant of this enzyme (1V9I, 2.95 Å).

Studies using inhibitors and mutations have motivated the majority of crystal structures of HCA I and II. The resolution of most of these structures is in the range of 2.0 ± 0.5 Å, which is adequate for modeling the interactions of the inhibitors in and around the active site, as well as for observing the effects of mutations on structure. X-ray structures of both native and mutant isozymes of HCA provide useful information on how inhibitors bind in the active site and at nearby hydrophobic sites (see section 4.6). Table 4 lists all of the structures in the PDB of native HCA with^{45,128,162,179–238} and without^{54,183,184,239–242} bound ligands. Table 5 lists the structures of mutant HCAs and the motivation for constructing each mutation.^{153,156,158,179,180,183,242–268}

Information gained from studies on mutants of HCA (mainly HCA II) has been invaluable in elucidating the mechanism of catalytic hydration of CO₂. Mutations of Thr199 alter the coordination sphere of Zn^{II} and create proteins that bind zinc both more strongly and more weakly than the w.t. enzyme.^{243,244} Mutations of the Zn^{II}-binding histidine residues have clarified the importance of plasticity of the Zn^{II}-binding site; these mutations often lead to loss (i.e., weak binding) of the Zn^{II} ion.^{245,246} Other studies have explored the importance of indirect ligands—that is, residues that interact with the Zn^{II}-bound residues but not directly with the Zn^{II}—by introducing mutations into the Zn^{II}OH–Thr199–Glu106 triad^{156,179,247} and into the rest of the indirect ligand–metal^{248,269} hydrogen-bonding network (see section 6 and Table 5).

Certain mutations enhance the binding of metal ions to HCA, and some metal ions bind readily to the native apoenzyme. To date, crystallized metallovariants include apo-HCA (protein with no metal in the binding site), Zn^{II} (w.t.), Cd^{II}, Co^{II}, Cu^{II}, Hg^{II}, Mn^{II}, and Ni^{II}. Tables 4 and 5 include many of these structures. Section 5 and Table 6 contain a more detailed discussion of these and other metallovariants of CA.

4.4.2. Structure Determined by NMR

While X-ray studies have provided useful structural data for mutated and native CA, both with and without bound ligands, they cannot provide information on solution-phase structural dynamics of the enzyme or its bound inhibitors.

Table 4. X-ray Crystal Structures of Native Carbonic Anhydrases of Human Origin

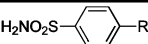
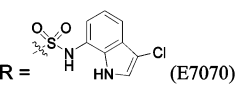
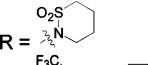
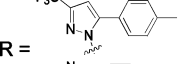
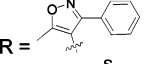
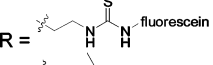
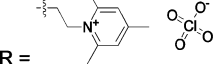
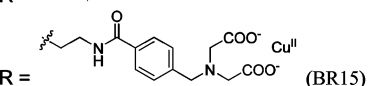
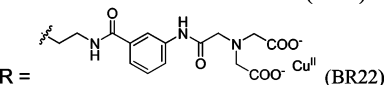
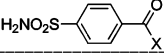
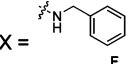
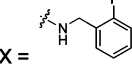
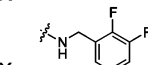
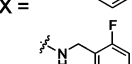
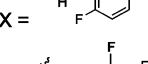
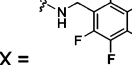
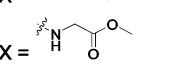
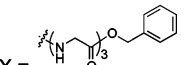
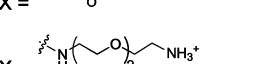
Compound	Complexed Ligand / Metal Substitute	Isoform	pH	PDB ID	Res (Å)	Ref.
Apo ^a		HCA II	8.0	2CBE	1.82	184
—		HCA I		2CAB	2.0	239
—		HCA II	7.8	2ILI	1.05	54
—		HCA II		1CA2	2.0	240
—		HCA II	7.8	2CBA	1.54	184
—		HCA II	6.0	2CBB	1.67	184
—		HCA II	7.0	1TBT	2.00	183
—(OH ⁻)		HCA II	9.0	1TEU	2.00	183
—		HCA II	10.0	1TEU	2.00	183
—		HCA II ^b	8.5	1XEV	2.20	n/a ^c
—		<i>d</i> -HCA II ^d	7.5	2AX2	1.50	241
—		HCA III ^e	8.0	1Z93	2.10	242
<i>Type:</i> 						
282	R = (CH ₂) ₂ NH ₃ ⁺	HCA II	7.7	2NNG	1.20	234
283	R = (CH ₂) ₂ NHCOCH ₃	HCA II	7.7	2NNS	1.03	234
		HCA I	7.0	2NMX	1.55	
284	R = (CH ₂) ₂ CO ₂ ⁻	HCA II	7.7	2NNO	1.01	234
		HCA I	7.0	2NN1	1.65	
285	R = (CH ₂) ₂ CO ₂ CH ₂ CH ₃	HCA II	7.7	2NNV	1.10	234
		HCA I	7.0	2NN7	1.85	
131		HCA II	8.2	n/a	1.9	229
292		HCA II	7.7	2Q1Q	1.90	238
230		HCA II	8.2	1OQ5	1.50	204
231		HCA II	8.4	2AW1	1.46	205
232		HCA II	8.5	2F14	1.71	206
233, 205		HCA II	8.5	1ZE8	2.00	207
234		HCA II	7.7	2FOQ	1.25	181
235		HCA II	7.7	2FOU	0.99	181
<i>Type:</i> 						
51	X = 	HCA II	8.0	n/a	2.3	202
55	X = 	HCA II	8.0	1G1D	2.04	180
56	X = 	HCA II	8.0	1G52	1.80	180
57	X = 	HCA II	8.0	1G53	1.94	180
58	X = 	HCA II	8.0	1G54	1.86	180
277	X = 	HCA II	8.0	n/a	2.0	202
70	X = 	HCA II	8.0	n/a	2.4	202
83	X = 	HCA II		1CNX	1.90	185
84	X = 	HCA II		1CNW	2.00	185

Table 4 (Continued)

Compound	Complexed Ligand / Metal Substitute	Isoform	pH	PDB ID	Res (Å)	Ref.
<i>Type:</i>						
85		HCA II		1CNY	2.30	185
	X =					
109		HCA II	8.0	1IF7	1.98	189
110		HCA II	8.0	1IF8	1.94	189
236		HCA II	8.0	1IF9	2.00	189
237		HCA II		1OKM	2.20	208
238		HCA II		1OKN	2.40	208
218		HCA II	7.7	2FOS	1.10	181
	X =					
219		HCA I	6.4	2FOY	1.55	181
	X =					
<i>Type:</i>						
239		HCA II	8.2	2HD6	1.80	209
240		HCA II	8.0	1ZFK	1.56	n/a ^c
241		HCA II	8.0	1ZH9	1.70	n/a ^c
287		HCA II	8.4	2HL4	1.55	235
	X =					
<i>Type:</i>						
207	4-fluoro	HCA II	8.0	1IF4	1.93	182
210	2,6-difluoro	HCA II	8.0	1IF5	2.00	182
211	3,5-difluoro	HCA II	8.0	1IF6	2.09	182
133		HCA II		1OKL	2.10	203
	(DNMA)					
137		HCA I		1AZM	2.00	211
	(acetazolamide, AZM)	HCA XII	4.8	1JD0	1.50	210
138		HCA I		1BZM	2.00	211
	(methazolamide)					
242		HCA II	8.2	2HOC	2.10	212
243		HCA II	8.2	2HNC	1.55	212
244		HCA II	8.0	2EU3	1.60	213
245		HCA II	8.0	2EU2	1.15	213
246		HCA II	8.0	1ZFQ	1.55	n/a ^c
146		HCA II	10.0	1BN1	2.10	199
147		HCA II	10.0	1BN4	2.10	199

Table 4 (Continued)

Compound	Complexed Ligand / Metal Substitute	Isoform	pH	PDB ID	Res (Å)	Ref.
148		HCA II	10.0	1BNW	2.25	199
155		HCA II		1CIM	2.10	214
156		HCA II		1CIN	2.10	214
157		HCA II		1CIL	1.60	214
158		HCA II	10.0	1BNU	2.15	199
159		HCA II	10.0	1BNT	2.15	199
160		HCA II	10.0	1BNQ	2.40	199
161		HCA II	8.0	1A42	2.25	162
	(brinzolamide)					
247		HCA II	8.0	1I90	2.00	215
162		HCA II	10.0	1BNN	2.30	199
163		HCA II	10.0	1BNM	2.60	199
164		HCA II	10.0	1BNV	2.40	199
165		HCA II	10.0	1BN3	2.20	199
248		HCA II	8.0	1I8Z	1.93	215
249		HCA II	8.0	1I91	2.00	215
186		HCA II	8.2	n/a	1.5	230
	(EMATE)					

Table 4 (Continued)

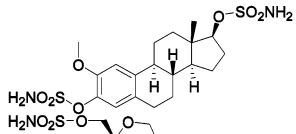
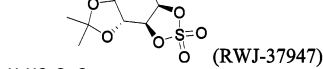
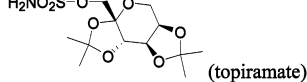
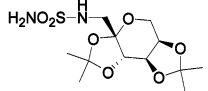
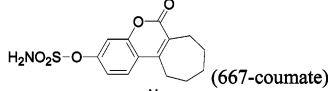
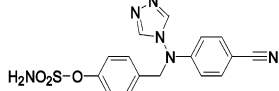
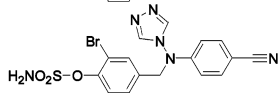
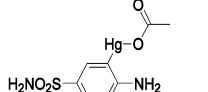
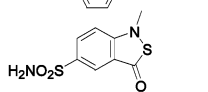
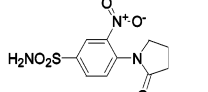
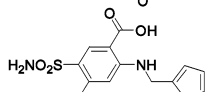
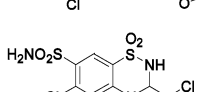
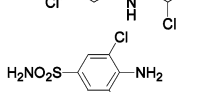
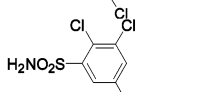
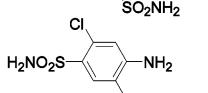
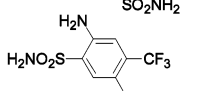
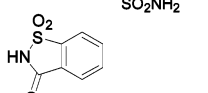
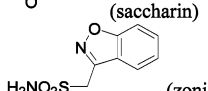
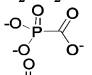
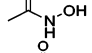
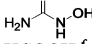
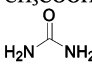
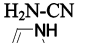
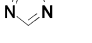
Compound	Complexed Ligand / Metal Substitute	Isoform	pH	PDB ID	Res (Å)	Ref.
186a		HCA II	8.5	2GD8	1.46	128
187	 (RWJ-37947)	HCA II	8.8	1E0U	2.10	216
187a	 (topiramate)	HCA II	8.2	n/a	1.8	233
187b		HCA II	7.7– 7.8	2H15	1.9	232
250	 (667-coumate)	HCA II	8.0	1TTM	1.95	217
251		HCA II	8.0	1XPZ	2.02	218
252		HCA II	8.0	1XQ0	1.76	218
253		HCA I		3CA2	2.00	186
254		HCA II	8.5	1KWR	2.25	219
255		HCA II	8.0	1KWQ	2.60	219
256		HCA II	8.0	1Z9Y	1.66	n/a ^c
257		HCA II	8.0	1ZGF	1.75	n/a ^c
258		HCA II	8.0	1ZGE	1.65	n/a ^c
288		HCA II	8.2	2POU	1.60	236
289		HCA II	8.2	2POV	1.60	236
290		HCA II	8.2	2POW	1.75	236
291	 (saccharin)	HCA II	8.5 8.0	2Q1B 2Q38	1.70 1.95	237 237
278	 (zonisamide)	HCA II	8.2	n/a	1.70	231

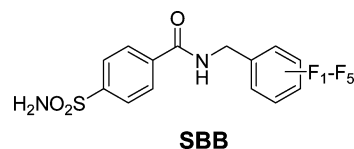
Table 4 (Continued)

Compound	Complexed Ligand / Metal Substitute	Isoform	pH	PDB ID	Res (Å)	Ref.
<i>Type: Organic Small Molecules</i>						
188	H ₂ NO ₂ S-CF ₃	HCA II	8.5	1BCD	1.90	201
192	H ₂ NO ₂ S-O ⁻	HCA II	8.2	n/a	1.4	228
279	H ₂ NO ₂ S-NH ₂	HCA II	8.2	n/a	1.6	228
280	H ₂ NO ₂ S-NHOH	HCA II	7.8	2O4Z	2.1	227
281		HCA I	9.0	2IT4	2.0	225
190		HCA II	8.0	1AM6	2.10	200
259		HCA II	7.7	2GEH	2.00	220
260	HCOOH ^f	HCA II		2CBC	1.88	184
261	CH ₃ COO ⁻	HCA II	8.5	1XEG	1.81	n/a ^c
262	CH ₃ COOH ^f	HCA II	8.5	1CAY	2.10	179
262	CH ₃ COOH	HCA XII	4.8	1JCZ	1.55	210
263		HCA II	7.7	1BV3	1.85	45
264		HCA II	7.7	1F2W	1.90	221
265		HCA II		1CRA	1.90	222
266	L-Histidine ^g	HCA I	9.0	2FW4	2.00	191
		HCA II	7.7	2ABE	2.00	190
267	D-Histidine ^g	HCA II	7.7	2EZ7	2.00	192
268	L-Phenylalanine ^g	HCA II	7.7	2FMG	1.60	193
269	D-Phenylalanine ^g	HCA II	7.7	2FMZ	1.60	193
199, 270	N ₃ ⁻ , Histamine ^g	HCA II	7.7	1AVN	2.00	194
286	L-Adrenaline ^g	HCA II	7.7	2HKK	1.90	226
<i>Type: Inorganic Anions</i>						
194	Cl ^{-f}	HCA II	6.1	1TB0	2.00	183
194	Cl ^{-f}	HCA II	7.8	1TE3	2.00	183
194	Cl ⁻ / Hg ^{II}	HCA I		1CRM	2.00	223
195	Br ⁻	HCA II	8.5	1RAZ	1.90	195
196	I ⁻	HCA I		1HUH	2.20	196
197	HS ⁻	HCA II	8.5	1CAO	1.90	197
199	N ₃ ⁻	HCA II	8.5	1RAY	1.80	195
201	SCN ⁻	HCA II		2CA2	1.90	186
203	HCO ₃ ⁻	HCA I		1HCB	1.60	198
203	HCO ₃ ⁻ / Co ^{II}	HCA II	8.0	1CAH	1.88	188
204	NO ₃ ⁻	HCA II		1CAN	1.90	197
271	HSO ₃ ⁻	HCA II		2CBD	1.67	184
272	SO ₄ ²⁻	HCA II	5.1	1T9N	2.00	183
272	SO ₄ ²⁻ / Co ^{II}	HCA II	8.5	1RZB	1.80	187
272	SO ₄ ²⁻ / Mn ^{II}	HCA II	8.5	1RZD	1.90	187
272	SO ₄ ²⁻ / Ni ^{II}	HCA II	8.5	1RZE	1.90	187
272	2 SO ₄ ²⁻ / 2 Zn ^{II}	HCA IV	5.1	1ZNC	2.80	224
273	O ₂ / Co ^{II}	HCA II	8.5	1RZA	1.90	187
273	O ₂ / Cu ^{II}	HCA II	8.5	1RZC	1.90	187
274	Au(CN) ₂ ^{-f}	HCA I		1HUG	2.00	196

^a The active site is free in this structure. ^b New crystal form. ^c Not published. ^d Perdeuterated HCA II. ^e Mutations C183S and C188S (opposite the active site) were made to enhance crystallization and did not affect catalysis. ^f The species is located in or near the active site but does not directly complex the metal. ^g CA activator.

For this kind of information, researchers have thus far turned to NMR. Most of the NMR studies involving complexes of benzenesulfonamides with CA have explored the stoichiometry,^{270–275} coordination,^{273,275–277} and internal motion^{270–274} of ligands bound to the active site. We discuss those studies here.

To the best of our knowledge, there are no high-resolution solution structures of CA determined by NMR-based techniques, as CA is marginally too large for NMR to be practical. Recent advances in NMR spectroscopy, however, may now make such structures obtainable.^{278,279} So far, only triple resonance experiments (¹H, ¹³C, ¹⁵N) and ¹⁵N heteronuclear NOE data on HCA I and perdeuterated HCA II with site-specific ¹⁵N-labeling have aided in the assignment of backbone and side-chain resonances, as well as in the determination of the secondary structure and global fold for



number	fluorination
51	none
55	2-fluoro
	4-fluoro
56	2,3-difluoro
	2,4-difluoro
	2,5-difluoro
57	2,6-difluoro
	2,3,4-trifluoro
	2,4,6-trifluoro
	3,4,5-trifluoro
58	pentafluoro

Table 5. X-ray Crystal Structures of Mutant Carbonic Anhydrases of Human Origin

Isoform	Mutation	Engineered ^a	Complex; Metal (non-Zn ^{II})	PDB ID	Res. (Å)	pH	Ref
Hydrophobic Pocket and Wall							
HCA II	V121A	widens hydrophobic pocket		12CA	2.40		153
HCA II	V143F	hydrophobic pocket depth affects catalytic activity		6CA2	2.50		158
HCA II	V143G	idem		7CA2	2.40		158
HCA II	V143H	idem		8CA2	2.40		158
HCA II	V143Y	idem		9CA2	2.80		158
HCA II	L198R	altered mouth of hydrophobic pocket, catalytic efficiency		1HEA	2.00		253
HCA II	L198E	idem		1HEB	2.00		253
HCA II	L198H	idem		1HEC	2.00		253
HCA II	L198A	idem		1HED	2.00		253
HCA II	L198E	side-chain mobility, charge and hydrophobicity affect substrate affinity	AZM ^b	1YDA	2.10		254
HCA II	L198R	idem	AZM ^b	1YDD	2.10		254
HCA II	L198F	idem/HCA III mimic	AZM ^b	1YDB	1.90		254
HCA II	L198F	idem/idem		1YDC	1.95		254
HCA III	F198L ^c	increased catalytic activity/HCA II mimic		1Z97	2.10		242
HCA II	F131V	electrostatics of ligand benzyl/Phe131 interaction	sulfamoyl benzamides ^d	see below ^d	1.8–1.96 ^d		180
HCA II	F131V	intermolecular interactions between bound ligands	sulfamoyl benzamides ^e	see below ^e	1.8–1.93 ^e		249
HCA II	P202A	decreased folded-state stability, maintained activity		1MUA	1.70		255
Direct and Indirect Ligands of Zn ^{II}							
HCA II	T200H	HCA I mimic	HCO ₃	1BIC	1.90		256
HCA II	T200S	increased esterase activity		5CA2	2.10		257
HCA II	T199C	tight Zn binder, engineered Zn coordination polyhedron		1DCA/1DCB	2.20/2.10		244
HCA II	T199D	fM Zn ^{II} binder; fourth Zn ^{II} ligand		1CCS	2.35		243
HCA II	T199E	idem		1CCT	2.20		243
HCA II	T199H	weak Zn ^{II} binder	SO ₄ ²⁻	1CCU	2.25		243
HCA II	T199P, C206S	novel binding interactions: Zn ^{II} -bound sulfur of ligand	2-ME	1LG5	1.75		258
HCA II	idem	tetraedrally coordinated SCN ⁻ binding to Zn ^{II}	SCN ⁻	1LG6	2.20		258
HCA II	idem	new bicarbonate binding site	HCO ₃	1LGD	1.90		258
HCA II	T199V	disrupts zinc OH-T199-E106 hydrogen bond network	N ₃ ⁻ /O ₄ ²⁻	1CVA/1CVB	2.25/2.40		156
HCA II	T199A	idem	none/HCO ₃	1CAL/1CAM	2.20/1.70		247
HCA II	E106A	idem	SO ₄ ²⁻	1CAI	1.80		247
HCA II	E106D	alters Zn ^{II} -OH-T199-E106 hydrogen bond network	SO ₄ ²⁻	1CAJ	1.90		247
HCA II	E106Q	idem	SO ₄ ²⁻	1CAK	1.90		247
HCA II	E106Q	alters hydrogen bond network and ligand binding	acetic acid	1CAZ	1.90		179
HCA II	H94C	engineering Zn ^{II} affinity, discrimination, functionality	apo	1HVA	2.30		250
HCA II	H94A	metal-binding site plasticity	apo	1CVF	2.25		245
HCA II	H94C	idem	2-ME; apo	1CNB	2.35		245
HCA II	H94C	idem		1CNC	2.20		245
HCA II	H119C	idem		1CVD	2.20		245
HCA II	H119D	idem		1CVE	2.25		245
HCA II	H96C	idem		1CVH	2.30		245
HCA II	H94D	redesigned Zn ^{II} binding site		1CVC	2.30		246
HCA II	H94N	electrostatic effects on Zn ^{II} binding affinity, coordination	tris (buffer)/AZM ^b	1H4N/2H4N	2.00/1.90		259
HCA II	H119N	idem		1H9N	1.85		259
HCA II	H119Q	idem		1H9Q	2.20		259
HCA II	E117Q	indirect ligand increases Zn ^{II} complexation kinetics	apo	1ZSA	2.50		252
HCA II	E117Q	idem/decreases ligand affinity	AZM ^b	1ZSB	2.00		252
HCA II	E117Q	idem/decreases catalytic activity		1ZSC	1.80		252
HCA II	E117A	indirect ligand–metal network	Cl ⁻	1CNG	1.90		248
HCA II	Q92E	idem		1CNH	2.05		248
HCA II	Q92A	idem		1CNI	1.80		248
HCA II	Q92N	idem		1CNJ	1.80		248
HCA II	Q92L	idem	SO ₄ ²⁻	1CNK	2.15		248

Table 5 (Continued)

Isoform	Mutation	Engineered ^a	Complex; Metal (non-Zn ^{II})	PDB ID	Res. (Å)	pH	Ref
Hydrophobic Core Residues							
HCA II	F95M, W97V	influence of hydrophobic core on metal binding, specificity		1FQL	2.00		251
HCA II	F93I, F95M, W97V	idem		1FQM	2.00		251
HCA II	idem	idem	apo	1FQN	2.00		251
HCA II	idem	idem	Co ^{II}	1FQR	2.00		251
HCA II	idem	idem	Cu ^{II} , SO ₄ ²⁻	1FR4	1.60		251
HCA II	F93S, F95L, W97M	idem		1FR7	1.50		251
HCA II	idem	idem	apo	1FSN	2.00		251
HCA II	idem	idem	Co ^{II}	1FSQ	2.00		251
HCA II	idem	idem	Cu ^{II}	1FSR	2.00		251
Proton Shuttle							
HCA II	Y7H	altered rate of proton transfer by proton shuttle H64		1LZV	2.30		262
HCA II	Y7F	removed hydrophilicity of proton-shuttle residues	SO ₄ ²⁻	2NXR	1.70	8.2	266
HCA II	idem	idem	SO ₄ ²⁻	2NXS	1.80	10.0	266
HCA II	idem	idem		2NXT	1.15	9.0	266
HCA II	N62L	idem		2NWO	1.70	8.2	266
HCA II	idem	idem	SO ₄ ²⁻	2NWP	1.80	6.0	266
HCA II	N67L	idem		2NWY	1.65	8.2	266
HCA II	idem	idem	SO ₄ ²⁻	2NWZ	1.80	6.0	266
HCA II	H64A	loss of the catalytic proton shuttle		1G0F	1.60		260
HCA II	idem	chemical (4-MI) rescue of the catalytic proton shuttle	4-methyl imidazole	1G0E	1.60		260
HCA II	idem	idem	4-methyl imidazole	1MOO	1.05		261
HCA II	H64W	idem		2FNK	1.80		267
HCA II	W5A, H64W	idem		2FNM	1.80		267
HCA II	idem	idem	4-methyl imidazole	2FNN	1.80		267
HCA II	H64A, N62H	effect of proton shuttle location and pH on H ⁺ transfer	SO ₄ ²⁻	1TG3	1.80	6.0	183
HCA II	idem	idem		1TG9	1.90	7.8	183
HCA II	H64A, N67H	idem	SO ₄ ²⁻	1TH9	1.63	6.0	183
HCA II	idem	idem		1THK	1.80	7.8	183
HCA II	H64A, T200H	idem	Cl ⁻	1YO0	1.80	6.0	263
HCA II	idem	idem	SO ₄ ²⁻	1YO1	1.70	7.8	263
HCA II	idem	idem		1YO2	1.80	9.3	263
HCA III	K64H, R67N ^c	partial recovery of the proton-transfer rate of HCA II		2HFW	2.50		268
HCA III	K64H ^c	idem		2HFX	1.70		268
HCA III	R67H ^c	idem		2HFY	2.60		268
HCA II	A65F	residue size, not polarity, hinders proton transfer		1UGA	2.00		264
HCA II	A65G	idem	N ₃ ⁻	1UGB	2.00		264
HCA II	A65H	idem		1UGC	2.00		264
HCA II	A65S	idem		1UGD	2.00		264
HCA II	A65L	idem		1UGE	1.90		264
HCA II	A65T	idem	N ₃ ⁻	1UGF	2.00		264
HCA II	A65S	idem		1UGG	2.20		264
HCA I	H67R	enhanced esterase activity, second Zn ^{II} binding site	ethylene glycol	1J9W	2.60		265
HCA I	idem	idem	Zn ^{II} ; ethylene glycol; Cl ⁻	1JV0	2.00		265

^a If the crystal structure corresponds to a mutation that has been engineered into the isoform, this column describes the purpose of this mutation. ^b 5-Acetamido-1,3,4-thiadiazole-2-sulfonamide (**137**). ^c Two additional mutations opposite the active site, Cys183Ser (Cys182Ser) and Cys188Ser, were made to enhance crystallization and did not affect catalysis. ^d Compounds, PDB IDs, and resolutions: none, 1G3Z, 1.86; **55**, 1G45, 1.83; **56**, 1G46, 1.84; **57**, 1G48, 1.86; **58**, 1G4J, 1.84; and **51**, 1G4O, 1.96. ^e Compounds (4-(aminosulfonyl)-N-[(X-phenyl)methyl]benzamide), PDB IDs, and resolutions: X = 4-fluoro, 1I9L, 1.93; X = 2,4-difluoro, 1I9M, 1.84; X = 2,5-difluoro, 1I9N, 1.86; X = 2,3,4-trifluoro, 1I9O, 1.86; X = 2,4,6-trifluoro, 1I9P, 1.92; and X = 3,4,5-trifluoro, 1I9Q, 1.80.

HCA I and HCA II.^{280,281} These studies provide the foundation for a complete solution structure, as well as for understanding the kinetics and pathway of folding, of HCA I and HCA II.

Kanamori and Roberts used ¹⁵N NMR to demonstrate that arylsulfonamides bind as the anion (ArSO₂NH⁻) to the Zn^{II} ion of HCA I, primarily through the sulfonamide nitrogen.²⁷⁶

Binding in this form requires deprotonation of the sulfonamide group. The pK_a of this group (e.g., 10) is, therefore, an important factor in binding. In sections 9 and 10, we describe in detail the influence of this pK_a on the observed binding affinity.

Arylsulfonamide inhibitors typically form 1:1 ligand/protein complexes with CA.^{270–273} Kim et al. observed 2:1

binding of fluoroaromatic ligands (SBB) to the Phe131Val mutant of HCA II (but not to native HCA II, which only formed 1:1 complexes with these inhibitors); X-ray structures showed that one sulfonamide bound to the active site of HCA II and the other sulfonamide bound at the interface between two HCA II proteins in the crystal lattice.^{180,249} NMR experiments, however, showed that these sulfonamides bound in a 1:1 complex in solution.²⁴⁹ By X-ray crystallography, Jude et al. observed 2:1 complexes for the binding of the two-pronged (sulfonamide and Cu^{II} ion) inhibitors **218**, **219**, **234**, and **235** to HCA I and HCA II.¹⁸¹ One of these inhibitors coordinated to Zn^{II} and His64, while the other bound at the rim of the active site near the N-terminus of the enzyme. This secondary binding site differs from the site that Kim et al. observed.^{180,249} Jude et al. confirmed that the 2:1 stoichiometry persists in solution by isothermal titration calorimetry (ITC). Dugad et al. proposed 2:1 complexes for the binding of compounds **207–209** and 2,5-difluorobenzene-sulfonamide to HCA I and HCA II with a pentacoordinated Zn^{II} ion in the active site, on the basis of ¹⁹F NMR experiments.^{274,275} Krishnamurthy et al. observed only 1:1 complexes for the binding of **209** to BCA II and HCA I by ¹⁹F NMR and confirmed this 1:1 stoichiometry for the binding of ligands **207–212** to BCA II by ITC and for the binding of **209** to HCA II by X-ray crystallography.¹⁸² In addition to structural information, NMR also characterizes the internal motion of bound inhibitors^{270–274} and of the enzyme active site itself.²⁷² Except for pentafluorobenzene-sulfonamide (**212**), which contains magnetically distinct environments for each fluorine atom when bound to HCA II,²⁷¹ the aromatic ring of benzenesulfonamides rotates rapidly on the NMR time scale about its C(1)–C(4) axis.^{270,273,274} BCA II forms a 1:1 complex with *p*-methylbenzenesulfonamide (**6**, Table 10) at pH 6.0.²⁷² While ¹³C–¹H NOE experiments suggested that the internal mobility of the α -carbons in the enzyme is restricted upon binding of the inhibitor, ¹⁵N[¹H] NOE experiments qualitatively indicated the existence of some internal mobility of the bound inhibitor.

Metal substitution facilitates the study of inhibitor binding. Metals that have a spin-1/2 nucleus (⁶⁷Zn, the only naturally occurring isotope of Zn with nonzero spin, has a spin of 5/2) provide a mechanism for efficient dipolar relaxation of ¹⁵N bound to the metal atom in the active site. ¹¹¹Cd and ¹⁵N NMR have shown that both arylsulfonamides and *N*-hydroxyarylsulfonamides bind to HCA I, BCA, and ¹¹¹Cd-BCA via an anionic nitrogen.^{276,277} ¹⁵N NMR alone cannot detect the binding of the *N*-hydroxyarylsulfonamide, since these species have no NMR-active atoms on the bound nitrogen to yield a nitrogen signal. Metal variants such as ¹¹¹Cd are, therefore, required for this study and other studies of this type. Metallovariants are discussed further in section 5.

These studies suggest that one must consider factors other than the static structure of an enzyme in the design of inhibitors. Upon binding of a ligand, the steric constraints in the active site may change, and the resulting structure is difficult to predict. In addition, the internal motion of ligands and of amino acid residues in the active site may influence the manner in which ligands bind. For example, ligands may form contacts with the protein that change as the ligands rotate within the active site and as the active site relaxes around the ligands. Thus, while X-ray structures are enormously useful, they alone do not completely detail the factors that should be included in the design of ligands for a given protein.

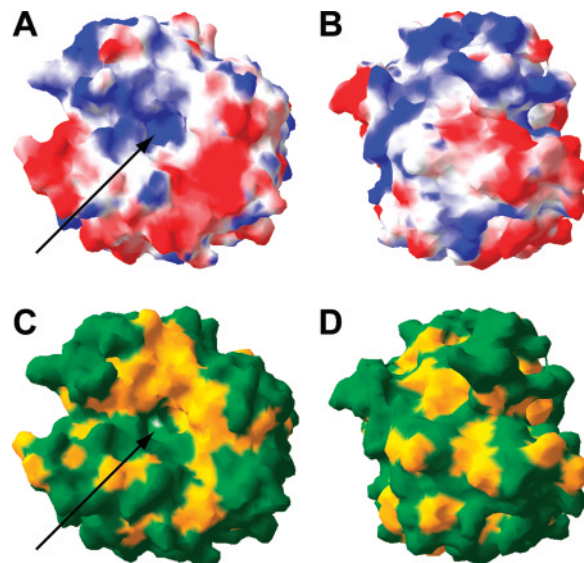


Figure 5. Surface rendering of opposite faces of HCA II (PDB/2CBA¹⁸⁴) showing (A and B) acidic residues in red and basic residues in blue and (C and D) hydrophobic residues in yellow and polar residues in green. At pH 7–8, the red regions have a negative charge; the blue regions have a positive charge. The arrows indicate the active site.

4.5. Global Structural Features

CA is a globular protein with a high degree of tertiary and secondary structural homology between isoforms. HCA II is roughly ellipsoidal in shape and has well-defined secondary structural elements. The enzyme has diameters of 40 and 42 Å along the minor axes and 56 Å along the major axis. (We estimated these values by measuring the distance between nuclei of farthest lying atoms along each axis using Deep View/Swiss-PdbViewer 3.7.)²⁸² These dimensions agree with those that Pocker and Sarkanen⁴⁰ and Eriksson et al.²⁴⁰ measured for HCA II: 40 × 42 × 55 Å and 39 × 42 × 55 Å, respectively. The structure of α -CAs is dominated by a central, ten-stranded, twisted β -sheet, β A to β J (running from front-left to back-right in Figure 4; see also Figure 2) and also contains seven α -helices surrounding the sheet.^{40,240} Another interesting structural feature of CA is the C-terminal knot (Figure 2)—that is, the knot that would form near the C-terminus if one were to grab both ends of the native structure and pull. Knots of this sort are rare (see section 15).

The global structure of HCA II changes minimally over a wide range of values of pH (5.7–8.4), upon binding of ligands and upon the removal of the Zn^{II} ion. The root-mean-square (rms) deviation of C α atoms in the superposition of structures with and without bound inhibitors for HCA II is 0.2 Å; few side chains have shifts > 1 Å.^{283,284} Most importantly, His64 undergoes a relatively large shift in position when the pH is reduced below 7 by rotating 64° about the χ_1 torsion angle.¹⁸³ Nair and Christianson measured an rms difference of 0.2 Å between their structure at pH 5.7 and that reported by Eriksson et al. for pH 8.5.^{240,285} Håkansson et al. observed that the structure of native HCA II at pH 6.0 is almost indistinguishable from that at pH 7.8; the rms deviation of C α atoms between the two structures is 0.044 Å.¹⁸⁴ Moreover, they measured an rms deviation of 0.098 Å for the C α atoms of the native and apo forms of the enzyme at pH 7.8.

Figure 5 shows maps of acidic and basic residues (parts A and B) as well as hydrophobic and polar residues (parts

C and D) of HCA II. While the surface of the enzyme opposite the active site (parts B and D of Figure 5) shows a majority of polar residues (Figure 5D), these residues are not arranged in any obvious pattern in terms of local acidity. In striking contrast, the “front” side of HCA II (i.e., the same side as the active site, which is marked by arrows in parts A and C of Figure 5) shows a large basic patch (blue) that surrounds the active site. On the other side of this patch, there is a large hydrophobic pocket (yellow, Figure 5C), which has been posited to be the binding site for carbon dioxide,⁴⁷ and below which lies a large acidic patch. These large polar patches may facilitate entry and exit of bicarbonate to and from the active site, where the substrate binds in the hydrophobic pocket.

The robust structure of CA makes the protein easy to manipulate. Invariance of the structure of CA (at least HCA II) as a function of pH suggests that changes in the binding properties of ligands at various values of pH are due to chemical effects in the active site (e.g., protonation of the enzyme or ligand) rather than to global structural effects. The structural homology between α -CA isozymes implies that findings for one isozyme are likely to be relevant for other isozymes and other species.

4.6. Structure of the Binding Cavity

The binding cavity of CA is a complex space surrounding the catalytic Zn^{II} ion and has been the focus of much research for the past three decades. The binding cavity includes three functional regions: (i) the primary coordination sphere around Zn^{II}, comprising histidine residues and a hydroxide ion or water (see section 4.7); (ii) the primary and secondary hydrophobic faces that bind ligands and substrates; and (iii) a hydrophilic face that is believed to regenerate the catalytic activity of the protein through a proton shuttle. Understanding the structure of this part of the protein is essential for effective biophysical and physical-organic studies of ligand binding.

All isoforms of CA have a conical cavity at the active site; this cavity is roughly 15 Å in diameter at its mouth and 15 Å deep.^{40,240} This conical cavity is visible at the centers of parts A and C of Figure 5. The catalytic Zn^{II} ion, Zn262, lies at the apex of the cone near the center of the protein and is coordinated in a distorted tetrahedral arrangement to a hydroxide ion or water molecule (water263) and three histidine residues, His94, His96, and His119, which are located on the central β -sheet—His94 and His96 on β D and His119 on β E.^{240,286,287}

There are small but noticeable changes in the geometry of the active site as a function of pH. The presence and location of various water molecules in and around the active site changes as the pH increases from 6.0 to 7.8.^{184,288} The geometry of the part of the active site comprising water263, Zn262, His94, His96, and His119, however, remains similar with bond distances and angles varying at most by 0.04 Å and 2.7°, respectively.¹⁸⁴ Perhaps the most important influence of pH on the structure of CA is that of water263, which is bound at the active site to Zn^{II}. The pK_a of this group, and its influence on the binding of ligands, are discussed further in sections 4.7 and 10, respectively.

The binding cavity of CA has hydrophobic and hydrophilic faces (Figure 5C). The residues of the *hydrophobic* face that make up primary and secondary binding sites are located above and to the right of the active site in Figure 5C. The primary site, known as the hydrophobic pocket, consists of

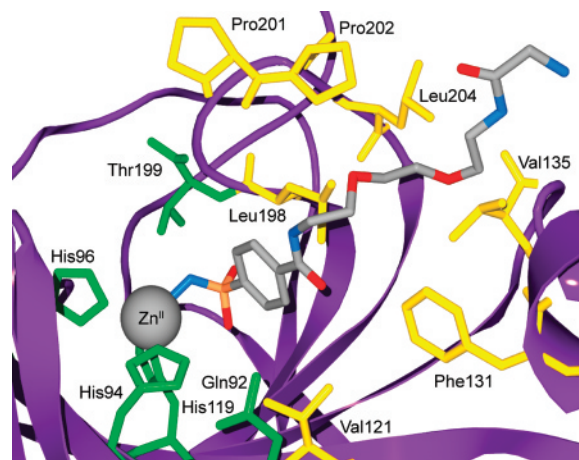


Figure 6. Model for the binding of compound **84** to HCA II based on the deposited X-ray crystallographic coordinates (PDB/1CNW).¹⁸⁵ Catalytically important residues and residues that contribute to the primary and secondary hydrophobic binding sites for this ligand are shown.

Val121, Val143, Leu198, and Trp209²⁸⁹ and is believed to bind CO₂ adjacent to the Zn^{II}-bound hydroxide.^{47,289,290} Silverman and Lindsog suggest that Val207 also contributes to this pocket.¹⁴

The secondary hydrophobic binding site is located farther from the active site than the primary hydrophobic pocket. Many inhibitors of CA bind to this region of the hydrophobic face in addition to the active site Zn^{II} itself. For example, Figure 6 shows an arylsulfonamide inhibitor with a triethylene glycol tail (Table 10, compound **84**) that contacts residues in the hydrophobic pocket.¹⁸⁵ Interactions with the secondary hydrophobic binding site require the use of long-chain linkers between a hydrophobic tail and a Zn^{II}-binding head group.

The *hydrophilic* face of the binding cavity was characterized first by Eriksson et al. (Figure 7).²⁴⁰ Of the eight residues on this face, Thr199 and Thr200 are nearest to the entrance to the cavity, while His64 is located on the opposite side of this entrance. The other five active site residues, Tyr7, Asn62, Asn67, Gln92, and Glu106, are involved in an intricate network of hydrogen bonds with nine ordered water molecules in the active site.^{240,287} Residues Tyr7, Asn62, and Asn67 refine the efficiency of proton transfer between the Zn^{II}-bound water and His64.²⁶⁶ Residues Glu117, His107, Asn244, and Arg246, which lie buried in the vicinity of the active site, are involved indirectly in the network. These residues orient the side chains that line the active site cavity and support their stable conformation.²⁴⁰

Figure 7 shows a network of hydrogen bonds among amino acid side chains and water molecules within the active site of HCA II. This network contributes to the catalytic activity of the enzyme, as well as to the affinity of the enzyme for Zn^{II}. Hydrogen bonds from the direct (those residues that coordinate Zn^{II}) to the indirect ligands, which orient the imidazole rings of the His residues coordinated to Zn, include the following: (i) N δ 1 of His94 to O ϵ 1 of Gln92; (ii) N δ 1 of His96 to O of Asn244; and (iii) N δ 2 of His119 to O ϵ 2 of Glu117, which also accepts a hydrogen bond from N δ 1 of His107 that orients Glu117. The O ϵ 1 atom of Glu106 accepts a hydrogen bond from the proton on the O γ 1 atom of Thr199. This bond aligns the O γ 1 atom on Thr199 to accept a hydrogen bond from the Zn-bound hydroxide ion and to orient the lone pair of the hydroxide ion for

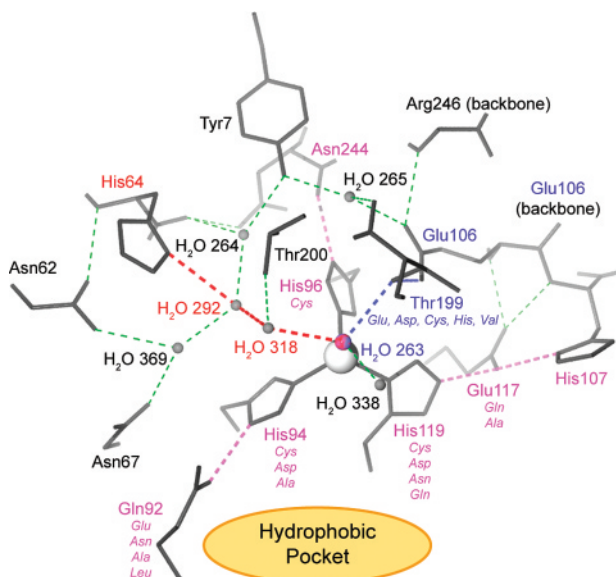


Figure 7. Hydrogen bonding in the active site of HCA II. All hydrogen bonds are shown in dashed lines. In pink are the hydrogen bonds and residues involved in orienting the imidazole rings of His94, His96, and His119. In blue are the residues involved in orienting the lone pairs on the zinc-bound hydroxyl ion for optimal nucleophilic attack. In red are the water molecules and His64 that make up the proton shuttle that regenerates the zinc-bound hydroxyl ion via deprotonation of the zinc-bound water molecule. The thin green dashed lines represent other, less crucial hydrogen bonds within the active site and further buried residues adjacent to the active site. The view is down an axis made up of the catalytic Zn^{II} cofactor (gray) and the zinc-bound hydroxyl ion (H₂O 263). The hydrophobic pocket (see Figure 6) lies in the area indicated by the orange ellipse and extends to the space above His119, His96, and Thr200. In italics are mutations of direct (Thr199, His119, His96, His94) and indirect (Glu117, Gln92) ligands to Zn^{II}, carried out by Fierke and Christianson (section 6). Modified with permission from ref 706. Copyright 2004 American Chemical Society.

nucleophilic attack on CO₂.^{184,240} When an inhibitor binds in the active site of CA, the Oγ1 atom on Thr199 can accept a hydrogen bond from the inhibitor. If, however, the inhibitor cannot donate a hydrogen bond to Thr199 (as is the case for SCN⁻), then Thr199 can repel the ligand and cause it to bind the Zn^{II} in a distorted pentagonal geometry.¹⁸⁶ A very high-field ligand, such as CN⁻, can also cause distortion to a pentagonal geometry.²⁹¹

When CO₂ binds to CA, computational,⁴⁷ ¹³C NMR^{292,293} and X-ray^{188,198,294} studies suggest that the CO₂ binds in the hydrophobic pocket and displaces the “deep water” (water338) that forms a hydrogen bond to the amide NH backbone of Thr199. Håkansson et al.¹⁸⁴ proposed that CO₂ binds to HCA II in the same location and orientation as cyanate.²⁹⁴ X-ray structures with HCA II showed that both cyanate (NCO⁻), which is isostructural and isoelectronic with CO₂, and cyanide (CN⁻) accept a hydrogen bond from the amide NH backbone of Thr199 but do not displace the zinc-bound water.²⁹⁴ Interestingly, cyanamide (264), which is also isostructural and isoelectronic with CO₂, binds to HCA II in a completely different manner: 264 coordinates to Zn^{II}, points away from the hydrophobic pocket, and forms hydrogen bonds with the Oγ1 atoms of Thr199 and Thr200.²²¹

Perhaps the most important catalytic feature involving the water molecules in the active site is the His64 residue, which acts as a “proton shuttle” that aids in the transfer of a proton from the Zn^{II}-bound water263 to buffer molecules in the final

step of the catalytic mechanism of CO₂ hydration (see section 2 and Figure 7: bold, red, hydrogen-bonded network).⁵³ A change in pH causes an important structural change in the conformation of His64 in HCA II that suggests the role of this residue in the mechanism of proton shuttling.^{55,183,240,285} For example, at pH 5.7, His64 appears to occupy an alternate conformation, in which the imidazole side chain is directed away from the active site by a 64° rotation about the χ₁ torsion angle.

While the hydrophilic face is essential for catalysis, the hydrophobic face remains the part of the active site to which most drugs are targeted. Understanding the structure of the hydrophobic face is, therefore, important in designing inhibitors with optimal affinities. Knowledge of the structure of the hydrophilic face is necessary for understanding the catalytic activity of CA.

4.7. Zn^{II}-Bound Water

The catalytic Zn^{II} cofactor in the active site of CA is coordinated in a tetrahedral geometry by three histidine residues and water263 (see Figures 2, 6, and 7). As a universal feature of all known Zn^{II}-metalloenzymes, the Zn^{II} ion activates this water molecule for catalysis; in the case of CA,²⁹⁵ this activation is believed to be carried out via deprotonation of the Zn-bound water (Zn^{II}-OH₂⁺) to yield a Zn^{II}-hydroxide (Zn^{II}-OH). The pK_a of the Zn^{II}-OH₂⁺ (pK_a(CA-Zn^{II}-OH₂⁺)) is believed to be 6.8 for HCA II,²⁶⁹ and defining this value has been the subject of substantial research, because it is important in understanding both the catalytic hydration of CO₂ and the binding of inhibitors. This section discusses both processes and focuses on the importance of the pK_a(CA-Zn^{II}-OH₂⁺) in the study of CA–ligand interactions.

The currently accepted mechanism for catalysis by CA of the hydration of CO₂ involves several steps:¹⁴ (i) attack on CO₂ by the Zn^{II}-bound hydroxide (deprotonated water263) to form bicarbonate; (ii) binding of a water molecule to the Zn^{II} at a position adjacent to the bicarbonate ion; (iii) leaving of bicarbonate; and (iv) transfer of a proton from the newly bound water (now water263, or Zn^{II}-OH₂⁺) to the buffer (Figure 1). The last step, in which water263 loses H⁺, is believed to be the rate-limiting step in this process.⁴⁸ The pH-dependence of the catalytic activity of CA, both as a hydratase and an esterase, strongly suggests the influence of a single ionizable group with pK_a 6.8 (for HCA II), and this group is widely believed to be water263.^{14,48,269,296,297} Lipton et al., however, used solid-state ⁶⁷Zn-NMR to infer that the species coordinated in the fourth position of Zn^{II} is hydroxide from pH 5 to 8.5.²⁹⁸ This proposal suggests a pK_a for the zinc-bound water that is <5. It is the only study that disagrees with a value of 6.8 for pK_a(CA-Zn^{II}-OH₂⁺). Fisher et al. observed Zn^{II}-bound water in a high-resolution (1.05 Å) X-ray structure of HCA II crystallized at pH 7.8; assuming a pK_a of 6.8, at this pH, water263 should be deprotonated to hydroxide.⁵⁴ The authors noted, however, that the ionization state of titratable groups in a crystal and in solution may be different.

Values for pK_a(CA-Zn^{II}-OH₂⁺) vary slightly among the different isozymes: Kiefer et al. estimated a value of 6.8 for HCA II by monitoring esterase activity as a function of pH;²⁶⁹ Coleman found a value of 8.1 for HCA I (also for Co^{II}-HCA I); and Kernohan inferred a value of 6.9 for BCA II using a similar procedure.^{296,297,299} Values ranging from 6.4 to 7.1 have been reported for Co^{II}-BCA II,^{300–302} with 6.8 prevailing as the accepted value.²⁹¹

The protein environment surrounding the Zn^{II} cofactor can have a significant influence on the value of $\text{p}K_{\text{a}}(\text{CA}-\text{Zn}^{\text{II}}-\text{OH}_2^+)$. For HCA II, mutations of Thr199,³⁰³ and of the residues involved directly³⁰⁴ and indirectly²⁶⁹ in coordinating Zn^{II} , modulate the value of $\text{p}K_{\text{a}}(\text{CA}-\text{Zn}^{\text{II}}-\text{OH}_2^+)$. Computer simulations of HCA II suggest that Glu106, Glu117, and Arg246 make the greatest contributions to the value of $\text{p}K_{\text{a}}(\text{CA}-\text{Zn}^{\text{II}}-\text{OH}_2^+)$.³⁰⁵ The linear relationship observed between $\text{p}K_{\text{a}}(\text{CA}-\text{Zn}^{\text{II}}-\text{OH}_2^+)$ and $\log(k_{\text{cat}}/K_{\text{m}})$ for CO_2 hydration among a series of mutants of HCA II implies that stabilization of the negative charge on the oxygen atom in $\text{Zn}^{\text{II}}-\text{OH}$ is a critical factor in catalysis.²⁶⁹ The effective charge on the Zn^{II} , which is influenced by all ligands in its coordination sphere, is believed to be an important factor in this stabilization.²⁸⁹

In parallel with studying the effects of the $\text{p}K_{\text{a}}(\text{CA}-\text{Zn}^{\text{II}}-\text{OH}_2^+)$ on the catalytic properties of CA, several groups explored the influence of the $\text{p}K_{\text{a}}(\text{CA}-\text{Zn}^{\text{II}}-\text{OH}_2^+)$ on the binding of ligands to CA.^{291,297,299,301,302,306} Several of these studies^{297,299,301} used enzymatic activity as a measure of binding. Since enzymatic activity falls off at and below $\text{pH} \sim 7$, presumably because of the protonation of $\text{Zn}^{\text{II}}-\text{OH}$ with formation of $\text{Zn}^{\text{II}}-\text{OH}_2^+$, these studies cannot unambiguously determine the effects of the $\text{p}K_{\text{a}}(\text{CA}-\text{Zn}^{\text{II}}-\text{OH}_2^+)$ on binding. Therefore, it is important that these effects were studied by nonenzymatic assays.

In an early study on the mechanism of arylsulfonamide inhibitors, Lindskog used stopped-flow fluorescence to monitor the kinetics and thermodynamics of the binding of several arylsulfonamides to $\text{Co}^{\text{II}}-\text{BCA II}$.³⁰⁷ The investigators used the Co^{II} variant because the UV-visible spectrum of the cobalt changes significantly on binding the sulfonamide, providing a spectroscopic handle. Their results suggest that ligand binding depends on two ionizable groups—one on the inhibitor, and one on the protein. The $\text{p}K_{\text{a}}$ values of the inhibitors were easy to confirm. The remaining $\text{p}K_{\text{a}}$ value was consistent at 6.6 across a series of inhibitors. This value, within the error of their experiments, correlates remarkably well to the accepted $\text{p}K_{\text{a}}(\text{CA}-\text{Zn}^{\text{II}}-\text{OH}_2^+)$ of 6.8 for $\text{Co}^{\text{II}}-\text{BCA II}$. Taylor et al. observed the same dependence of kinetics of association and affinity of sulfonamides on pH in HCA II with Zn^{II} .³⁰² The important conclusion is that both ligand binding and catalysis depend on the same ionizable group on the protein, which is very likely to be that of the Zn^{II} -bound water²⁶³.

Deerfield II et al. used density functional theory to evaluate the Zn-binding site in CA.³⁰⁸ Using the tetrahedral complex $\text{Zn}(\text{imidazole})_3(\text{H}_2\text{O})$ as their basic model, the investigators calculated a value for the $\text{p}K_{\text{a}}$ of the ligated water of ~ 7 ; this value is lower than the $\text{p}K_{\text{a}}$ of the zinc-coordinated imidazoles, and so, preferential deprotonation of the H_2O ligand should result.

5. Metalloenzyme Variants

Metallo variants of proteins present an interesting subject of study in order to rationalize why one metal is preferable for a catalytic function over another, what structural features of a protein determine metal specificity, and what structural changes occur upon substitution of a metal in enzymes. Different metal substituents are also useful as magnetic spin labels and scattering centers. CA is particularly well-suited for studies of metallo variants of the enzyme and their properties. The Zn^{II} ion can be easily extracted from the active site without denaturation of the protein and can be

readily replaced by a number of other divalent ions. There is minimal conformational change upon either removing the Zn^{II} ion or adding the non-zinc metal ions.

Hunt et al. developed a method for preparing *apo*-CA (BCA and HCA I) using flow dialysis against dipicolinic acid (pyridine-2,6-dicarboxylic acid).³⁰⁹ Flow dialysis removes $>97\%$ of the Zn^{II} from CA in <2 h, compared to the removal of 95% in 7–10 d using the original method developed by Lindskog and Malmström (using BCA II).^{309,310} Hunt et al. measured the presence of residual Zn^{II} by measuring the esterase activity of the enzyme—one commonly uses *p*-nitrophenyl acetate as the substrate—and by atomic absorption spectroscopy.³⁰⁹ A modified method using ultrafiltration is still used today.²⁵⁰ Alternatively, one can simply dialyze away the Zn^{II} by soaking CA in dipicolinic acid for 10–12 days.^{184,251} Metal derivatives are prepared by incubating the apoenzyme with a buffered solution of the chloride or sulfate salt of the desired metal for 24–48 h.^{187,188,311} The formation of cobalt complexes can be quantified by measuring esterase activity; the formation of other metal complexes (e.g., Cu^{II}) may be quantified by performing a colorimetric 4-(2-pyridylazo)resorcinol assay.^{188,311–313}

Table 6 lists the metallo variants of HCA II reported to date.^{184,187,188,223,245,246,250–252,259,311,314–318} Metals that bind to CA consist primarily of transition metals in the +2 oxidation state: Zn^{II} (w.t.), Cd^{II} , Co^{II} , Cu^{II} , Fe^{II} , Hg^{II} , Mn^{II} , and Ni^{II} . In^{III} from InCl_3 also binds to the active site of *apo*-BCA II.^{315,316} HCA II has been crystallized incorporating Co^{II} , Cu^{II} , Hg^{II} , Mn^{II} , and Ni^{II} ions.^{159,187,188,251,311,319}

Of these variant metalloenzymes, only the native Zn^{II} shows high enzymatic activity. The Co^{II} variant displays $\sim 50\%$ of the activity of the native protein. Lindskog and Nyman³¹⁴ formed various metal complexes with HCA I, HCA II, and BCA II and measured their activity. Proteins with Fe^{II} , Mn^{II} , and Ni^{II} show only 4%, 8%, and 2% activity, respectively, at 10–100 μM concentrations of the metal ions. Similar concentrations of Cd^{II} , Cu^{II} , and Hg^{II} show no activity beyond the residual Zn-activity (1–3% due to incomplete removal of Zn^{II}). Inhibition of the residual Zn-activity occurs at high concentrations (>10 – 100 μM) of Co^{II} , Fe^{II} , Mn^{II} , Ni^{II} , Cd^{II} , Cu^{II} , and Hg^{II} . No levels of Mg^{II} , Ca^{II} , or Ba^{II} —concentrations ranging from 10 μM to 2 mM—affect activity or inhibition; all three complexes are inactive.³¹⁴

The catalytically active metal ions, Zn^{II} and Co^{II} , coordinate to histidine residues in the active site of HCA II with distorted tetrahedral geometries, regardless of pH .¹⁸⁷ The Co^{II} variant of HCA II, however, when complexed with bicarbonate ion, showed nearly octahedral coordination, with the cobalt ion coordinated to the three histidine ligands, bicarbonate O-2 and O-3 oxygen atoms, and a water molecule.^{188,320} This propensity of Co^{II} to form expanded coordination complexes may explain the reduced CO_2 hydration activity of the Co^{II} -containing enzyme via reduction of the rate of product release.³²⁰ Other metals result in increased coordination number: Cu^{II} binds to HCA II in trigonal-bipyramidal and square-pyramidal geometries, while both Ni^{II} and Mn^{II} coordinate octahedrally.¹⁸⁷ These nontetrahedrally coordinated metals also perturb the solvent structure in the active site: water 318, which is usually hydrogen bonded to the Zn-bound water, is absent. From their thorough analysis of crystal structures of metal-substituted HCA II, Håkansson et al. concluded that the choice of Zn^{II} for catalysis by nature is due to the tetrahedral

Table 6. X-ray Crystal Structures of Metallo Mutants of HCA II^a

Metal	Residue mutation	Purpose of study	Coordination	Binding affinity ^b (K _d , nM)	pH ^c	PDB ID	Res. (Å)	Ref
Zn ^{II}		natural enzyme	4, tetrahedral	4 × 10 ⁻³	7.0	2CBA	1.54	184, 246
Apo		structural analysis	n/a	n/a	n/a	2CBE	1.82	184
Zn ^{II}		metal binding to native enzyme	4, tetrahedral	8 × 10 ⁻⁴	7.0	2CBA	1.54	184, 321
Cd ^{II}		idem		2.3	7.0			317
Co ^{II}		idem	4, tetrahedral	20	7.0	1RZA,1RZB	1.90, 1.80	187, 311
Cu ^{II}		idem	5, trigonal bipyramidal	1.7 × 10 ⁻⁵	7.0	1RZC	1.90	187, 311
Mn ^{II}		idem	6, octahedral			1RZD	1.90	187
Ni ^{II}		idem	6, octahedral	16	7.0	1RZE	1.90	187, 317
Hg ^{II}		idem	4, octahedral			1CRM	2.00	223
Co ^{II}		bicarbonate binding	6, octahedral			1CAH	1.88	188
Apo	H94C	engineering Zn affinity, functionality and discrimination	n/a	n/a	n/a	1HVA	2.30	250
Apo	H94C	metal-binding site plasticity	n/a	n/a	n/a	1CNB	2.35	245
Apo	H94A	idem	n/a	n/a	n/a	1CVF	2.25	245
Apo	E117Q	indirect ligand increases Zn complexation kinetics	n/a	n/a	n/a	1ZSA	2.50	252
Zn ^{II}	H94N	electrostatic effects on Zn binding affinity, coordination	5, trigonal bipyramidal	40	7.0	1H4N	2.00	259
Zn ^{II}	H119N	idem	5, trigonal bipyramidal	11	7.0	1H9N	1.85	259
Zn ^{II}	H119Q	idem	4, tetrahedral	69	7.0	1H9Q	2.20	259
Zn ^{II}	F95M, W97V	structural influence of hydrophobic core on metal binding	4, tetrahedral	1.6 × 10 ⁻³	7.0	1FQL	2.00	251, 321
Zn ^{II}	F93I, F95M, W97V	idem	4, tetrahedral	1.1 × 10 ⁻²	7.0	1FQM	2.00	251, 321
Apo	idem	idem	n/a	n/a	n/a	1FQN	2.00	251, 311
Co ^{II}	idem	idem	4, tetrahedral	66	7.0	1FQR	2.00	251, 311
Cu ^{II}	idem	idem	5, square pyramidal	3 × 10 ⁻⁶	7.0	1FR4	1.60	251, 311
Zn ^{II}	F93S, F95L, W97M	idem	4, tetrahedral	2.9 × 10 ⁻²	7.0	1FR7	1.50	251, 321
Apo	idem	idem	n/a	n/a	n/a	1FSN	2.00	251, 311
Co ^{II}	idem	idem	5, trigonal bipyramidal	145	7.0	1FSQ	2.00	251, 311
Cu ^{II}	idem	idem	5, trigonal bipyramidal	2 × 10 ⁻⁶	7.0	1FSR	2.00	251, 311
Cd ^{II}		binding to HCA I		6.3 × 10 ⁻¹	5.5			314
Co ^{II}		idem		6.3 × 10 ¹	5.5			314
Cu ^{II}		idem		2.5 × 10 ⁻³	5.5			314
Mn ^{II}		idem		1.6 × 10 ⁵	5.5			314
Mn ^{II}		idem		1.6 × 10 ³	8.5			318
Ni ^{II}		idem		3.2 × 10 ⁻¹	5.5			314
Zn ^{II}		idem		3.2 × 10 ⁻²	5.5			314
In ^{III}		γ- and K X-ray nuclear studies	not reported	—	5.7–7.7			315, 316

^a Unless otherwise stated. ^b Binding affinity for the metal to the *apo*-protein. ^c The pH at which the binding affinity was measured.

coordination chemistry of zinc, its natural abundance, and its weak interaction with other anions that may inhibit the enzyme *in vivo*.¹⁸⁷

Fierke and co-workers conducted a series of studies in which they measured the affinities of different metals to HCA II and its active site mutants to determine the basis of selectivity for zinc in this protein.^{251,311,321,322} The investigators looked at the influence of hydrophobic core residues Phe93, Phe95, and Trp97 on binding of metals and found that substitution of those residues with smaller side chains reduced the affinity of the protein to Zn^{II} and Co^{II} but increased the affinity to Cu^{II}.^{311,321} X-ray analysis of the mutants revealed new cavities formed in the core of the protein and shifts in the positions of metal-coordinating His94 and second-shell ligand Gln92.²⁵¹ The investigators concluded that the aromatic residues, although they do not directly coordinate the metal, preorient the metal-binding side chains in such a fashion as to favor tetrahedral zinc-binding geometry and to destabilize alternative geometries.

McCall and Fierke continued the study of factors that influence binding of metals by mutating the side chains of HCA II that directly coordinate the metal.³²² The investigators varied the polarizability of the coordinating atom, the relative size of the binding site and the metal ion, and the geometry of the binding site to determine which of these three was most important in determining the selectivity of HCA II for Zn^{II} over other metals. The investigators found that the selectivity for metals correlated with the geometry of the ligands in the active site and with the preferred coordination number of the metal (the investigators were able to vary the number of chelating residues by mutating Thr199 to Cys, Glu, or His, all of which can coordinate the metal). The polarizability of the coordinating atom (S vs O) or the size of the active site and the metal ion did not affect the selectivity as strongly as the coordination number and geometry. These series of studies emphasize the importance of number of direct ligands to the metal and of the core residues that support and orient the direct ligands in the

design of a metal-binding site with high selectivity and specificity.

The high affinity of binding of transition metals to *apo*-carbonic anhydrase and to its mutants³²³ can be utilized to construct sensors for low concentrations (\sim pM) of those metals.^{323–327} Fluorescent aryl sulfonamide inhibitors of CA, such as dansyl amide and others, can serve as probes for the zinc ion.³²³ Fluorophores that are covalently attached to a side chain of HCA II can serve as reporters for other metals, since their fluorescent properties (intensity, emission maximum, polarization, and lifetime) are sensitive to the presence of metal in the binding site.^{324,325,327} Since Mg^{II} and Ca^{II} are prevalent divalent cations in biological systems but do not bind to HCA II and interfere with the assay, these HCA II-based sensors are particularly useful for biological applications.^{328–330}

The ability to tune the affinity of various metals for HCA II allows one to perform a wider variety of experiments to probe the binding of inhibitors to HCA II than if the enzyme were restricted to complexing only Zn^{II} . The agreement of multiple assays, calculations, and fluorescence spectroscopic studies suggests that the binding of metals to CA is well-characterized, even if it is not yet completely understood.

6. Structure–Function Relationships in the Catalytic Active Site of CA

The structure of the binding pocket of CA is highly conserved among isozymes of CA. This high degree of structural homology suggests that evolution has given each residue in the binding pocket a specialized and optimized function in the catalytic processes. Since CA is a well-characterized enzyme, and CO_2 is among the simplest possible substrates, CA represents an ideal model system for examining the roles of active-site residues in the network of catalytic steps (see Figure 1). An extensive program of site-directed mutagenesis, evaluation of catalytic properties, and X-ray crystallography by Fierke and Christianson has assigned specific functions to the active-site residues in CA; this body of work has been reviewed previously.²⁸⁹ Here, we briefly summarize this work and suggest its relevance to the construction of artificial catalytic sites.

6.1. Effects of Ligands Directly Bound to Zn^{II}

Modifications of residues directly coordinated to the Zn^{II} ion (Figure 7) provide clues to the importance of cooperativity, geometrical constraints, and stereochemistry in the binding of the metal ion and its catalytic efficiency. Table 7 indicates that substitution of any of the directly zinc-bound His residues by Ala results in substantially increased dissociation constants for the Zn^{II} ion. Mutation of each His residue to Cys in the binding pocket of HCA II, and determination of the crystal structure of the mutants, revealed that His94Cys and His119Cys can coordinate to the metal ion while His96Cys does not.^{245,304} The β -sheet secondary structure around Cys96 is not sufficiently plastic to allow the thiolate to coordinate to Zn^{II} . In general, introduction of an acidic residue (Asp, Cys, or Glu) in place of one of the neutral His residues improves affinity to Zn^{II} by an order of magnitude relative to the introduction of an Ala (neutral) residue, but the catalytic activity (k_{cat}/K_m) of the mutants with acidic residues is still 3 orders of magnitude lower than that of the wild type. The decrease in catalytic activity may be due to electrostatics: an additional negative charge in the

Table 7. Properties of HCA II Mutants with Altered Zn^{II} Binding Site

Ligand type	Substitution ^a	pK_a^b	$k_{cat}/K_m \times 10^{-5}^c$ ($M^{-1} s^{-1}$)	K_d for Zn^{II} (nM)	Ref
direct	wild type	6.8	1100	0.004	
	His94Ala	n/a ^d	0.12	270	245, 304
	His94Asp	≥ 9.6	1.1	15	246, 304
	His94Cys	≥ 9.5	1.1	33	245, 250, 304
	His94Glu	n/a	≤ 0.1	14	304
	His96Ala	8.4	≤ 0.1	100	304
	His96Cys	8.5	0.73	60	245, 304
	His119Ala	n/a	1.2	≤ 1000	304
	His119Cys	n/a	1.1	50	245, 304
	His119Asp	8.6	38	25	245, 304
additional ligand:					
	Thr199Cys	n/a	1.1	0.0011	244, 332
	Thr199Asp	n/a	0.4	0.004	243
	Thr199Glu	n/a	0.4	0.0002	243
	Thr199His	n/a	0.2	0.08	243
indirect:					
	Gln92Ala	6.8	290	0.018	248, 269
	Gln92Leu	6.4	300	0.03	248, 269
	Gln92Asn	6.9	270	0.005	248, 269
	Gln92Glu	7.7	120	0.005	248, 269
	Glu117Ala	6.9	190	0.04	248, 269
	Glu117Asp	6.7	270	0.012	269
	Glu117Gln	≥ 9.9	0.02	4.4	252
	Gln92Ala/ Glu117Ala	6.8	280	0.160	269
	Thr199Ala	8.3	11	0.06	269, 156

^a See Figure 7 for explanation of nomenclature. ^b Refers to $pK_a(CA-Zn^{II}-OH_2^+)$ (see sections 4.7 and 10). ^c Values for hydration of CO_2 at pH 8.9. ^d Data not available or not applicable.

binding pocket should increase the pK_a of the Zn^{II} -bound water molecule and destabilize both $Zn^{II}-OH$ and the transition state for the hydration of CO_2 . Although the values of k_{cat}/K_m for hydration of CO_2 of these variants of HCA II are lower than k_{cat}/K_m of the wild type, they still exceed those of small molecule Zn-complexes.³³¹ These data indicate that the histidine ligands, although not essential for catalysis, are optimal for maximizing the electrostatic stabilization of both the ground-state zinc-hydroxide and the negatively charged transition state.

Because Thr199 is close to the Zn^{II} ion (in the wild-type enzyme, Thr199 accepts a hydrogen bond from the zinc-bound hydroxide group), and because the surrounding polypeptide chain is flexible, Thr199 can be replaced with another amino acid capable of coordinating to the metal. Fierke and Christianson^{243,244,332} generated four such mutants: Thr199Cys, Thr199Asp, Thr199Glu, and Thr199His, with the first three having identical or higher affinity for Zn^{II} than the wild-type enzyme. A Thr199Glu mutation, in particular, resulted in a very high affinity for binding of Zn^{II} ($K_d = 20$ fM). The Thr199Glu mutant bound Zn^{II} more tightly than the Thr199Asp mutant by 1 order of magnitude in K_d ; this result emphasizes the significance of the distance of separation between the metal and the ligand. The lack of improvement in metal affinity with the Thr199His mutation is presumably due to rotation of the imidazole side chain away from the metal. Although all of these mutations eliminate the essential $Zn^{II}-OH$ group and, thus, the CO_2 catalytic activity, these studies suggest principles useful in the de novo design of metal-binding sites of particularly high affinity.

6.2. Effects of Indirect Ligands

The data in Table 7 indicate that altering the residues directly chelating the metal in the active site results in a decrease in the catalytic activity of the enzyme by factors from 10^2 to 10^5 . Indirect ligands—that is, those residues that interact with the ligands bound to the metal rather than with the metal itself—provide another option for modulating the properties of a protein or of an artificially designed binding site. There are three important indirect ligands in the binding site of CA; these amino acid side chains hydrogen bond to the imidazole group of His residues and to the hydroxide group (Figure 7): (i) Gln92; (ii) Glu117; and (iii) Thr199. Christianson and Fierke examined the effects of these hydrogen bonds on the thermodynamics and kinetics of metal binding, the pK_a of the water molecule bound to Zn^{II} , and the catalytic efficiency of HCA II.^{156,248,252,269}

Substituting any of the indirect ligands with an Ala residue (Gln92Ala, Glu117Ala, Thr199Ala) decreased the affinity of the protein for Zn^{II} by 1 order of magnitude. The investigators suggest that this effect is mostly entropic in origin: indirect ligands favorably preorient the metal-binding site and minimize the conformational change that the direct ligands undergo upon binding the metal. In addition to the favorable entropic contribution, indirect ligands also provide some electrostatic stabilization for the binding of the metal.²⁸⁹ The network of hydrogen bonds also plays a role in the kinetics of association of Zn^{II} . Substituting residue Glu117 with Ala, Gln, or Asp reduces the rate of association with Zn^{II} by a factor of 10^2 – 10^4 .^{252,269}

Changes in direct ligands have a greater effect on catalytic activity than do changes in indirect ligands: in contrast to mutations of direct ligands (which often practically abolish catalytic activity), the catalytic activity of indirect mutants persists with only a modest 10-fold loss in k_{cat}/K_m relative to the wild type (Table 7). An exception is the Glu117Gln mutation, which increases the pK_a of Zn^{II} – OH_2^+ and abolishes catalytic activity. Since the mutation is essentially isosteric with the wild-type side chain, the investigators attributed the loss of activity to four processes: (i) reversal of polarity of the hydrogen bond between His119 and residue 117, (ii) stabilization of the negatively charged histidinate ligand, (iii) elevation of the pK_a of Zn-bound water, and (iv) elimination of the reactivity of Zn^{II} .²⁵² By site-directed mutagenesis, the investigators also determined the role of Thr199 in catalysis: via a hydrogen bond, Thr199 stabilizes the ground state Zn^{II} –OH and the transition state of the reaction pathway.¹⁵⁶ Removing the hydrogen bond by substituting Ala for Thr significantly reduced the catalytic activity.

These detailed studies of structure–function relationships of secondary ligands in an enzyme demonstrate the significance of position and orientation of side chains in the structure of the enzyme and of the level of optimization achieved by nature for a given catalytic function. Those who design artificial catalytic centers need to consider both the groups immediately and indirectly linked to the reaction site in order to achieve optimal binding and catalytic properties.

7. Physical-Organic Models of the Active Site of CA

Recreating the function of enzymes in small molecules is a way to test our understanding of the structural and mechanistic features of the enzyme. The wealth of informa-

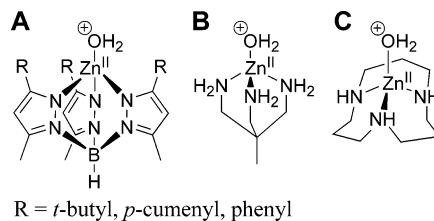
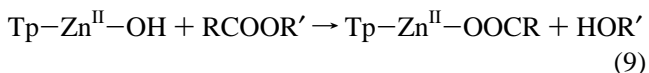


Figure 8. Examples of Zn^{II} -containing metallo-organic models of the active site of CA: (A) tris(pyrazolyl)borate family of ligand, (B) 1,1,1-tris(aminomethyl)ethane, and (C) 1,5,9-triazacyclodecane.

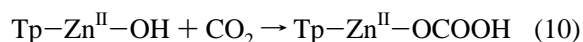
tion on carbonic anhydrase has stimulated multiple efforts to model its active site and to test hypotheses related to structure and catalytic activity of the enzyme and of molecules substantially simpler than the enzyme. Most work has focused on the most obvious part of the problem: that is, mimicking the Zn^{II} –OH group to carry out the usual functions of CA—hydration of CO_2 and the reverse dehydration of HCO_3^- , as well as hydrolysis of esters. Although this type of physical-organic chemistry is tangential to the central objective of this review, we include a brief overview. Several reviews exist that summarize the field of synthetic analogues of carbonic anhydrase and of other zinc enzymes.^{333–336}

A successful small-molecule mimic of the active site of CA should preserve as many of the features of the protein as possible: (i) tetrahedral geometry of coordination of the Zn^{II} ion to the molecule, with H_2O of $pK_a \approx 7$ as one of the ligands; (ii) formation of 1:1 complexes between the small molecule and the metal; (iii) catalytic activity and pH profile of the enzyme; and (iv) binding of arylsulfonamides in the anionic form. Here, we summarize several examples that satisfy several of these criteria.

The groups of Vahrenkamp and Parkin developed a series of tris(pyrazolyl)borate complexes ($Tp-Zn^{II}-OH$) as mimics of the active site of CA (Figure 8A).^{337–342} These tripodal ligands bind Zn^{II} in a tetrahedral geometry and reduce the pK_a of the fourth aqua ligand to ~ 6.5 .³⁴³ More importantly, the hydrophobic pocket, created by the pyrazole rings and the substituents at the 3-position, prevents the zinc ion from bridging two molecules of the ligand or a proton from bridging two zinc-containing complexes.^{336,339} These complexes, however, are not water-soluble, and since water cannot be introduced into the solution as a reagent, these complexes react *stoichiometrically* with esters (or amides and phosphates) according to eq 9, rather than catalyzing their hydrolysis.^{344,345}



$Tp-Zn^{II}-OH$ also reacts with CO_2 to form a complex with a bicarbonate ion according to eq 10 (to parallel the native function of CA—hydrolysis of CO_2):^{338,346}



Using the $Tp-Zn^{II}-OH$ complex as a mimic of the active site of CA, the investigators were able to show unequivocally that it is only the deprotonated form of the Zn^{II} –OH group that is able to carry out the catalysis of CO_2 .³⁴⁷ Protonation of $Tp-Zn^{II}-OH$ using simple acids always resulted in irreversible displacement of the aqua ligand by the counterion of the acid. The investigators, however, were able to

protonate the $\text{Tp-Zn}^{\text{II}}\text{-OH}$ complex with $(\text{C}_6\text{H}_5)_3\text{B}(\text{OH}_2)\text{-}$ a strong Brønsted acid that was unable to displace water due to steric constraints.³⁴⁸ The deprotonated form $\text{Tp-Zn}^{\text{II}}\text{-OH}$, as expected, was in equilibrium with the bicarbonate as $\text{Tp-Zn}^{\text{II}}\text{-OCOOH}$, while its conjugate acid $\text{Tp-Zn}^{\text{II}}\text{-OH}_2^+$ showed no reactivity toward CO_2 .^{347,348}

Sprigings and Hall reported a simple water-soluble tripodal complex of 1,1,1-tris(aminomethyl)ethane with Zn^{II} (Figure 8B), with water of $\text{p}K_{\text{a}} = 8.0$ as the fourth ligand.³⁴⁹ This complex exhibited enzyme-like Michaelis–Menten saturation kinetics during the hydrolysis of *p*-nitrophenyl acetate, but its second-order rate constant for the hydrolysis was 2 orders of magnitude lower than that of the native enzyme. The investigators did not report any kinetic study of the hydrolysis of CO_2 by this compound.

Kimura and co-workers developed a series of macrocyclic polyamine ligands as mimics of hydrolytic metalloenzymes: specifically, 1,5,9-triazacyclododecane ([**12**]aneN₃, Figure 8C) as a model of the active site of carbonic anhydrase.^{331,335,350,351} The investigators measured potentiometrically the value of $\text{p}K_{\text{a}}$ to be 7.3 for the Zn-bound water in this complex; this value is very close to that found in CA II (~6.9 for BCA II, 6.8 for HCA II).³³¹ Using either the tri(amine) or tetra(amine) macrocyclic scaffold, the investigators could vary the number of nitrogen ligands to Zn^{II} from 3 to 4 and, thus, were able to demonstrate that increasing the coordination state of Zn^{II} increased the value of $\text{p}K_{\text{a}}$ of $\text{Zn}^{\text{II}}\text{-OH}_2^+$. Thus, they were able to show that the value of $\text{p}K_{\text{a}}$ of the $\text{Zn}^{\text{II}}\text{-OH}_2^+$ group in the native protein is mainly determined by the coordination number of Zn^{II} , rather than by the hydrophobic environment in the binding pocket.³³¹ Kimura et al. also demonstrated that [**12**]aneN₃, like CA, was able to catalyze the hydration of acetaldehyde and hydrolysis of methyl acetate or *p*-nitrophenyl acetate, albeit with second-order rate constant 1 order of magnitude lower than those of BCA II. The pH profile of the rate of these reactions showed an inflection point near $\text{pH} = 7.3$, agreeing with potentiometric measurements for the value of $\text{p}K_{\text{a}}$ and indicating that the reaction mechanism involves a nucleophilic attack by $\text{Zn}^{\text{II}}\text{-OH}$.³³¹

The macrocyclic complex [**12**]aneN₃ with Zn^{II} also exhibited catalytic enhancement for the hydration of CO_2 and dehydration of HCO_3^- , with a pH profile that showed that the deprotonated form [**12**]aneN₃- $\text{Zn}^{\text{II}}\text{-OH}$ is the active species in the hydration reaction, while the protonated form [**12**]aneN₃- $\text{Zn}^{\text{II}}\text{-OH}_2^+$ is the active species in dehydration reaction, as in the native enzyme.³⁵¹ The rate constant for hydrolysis of CO_2 , catalyzed by [**12**]aneN₃- $\text{Zn}^{\text{II}}\text{-OH}$ ($k_{\text{cat, hyd}} \approx 6 \times 10^3 \text{ M}^{-1} \text{ s}^{-1}$), is, however, ~4 orders of magnitude lower than the rate constant in the presence of CA ($k_{\text{cat}}/K_{\text{m}} \approx 10^7 \text{ M}^{-1} \text{ s}^{-1}$; see Table 1). The difference clearly indicates the importance of the hydrophobic pocket of the enzyme, which may help preassociate CO_2 or facilitate the proton transfer.

Koike et al. also demonstrated the binding of sulfonamides (acetazolamide and others) as anions to [**12**]aneN₃- $\text{Zn}^{\text{II}}\text{-OH}$, with dissociation constants on the order of ~100 μM .³⁵⁰ Since, in this case, there are no effects of hydrophobicity or hydrogen bonding of the binding pocket of a protein, this value provides a measure of the strength of the $\text{Zn}^{\text{II}}\text{-N}$ bond between CA and sulfonamide. The lower dissociation constants of a CA–sulfonamide system (to low and sub μM) must, thus, reflect a hydrophobic component of binding (we discuss partitioning of affinities of sulfonamides to CA in

greater detail in section 10). This mimic of CA by Kimura and co-workers, however, appears to be the most successful one as it satisfies many criteria of the native enzyme (i.e., coordination of the metal, solubility in water, $\text{p}K_{\text{a}}$, activity, and sulfonamide binding).

In addition to the inorganic small molecule mimics of the active site of CA, there have been reports on using active sites of other proteins as templates for binding sites containing tetrahedrally coordinated Zn^{II} .^{352–355} These approaches were based on the mutation of three native residues to His residues in order to approximate the tripodal geometry in CA. Although these studies demonstrated the affinity of these mutated proteins for Zn^{II} and other divalent metal ions, the significance of these models has been solely structural—that is, no CA-type catalytic activity has been reported.

III. Using CA as a Model to Study Protein–Ligand Binding

Part 3 (sections 8–13) presents the use of CA as a model to study the thermodynamics and kinetics of protein–ligand binding in solution, at the surface of a solid, and in the gas phase. Section 8 presents the enzymatic and binding assays that have been useful in this effort. Sections 9 and 10 present the thermodynamics of CA–ligand binding. Section 9 presents an overview of the different ligands that bind to CA and the different approaches taken to discover those ligands. Section 10 focuses on the binding of arylsulfonamides (in particular, substituted benzenesulfonamides) and overviews the physical-organic chemistry of arylsulfonamide ligand design. It attempts to use the system of CA and arylsulfonamides as a model for the rational design of high-affinity ligands for proteins. Section 11 surveys the kinetics of binding of arylsulfonamides to CA in solution and presents models for the mechanism of association that are consistent with the data. Sections 12 and 13 discuss the kinetics and thermodynamics of binding of ligands to CA where one component is immobilized on the surface of a solid and where both components are in the gas phase, respectively.

8. Assays for Measuring Thermodynamic and Kinetic Parameters for Binding of Substrates and Inhibitors

8.1. Overview

Several assays have been used to study the interactions of CA with its substrates and ligands (Tables 8 and 9). CA has also been used as a model enzyme with which to develop new techniques for use with CA and other proteins (e.g., affinity capillary electrophoresis, sections 8.3.3 and 8.4.2). In this section, we discuss the most frequently used assays for determining the enzymatic activity of CA (section 8.2), as well as for the thermodynamics (section 8.3) and the kinetics (section 8.4) of the binding of ligands to CA. These assays measure the binding of ligands to CA directly or indirectly by measuring competitive binding or inhibition of the catalytic activity of CA. The most popular assays use the inhibition of the CA-catalyzed hydrolysis of *p*-nitrophenyl acetate (*p*-NPA) (sections 8.3.2 and 8.4.1) and the difference in fluorescence of CA when bound to dansylamide (DNSA, **133**) and when bound to other ligands (sections 8.3.1 and 8.4.1) to determine the thermodynamics and kinetics of the binding of ligands to CA. We present the experimental details and results of these assays in sections 10–13.

Table 8. Comparison of Techniques Used to Measure Binding to CA

Technique	Observable	Advantages	Disadvantages	Useful range of concentration (M)	Ref
fluorescence	emission of light	high sensitivity rapid measurements large dynamic range			
intrinsic	tryptophan residues	no chemical modification of CA or ligand is required	strong background interactions may not alter the fluorescence of indoles	5×10^{-5} – 10^{-8} (CA)	366, 367, 458
extrinsic	extrinsic luminophores	excitation in the visible and near-UV regions	may require chemical modification of CA or the ligand	10^{-2} – 10^{-10} (luminophore)	317, 368, 373–375
dansylamide competition	bound dansylamide	no chemical modification of CA or ligand is required enables a large range of binding affinities to be measured	indirect observation of binding	10^{-4} – 10^{-8} (competitor)	180, 189, 368, 377, 378
spectrophotometry	UV/visible absorption shift in Co ^{II} absorbance	rapid widely accessible	small dynamic range must use Co ^{II} in place of Zn ^{II}	10^{-4} – 10^{-7} (chromophore)	41, 269, 291, 296, 297, 301, 317, 390, 425, 612, 613
pH stat assay	hydrolysis of <i>p</i> -nitrophenyl acetate rate of NaOH addition needed to keep pH constant	Co ^{II} method directly measures binding no chemical modification needed widely accessible	indirect observation of binding	10^{-5} – 10^{-8} (CA)	509, 517, 518
CD ^a spectroscopy	ellipticity due to the absorption of:		large concentrations required		
far UV	peptide bonds	monitors changes in the secondary structure of CA	slow narrow dynamic range	10^{-5} – 10^{-3} (amino acid residue)	426–429
near UV	aromatic residues	monitors changes in the tertiary structure of CA	slow	10^{-5} – 10^{-3} (amino acid residue)	426–429
ICD ^b	disulfide bonds extrinsic chromophore incorporated in asymmetric environment	good signal-to-noise ratio reflects binding affinity	narrow dynamic range limited by the optical density of the chromophore	10^{-6} – 10^{-3} (chromophore)	430
ACE ^c	electrophoretic mobility	multiple isoforms can be studied at once	neutral ligands require competitive assays	$\sim 10^{-6}$ (CA)	391–398, 653
calorimetry	generation of heat	information about enthalpy, entropy, and heat capacity	requires large amounts of protein		405
ITC ^d	heat change during binding	constant temperature measures enthalpy directly	high binding (i.e., $K_d < \sim 10^{-10}$ M) cannot be measured directly	10^{-3} – 10^{-9}	182, 409, 412, 415
PAC ^e	pressure wave generated from fast nonradiative decay of electronically excited chromophore	rapid measurement localized heating	requires presence of a chromophore	$> \sim 10^{-5}$ (CA)	375, 418
SPR ^f	change in refractive index at a surface upon binding	measures binding at a surface real-time observation kinetics and thermodynamics	mass-transport issues	10^{-3} – 10^{-8}	412, 467, 468, 620
mass spectrometry	m/z	high resolution small amount of sample	qualitative solvent-free environment can distort structure of CA	$> \sim 10^{-12}$ (CA)	443–446
magnetic resonance (NMR, ESR)	nuclear or electronic spin resonance	fast structural information	destroys sample low sensitivity	$> 10^{-4}$	182, 270, 271, 273–277, 298, 377, 419–422, 424, 425

^a CD = circular dichroism. ^b ICD = induced circular dichroism. ^c ACE = affinity capillary electrophoresis. ^d ITC = isothermal titration calorimetry. ^e PAC = photoacoustic calorimetry. ^f SPR = surface plasmon resonance.

8.2. Enzymatic Catalysis

Various assays measure the enzymatic activity of CA (Table 9).^{17,48,356–365} These assays fall into three main categories: (i) detection of the release of protons, (ii) measurement of the consumption of CO₂, and (iii) observa-

tion of the esterase activity of CA. Carbon dioxide and carbonates are frequently used as substrates for measuring the enzymatic activity of CA. In addition to its hydration of CO₂, α -CA displays esterase activity, which has led to spectrophotometric methods based on the hydrolysis of *p*-NPA (section 8.3.2).³⁵⁶

Table 9. Techniques Used to Measure the Catalytic Activity of CA

Technique	Observable	Advantages	Disadvantages	Ref
production of H ⁺ : pH indicator dyes	color/absorbance change	spectrophotometric detection sensitive (± 0.001 pH units)	slow response some dyes inhibit CA activity is pH-dependent activity is pH-dependent	17
pH electrodes	potential	sensitive (0.001 pH units) rapid (ms) requires small volumes	activity is pH-dependent	359, 360
pH stat	used in conjunction with one of the above methods	requires small volumes activity measured at constant pH	slow response	357
consumption of CO ₂ : pCO ₂ manometer	volume change		slow cumbersome requires large volumes	362
pCO ₂ electrode	potential	sensitive requires small volumes	slow (response time ≥ 10 s)	358
continuous-flow mixing apparatus	used in conjunction with one of the methods above	fast	expensive	363
stopped-flow apparatus	used in conjunction with one of the methods above	fast	expensive	364
calorimetry	heat of reaction	rapid (0.01 ms) sensitive (± 0.00002 °C)	also measures the heat from dilution, fluid friction, and heat conduction to/from thermocouples	365
isotope exchange	disappearance of ¹⁸ O	measures activity at constant pH sensitive (> 0.1 nM) can measure activity inside cells	instrumentation (mass spectrometer)	361
magnetic resonance	¹³ C exchange (CO ₂ /HCO ₃ ⁻) causes ¹³ C line broadening	lends structural information	instrumentation (NMR)	48
hydrolysis of 4-nitrophenyl acetate	absorbance change	spectrophotometric detection	measures rate of esterase activity, not hydratase	356

Since protons are released at physiological pH in the CA-catalyzed hydration of CO₂, methods for measuring the change in the pH of the media are the basis for a simple assay of the catalytic activity of CA. These methods typically rely on measuring a change in pH using indicators or pH electrodes, or on keeping the pH constant by continuous titration (pH stat).³⁵⁷ Carbon dioxide electrodes are also widely used to measure the catalytic activity of CA.³⁵⁸

The use of stopped-flow spectrophotometry to measure the ionization state of a dye dramatically improved these methods.¹⁷ The use of pH electrodes avoids inhibition of CA by some dyes; both continuous-flow and stopped-flow mixing instruments can incorporate them.^{359,360}

Silverman estimated the activity of HCA II and BCA II in intact cells using mass spectrometry to detect the exchange of ¹⁸O between CO₂ and water at equilibrium.³⁶¹ Alternatively, ¹³C NMR can assess the activity of CA by measuring the exchange of ¹³C between CO₂ and HCO₃⁻.⁴⁸

8.3. Thermodynamic Assays for Ligand Binding

The equilibrium dissociation constant (K_d) and the inhibitory constant (K_i) are among the most commonly used metrics for comparing the *in vitro* efficacies of the binding of small-molecule-based ligands to their macromolecular targets. In choosing a technique for measuring these constants, there are two main requirements: (i) the binding constant should be within the reliable dynamic range of the technique and (ii) a statistically significant change in the observable signal should occur upon binding. Table 8 provides a summary of techniques used for measuring binding constants of CA to various ligands. A brief description of these techniques follows.

8.3.1. Fluorescence and Luminescence Spectroscopy

The principal advantages of emission spectroscopy (fluorescence and phosphorescence) are its high sensitivity and

large linear dynamic range (up to 12 orders of magnitude). A major limitation, however, is the requirement for a reporter molecule that has a large quantum yield of fluorescence or luminescence and that is sensitive to the binding event. Despite the advantages of fluorescence spectroscopy, there are relatively few reports that have used the *intrinsic* fluorescence of CA to measure the binding of ligands.^{302,366,367} The principal fluorophore in CA is the indole ring of tryptophan residues; it has an excitation wavelength of 280–290 nm (using 290 nm minimizes absorption by tyrosine residues) and a broad emission band of 330–350 nm ($\lambda_{\max} = 336$ nm).³⁶⁸ Because of differences in chemical environment, there is a large difference in the contributions of the individual fluorophores to the total emission of the protein. For example, 90% of the intensity of fluorescence of HCA II results from the radiative decays of Trp97 and Trp245.³⁶⁹ The substantially lower values of quantum yields of fluorescence of the other five tryptophans are due either to electron transfer to a nearby protonated histidine or arginine or to energy transfer to a tryptophan that is adjacent to a quencher.

A compound must alter (usually quench) the fluorescence of the tryptophans of CA in order to detect binding of that compound or a competitive compound to CA. The significant quenching of the fluorescence of *apo*-BCA upon binding Co^{II}, Cu^{II}, and Hg^{II} (Zn^{II} increases the fluorescent yield) demonstrates the sensitivity of the properties of the excited-state indoles to changes in their microenvironments.³⁶⁷ Kernohan studied four sulfonamide ligands (**227**–**229** and **140**) that, upon binding to BCA, quenched 58–84% of the fluorescence of its tryptophan residues.³⁶⁶ Direct titration of fluorescence is sufficiently sensitive that it can measure dissociation constants of ~ 10 nM. Kernohan used indirect techniques that employed competitive binding to study more strongly binding compounds that quench fluorescence. Indirect techniques are also suitable for measuring the binding properties of nonquenching ligands (e.g., **136**–**138**).³⁶⁶

Measurements of phosphorescence quenching^{370,371} and delayed fluorescence³⁷² are alternative emission techniques for investigating the binding properties of CA. The low quantum yields of phosphorescence, due to intersystem crossing and to the requirement for cryogenic conditions, diminish the practical importance of methods involving the triplet excited state.

Using *extrinsic* luminophores in emission assays increases sensitivity and allows the probe of interest to be selectively excited. Binding assays can make use of emissive probes that are (i) covalently bound to the protein, (ii) part of the ligand or competitor, or (iii) indicators for monitoring changes in the sample (e.g., pH) during an assay. Binding assays that employ fluorescent ligands are technically straightforward, easy to perform, and can achieve high sensitivity.^{317,368,373–375} The binding of DNSA (**133**) to BCA II results in (i) quenching of the tryptophan fluorescence, (ii) increasing the quantum yield of fluorescence of DNSA from 0.055 to 0.84, and (iii) blue-shifting the emission of DNSA from 580 to 468 nm.³⁶⁸ Banerjee et al. obtained similar results upon binding of other naphthalenesulfonamide derivatives to HCA I and HCA II.³⁷⁶ Simultaneous monitoring of any of these changes during the fluorescence titration improves the reliability of the recorded data and can result in expansion of the dynamic range of this method. Jain et al. reported the binding constant for dansylamide to BCA II as 0.38 μM ,³⁷⁷ and Grzybowski et al. reported a K_d value of 0.83 μM for DNSA in its complex with HCA II.¹⁸⁹ We recommend these values of K_d for binding studies with these isoforms.

The change in fluorescence intensity upon binding of CA by DNSA is the basis for a widely used competition binding assay, in which the ligand of interest is titrated into a sample of the CA–DNSA complex. The displacement of DNSA by the ligand of interest is monitored, as a function of the concentration of the ligand, by following the decrease in intensity of fluorescence at 460–470 nm upon excitation of the sample at either 280–290 nm (to excite the Trp residues of CA) or 320 nm (to excite directly the bound DNSA).^{180,189,368,377,378} This assay has all the benefits of fluorescence assays, with three additional advantages: (i) it requires no chemical labeling of the ligand or CA; (ii) it enables the measurement of dissociation constants as low as pM; and (iii) when the wavelength used for excitation is 280–290 nm, there is almost no background fluorescence.

An alternative emission assay involves monitoring the increase in fluorescence anisotropy of a fluorescent ligand upon binding to CA. Thompson et al. described an assay for the binding of Zn^{II} ions to *apo*-HCA II that measured the change in the anisotropy of the emission of a fluorophore, ABD-M (**134**), that was added to the samples.³⁷⁹

Baltzer and co-workers reported an interesting example of the use of fluorescence to characterize the binding of a sulfonamide ligand to HCA II.^{380,381} They used a small helix–turn–helix peptide that was conjugated at one of its Lys residues to a *p*-hexylamidobenzene sulfonamide (similar to compound **28**) and at another of its Lys residues to a dansyl group. Upon binding to HCA II via the sulfonamide group, the local environment around the dansyl group changed such that its fluorescence increased by 60–80%, depending on the peptide sequence. This study provides a unique method for the fluorescent sensing of proteins using synthetic constructs and demonstrates how CA can be used to develop new types of assays for protein–ligand recognition.

Binding assays can also use auxiliary fluorophores that are covalently bound to the enzyme. Viappiani observed quenching of the emission of fluorescein isothiocyanate (FITC)-labeled CA (unspecified isozyme) upon the addition of iodide.³⁷⁵ The measured binding constant from Stern–Volmer analysis was 0.2 M; this value is significantly higher than the K_i of 8.7 mM that Pocker and Stone measured (see section 9) for iodide using the inhibition of the BCA-catalyzed hydrolysis of *p*-NPA (section 8.3.2).¹⁵⁷ More recently, Bozym et al. developed an assay to measure the intracellular concentration of exchangeable zinc at picomolar levels.³⁸² This assay used a fluorescent label, Alexa Fluor 594 (AF594), covalently attached to *apo*-HCA II double mutant (Cys206Ser and His36Cys) via an engineered residue. Excitation at 365 nm, followed by fluorescent resonance energy transfer (FRET) to AF594 from a bound ligand, dapoxy sulfonamide (this ligand binds to HCA II but not to *apo*-HCA II), leads to fluorescent emission at 617 nm from the AF594. Increased emission at 617 nm indicates the presence of zinc bound to HCA II.

8.3.2. Absorption Spectrophotometry

Although absorption spectrophotometry is less sensitive than fluorescence spectroscopy, absorption studies have the advantage that they do not require the chromophores to be fluorescent. The speed and widespread availability of absorption spectrophotometers make spectrophotometric assays convenient tools for screening large numbers of ligands.^{383,384} There are two major approaches used in spectrophotometric assays of CA: (i) the chromophore is an indicator of changing pH in the medium upon consumption of HCO_3^- or CO_2 by the enzyme; and (ii) the ligand contains a chromophore whose absorption (e.g., the wavelength of maximum absorption or the extinction coefficient at a particular wavelength) changes upon binding. The former approach has been a basis for kinetic assays using stopped-flow spectrophotometry.

A popular spectrophotometric assay that detects a change in pH uses the Brinkman approach, which has been widely commercialized.^{385,386} This method consists of adding CA to a solution that is saturated with CO_2 and monitoring the change in the color of a pH indicator.³⁸⁷ The change in pH results from the enzymatic activity of CA. The indicator that Brinkman originally used was phenol red ($\text{p}K_a = 7.4$), which changes color from red to yellow when the pH of the media drops below ~ 7 .³⁸⁷ Coleman used bromothymol blue ($\text{p}K_a = 8.9$) to monitor the change in the pH caused by CA-catalyzed hydrolysis.²⁹⁷

Another popular and convenient spectrophotometric assay measures the esterase activity of CA by monitoring the CA-catalyzed hydrolysis of *p*-NPA.^{269,291,296,297,301,302} The formation of *p*-nitrophenolate is monitored by the appearance of its absorption band at 410 nm. Wilson et al. used this approach to monitor the inhibition of BCA II by saccharin and *o*- and *p*-carbobenzoxybenzene sulfonamide.³⁸⁸

An important spectroscopic technique monitors binding of ligands to the Co^{II} variant of CA by using the fact that the UV–visible spectrum of Co^{II} is highly sensitive to changes in its coordination sphere and to changes in pH.^{291,301,302,389} This technique has the advantage that it monitors binding directly, rather than as a function of enzymatic activity. It has the disadvantages that the Co^{II} metalloenzyme requires preparation and only indirectly represents the native protein.

While the *p*-NPA and Co^{II} assays are the most commonly reported techniques for measuring binding, several other assays have been demonstrated. Difference absorption spectroscopy is a technique for measuring weak signals in samples with high optical density. King and Burgen studied the difference spectra of eight sulfonamide ligands bound to HCA I and HCA II, in which the reference sample was a solution of pure enzyme.³⁹⁰ Nguyen and Huc described an interesting approach for generating bifunctional ligands of BCA II using the binding site and the surface of the enzyme as a “mold” (see section 9.4).³⁸⁴ In this study, they used spectrophotometric high-performance liquid chromatography (HPLC) methods to monitor the affinities of various ligands to BCA II. McCall and Fierke developed spectrophotometric and fluorometric assays for measuring the concentration of metal ions in solution. These assays employed ligands (PAR and Fura-2) that had absorption and fluorescence properties that changed drastically upon chelation of various metal ions. The investigators used these assays to measure the affinity of *apo*-HCA II for Ni^{II} and Cd^{II} (see section 5).³¹⁷

8.3.3. Affinity Capillary Electrophoresis

Affinity capillary electrophoresis (ACE) is a technique for measuring binding constants between proteins and ligands based on the difference in the electrophoretic mobility of the free protein and the ligand-bound protein.^{391–394} ACE can also separate chemically modified derivatives of CA to determine the role of electrostatics in the binding of ligands to proteins (see section 14.1). The electrophoretic mobility, μ (eq 11), of a molecule is proportional to its charge, Z , and inversely proportional to its molecular weight, M ,³⁹⁵ where the exponent α relates the molecular weight of the protein to its hydrodynamic drag and C_p is a proportionality constant.^{394,396–398} Equation 11 shows that a change in the electrophoretic mobility of the protein can be altered by a ligand that changes (i) the charge of the receptor, (ii) the hydrodynamic drag of the receptor, or (iii) both.

$$\mu = \frac{C_p Z}{M^\alpha} \quad (11)$$

When CA binds to an arylsulfonamide, the change in the hydrodynamic drag of the protein is negligible, and the assay relies on having a *charged* ligand to produce a significant change in the charge of the protein–ligand aggregate and, thus, a change in the electrophoretic mobility of the receptor (Figure 9A). Experimentally, μ is measured by capillary electrophoresis and calculated using eq 12,³⁹⁴ where L_d and L_t are lengths of the capillary from the inlet to the detector and to the outlet, respectively; V is the applied voltage; t_{nm} is the migration time of an electrically neutral, noninteracting molecule, used as an internal standard to monitor electroosmotic flow; and t is the migration time of the analyte.

$$\mu = \frac{L_d L_t}{V} \left(\frac{1}{t_{nm}} - \frac{1}{t} \right) \quad (12)$$

A Scatchard plot of $\Delta\mu_{p,L}/[L]$ versus $\Delta\mu_{p,L}$ results in a line with slope equal in magnitude to the binding constant, where $\Delta\mu_{p,L}$ is the difference between the mobility of the protein (P) at a given concentration of ligand, $[L]$, and the mobility of the protein without the ligand.^{394,396–398}

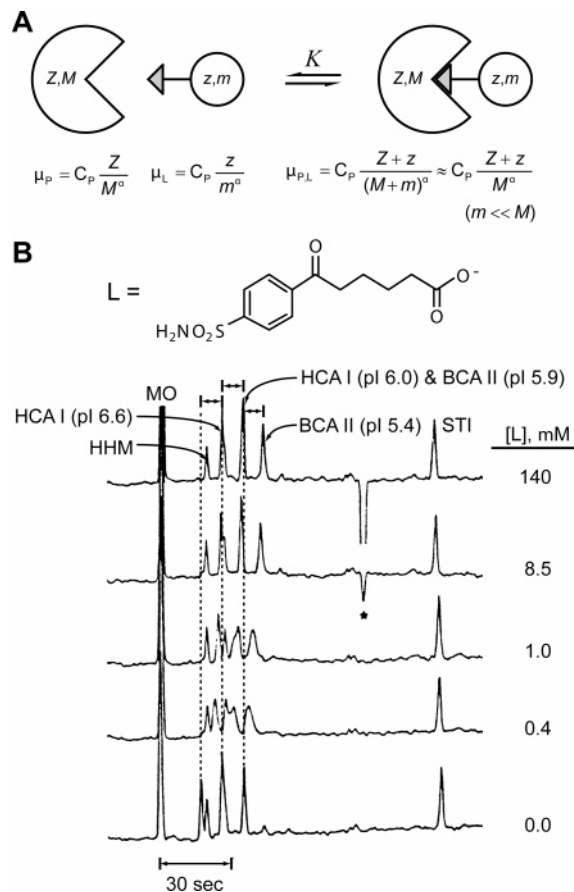


Figure 9. (A) Diagram sketching the species involved in an experiment comprising a receptor of molecular weight M and charge $\pm Z$ and a ligand of molecular weight m ($m \ll M$) and charge z (both Z and z can be either positive or negative). (B) Electropherograms (by ACE) conducted on the mixture of isozymes of carbonic anhydrase: HCA I (pI = 6.6), HCA I (pI = 6.0), BCA II (pI = 5.9), and BCA II (pI = 5.4). An electrically neutral marker (mesityl oxide, MO) and two noninteracting proteins (soybean trypsin inhibitor (STI) and horse heart myoglobin (HHM)) were added to the mixture. Shifts in mobility were observed for the isozymes of carbonic anhydrase with increasing concentration of negatively charged ligand L (shown), while the mobility of noninteracting proteins remained constant. The dissociation constant K_d between BCA II and the ligand was determined to be $1.7 \mu\text{M}$. Adapted with permission from ref 398. Copyright 1998 Wiley-VCH.

Determination of the binding constant of CA to neutral ligands requires a competitive binding assay because small neutral ligands do not cause a shift in the mobility of the protein. The competitive assay involves the addition of a neutral ligand to a sample of CA containing a fixed concentration of a charged ligand of known affinity. The mobility of CA is then a concentration-weighted average of the mobility of the complex of CA with the charged ligand and of the complex of CA with the neutral ligand. Scatchard analysis leads to the binding constant of the neutral ligand.

Figure 9B shows a set of ACE experiments with various isozymes of CA and a negatively charged sulfonamide. The elution time (and, thus, the mobility) of the protein increases with increasing concentration of ligand. The figure illustrates the ability of ACE to determine simultaneously values of K_d for multiple isoforms of CA. Another advantage of ACE is that it requires only small quantities of the protein (nanoliters of $\sim 10 \mu\text{M}$ solution and tens of picograms of protein per run). ACE also does not require knowledge of

precise concentrations of the protein because the assay is based on mobilities and concentrations of ligand, rather than on peak areas.

Affinity gel electrophoresis (AGE) is a technique similar to ACE. In AGE, a change in the migration of a protein through a slab gel is measured as a function of ligand immobilized in the gel.³⁹⁹ When compared to the capillary-based assay, AGE has a number of disadvantages, which include the necessity for (i) immobilized ligands in the gel, (ii) larger quantities of both the protein and the ligand than in the ACE assay, (iii) significantly longer times for analysis than required by ACE, and (iv) difficulty in numerical quantitation of values of K_d .

8.3.4. Calorimetry

Calorimetry is the only technique that directly measures the enthalpy of binding. Calorimetric measurements yield useful information about the contributions of enthalpy and entropy to binding, as well as about the effects of compensation between entropy and enthalpy.^{400–403} Flow- or batch-calorimeters are able to measure the binding of metals (see section 5)⁴⁰⁴ and sulfonamides (see section 10.6)⁴⁰⁵ to CA.

Differential scanning calorimetry (DSC) measures the temperature dependence of the heat capacity of a sample.⁴⁰⁶ DSC has proven to be a good technique for studying equilibria between folded and molten-globule conformations of BCA II.⁴⁰⁷ One disadvantage of using DSC for studies of binding is the difficulty in decoupling the unfolding process from the effects of temperature on the conformation of the protein.

Isothermal titration calorimetry (ITC) is the method of choice for conducting calorimetric binding assays.^{5,182,402,406,408–417} In an ITC experiment, a sample cell, which contains enzyme, and a reference cell are heated slightly and kept at a constant, equal temperature.⁴⁰⁸ As ligand is titrated into the sample cell, heat is produced from an exothermic binding event and is consumed by an endothermic binding event. The calorimeter compensates by providing less power (exothermic binding) or more power (endothermic binding) to the sample cell in order to keep the two cells at the same temperature. The power is integrated over time to provide the heat of the binding event, and normalizing this heat to the amount of ligand added gives the enthalpy (ΔH°) of binding. Titrating the ligand over many aliquots results in a binding isotherm, from which the binding constant (K_d) and, thus, the standard free energy of binding (ΔG°) are obtained. The entropy of interaction (ΔS°) is given by eq 13.

$$\Delta S^\circ = (\Delta H^\circ - \Delta G^\circ)/T \quad (13)$$

ITC is capable of measuring the binding of metals (section 5)⁴¹¹ and ligands (section 10.6)⁴⁰⁹ to CA.

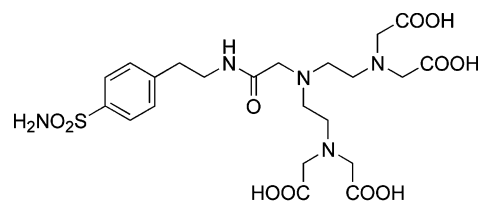
Photoacoustic calorimetry (PAC) is applicable to assays in which the binding of a ligand to CA results in a change in the ratio between the radiative and nonradiative rates of decay of electronically excited species that are part of either the enzyme or the ligand. The observable signal is the intensity of a pulse of pressure generated from a local heat gradient, which is formed when a chromophore decays nonradiatively after flash-excitation. Jain et al. used BCA and dansylamide to investigate the reliability of PAC for binding assays.⁴¹⁸ They monitored the increase in the quantum yield of fluorescence of dansylamide upon binding

to BCA and obtained a K_d for the BCA–dansylamide complex that was about one-half of the value measured for the same system by fluorescence titration.³⁶⁸ Similarly, the values for the dissociation constant of iodide to CA (unspecified isozyme) modified with FITC was about one-half of the value for the same constant measured by fluorescent emission assays.³⁷⁵ The origin of this discrepancy remains unclear, but it is, in any event, small relative to the uncertainties in many binding assays.

8.3.5. Magnetic Resonance Spectroscopy

Techniques based on magnetic resonance are useful for studying the solution-phase structure and dynamics of protein–ligand interactions, although these techniques have relatively low sensitivity and typically require the concentrations of the samples to be 100 μM or larger. Various nuclear magnetic resonance (NMR) studies—for example, ^1H and ^{13}C NMR,⁴¹⁹ ^1H NMR with Ni–BCA II,^{420,421} ^3H NMR,²⁷⁰ ^{15}N NMR,²⁷⁶ ^{19}F NMR,^{182,271,273–275} and ^{111}Cd NMR²⁷⁷—have determined the stoichiometry, coordination, and internal motion of ligands bound to CA. We present the details of these studies in section 4.4.2.

Anelli et al. used nuclear magnetic relaxation dispersion (NMRD) to study the binding of a Gd^{III} –diethylaminetriaminepentaacetic acid (DTPA) chelate, Gd –DTPA–benzenesulfonamide, to BCA.⁴²² The investigators reported the NMRD profiles from plots of the relaxation time of the protons as a function of the strength of the applied magnetic field.



DTPA-benzenesulfonamide

Cleland and Randolph used electron spin resonance (ESR) spectroscopy to observe the nonspecific, weak binding of PEG to BCA II in the molten-globule form, where either the PEG or the BCA II were spin-labeled.⁴²³ Two other groups have also used ESR with spin-labeled ligands (TEMPO-benzenesulfonamides) to study binding to CA.^{424,425}

8.3.6. Circular Dichroism Spectroscopy

The rotatory strength of proteins is extremely sensitive to alterations in their secondary structure. Circular dichroism (CD) is, therefore, a useful tool for assaying binding.^{426–429} The optical activity of CA in the far-UV region ($\lambda < \sim 230$ nm) results from electronic transitions in the amide bonds, while absorption of the aromatic residues is responsible for the ellipticity observed in the near- and middle-UV (about 320 and 240 nm). Gianazza et al. reported an extensive study on binding of acetazolamide (**137**), dorzolamide (**156**), and methazolamide (**138**) to BCA II in the presence and absence of sodium dodecyl sulfate (SDS).⁴²⁷ Although the molar ellipticity of CA in the far-UV region is significantly higher than in the 300 nm region, the binding of ligands to CA leads to minor changes in the spectra in the 200–230 nm region; under the same conditions, the CD bands ~ 280 –300 nm change not only shape but also sign.⁴²⁷ One must,

however, approach the interpretation of such results with caution. Most arylsulfonamide ligands exhibit moderate or strong absorption in the near-UV region, and hence, the observed spectral changes may result from changes in either the environment of the aromatic residues or from the induced CD (ICD) signal of the ligand.

ICD can achieve high sensitivities because of the capacity to generate complexes with high molar ellipticities ($\sim 1 \times 10^5 \text{ deg cm}^2 \text{ dmol}^{-1}$) in the visible region, where possible impurities in the samples would not have any optical activity. The sensitivity of CD spectrometers is higher in the near-UV and visible regions than in the far-UV. For example, Coleman reported the use of optical rotatory dispersion and CD spectroscopy to study the binding of the *azo*-chromophore **132** to Zn^{II} and Co^{II} derivatives of HCA I.⁴³⁰ The extinction coefficient of this dye at 500 nm is $\sim 2.5 \times 10^4 \text{ M}^{-1} \text{ cm}^{-1}$, and the value of the molar ellipticity at 486 nm reached $10^5 \text{ deg cm}^2 \text{ dmol}^{-1}$ upon binding to HCA I.

8.3.7. Mass Spectrometry

The analysis of proteins by mass spectrometry has been reviewed extensively.^{431–442} To study protein–ligand complexes in the gas phase, it is important to vaporize the complexes without dissociation and to dissociate them without destroying the protein (the mass of the protein must not be affected). The system of CA and arylsulfonamides has provided a model for studies of protein–ligand binding in the gas phase. We discuss the experimental data in section 13 and here only discuss the technical aspects of these experiments.

Electrospray ionization followed by Fourier transform ion cyclotron resonance mass spectrometry (ESI-FTICR-MS) allowed the generation and trapping of ions of CA II–ligand complexes (HCA II or BCA II).^{443–446} The relative intensities of BCA II–ligand complex ions gave the relative abundances of the BCA II–ligand complexes in the gas phase (and also in solution).⁴⁴³ Whitesides, Smith, and co-workers demonstrated that these BCA II–ligand complex ions could be completely dissociated by the application of an electromagnetic pulse in the presence of nitrogen gas molecules.^{443,444} This process generated free ligand ions, which could be quantified to determine the relative abundances of the precursor protein–ligand complex ions. The investigators also demonstrated that sustained off-resonance irradiation CID (SORI-CID)—the application of an electromagnetic pulse with a frequency lower than the cyclotron frequency of the protein in the presence of nitrogen gas—induced the loss of some of the ligands from the protein–ligand complex ions, in a manner that scaled with the intensity of the pulse.^{445,446} The intensity of the pulse that generated equal ion intensities for the CA II–ligand complex and free CA II was termed E_{50} and was used to compare the relative stabilities of different CA II–ligand complexes in the gas phase.^{445,446}

8.4. Kinetic Assays for Ligand Binding

8.4.1. Fluorescence and Absorbance Spectroscopy

The earliest experiments to determine the kinetics of CA measured the rate of CO_2 hydration either directly, by monitoring the absorption of gas in a sealed container,^{447–449} or indirectly, by measuring the change in pH of the solution.^{450–452} Binding of a ligand is measured by a change in the rate of hydration of CO_2 in the presence of the ligand.

Many studies used stopped-flow methods with a pH indicator to increase the accuracy of the measure of the rate of hydration.^{296,299,300,307,453,454}

Pocker and Stone reported that BCA acts as an esterase and measured the hydrolysis of *p*-NPA by monitoring the absorption of the product, *p*-nitrophenolate, at 400 nm ($\epsilon \approx 2.1 \times 10^4 \text{ M}^{-1} \text{ cm}^{-1}$).⁴⁵⁵ Using this technique, Pocker measured the kinetics of binding of many ligands by determining the decrease in esterase activity as a function of time.^{38,157,456,457}

Other stopped-flow experiments, based on fluorescence quenching of tryptophan residues, have been used to measure the kinetics of binding of sulfonamides to CA directly (see section 11 for further discussion).^{389,390,458} Any sulfonamide with spectral transitions overlapping the tryptophan emission band is an effective quencher of the native fluorescence of the protein. The binding of these sulfonamides, including the *azo*-sulfonamides, DNSA (**133**), and many nitro- and aminosulfonamides,^{368,390,458} leads to a decay in fluorescence intensity as a function of time; this decay is a direct measure of ligand binding. If a ligand does not quench the enzyme fluorescence sufficiently, the kinetics can be determined by competition with either *p*-nitrobenzenesulfonamide (**3**) or DNSA.^{368,389}

Ligands with much more rapid kinetics of binding have been studied using temperature-jump relaxation, which exploits the absorbance of Co^{II} –BCA II.²⁹¹ Joule heating induces a sudden increase in the temperature of the analyte mixture, after which the absorption of Co^{II} at 599 nm is measured as a function of time. In the absence of ligand, the absorption of Co^{II} –BCA II has an intrinsic relaxation rate on the millisecond time scale. Hence, this technique is appropriate only for ligands with relaxation rates faster than milliseconds, including cyanate, thiocyanate, and cyanide. It is not clear what causes the millisecond relaxation because the molecular details of this intrinsic relaxation have not been reported.

8.4.2. Affinity Capillary Electrophoresis

Section 8.3.3 outlined the principles of ACE. The binding constants of a charged ligand (or an uncharged ligand in competition with a charged ligand) can be determined by measuring the change in mobility of a protein as a function of the concentration of ligand(s). In addition to determining binding constants, ACE can, in some circumstances, be used to determine the on- and off-rates of complex formation.³⁹² If the off-rate is comparable to the time required to obtain the electropherogram, the peaks in the electropherogram shift and broaden as the concentration of a charged ligand increases, until the protein is saturated with ligand. The broadening of peaks is due to equilibration between species with different electrophoretic mobilities (free and complexed protein). At saturating concentrations of ligands, in which all of the enzyme has bound ligand, the peak narrows again. The broadening is most pronounced when the dissociation time is of the same magnitude as the migration time of the protein. Therefore, ACE can be used only to analyze the kinetics of ligands with a dissociation time similar to the migration time, typically where $k_{\text{off}} \approx 0.01–0.1 \text{ s}^{-1}$. Fitting the displacement and shape of the peak in the electropherogram gives the rate constants of association (k_{on}) and dissociation (k_{off}). The values of k_{on} and k_{off} are constrained to give the experimentally obtained binding constant (K_{d}).

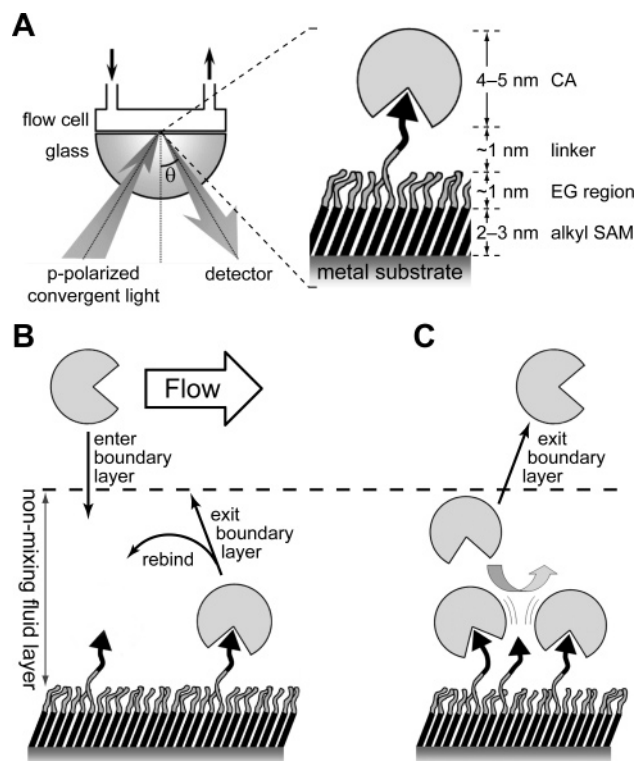


Figure 10. Measuring the binding of CA to self-assembled monolayers using surface plasmon resonance: (A) schematic of the apparatus and the overall molecular structure at the solid–liquid interface, (B) effects of mass transport on measurements of binding, and (C) effects of lateral sterics on binding of CA at densely populated surfaces.

8.4.3. Surface Plasmon Resonance Spectroscopy

Surface plasmon resonance spectroscopy (SPR) measures the rates of molecular association (k_{on}) and dissociation (k_{off}) at surfaces—provided that the rates are not mass-transport limited—and the thermodynamic dissociation constant, K_{d} . The dependence of binding on temperature must be determined in order to separate ΔG° into ΔH° and ΔS° (see section 10). SPR is based on the measurement of the intensity of monochromatic, plane-polarized light reflected from the backside of a semitransparent, gold-coated glass slide (Figure 10a). The reflected light has a minimal intensity at a specific angle of incident light, θ_{m} . The instrument monitors θ_{m} as a function of time while the surface is treated with an analyte. Changes in θ_{m} correlate to changes in the refractive index at the interface between the gold surface and the solution; the distance from the surface at which the change occurs is within approximately one-quarter wavelength of the incident visible light.^{459,460} For a family of compounds (e.g., proteins), changes in θ_{m} correlate linearly with the mass of compound adsorbed per unit area of the surface.^{461,462} For proteins, a change in θ_{m} of 1° corresponds to an adsorption of ~ 10 ng mm^{-2} .⁴⁶³

Instruments for SPR⁴⁶⁴ are capable of measuring values of k_{on} (10^3 – 10^7 $\text{M}^{-1} \text{s}^{-1}$) and k_{off} (10^{-6} – 10^{-1} s^{-1}) at temperatures between 4 and 40 $^{\circ}\text{C}$.⁴⁶⁵ The corresponding equilibrium dissociation constant, K_{d} (10^{-13} – 10^{-4} M), can be determined by calculating the ratio $k_{\text{off}}/k_{\text{on}}$ or by constructing a Scatchard plot to values of θ_{m} at different concentrations of ligand.

The two types of model surfaces commonly used for studying protein–ligand interactions (especially by SPR) are

as follows: (i) commercially available dextran-coated substrates⁴⁶⁶ and (ii) self-assembled monolayers (SAMs) of alkanethiols on gold or palladium.^{467–473} The dextran-coated surfaces are convenient to use, but they have disadvantages, including (i) the influence of the gel on mass transport of the analyte, (ii) the rebinding of analyte molecules that become “trapped” in the gel environment, (iii) exclusion of macromolecular analytes from the gel matrix, and (iv) nonspecific binding.^{469,474}

Exposing a clean, gold surface to a solution of alkanethiols forms SAMs. These compounds are bound to the gold surface as alkanethiols with their ω -terminal functional group oriented into the bulk solution. This functional group defines the interface between the solid and the solution. SAMs of alkanethiols on gold have three characteristics that make them particularly well-suited to the study of protein–ligand interactions at surfaces. SAMs (i) allow flexibility in both the composition and reactivity of the surface,^{467,468,474–480} (ii) can be designed to resist the nonspecific adsorption of proteins,^{481–486} and (iii) provide excellent compatibility with the techniques of SPR^{467,468,487–490} and quartz crystal microbalance (QCM).^{489,491}

SAMs presenting oligo(ethylene glycol) are particularly important in studies of protein–ligand interactions at surfaces, since they effectively resist the nonspecific adsorption of proteins and cells^{481,483–485} and provide an excellent baseline against which the specific binding of proteins to surface-bound ligands,^{467–469,492} or the nonspecific binding of proteins to hydrophobic sites, can be measured.⁴⁹³

8.5. Most Convenient Assays

As an aside, to researchers new to this area, our experience suggests that the most convenient assays for thermodynamic binding studies are the dansylamide displacement assay (section 8.3.1) and the inhibition of CA-catalyzed hydrolysis of *p*-NPA (section 8.3.2), and, if the ligand is charged, affinity capillary electrophoresis (section 8.3.3). For kinetics, we find that SPR (section 8.4.1) and stopped-flow fluorescence spectroscopy (section 8.4.1) are the most convenient.

9. Structure–Activity Relationships for Active-Site Ligands

9.1. Overview of Structure–Activity Relationships

CA has been a therapeutic target for many years, as gauged by the considerable effort focused on developing high-affinity inhibitors of CA and the more recent development of activators of CA. Activators of CA (e.g., L- and D-histidine,^{190–192} L- and D-phenylalanine,¹⁹³ β -Ala-His,⁴⁹⁴ histamine,¹⁹⁴ tri- and tetrasubstituted pyridinium azole compounds,^{495,496} and L-adrenaline²²⁶) bind to the entrance of the active site (near His64) and increase k_{cat} for the hydration of CO_2 by enhancing the activity of the proton shuttle (see section 4.6). We will not focus on activators in this review because Supuran and co-workers have comprehensively reviewed them.^{497–499} In addition, the development of inhibitors of CA has been well-reviewed elsewhere.^{2,15,500–502} Previous reviews on inhibitors of CA have focused mainly on in vivo activity, as determined by the effect of topically administered inhibitors on the reduction in intraocular pressure. We focus here on in vitro approaches that develop tight-binding (low K_{d}) sulfonamide inhibitors. In this section, we discuss relationships between the structure of an inhibitor

and its affinity, and in section 10, we discuss the use of CA as a model for physical-organic studies in the design of ligands.

We classify the myriad inhibitors of CA into three main groups: (i) sulfonamides ($R-SO_2NH_2$), (ii) other sulfonic acid derivatives ($R-SO_2-X$, $X \neq NH_2$), and (iii) small monoanions (e.g., halides, azide, and thiocyanate). The sulfonamides and sulfonic acid derivatives have values of K_d in the picomolar to micromolar range, whereas the inorganic monoanions bind CA with values of K_d in the micromolar to millimolar range. We describe each class of inhibitors in more detail below, with representative examples listed in Table 10 (see also refs 157, 181, 182, 185, 189, 199, 200, 214, 216, 225, 227, 229–233, 284, 366, 368, 377–379, 384, 389, 392, 413, 415, 417, 430, 458, 503–523). Although this table contains many structures, it is not a comprehensive listing of inhibitors for CA: those compilations are elsewhere.^{2,15,500,501} Instead, it lists compounds, and families of compounds, that are (in our opinion) particularly relevant to understanding the physical-organic chemistry of CA–ligand binding: What ligands bind tightly and why? What is the mechanism of association and dissociation?

The structure of a sulfonamide inhibitor can be divided into four parts (Figure 11). Each part can be varied in structure independently, and each has an important characteristic or functionality that can modulate the affinity of the ligand for CA. Perhaps the most significant region of the molecule is the sulfonamide head group, which binds as the RSO_2NH^- monoanion to the Zn^{II} ion in the active site of CA.²⁷⁶ Deprotonation of the sulfonamide is, therefore, necessary for binding, and so the pK_a of the sulfonamide group often correlates with the rate constant of association and with the equilibrium dissociation constant for binding to CA. This relationship is particularly strong within classes of similar compounds and is elaborated in section 9.2.2.³⁸⁹

In addition to aromatic sulfonamides, there are now several examples of powerful *aliphatic* sulfonamide and *sulfamate* inhibitors. Typically, however, the group attached to the sulfonamide is a 5- or 6-membered aromatic ring or fused ring system, often containing nitrogen, oxygen, and/or sulfur heteroatoms.² In order to modulate the properties of the inhibitor (such as pK_a and solubility), many functional groups have been conjugated to the aromatic rings; these groups are often called “tails”.

Tail groups may vary in length from 1 to 100 Å and may affect the in vitro and in vivo activity of the inhibitor by changing the solubility, flexibility, polarity, and biocompatibility of the compound.² Additionally, tails may be used as linkages to secondary recognition elements (SREs), which target sites on the protein that are adjacent to the primary binding site. This approach can significantly modulate the affinity of an inhibitor by effectively creating a bivalent ligand (see section 10). In addition, tails have been used as a convenient variable region in several combinatorial studies of sulfonamide inhibitors.

9.2. Thermodynamic Binding Data

We divide the many approaches to developing inhibitors of CA into four categories: (i) lead-based design, (ii) combinatorial approaches, (iii) rational design, and (iv) computational approaches. Lead-based design, which is the most common approach in the development of pharmaceuticals, uses particularly active compounds—that is, leads—as the starting point in an iterative process of varying the

structure of the lead and selecting, from the small library resulting from this variation, new lead compounds that have improved properties (e.g., efficacy in predictive disease models, profile of absorption, distribution, metabolism and excretion (ADME), and toxicity). This approach has been applied successfully to the development of sulfonamide-based inhibitors of CA.

9.2.1. Inhibitors with Aromatic Rings

In 1940, Mann and Keilin observed that sulfanilamide (**4**) can inhibit CA.⁵²⁴ This compound was the early lead in the eventual development of the four systemic drugs now used for the treatment of glaucoma: acetazolamide (**137**), methazolamide (**138**), ethoxzolamide (**140**), and dichlorophenamide (**136**) (see Table 10). A common approach used in the early design of sulfonamide-based inhibitors involved modifying the aromatic ring system attached directly to the sulfonamide group. Supuran and co-workers coined this tactic the “ring approach”, and they provide an excellent review of the clinical relevance of ~500 compounds generated using the ring and tail approaches.² The phenyl moiety of sulfanilamide has been changed to many different rings, including furan (**142**), thiophene (**145**), thiadiazole (**137** and **138**), indole (**141**), benzofuran (**143**), benzothiophene (**149**), benzothiazole (**140**), thienofuran (**144**), thienothiophene (**149** and **150**), thienothiopyran (**152**, **153**, **156**, **157**, **160**, **161**, **163**, and **164**), and thienothiazine (**166**). Table 10 includes representative compounds from each of these classes that were among the most effective inhibitors of CA. It is clear from this list, and the references included therein, that most of these compounds tested were bicyclic, contained at least one sulfur atom, and had similar, nanomolar dissociation constants but different in vivo activities. Affinity, therefore, is not the primary factor in developing an effective therapeutic; essential criteria also include, among other factors, pK_a , hydrophobicity, and solubility (and other properties that contribute to ADME/TOX/PK/PD).

Although the systemic drugs, **136**–**138** and **140**, were effective antiglaucoma agents, they inhibit several CA isozymes in tissues outside of the eye and cause wide-ranging side effects. Topical antiglaucoma agents circumvent this shortcoming. Compound **140** was the lead used to develop the two topical antiglaucoma agents, dorzolamide (**157**) and brinzolamide (**161**). HCA II was the primary target of inhibition because it is the critical CA isozyme that controls the secretion of ocular aqueous humor.^{2,525} In section 9.2.4, we describe attempts to develop isozyme-specific inhibitors.

9.2.2. Sulfamates and Non-aromatic Sulfonamides

While initially it was believed that only *aromatic* sulfonamides could serve as potent inhibitors of CA,⁵⁰⁰ it was discovered subsequently that a “spacer” between the sulfonamide moiety and the ring could be incorporated into tight-binding inhibitors. The tight binding of zonisamide (**278**) to HCA II ($K_i = 35$ nM) demonstrates that the aryl ring of a sulfonamide inhibitor can also be separated from the sulfonamide moiety by a methylene group.²³¹ In another example, a series of aryl sulfamates (**183**–**185**, compounds of the type $R-O-SO_2NH_2$ where R represents a substituted benzene ring) was synthesized and gave values of IC_{50} in the range of 40–100 nM.⁵⁰⁴ Contrary to results with substituted benzenesulfonamides, the *meta*-substituted sulfa-

Table 10. Thermodynamic Data for the Binding of Ligands to CA II

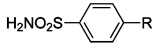
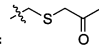
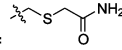
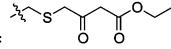
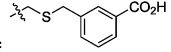
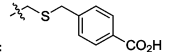
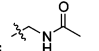
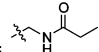
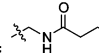
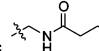
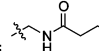
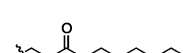
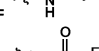
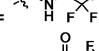
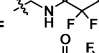
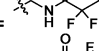
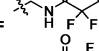
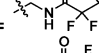
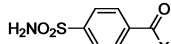
Compound	Structure	CA II Variant	Dissociation Constant (nM)	K_d or K_i^a	p <i>K</i> _a	Ref.
<i>Type:</i> 						
1	R = H	HCA	200–1500	K_d	10.1	389,458
2	R = Cl	HCA	120	K_d	9.9	458
3	R = NO ₂	HCA	63	K_d	9.0	458
4	R = NH ₂	BCA	3000–23 000	K_i	10.5	413,503
5	R = NHCH ₃	BCA	15 000	K_i	11.0	503
222	R = CH ₂ NH ₃ ⁺	BCA	36 000	K_d	8.4	417
6	R = CH ₃	HCA	82	K_d	10.2	389
7	R = CH ₂ CH ₃	HCA	29	K_d	10.4	389
8	R = (CH ₂) ₂ CH ₃	HCA	17	K_d	10.3	389
9	R = (CH ₂) ₃ CH ₃	HCA	5.0	K_d	10.4	389
10	R = (CH ₂) ₄ CH ₃	HCA	1.4	K_d	--	389
11	R = 	HCA	180	K_i	--	384
12	R = 	HCA	770	K_i	--	384
13	R = 	HCA	130	K_i	--	384
14	R = 	HCA	59	K_i	--	384
15	R = 	HCA	84	K_i	--	384
16	R = 	BCA	850	K_d	10.2	508
17	R = 	BCA	720	K_d	9.9	508
18	R = 	BCA	610	K_d	--	508
19	R = 	BCA	440	K_d	--	508
20	R = 	BCA	230	K_d	--	508
21	R = 	BCA	190	K_d	--	508
22	R = 	BCA	270	K_d	10.1	508
23	R = 	BCA	140	K_d	9.8	508
24	R = 	BCA	85	K_d	--	508
25	R = 	BCA	44	K_d	--	508
26	R = 	BCA	23	K_d	--	508
27	R = 	BCA	19	K_d	--	508
28	R = CH ₂ NHCO(CH ₂) ₄ CO-NHC[CH ₂ O(CH ₂) ₃ SCH ₂ COOH] ₃	BCA	6.1	K_d	--	392
<i>Type:</i> 						
29	X = OH	HCA	270	K_i	--	458
30	X = OCH ₃	HCA	10	K_i	9.8	389
31	X = OCH ₂ CH ₃	HCA	3.2	K_i	9.7	389

Table 10 (Continued)

Compound	Structure	CA II Variant	Dissociation Constant (nM)	K_d or K_i^a	pK_a	Ref.
Type:						
32	X = O(CH ₂) ₂ CH ₃	HCA	1.7	K_i	9.8	389
33	X = O(CH ₂) ₃ CH ₃	HCA	0.77	K_i	9.7	389
34	X = O(CH ₂) ₄ CH ₃	HCA	0.41	K_i	10.1	389
35	X = O(CH ₂) ₅ CH ₃	HCA	0.41	K_i	--	389
36	X = NH ₂	HCA	120	K_d	--	284
37	X = NHCH ₃	HCA	83	K_i	10.3	389
38	X = NHCH ₂ CH ₃	HCA	30	K_d	10.1	389
39	X = NH(CH ₂) ₂ CH ₃	HCA	8.3	K_d	10.1	389
40	X = NH(CH ₂) ₃ CH ₃	HCA	3.3	K_d	10.1	389
41	X = NH(CH ₂) ₄ CH ₃	HCA	1.8	K_d	10.2	389
42	X = NH(CH ₂) ₅ CH ₃	HCA	1.3	K_d	--	389
43	X = NH(CH ₂) ₆ CH ₃	HCA	1.2	K_d	--	389
44	X = NH(CH ₂) ₇ CH ₃	HCA	2.5	K_d	--	284
45	X = NHCH ₂ CF ₃	BCA	21	K_d	--	508
46	X = NHCH ₂ CF ₂ CF ₃	BCA	5.6	K_d	--	508
47	X = NHCH ₂ (CF ₂) ₂ CF ₃	BCA	0.91	K_d	--	508
48	X = NHCH ₂ (CF ₂) ₆ CF ₃	BCA	0.3	K_d	--	284
49	X =	HCA	1.1	K_d	--	284
50	X =	HCA	2.1	K_d	--	284
51	X =	HCA	1.1	K_d	--	284
52	X =	HCA	2.2	K_d	--	284
53	X =	HCA	2.0	K_d	--	284
54	X =	HCA	1.4	K_d	--	284
55	X =	HCA	0.36	K_d	--	515,516
56	X =	HCA	0.29	K_d	--	515,516
57	X =	HCA	0.91	K_d	--	515,516
58	X =	HCA	1.5	K_d	--	515,516
59	X =	HCA	4.3	K_d	--	284
60	X =	HCA	4.0	K_d	--	284
61	X =	HCA	1.4	K_d	--	284
62	X =	HCA	0.6	K_d	--	284

Table 10 (Continued)

Compound	Structure	CA II Variant	Dissociation Constant (nM)	K_d or K_i^a	pK_a	Ref.
Type:						
92	X = Gln	HCA	140	K_d	--	507
93	X = Ser	HCA	240	K_d	--	507
94	X = Thr	HCA	53	K_d	--	507
95	X = Gly	HCA	310	K_d	--	507
96	X = Ala	HCA	120	K_d	--	507
97	X = Arg	HCA	220	K_d	--	507
98	X = Pro	HCA	230	K_d	--	507
99	X = Val	HCA	15	K_d	--	507
100	X = Met	HCA	10	K_d	--	507
101	X = Ile	HCA	9	K_d	--	507
102	X = Leu	HCA	9	K_d	--	507
103	X = Phe	HCA	13	K_d	--	507
104	X = L-PheGlyGlyO ⁻	HCA	21	K_d	--	284
105	X = L-PheGlyGlyOBn	HCA	5.3	K_d	--	284
106	X = L-PhgGlyGlyOBn	HCA	0.9	K_d	--	284
107	X = D-PheGlyGlyOBn	HCA	36	K_d	--	284
108	X =	HCA	4	K_d	--	506
109	X =	HCA	0.03	K_d	--	189 ^b
110	X =	HCA	0.23	K_d	--	189 ^b
111	X =	BCA	91	K_d	--	508
112	X =	BCA	59	K_d	--	508
113	X =	BCA	53	K_d	--	508
Type:						
114	X = OCH ₃	HCA	700	K_d	9.8	389
115	X = OCH ₂ CH ₃	HCA	610	K_d	9.6	389
116	X = O(CH ₂) ₂ CH ₃	HCA	365	K_d	9.7	389
117	X = O(CH ₂) ₃ CH ₃	HCA	113	K_d	9.6	389
118	X = O(CH ₂) ₄ CH ₃	HCA	138	K_d	9.9	389
Type:						
119	X = OCH ₃	HCA	39 000	K_d	9.3	389
120	X = OCH ₂ CH ₃	HCA	16 000	K_d	9.5	389
121	X = O(CH ₂) ₂ CH ₃	HCA	5200	K_d	9.7	389
122	X = O(CH ₂) ₃ CH ₃	HCA	1800	K_d	9.8	389
123	X = O(CH ₂) ₄ CH ₃	HCA	660	K_d	9.9	389

Table 10 (Continued)

Compound	Structure	CA II Variant	Dissociation Constant (nM)	K_d or K_i^a	p <i>K_a</i>	Ref.
Type:						
124		HCA	23	K_i	--	510
125		HCA	25	K_i	--	510
127		HCA	18	K_i	--	510
128		HCA	16	K_i	--	510
129		HCA	12	K_i	--	510
130		HCA	15	K_i	--	510
131		HCA	15	K_i	--	229
132		HCA	1000	K_i	--	430
133		HCA	250	K_d	9.8	189,368,458
134		HCA	300	K_d	--	379
135		HCA	220	K_d	9.7	458
136		HCA	38	K_i	--	232,233
137		HCA	12	K_i	7.4	232,233,521
138		HCA	14	K_i	7.4	232,233,521
139		HCA	9	K_i	--	511
140		HCA	8	K_i	8.0	232,233,521
141		HCA	11	K_i	--	512
142		HCA	2.3	K_d	8.1	517
143		HCA	3.0	K_i	--	512
144		HCA	1.2	K_d	9.2	518
145		HCA	1.4	K_d	8.8	517
146		HCA	0.46	K_d	--	199
147		HCA	0.49	K_d	--	199

Table 10 (Continued)

Compound	Structure	CA II Variant	Dissociation Constant (nM)	K_d or K_i^a	p <i>K</i> _a	Ref.
148		HCA	0.83	K_d	--	199
149		HCA	4.0	K_i	--	512
150		HCA	2.7	K_d	--	513
151		HCA	1.1	K_d	--	513
152		HCA	0.61	K_d	--	514
153		HCA	71	K_d	--	514
154		HCA	3.5	K_d	8.5	378
155		HCA	1.5	K_i	--	214
156		HCA	1.9	K_i	--	214
157		HCA	0.37	K_i	--	214
158		HCA	0.20	K_d	--	199
159		HCA	0.16	K_d	--	199
160		HCA	0.32	K_d	--	199
161		HCA	0.13	K_d	--	199
162		HCA	0.10	K_d	--	199
163		HCA	0.10	K_d	--	199
164		HCA	1.7	K_d	--	199

Table 10 (Continued)

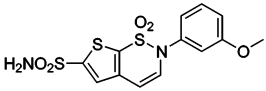
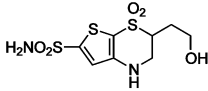
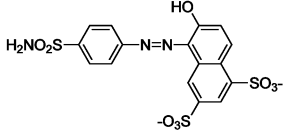
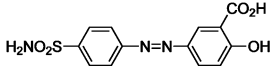
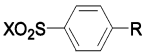
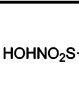
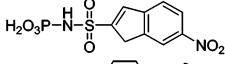
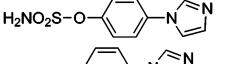
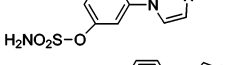
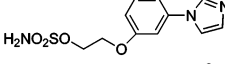
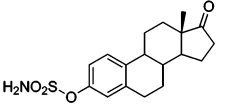
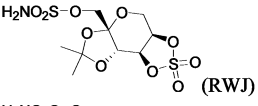
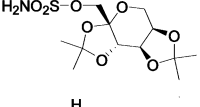
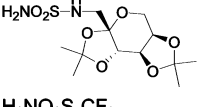
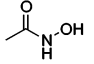
Compound	Structure	CA II Variant	Dissociation Constant (nM)	K_d or K_i^a	p <i>K</i> _a	Ref.
165		HCA	0.13	K_d	--	199
166		HCA	1.2	K_d	8.5	509
167		HCA	130	K_d	--	458
168		HCA	2.9	K_d	--	458
<i>Type:</i> 						
169	R = CH ₃ X = OH	BCA	460 000	K_i	--	519
170	R = CH ₃ X = SH	BCA	10 000	K_i	--	519
171	R = CH ₃ X = N ₃	BCA	45 000	K_i	--	519
172	R = CH ₃ X = NO	BCA	24 000	K_i	--	519
173	R = CH ₃ X = NCS	BCA	18 000	K_i	--	519
174	R = CH ₃ X = NHNH ₂	BCA	53 000	K_i	--	519
175	R = CH ₃ X = NHOH	BCA	9 000	K_i	--	519
176	R = CH ₃ X = NHOMe	BCA	170 000	K_i	--	519
177	R = CH ₃ X = NHCl	BCA	2 100	K_i	--	519
178	R = COOH X = NCl ₂	BCA	3 600	K_i	--	519
179	R = CH ₃ X = NHCN	BCA	130 000	K_i	--	519
180	R = CH ₃ X = NHOCH ₂ COO ⁻	BCA	85 000	K_i	--	519
181		HCA	0.8	K_i	--	522
182		HCA	2	K_i	--	520
183		BCA	120	K_i	8.0	504
184		BCA	42	K_i	9.1	504
185		BCA	69	K_i	8.9	504
186		HCA	10	K_i	--	523
187		HCA	36	K_i	--	216
187a		HCA	5	K_i	--	233
187b		HCA	2 100	K_i	--	232
188	H ₂ NO ₂ S-CF ₃	HCA	2–13	K_i	6.3	505,528
189	H ₂ NO ₂ S-CH ₃	HCA	70 000–320 000	K_i	10.8	505,528
190		HCA	47 000	K_i	--	200

Table 10 (Continued)

Compound	Structure	CA II Variant	Dissociation Constant (nM)	K_d or K_i^a	pK_a	Ref.
191		HCA	3800	K_i	--	200
192	$H_2NSO_3^-$	HCA	390 000	K_i	--	413
192	$H_2NSO_3^-$	BCA	390 000	K_i	--	519
193	F^-	BCA	1.2×10^9	K_i	3.2 ^c	157
194	Cl^-	BCA	1.9×10^8	K_i	-7.0 ^c	157
195	Br^-	BCA	6.6×10^7	K_i	-9.0 ^c	157
196	I^-	BCA	8.7×10^6	K_i	-10.0 ^c	157
197	HS^-	BCA	1.1×10^4	K_i	7.0 ^c	157
198	CN^-	BCA	2.6×10^3	K_i	9.2 ^c	157
199	N_3^-	BCA	5.9×10^5	K_i	4.7 ^c	157
200	NCO^-	BCA	1.1×10^5	K_i	3.5 ^c	157
201	SCN^-	BCA	5.9×10^5	K_i	0.9 ^c	157
202	OAc^-	BCA	8.5×10^7	K_i	4.7 ^c	157
203	HCO_3^-	BCA	2.6×10^7	K_i	6.5 ^c	157
204	NO_3^-	BCA	4.8×10^7	K_i	-1.5 ^c	157
205	ClO_4^-	BCA	1.6×10^7	K_i	-10.0 ^c	157
Type:						
207	2-fluoro	BCA	230	K_d	9.6	182
208	3-fluoro	BCA	75	K_d	9.7	182
209	4-fluoro	BCA	590	K_d	10.0	182
210	2,6-difluoro	BCA	190	K_d	9.1	182
211	3,5-difluoro	BCA	57	K_d	9.4	182
212	pentafluoro	BCA	25	K_d	8.2	182
Type:						
213	$X =$	BCA	620	K_d	--	415
214	$X =$	BCA	300	K_d	--	415
215	$X =$	BCA	340	K_d	--	415
216	$X =$	BCA	410	K_d	--	415
217	$X =$	BCA	450	K_d	--	415
218	$X =$	HCA	27	K_d	--	181
219	$X =$	HCA	28	K_d	--	181
227		BCA	1738	K_i	7.5	366
228		BCA	93	K_i	7.5	366
229		BCA	1.4	K_i	7.5	366
278		HCA	35	K_i	--	231
279	$H_2NO_2S-NH_2$	BCA	1.1×10^6	K_i	10.9	227,519
280	$H_2NO_2S-NHOH$	HCA	570	K_i	13.9	227
281		HCA	1.4×10^7	K_i	--	225

^a Values of K_d were determined either by fluorescence titration (directly or with DNSA as the competitor) or by calorimetry; values of K_i were determined by monitoring the hydratase (pH) or esterase (cleavage of *p*-nitrophenyl acetate) activity of CA II as a function of added ligand. ^b Note that the structures are accidentally switched in the original paper.¹⁸⁹ ^c Value is the pK_a of the conjugate acid.

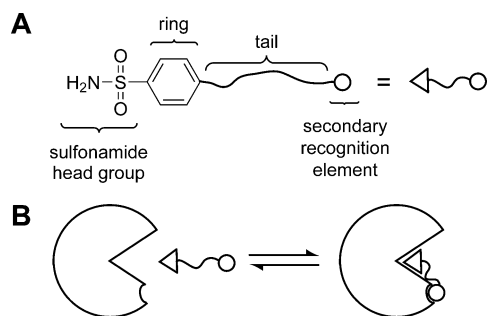


Figure 11. Binding of arylsulfonamide to carbonic anhydrase (CA). (A) Structure of a general arylsulfonamide ligand showing the structural features that can be modified (to a first approximation) independently. (B) The interactions between the different structural components of a general arylsulfonamide ligand and CA.

mates (**184** and **185**) were more potent inhibitors than their *para*-substituted analogues (**183**) (Table 10). In the same study, aryloxyalkyl sulfamates (compounds of the type $R-O-CH_2CH_2-O-SO_2NH_2$, e.g., **185**), in which methylene units intervene between the aryl ring and the sulfamate, gave compounds with roughly the same values of K_i as did the aryl sulfamates (cf. **185** and **184**; Table 10).

More recent examples of aryl sulfamates (EMATE, **186**; 2-MeOE2bisMATE, **186a**; RWJ-37947, **187**; topiramate, **187a**; 667-coumate, **250**; **251**; and **252**) were crystallized with HCA II.^{128,216–218,230,233} Although the values of K_i for EMATE (10 nM) and topiramate (5 nM) were similar, these two sulfamates bound with different geometries in the active site of HCA II.^{230,233,523} Whereas topiramate made several hydrogen bonds to the hydrophilic face of the active site,²³³ EMATE bound entirely to the hydrophobic wall (Val121, Phe131, Val135, and Pro202).²³⁰ Interestingly, although 2-MeOE2bisMATE (**186a**) is similar in structure to EMATE (**186**, see Table 4), and although ionization of the sulfamate on the aryl ring is more favorable than ionization of the sulfamate on the cyclopentyl ring, **186a** binds to HCA II by means of the sulfamate on the cyclopentyl ring (presumably because of steric interactions between the enzyme and the methoxy group on the aryl ring of **186a**).¹²⁸

EMATE and 667-coumate bind to HCA II with similar geometries, but the $Zn^{II}-N$ bond is 0.36 Å shorter in the EMATE–HCA II complex.²¹⁷ The short $Zn^{II}-N$ bond (1.78 Å) with the sulfamate nitrogen atom of EMATE, contrary to most substituted benzenesulfonamides (1.9–2.15 Å), may contribute to the high affinity of EMATE for HCA II.²³⁰ A similarly shortened $Zn^{II}-N$ bond exists for compounds containing fluorinated benzene rings **55**, **57**, **210**, and **211**, as well as the tight-binding compound **110** ($K_d = 0.23$ nM).^{180,182,189}

The next step in violating the conventional dogma for inhibitors of CA was the complete removal of the aromatic moiety. Supuran and co-workers investigated the binding of sulfamic acid (**192**, $K_i = 0.39$ mM, HCA II) and sulfamide (**279**, $K_i = 1.13$ mM, HCA II) to HCA I, HCA II, BCA II, and BCA IV,^{228,233,413,519} and, more recently, of *N*-hydroxy-sulfamide (**280**, $K_i = 566$ nM, HCA II) to HCA I, II, IX, and XII.²²⁷ X-ray structures of these compounds with HCA II show new hydrogen bonds (not observed with aryl sulfonamides) in an intricate hydrogen-binding network between the inhibitor, enzyme, and solvent molecules.^{227,228} Tight binding to HCA I and II is restored for arylsulfonyl- and arylsulfonylureido-derivatives of sulfamates and sulfamides.^{228,526} Many of these derivatives bind more tightly

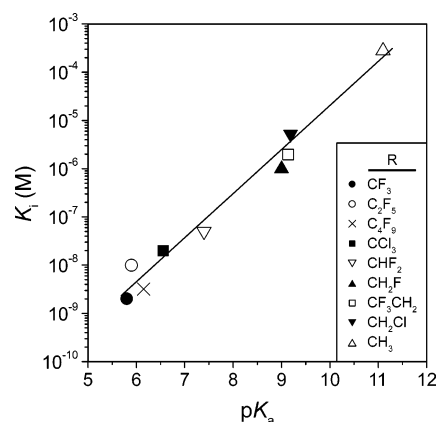


Figure 12. Linear dependence between K_i (on a logarithmic scale) and pK_a for a series of halogen-substituted unbranched aliphatic sulfonamides ($R-SO_2NH_2$). Data taken from ref 528.

to some isozymes than do the arylsulfonamides with the same aromatic moiety.⁵²⁷ Some derivatives have a higher affinity for HCA I than for HCA II; thus, arylsulfamates and arylsulfamides may be useful as isozyme-specific inhibitors (see section 9.2.4).

Scholz et al. first characterized trifluoromethanesulfonamide (**188**) as an inhibitor of HCA II.⁵⁰⁵ The surprising result was that this relatively simple molecule had a very high affinity ($IC_{50} = 13$ nM, $K_d = 50$ nM). The result was all the more astonishing given the low affinity of methanesulfonamide (**189**) ($IC_{50} = 70$ μM). The greater potency of the fluorinated sulfonamide **188** was attributed to the fact that it has a much lower value of pK_a than does **189** (6.3 vs 10.8) (current understanding of the high affinity of **188** also includes contacts between the trifluoromethyl group and the enzyme; see section 10.3.4). Further work by Maren et al. found a linear dependence between $\log K_i$ and pK_a across a number of fluorine- and chlorine-substituted methanesulfonamides⁵²⁸ (Figure 12). Such a trend had been found previously for the *para*-substituted benzenesulfonamides.⁵⁰³ The dependence of affinity on pK_a is discussed in detail in section 10.3.

Scholz et al. suggested a more extensive, quantitative structure–activity relationship (QSAR) to describe the binding of aliphatic sulfonamides to HCA II.⁵⁰⁵ In their model, inhibitory activity is determined by the inductive effects of substituents vicinal to the sulfonamide moiety (these substituents presumably influence the pK_a of the sulfonamide) combined with the steric bulk of these substituents (steric repulsion in the congested active site region near the Zn^{II} cofactor). The third term in the QSAR represents an increase in affinity with increasing hydrophobicity ($\log P$) of the aliphatic chain attached to the sulfonamide. Increasing the hydrophobicity of the chains was hypothesized to increase the interaction of the inhibitor with the hydrophobic wall of the active site of the enzyme (see section 4) and, thus, to contribute to the stability of the complex. The influence of $\log P$ and hydrophobic surface area on affinity are discussed in detail in section 10.4.

9.2.3. “Tail Approach”

The “tail approach”—a term coined by Supuran and co-workers²—is an approach to the development of leads that is complementary to the “ring approach” described in section 9.2.1. The goal of this approach was to increase aqueous solubility at neutral pH in order to obviate the clinical side

effects of such inhibitors as dorzolamide, which are only soluble in acidic media. It involved the derivatization of well-characterized aromatic sulfonamides with ionizable moieties, such as secondary or primary amines or carboxylates. The intent of this approach was to optimize characteristics required for applications *in vivo* (e.g., to ensure penetration via the cornea for topical therapeutic applications) and so is outside of the scope of this review. We, therefore, present only a few comments here.

The first example of this approach involved modifying the exocyclic acetyl group of acetazolamide by the attachment of a variety of amino acids.⁵²⁹ Antonaroli et al. adopted a similar approach but utilized dioic fatty acids as their acylating agents.⁵³⁰ Values of K_i on the order of low micromolar were observed in both cases. Supuran et al. developed this approach by using a range of ionizable moieties and precursor molecules and by characterizing the inhibitors using *in vivo* models. This material has been reviewed elsewhere.^{2,15}

9.2.4. Isozyme-Specific Inhibitors

When targeting isozymes other than HCA II, most of the side effects of the clinically used sulfonamides—for example, acetazolamide (**137**), methazolamide (**138**), ethoxzolamide (**140**), dorzolamide (**157**), and brinzolamide (**161**)—are probably due to inhibition of HCA II; many tissues and organs, in which targeting HCA II may be undesirable, contain large amounts of this isozyme.¹⁵ It is, therefore, desirable to design inhibitors that bind more weakly to HCA II than to other isozymes. The high degree of sequence and structural homology among HCA I, II, and IV (see section 4) has made the synthesis of isozyme-selective inhibitors very difficult. The initial generalization (from the use of HCA I and BCA II and IV)⁵³¹ that sulfonamides appear to bind more tightly to CA II and IV than to CA I, while inorganic anions seem to bind more tightly to CA I than to CA II and IV, seems to hold.² HCA II and BCA IV show remarkably similar affinities to inhibitors.⁵²⁸ Distinguishing between these two major drug targets (specifically, HCA II and HCA IV) has, therefore, proven particularly difficult; attempts to design inhibitors selective for CA IV over CA II are presented briefly here.

Given their extensive structural homology, including a similar orientation of His64 in the proton shuttle (see section 4.6), the most successful approaches to designing inhibitors capable of differentiating between CA II and IV have involved exploiting their different subcellular locations. CA II is a cytosolic protein, while CA IV is membrane-associated, with its active site oriented toward the extracellular space. Thus, membrane-impermeable inhibitors should be capable of inhibiting CA IV without affecting CA II. This possibility has been realized both *in vitro* and *in vivo* by using polymeric^{532,533} and cationic^{2,7} sulfonamides.

Isozyme-specific inhibitors may also be useful for targeting isozymes involved in tumorigenesis (such as HCA IX and XII)^{88,534} or in lipogenesis (HCA VA and HCA VB).^{27,535} Supuran and co-workers employed sugar tails (e.g., **124–130**) to design sulfonamides that were water-soluble and specific for isozyme IX.^{510,536} Winum et al. investigated the inhibition of 10 isozymes of HCA by the sulfamide analogue (**187b**) of topiramate (**187a**).²³² Compound **187b** was a less potent inhibitor of HCA II than **187a** (by a factor of $\sim 10^2$) but effectively inhibited isozymes VA, VB, VII, XIII, and XIV (with K_i values in the range 21–35 nM). The X-ray

structure of **187b** with HCA II showed that its weak inhibition of HCA II was due to a clash between a methyl group of the inhibitor and Ala65, which is a residue unique to HCA II¹³⁹ (e.g., the corresponding residue is Ser in HCA I,²³⁹ IV,²²⁴ VB,⁵³⁷ VII,⁵³⁸ IX,⁵³⁹ XII,²¹⁰ and BCA II,¹⁴⁷ Thr in HCA III,²⁴² VI,⁵⁴⁰ and VIII;⁵⁴¹ and Leu in HCA VA,⁵³⁷ see Table 4 for the PDB numbers of HCA I–IV and XII and Table 3 for BCA II). Other compounds may, therefore, be designed to have a low affinity for HCA II by exploiting this interaction.

9.2.5. Inhibition by Small Monoanions

Simple monoanions can inhibit CA, although more weakly than arylsulfonamides (**192–205**, Table 10). These studies are important not only for understanding protein–ligand interactions but also for knowing how anions present as constituents in the buffer medium may influence binding studies. Roughton and Booth first showed that small inorganic anions could inhibit CA.⁴⁴⁸ In 1965, Kernohan reported the use of stopped-flow fluorescence to measure the kinetics of the binding of Cl^- and NO_3^- to BCA II as a function of pH.²⁹⁹ Lindskog examined a larger series of anionic inhibitors (F^- , Cl^- , Br^- , I^- , NO_3^- , and NCO^-) of Co^{II} –BCA II using the CO_2 kinetic assay and spectrophotometric titrations.³⁰¹ Prabhananda et al. reported values of K_d , determined by spectrophotometric titration, for Co^{II} –BCA II binding to NCO^- , SCN^- , and CN^- .²⁹¹

Pocker et al. reported values of K_d for a large series of small, anionic inhibitors, and these values are listed in Table 10.¹⁵⁷ X-ray structural data (Table 4) show that most anions (e.g., Br^- and N_3^- ,¹⁹⁵ I^- ,¹⁹⁶ HS^- ,¹⁹⁷ HCO_3^- ,¹⁹⁸ HSO_3^- ,¹⁸⁴ H_2NSO_3^- ,²²⁸ SO_4^{2-} ,¹⁸³ and foscarnet ($-\text{O}_2\text{C}-\text{PO}_3^{2-}$)²²⁵) displace the Zn^{II} -bound water and bind to the Zn^{II} cofactor in a tetrahedral geometry, whereas SCN^- ¹⁸⁶ and NO_3^- ¹⁹⁷ do not displace the water. These two anions expand the coordination sphere of the Zn^{II} cofactor and bind to Zn^{II} in a distorted pentagonal geometry (see section 4.6). A trend in the values of K_d for the halides favors binding of the largest, most polarizable, least strongly solvated ion, iodide. The obvious outlier in the series, CN^- , is the best σ -donor of all the compounds listed, and although d_{10} metals are relatively poor electron donors, the cyanide ligand is also the strongest π -acceptor in the series. Moreover, due to the strong ligand field of the CN^- ion, two equivalents can bind to the Zn^{II} cofactor and distort the tetrahedral geometry.²⁹¹

Studies of protein–ligand interactions are typically performed in buffered solution. The binding data discussed in this section indicate that the identity and concentration of the small, anionic component(s) of the buffer are important in the analysis of binding constants and X-ray structures (see section 4.3). In a buffer containing a concentration of inorganic anion that approximates or exceeds its K_d , one must consider the binding of a ligand, such as an arylsulfonamide, to be a competition reaction—that is, the observed equilibrium involves exchange of inorganic anion with sulfonamide anion.

9.2.6. Derivatives of Arylsulfonic Acids

Binding of the sulfonamide group, $\text{R}-\text{SO}_2\text{NH}_2$, as its anion, $\text{R}-\text{SO}_2\text{NH}^-$, to the Zn^{II} ion in the binding site of CA has been the basic foundation for the design of CA inhibitors for over 50 years.⁵⁴² Other functional groups are, however, not only possible but moderately effective. Supuran and co-workers have explored a wide range of alternative arylsul-

fonic acid derivatives of formula $R-SO_2-X$ (**168–179**, Table 10), and they have reviewed this topic elsewhere.² Among the $R = p\text{-MePh}$ series, the most potent inhibitor of HCA II was $X = \text{NHCl}$ with $K_i = 2.1 \mu\text{M}$.⁵¹⁹ Although these compounds are relatively weak inhibitors of CA, they were used as leads to develop numerous nM inhibitors of HCA II (**138–140**, Table 10). In contrast to sulfonamide-based inhibitors, which have little isozyme selectivity, numerous sulfonic acid derivatives showed significant selectivity (up to 20-fold) for either HCA I or HCA II (see sections 9.2.2 and 9.2.4). These examples serve to illustrate that the sulfonamide head group is not necessary for effective inhibition of CA.

9.3. Kinetics of Binding

Studies of the kinetics of binding for inhibition of CA have revealed important features regarding the mechanism of inhibition by arylsulfonamide inhibitors and their derivatives. We outlined methods for measuring the kinetics of binding in section 8.3. Burgen and co-workers reported several important experiments that used stopped-flow fluorescence to establish a correlation between the pH of the inhibitor and the dissociation constant (K_d) and between K_d and the apparent rate constant for bimolecular association (k_{on}).^{302,389,458} In addition, the rates of binding measured by affinity capillary electrophoresis (ACE; see sections 8.3.3 and 14) and surface plasmon resonance spectroscopy (SPR; see section 12) have been reported. These data are discussed further, along with possible mechanisms for CA–sulfonamide binding, in section 11.

9.4. Combinatorial Approaches to Ligand Design

An approach to the design of effective inhibitors of CA involves combinatorial methods—that is, the generation of libraries of possible candidates and the selection of interesting compounds from these libraries. Several combinatorial approaches have utilized CA as the model enzyme. Supuran and co-workers reported the synthesis and screening of a library of arylsulfonamide inhibitors of HCA I and II using solid-phase synthesis; interestingly, their screening method assayed the resin-bound inhibitors.⁵⁴³

Burbaum et al. used BCA II as the model enzyme to test the concept of encoded combinatorial libraries for small-molecule drug discovery due to the synthetic accessibility of arylsulfonamides and the extensive structural and medicinal knowledge of their interactions with BCA II.⁵⁰⁶ They constructed two libraries based on benzenesulfonamide—one containing 1143 compounds and the other containing 6727 compounds. Using the dansylamide (DNSA, **133**) displacement assay to measure binding affinity, their technique identified two inhibitors, one of which (**108**) had a K_d of 4 nM.

Sigal et al. reported a library of peptide conjugates based on *para*-substituted derivatives of compound **36**.⁵⁰⁷ The compounds of general formula, $H_2NSO_2C_6H_4-(Gly)_n-AA$, kept the benzene sulfonamide portion constant while varying the number of Gly residues ($n = 0–3$) and the identity of the terminal amino acid residue (AA). For the most effective series ($n = 0$, **89–103**), hydrophobic amino acids increased the affinity by 1–2 orders of magnitude (from $K_d \approx 100–1000$ nM to $K_d \approx 10$ nM), whereas hydrophilic residues did not enhance affinity. The series with $n = 1–3$ displayed little change in affinity as a function of the amino acids incorporated (see section 10.5).

Huc and Lehn described the use of virtual combinatorial libraries—the reversible formation of inhibitors from a library of components or fragments—to form sulfonamide inhibitors from amine and aldehyde components.⁵⁴⁴ They used BCA II as the model system to develop this technique because the mechanism of binding is well-understood and because arylsulfonamide inhibitors are structurally simple and synthetically accessible.⁵⁴⁴ The presence of BCA II enhanced the production of certain combinations, suggesting specificity of the enzyme for particular sulfonamides. This “dynamic combinatorial library” approach was extended to include *irreversible* covalent interactions as the basis for combining components of the library to generate compounds of structure $H_2NSO_2C_6H_4CH_2SCH_2R$ (**11–15**) from the fragment thiols and alkyl chlorides.³⁸⁴ For a given pair of sulfonamide products, the presence of BCA II in the reaction mixture enhanced the formation of the product with the higher affinity for BCA II. In addition, the labs of Sharpless, Wong, and Kolb have developed inhibitors for HCA II using “click chemistry” (the [1,3]-dipolar cycloaddition reaction between azides and acetylenes)⁵⁴⁵ in combination with selection methods.⁵⁴⁶

DNA-based libraries have been useful in identifying inhibitors of BCA.^{414,547} Doyon et al. reported a technique for using BCA to enrich the concentration of their target inhibitors within a small library of inhibitors.⁵⁴⁷ They linked each inhibitor to a unique sequence of DNA, which served as a means to amplify and identify the enriched species. They used *para*-phenylglycine-linked benzenesulfonamide, which is similar to the highly effective compound **106**, as the target for BCA. Among the seven proteins in their study, BCA was among the most effective in terms of needing a minimum quantity of protein in order to provide an enrichment factor of >50-fold. This type of study illustrates how CA, among other proteins, can be used as a model for developing new methods in combinatorial selection.

Smith, Whitesides, and co-workers described the use of electrospray ionization Fourier transform ion cyclotron resonance spectrometry (ESI-FTICR-MS; see section 8.3.7) to select for high-affinity ligands for BCA II.^{443,444} We discuss this approach in section 13.2.

9.5. Computational Approaches to Ligand Design

With the increase in availability of high-resolution structures of proteins, computational chemistry is becoming a useful approach to designing drugs and to understanding the basis for drug–protein interactions.^{5,548–553} Grzybowski et al. reported an *in silico* combinatorial method (CombiSMoG^{554,555}) that employs simulation to generate a virtual library of inhibitors and then to rate the candidate inhibitors by their binding free energies generated using knowledge-based potential functions.¹⁸⁹ HCA II was used as the model enzyme for this study for several reasons: (i) The location of the benzenesulfonamide group could be specified. (ii) The inhibitors were small, uncharged, and easy to test experimentally. (iii) The enzyme is relatively rigid, and the active site is relatively plastic. (iv) The inhibitors have low molecular weight, and the benzenesulfonamide moiety is rigid. (v) The orientation of the inhibitor in the active site is well-defined. The first demonstration of this technique produced **109** (Table 10), which is the highest-affinity inhibitor of CA known to date ($K_d = 0.03$ nM as measured by the DNSA competitive binding assay). This compound bound to HCA II approximately 8-fold more

tightly than its enantiomer, **110**, in agreement with relative ordering of affinities for these two ligands from the CombiSMoG approach. In addition, the calculated structure of the HCA II–ligand complex was in satisfactory agreement with the observed X-ray crystal structure of the complex, for both of the ligands. This technique demonstrated the potential for the combination of structure and computation in the design of high-affinity inhibitors of proteins. We discuss the binding of this ligand to HCA II in detail in section 10.5.

Rossi et al. reported the use of HCA II to assess the efficacy of using the free energy perturbation (FEP) method to predict relative free energies ($\Delta\Delta G$) and the concomitant structural changes among different complexes of HCA II with arylsulfonamides.⁶⁰ FEP is a computational approach that starts with one molecule (e.g., a CA–sulfonamide_A complex) and slowly modifies it to another molecule (e.g., CA–sulfonamide_B) by adjusting the parameters that describe the molecule. In the reported study, they compared the complexes of HCA II with several inhibitors that were closely related in structure. They found that, although FEP did not accurately predict the exact structural perturbation of HCA II, it did predict the energetic trends among the three compounds with acceptable accuracy. FEP predicted the best inhibitor in the small set examined, but it did not predict the structural details of that complex as effectively. While this study shows that the FEP method is applicable to studies in ligand design, it suggests caution in such studies.

Grüneberg et al. reported the use of structure-based algorithms to score the relative predicted binding affinities for a group of compounds with HCA II.⁵⁵⁶ They found, however, that there was relatively little correlation between the predicted affinities and the measured inhibition constants.

9.6. Conclusions

Ligands of very diverse structure (e.g., small monoanions, alkyl sulfamates, etc.) bind to and inhibit CA. There do not seem to be any “essential components” for moderate-affinity ($\sim\mu\text{M}$) ligands: the sulfonamide, aryl ring, tail, and secondary recognition element can all be removed to generate ligands with some affinity (indeed, can there be any structurally simpler ligands than the small inorganic monoanions?). In spite of the broad structural diversity of ligands that have been examined, the highest-affinity class of ligands remains the arylsulfonamides. In section 10, we attempt to determine why the arylsulfonamides bind with such high affinity. Further, we use the system of arylsulfonamides and CA as a model to understand how to design high-affinity ligands for proteins rationally (or, more precisely, what the opportunities and challenges of designing ligands rationally are).

10. Using CA to Study the Physical-Organic Chemistry of Protein–Ligand Interactions

10.1. Overview

We have four objectives in this section: (i) to review why the system comprising carbonic anhydrase (CA) and arylsulfonamides is a good choice for a model system with which to study protein–ligand binding; (ii) to clarify details of the thermodynamic model of binding of arylsulfonamides to CA; (iii) to explain how to use CA and arylsulfonamides as a model for ligand design through the separation of the influence on affinity of the different structural components

of the arylsulfonamide; and (iv) to use that understanding to explore methods for using CA to test methods in ligand design (e.g., Lewis basicity, hydrophobicity, and multivalency).

Section 9 describes the different classes of ligands for CA. Here, we focus on *para*-substituted arylsulfonamides (particularly *p*-substituted benzenesulfonamides, *p*-RC₆H₄SO₂NH₂; Figure 11A), because (i) these compounds are easy to synthesize in great variety, (ii) the mode of binding of these sulfonamides to CA is essentially conserved for all arylsulfonamides and many isozymes of CA, and (iii) for *p*-RC₆H₄SO₂NH₂, the mode of binding is independent of the substituent R. We focus our analysis on the binding of arylsulfonamides to carbonic anhydrase II (both the human, HCA, and bovine, BCA, versions), because this isozyme is the best characterized biophysically of the carbonic anhydrases (see section 2). The important interactions (Figures 11 and 12; see sections 4.6–4.8) between the sulfonamide and CA are between (i) the ionized sulfonamide and the Zn^{II} cofactor of CA (forming *p*-RC₆H₄SO₂NH–Zn^{II}–CA and resulting in displacement of the zinc-bound water, CA–Zn^{II}–OH₂⁺/CA–Zn^{II}–OH), (ii) the sulfonamide head group, SO₂NH, and hydrogen-bond acceptors and donors of residues of the active site of CA, (iii) the aryl ring and the hydrophobic pocket of CA, (iv) the tail region and a nonpolar surface of CA just outside of the active site, and (v) the secondary recognition element (SRE) and a surface outside of the active site and near the periphery of the conical cleft of the enzyme (the so-called “hydrophobic wall”).

In this section, we exploit the conserved mode of binding of arylsulfonamides to CA to examine these different interactions *separately* as the structure of the ligand is changed. This analysis suggests that all of the interactions listed above (i–v) contribute to the affinity of arylsulfonamides for CA. For instance, using an aryl ring larger than a phenyl ring (iii), a tail (iv), and/or an SRE (v) in ligand design can generate ligands with affinities higher than a hypothetical benzenesulfonamide with the same value of p*K*_a (and, thus, with the same strengths of the Zn^{II}–N bond and hydrogen bonds) as the ligand.

Since we are only examining arylsulfonamides in this section, the –SO₂NH₂ moiety of the ligand is conserved. We do not separate structural perturbations that affect the hydrogen-bond network of the SO₂NH from those that affect the ionized sulfonamide, ArSO₂NH[–]; instead, we consider perturbations that affect the total “head group” together (Figure 11A).

We adopt a four-part organization in this section:

(i) we discuss briefly the challenges in the rational design of ligands that bind with high affinity to proteins based on structural information, the utility of the system comprising CA and arylsulfonamides in developing rules or principles useful in this kind of design, and the interactions that make arylsulfonamides good ligands for CA (section 10.2);

(ii) we explore separately the influence of variations in the structure of arylsulfonamides that affect the head region (section 10.3), aryl ring (section 10.3), tail region (section 10.4), and secondary recognition element (the concept of multivalency, section 10.5) on the affinity (*K*_d^{obs}) of arylsulfonamides for CA (Figure 11B);

(iii) we dissect the thermodynamics of binding of arylsulfonamides to CA into enthalpy and entropy of binding and separately discuss the influence of perturbations in the

regions of the head, ring, and tail on these observed thermodynamic parameters (section 10.6); and

(iv) we summarize what the study of the system of CA/arylsulfonamides teaches us about the rational design of ligands that can (in principle) be applied to other systems (section 10.9).

10.2. Challenges in Rational Ligand Design

We only discuss the challenges of designing high-affinity ligands for proteins (and the system of CA and arylsulfonamides as a model in this effort) and do not discuss those of designing *drugs*. There are a number of issues involved in converting a high-affinity ligand into a drug, but these issues have more to do with physiology and in vivo pharmacology than with physical-organic chemistry. There are several worthwhile reviews that discuss CA as a *drug* target.^{2,15}

10.2.1. General Concepts

Although the subject of more than 50 years of study, designing high-affinity ligands for proteins of known structure—a problem of molecular recognition in aqueous solution that is presumably tailor-made for chemistry—remains an elusive goal. The primary reason for our inability to do so seems to be our lack of adequate understanding of the physical principles that underlie the association of protein and ligand in water.^{4,5}

(1) Water and the hydrophobic effect: The hydrophobic effect—the propensity of hydrophobic molecular surfaces to coalesce in aqueous solution—is dominated by entropy at room temperature and is accompanied by a large negative change in the specific heat capacity.^{4,557} The hydrophobic effect has been rationalized by invoking the entropically favorable release of ordered water molecules (which surround hydrophobic surfaces) when the hydrophobic surfaces coalesce and/or the energetic penalty of creating a cavity in water; the relative importance of the two is still unclear.^{4,557–560} Conceptually, we still do not understand the structure of water around hydrophobic groups or the influence of hydrogen bonding (as opposed to the size) of water on the hydrophobic effect. Since many protein–ligand binding events are believed to be dominated by the hydrophobic effect, understanding the origin of this effect is clearly important in efforts to engineer these interactions rationally.

(2) Electrostatic interactions in water: In vacuum, the free energies of attraction of unlike point charges, and of repulsion of like ones, are given by Coulomb's law.⁵⁶¹ In solution, solvation complicates the calculation of such free energies. The key issues that have not been clearly addressed include the dielectric constant at the interface of protein and ligand (crucial because the energy of association is inversely proportional to the dielectric constant), the thermodynamic driving force for electrostatic interactions (while, intuitively, it might be expected to be enthalpy, recent analyses reviewed by Gitlin et al.³⁹⁷ suggest that it is, in fact, entropy), and the charge compensation between ionizable residues of a protein.^{4,397,561}

(3) Protein plasticity: As Beece⁵⁶² stated, “A protein is not like a solid house into which the visitor (the ligand) enters by opening doors without changing the structure. Rather it is like a tent into which a cow strays.” Many proteins undergo large conformational changes upon binding ligands or substrates; this plasticity is one reason why rationally designing a ligand to bind to a protein—a flexible structure—has been difficult.^{563–565} Vamvaca et al. reported that a

monomeric, structurally disordered chorismate mutase could be ordered into a structured binding site with catalytic activity by binding a transition-state analogue ligand.⁵⁶⁴ Benkovic and Hammes-Schiffer analyzed the catalytic activity of a number of mutants of dihydrofolate reductase and demonstrated that amino acid residues far (~ 20 Å) from one another in the tertiary structure of a protein can influence the binding of ligands in a cooperative (or synergistic) fashion.⁵⁶⁵ This idea of structural, energetic coupling of well-separated amino acid residues is still a difficult one to understand and makes the rational design of high-affinity ligands particularly difficult.

(4) Estimating the change in entropy: The entropy of protein–ligand complexation is an aggregate value taking into account the losses in translational and rotational entropy of the ligand (and the protein, see (3) above),^{5,566,567} the loss in conformational mobility of the ligand (and the protein),^{5,566–568} new vibrational modes of the protein–ligand complex,⁵⁶⁶ loss of vibrational modes of the free protein,⁵⁶⁶ the burial of hydrophobic surface area upon complexation,^{4,557} and the release of solvent (and, perhaps, buffer or additive) molecules.⁵⁶⁶ The inability to estimate theoretically, or at the least to ascribe the observed change in entropy to, these individual components has been one of the more intractable problems in this area.

(5) Enthalpy/entropy compensation: In many cases of protein–ligand binding, the enthalpies of binding of a series of ligands are positively correlated with their entropies of binding; that is, as the structure of the ligand varies, changes in enthalpy are compensated by changes in entropy.^{403,569–573} This compensation has the effect of reducing changes in the free energy of binding with modifications to ligand structure and can even make the free energy of binding constant (although the fundamental thermodynamics and interactions vary) within a series of ligands. While qualitative theoretical models have been proposed,^{571,572} the quantitative physical basis for this phenomenon, and even the qualitative aspects of the model, remain undefined and are still subjects of debate.^{573–576} Understanding when and why enthalpy/entropy compensation should be expected (and the role, if any, of solvent and solvent release in the process) would facilitate the rational design of high-affinity ligands.

10.2.2. Enthalpy and Entropy of Binding

10.2.2.1. Why Separate Enthalpy and Entropy? Why Not Just Use Free Energy? The free energy of binding (ΔG°), which is directly proportional to the logarithm of the dissociation constant (K_d), has components of enthalpy (ΔH°) and entropy (ΔS°) of binding, although it is common that ΔH° and ΔS° are not distinguished in discussions of binding processes. In noncovalent interactions, complexation is often assumed to be driven by ΔH° , but ΔS° can play a major—even dominating—role in the thermodynamics of binding in water (see section 10.2.1). A primary contributor to a favorable ΔS° is the hydrophobic effect.^{4,557–560} Another contributor to a favorable ΔS° can be the residual mobility of the protein–ligand complex.⁴⁰³ For instance, the ligand can maintain significant mobility (and, thus, maintain a favorable entropy) in the complex, because good binding often seems to be surprisingly loose (in stark contrast to the historically honored model for the binding of a ligand to an enzyme³⁰—the insertion of a key into a lock or a hand into a glove (“induced fit”)).

Many investigators have argued that separating ΔH° and ΔS° is neither possible (due to experimental artifacts and

theoretical issues related to the temperature dependence of both terms) nor worthwhile and that the only important thermodynamic parameter is ΔG° .³⁰ We believe, however, that separating the two is possible with current experimental techniques (in particular, isothermal titration calorimetry)⁴⁰⁸ and that understanding the separate influence of ΔH° and ΔS° on protein–ligand binding should improve our ability to *design* high-affinity ligands. For instance, we must know accurately the magnitude of ΔS° in order to test models for protein–ligand binding based on hydrophobic contacts or on the residual mobility of the ligand in the protein–ligand complex.

The remainder of this section covers the two major techniques used to measure ΔH° and ΔS° of protein–ligand interactions—van't Hoff analysis and isothermal titration calorimetry (ITC)—as well as the compensation often observed between ΔH° and ΔS° . Section 10.5 discusses systematic studies of the separated thermodynamics of binding of arylsulfonamides to CA.

10.2.2.2. van't Hoff Analysis to Estimate Enthalpy and Entropy of Binding. Most estimates of enthalpy and entropy of binding of arylsulfonamides to CA (and, in general, of most ligands to proteins) have measured the temperature-dependence of the dissociation constant (K_d) and analyzed the data using the method of van't Hoff (eq 14),

$$\ln K_d = \frac{\Delta H^\circ}{RT} - \frac{\Delta S^\circ}{R} \quad (14a)$$

$$\frac{d \ln K_d}{d(T^{-1})} = \frac{\Delta H^\circ}{R} \quad (14b)$$

where T is the temperature in K, R is the ideal gas constant in kcal mol⁻¹ K⁻¹, ΔH° is the enthalpy of binding in kcal mol⁻¹, and ΔS° is the entropy of binding in kcal mol⁻¹ K⁻¹. Plotting $\ln K_d$ vs T^{-1} provides ΔH° from the slope and ΔS° from the y-intercept.

Because ΔH° and ΔS° are assumed to be temperature-independent, this analysis is predicated on a negligible change in heat capacity (ΔC_p) upon binding.⁵⁷⁷ Large changes in heat capacity are often observed for hydrophobic interactions in water (see section 10.2.1)^{4,557} and can result in deviations from eq 14 and in curvature in van't Hoff plots. Further, the dielectric constant of water has an anomalously strong dependence on temperature; this dependence changes the magnitude of electrostatic interactions with temperature.³⁹⁷ Only a limited range of temperatures can be examined by van't Hoff analysis of proteins (because the structure of the protein can itself be temperature-dependent), and extrapolation to a very distant y-intercept is necessary to estimate the entropy of binding. This sort of extrapolation notoriously yields uncertain values of enthalpy and entropy.⁵⁷⁴

Equation 15 shows a more complicated form of eq 14a that allows for a nonzero, temperature-independent change in heat capacity (ΔC_p) upon binding^{577,578}

$$\ln \left(\frac{K_d}{K_d^0} \right) = \frac{\Delta H_0 - T_0 \Delta C_p}{R} \left(\frac{1}{T_0} - \frac{1}{T} \right) + \frac{\Delta C_p}{R} \ln \left(\frac{T}{T_0} \right) \quad (15)$$

where T_0 is an arbitrarily selected reference temperature (usually 298 K), K_d^0 is the dissociation constant at T_0 , and ΔH_0 is the enthalpy of binding at T_0 . This equation, however, can still give thermodynamic parameters that differ from

those obtained calorimetrically,^{578–580} and it is still subject to errors from probing a limited range of temperature.

10.2.2.3. Isothermal Titration Calorimetry to Measure Directly Enthalpy and Entropy of Binding. Isothermal titration calorimetry is currently the most accurate technique for estimating the dissected thermodynamic contributions to binding because it measures directly the heat released (and so, the enthalpy of binding) when protein is titrated with ligand at constant temperature.⁴⁰⁸ The sensitivity of commercially available microcalorimeters (see section 8.2.4) allows for the measurement of heat released at each step during a titration and, thus, provides ΔG° in addition to ΔH° , from which ΔS° can be calculated.

10.2.2.4. Enthalpy/Entropy Compensation. As mentioned in section 10.2.1, the correlation between the enthalpy of binding for a series of ligands and the entropy of binding—a correlation that often minimizes changes in K_d with ligand structure^{403,569–573}—has complicated the rational design of high-affinity ligands. Gilli et al. undertook an extensive literature survey of values of enthalpy and entropy, determined by van't Hoff analysis, that characterized receptor–ligand binding.⁵⁶⁹ Their results revealed that enthalpy and entropy of binding were almost perfectly compensating for the association of 136 structurally unrelated, but therapeutically useful, ligands with 13 distinct macromolecular targets. They speculated that the limit in affinity ($K_d \approx 10$ pM) resulted (somehow) from this compensation between the entropy and enthalpy of binding.

Dunitz and Williams and co-workers sketched a theoretical framework for enthalpy/entropy compensation by approximating a protein–ligand complex as a potential energy well.^{571,572} Dunitz approached the issue semiquantitatively and used the Morse potential to estimate the dependence of the entropy of the complex (primarily due to the residual mobility of the ligand in the complex) on its enthalpy (bond dissociation energy).⁵⁷¹ From this analysis, he concluded that enthalpy/entropy compensation is associated with weak, intermolecular interactions in general and is not merely restricted to complexation in water. This theoretical model suggests an origin for the compensation between enthalpy and entropy of binding: a more tightly held protein–ligand complex (one with a more favorable enthalpy of binding) has less residual mobility (and a less favorable change in entropy due to greater entropic cost of complexation) than a less tightly held one.

Williams and co-workers have explored the dimerization of glycopeptide antibiotics in water as a model system for understanding protein–ligand complexation.^{581,582} They probed the “tightness” of the dimer interface (that is, the physical separation of monomer subunits) by NMR. They demonstrated that a tighter dimer interface was associated with both a more favorable free energy and a more favorable enthalpy of dimerization than a looser one.^{581,582} The more favorable enthalpy of dimerization was partially compensated by a more unfavorable entropy of dimerization: enthalpy/entropy compensation.⁵⁸² The observed compensation was not exact: the free energy of binding decreased (became more favorable) with decreasing (more favorable) enthalpy and with increasing tightness of the dimer interface.

10.2.3. Utility of the System of CA/Arylsulfonamides in This Effort

The system of carbonic anhydrase and arylsulfonamides offers four advantages in exploring approaches to the rational design of high-affinity ligands for proteins:

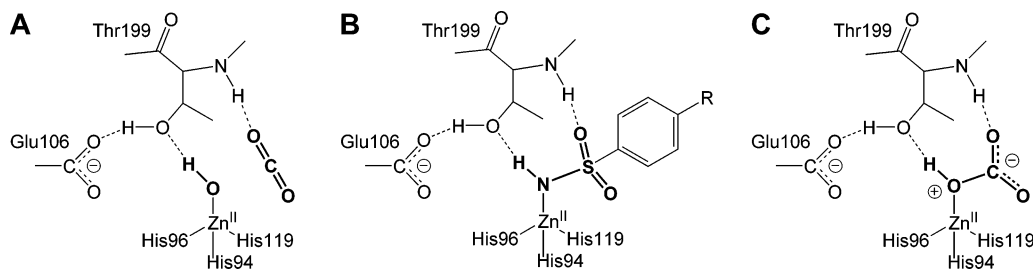


Figure 13. Diagram comparing (A) carbon dioxide (putative interactions), (B) an arylsulfonamide, and (C) bicarbonate bound in the active site of HCA II. The arylsulfonamide can be viewed as a transition-state analogue of the hydratase reaction ($\text{H}_2\text{O} + \text{CO}_2 \rightleftharpoons \text{HCO}_3^- + \text{H}^+$).

(i) CA is readily available from commercial sources (HCA I, HCA II, and BCA II) and its site-specific mutants from facile overexpression in *E. coli* (see section 4.2).

(ii) CA does not undergo *gross* conformational changes upon binding sulfonamides (see section 4.5). This lack of plasticity (see section 10.2.1) allows for a relatively straightforward interpretation of thermodynamic and kinetic data because the protein, to a first approximation, can be treated as rigid (rms deviation $\approx 0.2\text{--}0.3$ Å between ligand-free and ligand-bound forms of HCA II).^{283,284} The individual amino acid side chains lining the active site, particularly His64, are, however, still conformationally mobile. Subtle conformational changes or dynamics of these residues might affect affinity in ways that are hard to predict.

(iii) There are several convenient assays to measure binding (e.g., the inhibition of catalysis and the competitive displacement of fluorescent sulfonamides from the active site) (see section 8).

(iv) Compounds of structure $p\text{-RC}_6\text{H}_4\text{SO}_2\text{NH}_2$ (Figure 11A), *para*-substituted benzenesulfonamides, are easy to synthesize in great variety (see section 10.1). All of the relevant regions (head, ring, tail, and secondary recognition element) of their structure can be changed independently, and the influence of these changes on binding to CA can be assessed separately. For example, the system allows the separate study, and evaluation of importance to affinity, of the influence of substituents (R) on the nucleophilicity of $\text{RC}_6\text{H}_4\text{SO}_2\text{NH}^-$ toward the Zn^{II} cofactor and on the hydrophobicity of the ligand.

10.2.4. Why Are Arylsulfonamides Such Good Ligands for CA?

10.2.4.1. Sulfonamides as Transition-State Analogues for the Hydration of Carbon Dioxide. In this section, we address the particular structural features that make sulfonamides superior to other classes of molecules for binding to CA. For many enzymes, molecules that mimic the transition state of the catalyzed reaction make good ligands.³⁰ This concept seems to apply to CA. The structure of CA with a bound sulfonamide resembles the structure of CA with the native substrates, hydroxide and CO_2 (putative) or HCO_3^- , bound in its active site (Figure 13).^{64,184,198,199,583} In a CA–sulfonamide complex, the sulfonamide nitrogen anion coordinates to the Zn^{II} cofactor, the sulfonamide NH donates a hydrogen bond to the O_γ of Thr199, one sulfonamide oxygen accepts a hydrogen bond from the backbone NH of Thr199, and the other sulfonamide oxygen coordinates weakly at a fifth position on the Zn^{II} (Figures 11B and 12B). This arrangement mimics the structure of CA bound to bicarbonate (Figure 13C), where the bicarbonate oxygen coordinates to the Zn^{II} cofactor, the bicarbonate OH donates a hydrogen bond to the O_γ of Thr199, one bicarbonate

oxygen accepts a hydrogen bond from the backbone NH of Thr199, and the other bicarbonate oxygen coordinates weakly at a fifth position on the Zn^{II} cofactor.

10.2.4.2. $\text{Zn}^{\text{II}}\text{--N}$ Bond. Upon binding, the *ionized* sulfonamide nitrogen displaces the zinc-bound water ($\text{Zn}^{\text{II}}\text{--OH} / \text{Zn}^{\text{II}}\text{--OH}_2^+$) and interacts directly with the Zn^{II} cofactor (see section 4). To our knowledge, all high-affinity ligands that have been reported make use of the $\text{Zn}^{\text{II}}\text{--N}$ bond. For instance, Scolnick et al. have shown that hydroxamic acids (RCONHOH), which bind to Zn^{II} -containing metalloproteases by bidentate chelation of the Zn^{II} by the carbonyl and hydroxyl groups of the ligand, bind to HCA II in a mode similar to that used by sulfonamides: the ionized nitrogen binds directly to Zn^{II} and the carbonyl group of the ligand accepts a hydrogen bond from the backbone NH group of Thr199.²⁰⁰

10.2.4.3. Hydrogen-Bond Network. The “hydrogen-bond network” between ligand and CA is also crucial for high-affinity binding (Figure 7). On the basis of free-energy perturbation simulations of the binding of a benzenesulfonamide and a benzenesulfonate to HCA II, Merz et al. argued that an important reason that sulfonates are weaker ligands for HCA II than are sulfonamides is because a sulfonate bound to HCA II lacks the ability of a sulfonamide to donate a hydrogen bond to O_γ of Thr199.⁵⁸⁴ Their simulations suggested that binding of the sulfonate results in a repulsive $\text{O}\cdots\text{O}$ interaction between the anionic sulfonate oxygen and O_γ of Thr199, and that, in order to reduce this repulsion, Thr199 rotates and loses its hydrogen bond with Glu106.⁵⁸⁴ They concluded that the interaction between the sulfonamide NH and O_γ of Thr199 is an essential component of the specificity of HCA II for sulfonamides. While their results qualitatively supported one possibility for why sulfonates have lower affinities than sulfonamides, their simulations could not quantitatively explain the data. The experimental difference in free energy of binding (~ 10 kcal mol⁻¹) between benzenesulfonate and benzenesulfonamide is much greater than their calculated value (~ 5 kcal mol⁻¹).⁵⁸⁴ A large contribution to this difference could be the difference in energies between the $\text{Zn}^{\text{II}}\text{--N}$ bond (for sulfonamides) and the $\text{Zn}^{\text{II}}\text{--O}$ bond (for sulfonates); their simulations could probably not calculate these energies accurately because of difficulties in treating the Zn^{II} cofactor computationally.⁵⁸⁴ Regardless, Thr199 is believed to make important contacts to Zn^{II} -bound ligands, and this central role in determining ligand accessibility to the active site has led to Thr199 being termed the “doorkeeper residue”.^{184,289,294,585}

Suitable data to enable a direct estimate of the contribution of the hydrogen bond network to the free energy of binding of arylsulfonamides have not been reported. Liang et al. have reported that dansylamide (133) binds to a Thr199Ala mutant (a mutation that abolishes the hydrogen bond between the

sulfonamide NH and O γ of Thr199) of HCA II with a 4-fold lower affinity (difference in ΔG° of ~ 0.8 kcal mol $^{-1}$) than to wild-type HCA II.³⁰³ No estimate is available for the hydrogen bond between the backbone NH of Thr199 and the sulfonamide oxygen.

As mentioned in section 10.1, we do not explicitly discuss structural perturbations that affect the hydrogen-bond network alone, but rather discuss the influence of structural perturbations on the head group of the arylsulfonamide as a whole (Figure 11A).

10.2.4.4. Interactions between the Aryl Ring and the Hydrophobic Pocket of CA. Crystal structures of HCA II complexed with arylsulfonamides have revealed contacts between the aryl ring of the sulfonamide and the hydrophobic pocket of the enzyme (section 4.6).^{47,289,290} These contacts are believed to be primarily hydrophobic and to contribute to the free energy of binding;¹⁸² for instance, benzene-sulfonamide (**1**) binds to HCA II with $\sim 10^3$ -fold higher affinity than does methanesulfonamide (**189**). While QSAR analyses have suggested that the hydrophobicity of the aryl ring of the sulfonamide is important in affinity (see section 9.2.1),^{9,503,586,587} this idea has not been tested rigorously through a systematic examination of the affinity of simple sulfonamides of varying hydrophobicity. Most reports have complicated the issues of hydrophobicity and Lewis basicity of the sulfonamide on affinity. We attempt to examine these factors separately in section 10.3.

10.2.5. Conclusions

Rational ligand design has been, and remains, challenging because we do not understand the fundamental, underlying thermodynamic principles of molecular recognition in water. Using isothermal titration calorimetry to separate the influence of enthalpy and entropy on affinity will, we believe, make it possible to begin to understand (or rationalize) the thermodynamics of these systems. The system of CA and arylsulfonamides provides a useful model system to try to understand this subject because so many biophysical and thermodynamic (binding) data are available for it. It is a “simple” system (e.g., negligible conformational change of CA upon complexation with arylsulfonamides, conformationally rigid ligand, and relatively well-defined protein–ligand interactions) that generates as uncomplicated thermodynamic data as any system of protein and ligand now available. Even so, accurate and extensive thermodynamic data will be necessary, but not sufficient, for understanding even this simplest example of protein–ligand interactions. A complete description will also require physical models, statistical mechanics, perhaps molecular dynamics, and direct observation of water.

10.3. Influence of the Head Group of Arylsulfonamides on Their Binding to CA

10.3.1. General Approach

This section summarizes the influence of the sulfonamide head group on the affinity of arylsulfonamides for CA (Figure 11A); section 10.4 examines the influence of the tail region on affinity. Section 10.5 discusses the influence of structural perturbations on the enthalpy and entropy of binding of the sulfonamide head group. We conclude that much of the reported variation in affinity of arylsulfonamides can be explained by the influence of the pK_a of the arylsulfonamide on the head group; sulfonamides that deviate from our

analysis are likely taking advantage of contacts (especially hydrophobic contacts) between the aryl ring and CA.

10.3.2. pK_a Determines the Fraction of Arylsulfonamide Present in the Active, Ionized ($ArSO_2NH^-$) Form

We wish to separate the influence of the pK_a (a value that is affected by the structure of the ligand) of the arylsulfonamide on the fraction available in the “active” form (either anion or neutral) and on the Lewis basicity of $ArSO_2NH^-$ toward CA (toward the Zn^{II} cofactor and toward hydrogen-bond acceptors and donors in the active site; Figure 13B). Our objective in this section is to summarize the literature and to rationalize future efforts to design ligands that have the “best” pK_a for binding.

There are four possible schemes, which vary in the protonation states—that is, the active forms—of the two components, that might describe the binding of arylsulfonamides to CA (eqs 16–19). While the ionizable group (value of $pK_a \approx 6.6$ – 7.0 for CA II) on the enzyme has not been unambiguously identified and has been the subject of controversy in the literature, here we adopt the prevailing view that ionization occurs at the zinc-bound hydroxide/water ($CA-Zn^{II}-OH/CA-Zn^{II}-OH_2^+$).^{302,307,454,588}

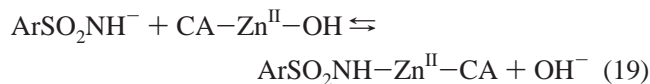
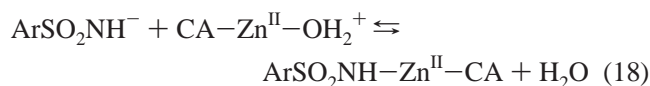
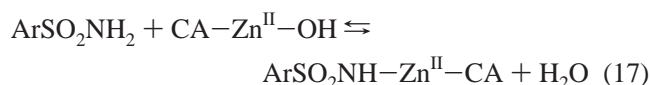
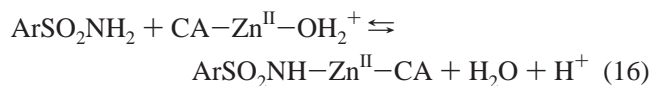


Figure 14A shows the fractions of arylsulfonamide and $CA-Zn^{II}-OH_2^+$ in the protonated and deprotonated forms, as a function of pH. Figure 14B shows simulated curves for the pH-dependence of the affinity of arylsulfonamides for CA II: the product of fractions of CA II and arylsulfonamide in the active forms specified in eqs 16–19. This figure also shows experimental data for the pH-dependence of K_d^{obs} for the complex between HCA II and *p*-nitrobenzenesulfonamide (**3**). Only the simulations to eqs 17 and 18 are compatible with these data; eqs 16 and 19 are not compatible with this pH-dependence, and so we rule out these thermodynamic models.

10.3.3. Selection of Standard Reaction for the Binding of Arylsulfonamides to CA

Scheme 1 shows the equilibria between the active forms of CA and arylsulfonamide specified in eqs 17 and 18. Equations 17 and 18 are thermodynamically indistinguishable (Figure 14B). We take the pathway involving $K_d^{ArSO_2NH^-}$ as the predominant one (although analyzing the pathway involving $K_d^{ArSO_2NH_2}$ would lead to the same conclusions for the “best” sulfonamides to bind to CA). We then calculate values of $K_d^{ArSO_2NH^-}$ using eqs 20 and 21, with literature values of pK_a for arylsulfonamides and for $CA-Zn^{II}-OH_2^+$ (we take this pK_a to be 6.8 for HCA II and 6.9 for BCA

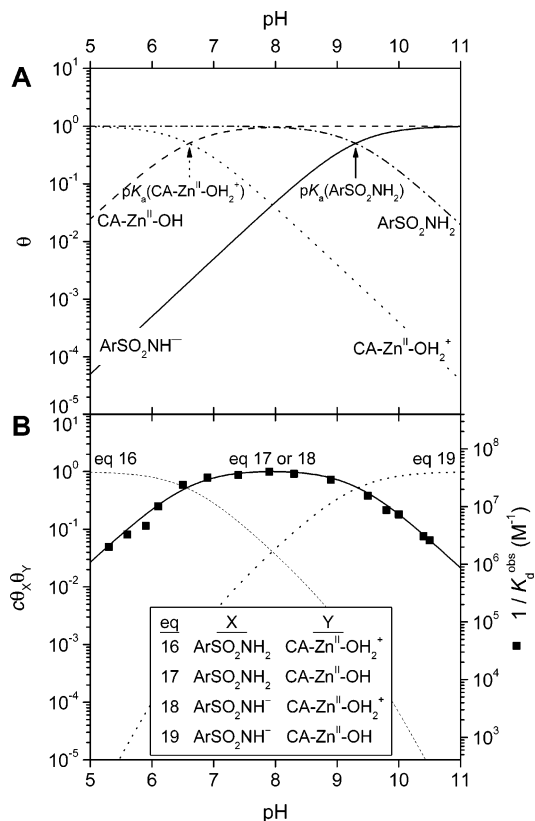
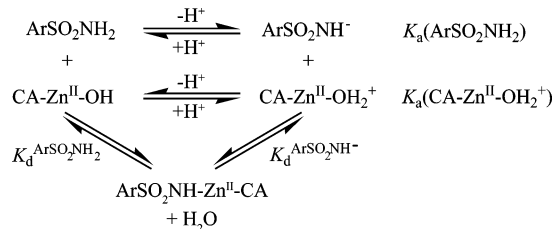


Figure 14. Fractions of arylsulfonamide and carbonic anhydrase II in their protonated and deprotonated forms, and the affinity of arylsulfonamides for HCA II, as a function of pH. (A) pH-dependence of the fractions (θ) of arylsulfonamide (ArSO_2NH_2 and ArSO_2NH^- , eq 20a) and carbonic anhydrase II ($\text{CA-Zn}^{\text{II}}-\text{OH}_2^+$ and $\text{CA-Zn}^{\text{II}}-\text{OH}$, eq 20b) in protonated and deprotonated forms. The values of $\text{p}K_{\text{a}}$ used were 6.6 for $\text{CA-Zn}^{\text{II}}-\text{OH}_2^+$ and 9.3 for ArSO_2NH_2 . (B) Simulations (shown as lines) and experimental data (shown as black squares for *p*-nitrobenzenesulfonamide, **3**; data taken from ref 302) of the affinity of arylsulfonamides for HCA II. The simulated curves are the products of the fractions of HCA II and arylsulfonamide in the reactive forms given in eqs 16–19 (see text). The curves have been scaled to give a maximum value of unity (using constant *c*) to facilitate comparisons between curves. Simulated curves using eqs 17 and 18 are identical, and thus, the two equations are thermodynamically indistinguishable.

Scheme 1. Equilibria for the Association of Arylsulfonamide ($\text{ArSO}_2\text{NH}_2/\text{ArSO}_2\text{NH}^-$) with Carbonic Anhydrase ($\text{CA-Zn}^{\text{II}}-\text{OH}_2^+/\text{CA-Zn}^{\text{II}}-\text{OH}$) (Reproduced with Permission from Ref 182; Copyright 2007 Wiley-VCH)



II,^{269,296,299} see section 4.7), the dissociation constant of binding ($K_{\text{d}}^{\text{obs}}$; Table 10), and the pH at which binding was measured:

$$\theta_{\text{ArSO}_2\text{NH}^-} = [1 + 10^{\text{p}K_{\text{a}}(\text{ArSO}_2\text{NH}_2) - \text{pH}}]^{-1} \quad (20\text{a})$$

$$\theta_{\text{CA-Zn}^{\text{II}}-\text{OH}_2^+} = [1 + 10^{\text{pH} - \text{p}K_{\text{a}}(\text{CA-Zn}^{\text{II}}-\text{OH}_2^+)}]^{-1} \quad (20\text{b})$$

$$K_{\text{d}}^{\text{ArSO}_2\text{NH}^-} = K_{\text{d}}^{\text{obs}} \theta_{\text{ArSO}_2\text{NH}^-} \theta_{\text{CA-Zn}^{\text{II}}-\text{OH}_2^+} \quad (21)$$

This analysis allows us to calculate a dissociation constant for the reaction between $\text{CA-Zn}^{\text{II}}-\text{OH}_2^+$ and the ionized (anionic) form of the sulfonamide, ArSO_2NH^- (eq 18; Table 11²⁴) or inorganic ligand, L^- (Table 12).^{157,589–591}

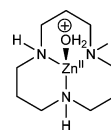
10.3.4. Brønsted Relationships Reveal the Role of Basicity of the Sulfonamide Anion

A Brønsted relationship between the logarithm of $K_{\text{d}}^{\text{ArSO}_2\text{NH}^-}$ and $\text{p}K_{\text{a}}$ of ArSO_2NH_2 (with a slope of β) would establish the extent to which the interactions of ArSO_2NH^- with the Zn^{II} cofactor of CA and with a proton are related. Deviations of individual arylsulfonamides from the general linear relationship would suggest the contribution of other factors (e.g., hydrophobicity) to affinity. We consider the key question of “What is the value of β ?” first.

While the maximum value of β is plausibly unity for this type of reaction, we anticipate that it is probably significantly lower because we expect the $\text{CA-Zn}^{\text{II}}-\text{NHSO}_2\text{Ar}$ bond to be significantly more ionic (less covalent) than the $\text{H-NHSO}_2\text{-Ar}$ bond. We attempted to determine the value empirically by constructing a plot of $\log K_{\text{d}}^{\text{ArSO}_2\text{NH}^-}$ vs $\text{p}K_{\text{a}}$ for the binding of a number of structurally related arylsulfonamides to CA II (Figure 15). Linear fits to these data gave values of β between 0.4 and 0.7, but the quality of the fits was poor ($R^2 = 0.20\text{--}0.26$), presumably because of the heterogeneity in the interaction of these ligands with CA II.

We consider three model studies that should allow more reliable estimates of β ; these studies explore the binding of (i) arylsulfonamides and simple monoanions to a small-molecule model of the active site of CA, (ii) anionic nitrogen heterocycles to HCA I, and (iii) fluorinated benzenesulfonamides to BCA II. From these studies, we believe that the best estimate for the value of β is ~ 0.6 .

Kimura and co-workers examined the binding of arylsulfonamides and anions to a macrocyclic triamine chelated to Zn^{II} (**206**) in aqueous buffer (with 10% acetonitrile for solubility).^{335,350} This small molecule (**206**) seems to provide a good model for the active site of CA because it (i) has a distorted tetrahedral geometry about Zn^{II} with the fourth site occupied by a water molecule with a $\text{p}K_{\text{a}}$ of 7.3 (similar to the $\text{p}K_{\text{a}}$ of $\text{CA-Zn}^{\text{II}}-\text{OH}_2^+$; section 10.3.3), (ii) catalyzes the hydrolysis of *p*-nitrophenyl acetate (a model substrate for CA), and (iii) binds arylsulfonamides as anions with concomitant displacement of the Zn^{II} -bound water. A Brønsted plot derived from their data for the dependence of $\log K_{\text{d}}^{\text{ArSO}_2\text{NH}^-}$ on $\text{p}K_{\text{a}}$ ($R^2 = 0.88$) reflects only the effect of $\text{p}K_{\text{a}}$ (e.g., Brønsted or proton basicity) on the strength of the $\text{Zn}^{\text{II}}-\text{N}$ bond because the arylsulfonamide cannot engage in hydrophobic contacts of its aryl ring or hydrogen bonds of its head group, in the bound complex. They obtained a value for β of 0.29 ± 0.05 .



206

Khalifah et al. undertook a Brønsted analysis of the binding of four aromatic nitrogen heterocycles (imidazole analogues) to HCA I. They observed a linear dependence of the

Table 11. Dissociation Constants, K_d^{obs} and $K_d^{\text{ArSO}_2\text{NH}^-}$ (Calculated for the Binding of the Anion to $\text{CA-Zn}^{2+}-\text{OH}_2^+$; eq 18)

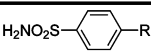
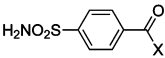
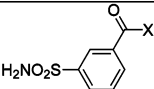
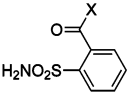
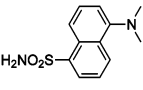
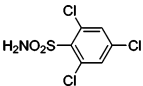
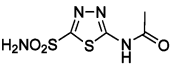
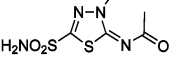
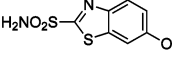
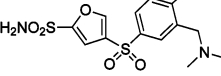
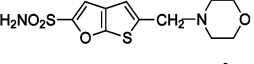
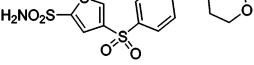
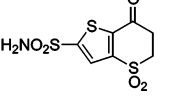
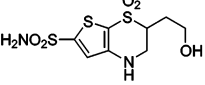
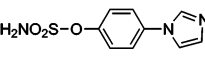
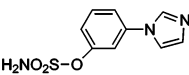
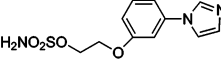
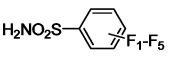
Compound	Structure	$\text{p}K_a$	pH^a	CA II Variant	$K_d^{\text{obs } b}$ (nM)	$K_d^{\text{ArSO}_2\text{NH}^- c}$ (nM)	Ref.
<i>Type:</i> 							
1	R = H	10.1	6.5	HCA	200	0.033	389,458
2	R = Cl	9.9	6.5	HCA	120	0.032	458
3	R = NO ₂	9.0	6.5	HCA	63	0.13	458
4	R = NH ₂	10.1	7.5	BCA	300	0.13	413,503
222	R = CH ₂ NH ₃ ⁺	8.4	7.0	BCA	36 000	690	417
6	R = CH ₃	10.2	6.5	HCA	82	0.011	389
7	R = CH ₂ CH ₃	10.4	6.5	HCA	29	0.0024	389
8	R = (CH ₂) ₂ CH ₃	10.3	6.5	HCA	17	0.0018	389
9	R = (CH ₂) ₃ CH ₃	10.4	6.5	HCA	5.0	0.00042	389
<i>Type:</i> 							
30	X = OCH ₃	9.8	6.5	HCA	10	0.0033	389
31	X = OCH ₂ CH ₃	9.7	6.5	HCA	3.2	0.0013	389
32	X = O(CH ₂) ₂ CH ₃	9.8	6.5	HCA	1.7	0.00057	389
33	X = O(CH ₂) ₃ CH ₃	9.7	6.5	HCA	0.77	0.00032	389
34	X = O(CH ₂) ₄ CH ₃	10.1	6.5	HCA	0.41	0.000069	389
37	X = NHCH ₃	10.3	6.5	HCA	83	0.0088	389
38	X = NHCH ₂ CH ₃	10.1	6.5	HCA	30	0.0050	389
39	X = NH(CH ₂) ₂ CH ₃	10.1	6.5	HCA	8.3	0.0014	389
40	X = NH(CH ₂) ₃ CH ₃	10.1	6.5	HCA	3.3	0.00055	389
41	X = NH(CH ₂) ₄ CH ₃	10.2	6.5	HCA	1.8	0.00024	389
<i>Type:</i> 							
114	X = OCH ₃	9.8	6.5	HCA	700	0.23	389
115	X = OCH ₂ CH ₃	9.6	6.5	HCA	610	0.32	389
116	X = O(CH ₂) ₂ CH ₃	9.7	6.5	HCA	370	0.15	389
117	X = O(CH ₂) ₃ CH ₃	9.6	6.5	HCA	110	0.060	389
118	X = O(CH ₂) ₄ CH ₃	9.9	6.5	HCA	140	0.037	389
<i>Type:</i> 							
119	X = OCH ₃	9.3	6.5	HCA	39 000	41	389
120	X = OCH ₂ CH ₃	9.5	6.5	HCA	16 000	11	389
121	X = O(CH ₂) ₂ CH ₃	9.7	6.5	HCA	5200	2.2	389
122	X = O(CH ₂) ₃ CH ₃	9.8	6.5	HCA	1800	0.60	389
123	X = O(CH ₂) ₄ CH ₃	9.9	6.5	HCA	660	0.17	389
133	 (DNSA)	9.8	7.4	HCA	826	0.66	189,368,458
135		9.7	6.5	HCA	220	0.092	458

Table 11 (Continued)

Compound	Structure	pK_a	pH ^a	CA II Variant	$K_d^{obs\ b}$ (nM)	$K_d^{ArSO_2NH^-\ c}$ (nM)	Ref.
137		7.2	7.5	HCA	7	0.78	528
138		7.4	7.5	HCA	7	0.65	528
140		8.1	7.5	HCA	0.5	0.017	528
142		8.1	7.4	HCA	2.3	0.077	517
144		9.2	8.3	HCA	1.2	0.0041	518
145		8.8	7.4	HCA	1.4	0.011	517
154		8.5	8.3	HCA	3.5	0.042	378
166		8.5	8.3	HCA	1.2	0.014	509
183		9.1	8.2	BCA	42	0.18	504
184		8.0	8.2	BCA	100	2.3	504
185		8.9	8.2	BCA	70	0.45	504
188	$H_2NO_2S-CF_3$	6.3	7.5	HCA	2	0.31	528
189	$H_2NO_2S-CH_3$	10.5	7.5	HCA	300 000	50	528
Type:							
207	2-fluoro	9.6	7.5	BCA	230	0.39	182
208	3-fluoro	9.7	7.5	BCA	75	0.11	182
209	4-fluoro	10.0	7.5	BCA	590	0.40	182
210	2,6-difluoro	9.1	7.5	BCA	190	1.0	182
211	3,5-difluoro	9.4	7.5	BCA	57	0.16	182
212	Pentafluoro	8.2	7.5	BCA	25	0.80	182

^a pH at which K_d^{obs} was reported. ^b Values of K_d^{obs} were taken from values for K_d and K_i from references in Table 10. ^c Calculated from eq 18.

logarithm of $K_d^{N^-}$ on the pK_a of the neutral species for these ligands; the best-fit line gave a value for β of 0.43 ± 0.07 with $R^2 = 0.95$.⁴⁰⁹ This low value for β is in reasonable agreement with that from the small-molecule study of Koike et al. and suggests that the Zn^{II} of CA is a hard acid and that the interaction of $ArSO_2NH^-$ with Zn^{II} of CA is more ionic than is its interaction with a proton.

While these studies are interesting, they are far from ideal as models for the binding of the arylsulfonamide anion to CA II: Koike et al. used a small-molecule model of the active site of CA in which the Zn^{II} was chelated by secondary amines and not His residues (and their study neglects the pK_a -dependence of the hydrogen-bond network), and Khalifah et al. examined the binding of aromatic

Table 12. Thermodynamics of Binding of Anions to CA II

Compound	Anion (L ⁻)	pK _a ^a	BCA II			HCA II			
			pH ^b	K _d ^{obs c} (mM)	K _d ^{L⁻ d} (mM)	pH ^b	K _d ^{obs} (mM)	K _d ^{L⁻ d} (mM)	
193	F ⁻	3.2	7.55	1200	220	6.9	>300	<i>e</i>	130
194	Cl ⁻	-7.0	7.55	190	35	6.9	200	<i>e</i>	89
195	Br ⁻	-9.0	7.55	66	12	6.9	200	<i>e</i>	89
196	I ⁻	-10.0	7.55	8.7	1.6	6.9	26	<i>e</i>	12
						9.2	500	<i>f</i>	2.0
197	HS ⁻	7.0	7.55	0.011	0.001 6	7.5	0.04	<i>g</i>	0.005 1
198	CN ⁻	9.2	7.55	0.002 6	0.000 010	7.5	0.02	<i>g</i>	0.000 065
199	N ₃ ⁻	4.7	7.55	0.59	0.11	8.7	21	<i>f</i>	0.26
200	NCO ⁻	3.5	7.55	0.11	0.020	6.9	0.02	<i>e</i>	0.008 9
						8.7	0.3	<i>f</i>	0.003 7
201	SCN ⁻	0.9	7.55	0.59	0.11	9.0	25	<i>f</i>	0.16
						7.4	1.8	<i>f</i>	0.36
						6.9	0.6	<i>e</i>	0.27
						6.4	0.32	<i>f</i>	0.23
202	OAc ⁻	4.7	7.55	85	16	6.9	70	<i>e</i>	31
203	HCO ₃ ⁻	6.5	7.55	26	4.4	6.9	70	<i>e</i>	22
204	NO ₃ ⁻	-1.5	7.55	48	8.8	6.9	35	<i>e</i>	15
205	ClO ₄ ⁻	-10.0	7.55	16	2.9	6.9	1.3	<i>e</i>	0.58

^a pK_a of the conjugate acid. ^b pH at which K_d^{obs} was reported. ^c Values of K_d^{obs} were taken from values of K_i reported in ref 157. ^d Calculated from eqs 18, 20, and 21. ^e Values of K_d^{obs} were taken from values of IC₅₀ reported in ref 589. ^f Values of K_d^{obs} were taken from values of K_i reported in ref 590. ^g Values of K_d^{obs} were taken from values of K_i reported in ref 591.

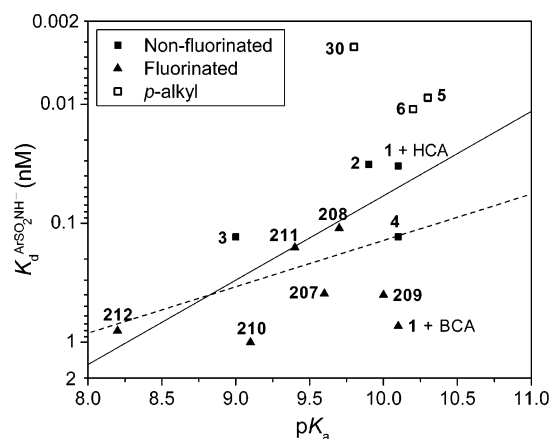


Figure 15. Brønsted plot for the variation of $K_d^{\text{ArSO}_2\text{NH}^-}$ (defined in eq 21) for the binding of substituted benzenesulfonamide anions to carbonic anhydrase II (CA II) with pK_a of the sulfonamide (see Table 11). The y-axis is plotted such that tighter-binding ligands are at the top of the graph. We included substituted benzenesulfonamides that we presume do not have hydrophobic contacts with CA II other than a conserved interaction of their phenyl rings. Compounds **6**, **30**, and **37** (shown as open squares) contain methyl groups attached to the phenyl ring and so could have additional hydrophobic contacts with CA II. The solid line shows a fit to all of the experimental points and gives a value for β of 0.7 with R^2 of 0.26. The dashed line shows a fit to the data omitting the open squares; it gives a value for β of 0.4 with R^2 of 0.20. The poor fits for both lines suggest that the binding of these compounds to CA II involves substantially different balances of contributions from different types of interactions (e.g., Zn^{II}-N bond, hydrogen-bond network, and hydrophobic effects).

nitrogen heterocycles (not arylsulfonamides) to HCA I (not CA II). In a study relevant to the binding of arylsulfonamides to CA II, Krishnamurthy et al. have recently reported the binding of fluorinated benzenesulfonamides (**207**–**212**) to BCA II.¹⁸² By constructing a quantitative structure–activity relationship (QSAR), the investigators separated the influence of fluorination of the ring on electrostatic–Lewis basicity of ArSO₂NH⁻ toward the Zn^{II} cofactor and toward the hydrogen-bond network (interactions that they assumed were dependent on pK_a)—and hydrophobic—contacts of the phenyl

ring with the enzyme (an interaction that they assumed was dependent on $\log P$, the logarithm of the octanol/aqueous buffer partition coefficient)—interactions (eq 22; Figure 16A). Their plot suggests a value for β of ~ 0.6 (with $R^2 = 0.83$), which is consistent with the more ionic (less covalent) character of the Zn^{II}-NHSO₂Ar bond than of the H-NHSO₂Ar bond.

$$-\log K_d^{\text{ArSO}_2\text{NH}^-} = 0.62(\pm 0.17)\text{pK}_a + 0.87(\pm 0.29)\log P + 3.2(\pm 1.7) \quad (22)$$

From these simple studies, we take the value for β for the binding of arylsulfonamides to CA II to be ~ 0.6 . This value takes into account the pK_a -dependence of the Lewis basicity of the arylsulfonamide anion for the Zn^{II} cofactor and of the hydrogen-bond network. We discuss the affinity of arylsulfonamides relative to a Brønsted plot constructed with that slope below.

10.3.4.1. Comparison of Affinity of Arylsulfonamides for CA Relative to Brønsted Relationships. Figure 17A shows a plot of the dependence of K_d^{obs} on the pK_a of arylsulfonamides where values of pK_a are available (Table 10). Figure 17B shows a similar plot for $K_d^{\text{ArSO}_2\text{NH}^-}$. The values of $K_d^{\text{ArSO}_2\text{NH}^-}$ generally decrease (that is, $1/K_d^{\text{ArSO}_2\text{NH}^-}$ and affinity increase) as values of pK_a increase (that is, ArSO₂NH⁻ becomes a stronger Brønsted base). One sulfonamide (**109**) seems to bind with exceptional affinity. We discuss this ligand, which we believe is able to exploit both multivalency and hydrophobic contacts, further in section 10.6.2.

We have drawn two theoretical lines with slopes of 0.6 (based on our analysis for β in the previous section) in Figure 17B. The lines pass through unsubstituted benzenesulfonamide (**1**) and represent the affinities for a hypothetical set of arylsulfonamides that have variable pK_a (and, thus, different strengths for the Zn^{II}-N bond and hydrogen-bond network) but the same strengths for hydrophobic contacts (assumed to be pK_a -independent) as benzenesulfonamide (see section 4.6); the solid line describes the binding of benzenesulfonamide to HCA II, and the dashed line describes binding

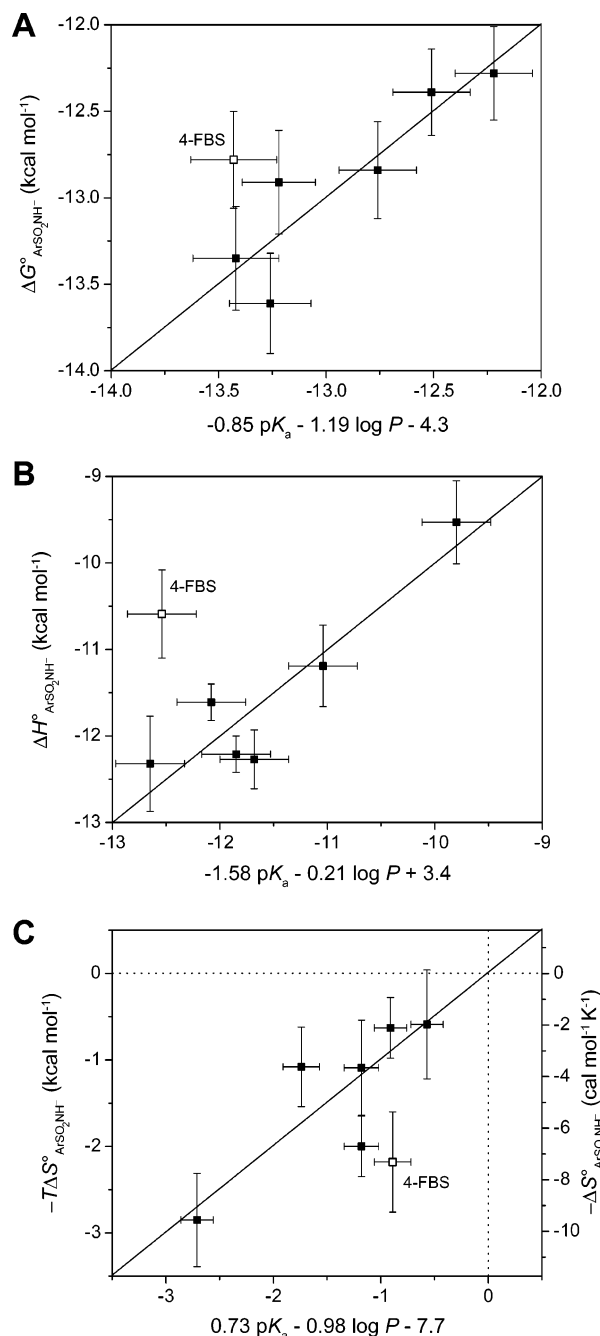


Figure 16. Quantitative structure–activity relationships (QSARs) between $\Delta G^\circ_{\text{ArSO}_2\text{NH}^-}$ (A), $\Delta H^\circ_{\text{ArSO}_2\text{NH}^-}$ (B), and $-T\Delta S^\circ_{\text{ArSO}_2\text{NH}^-}$ (C) and $\text{p}K_a$ and $\log P$ for the binding of fluorine-substituted benzenesulfonamides (207–212) to BCA II. Data are shown for QSARs in which those for 4-fluorobenzenesulfonamide (209, 4-FBS) were omitted; Krishnamurthy et al. have suggested that this ligand interacts in a different way with the enzyme than do the other ligands.¹⁸² The y-error bars are uncertainties described in Table 14, and the x-error bars were obtained by propagating uncertainties in $\text{p}K_a$ and $\log P$. The horizontal and vertical dotted lines in (C) separate favorable ($-T\Delta S^\circ < 0$) from unfavorable ($-T\Delta S^\circ > 0$) entropy of binding. Modified with permission from ref 182. Copyright 2007 Wiley-VCH.

to BCA II and only relates to the sulfonamides represented by closed triangles and closed circles. A number of arylsulfonamides lie above the solid line (that is, to higher affinities) and, we infer, are able to take advantage of interactions not available to benzenesulfonamide. For instance, the open symbols that lie above benzenesulfonamide (in the dotted ellipse in Figure 17B)—*para*-substituted benzenesulfonamides with

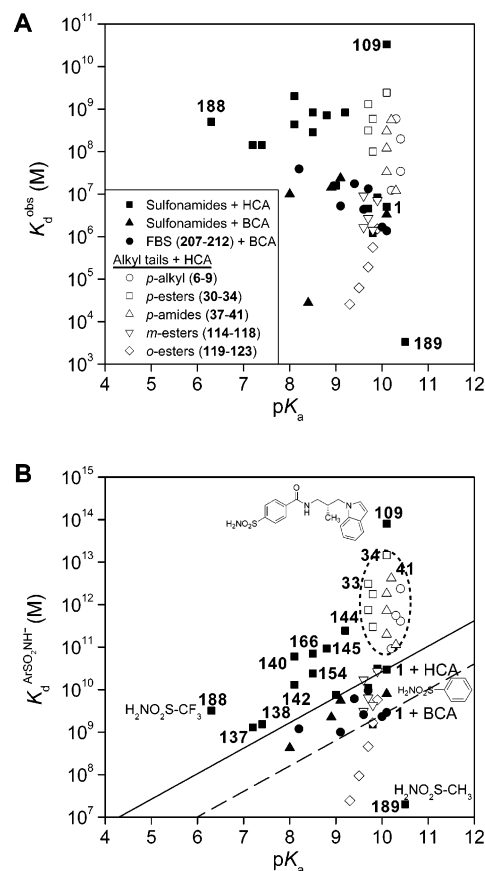


Figure 17. Variation of (A) K_d^{obs} and (B) $K_d^{\text{ArSO}_2\text{NH}^-}$ (defined in eq 21) with $\text{p}K_a(\text{ArSO}_2\text{NH}_2)$ for the binding of arylsulfonamides (shown in Table 11) to human (HCA) and bovine carbonic anhydrase II (BCA). The filled circles and filled triangles are data for the binding of ligands to BCA; the other symbols are data for the binding of ligands to HCA. The $\text{p}K_a$ of compound 109 has not been reported in the literature; we take it to be 10 based on its structure. The open symbols represent the binding of three series of benzenesulfonamides with alkyl chains to HCA. These compounds demonstrate that the affinity of substituted benzenesulfonamides with alkyl chains for CA increases with the length (and, thus, hydrophobicity) of the chain. We placed the dashed and solid lines (with slopes of 0.6; see text) to pass through the value of $K_d^{\text{ArSO}_2\text{NH}^-}$ for unsubstituted benzenesulfonamide (1) complexed with HCA (solid line) and with BCA (dashed line). The dotted ellipse segregates compounds that bind more tightly than benzenesulfonamide by virtue of hydrophobic contacts with the surface of the conical cleft just outside of the active site. We discuss 109 separately in the text.

alkyl tails—represent compounds that are probably able to exploit hydrophobic contacts between their alkyl tails and the surface of HCA II peripheral to, but outside of, the active site region (see section 10.4). The closed squares that lie above the solid line probably have more favorable contacts of their structurally complex aryl rings with HCA II than does benzenesulfonamide. Thus, interactions between arylsulfonamides and two hydrophobic sites on CA—the hydrophobic pocket in the active site (by using a large or hydrophobic aryl ring) and the hydrophobic wall along the surface of the conical cleft (by using a hydrophobic tail; see section 10.4)—can be used to generate high-affinity arylsulfonamides. We discuss the affinity of fluorinated benzenesulfonamides (207–212; represented by filled circles) for BCA II relative to the dashed line at the end of this section.

The structurally simple sulfonamide trifluoromethanesulfonamide (188) lies significantly above the solid line in

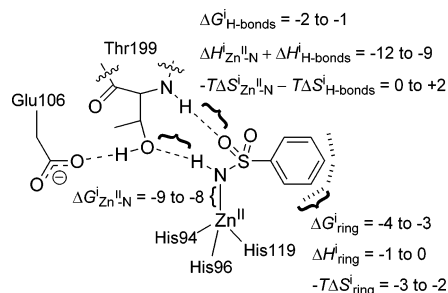


Figure 18. Estimated free energies, enthalpies, and entropies (all in kcal mol⁻¹) for the different structural interactions between fluorinated benzenesulfonamide anions and CA–Zn^{II}–OH₂⁺. Reproduced with permission from ref 182. Copyright 2007 Wiley-VCH.

Figure 17B (even though this compound lacks a phenyl ring) and far above a line with a slope of 0.6 that passes through methanesulfonamide (**189**). Håkansson and Liljas reported the X-ray crystal structure of trifluoromethanesulfonamide complexed with HCA II; the structure revealed that trifluoromethanesulfonamide was rotated by 180° around the sulfur–nitrogen bond relative to all arylsulfonamides.²⁰¹ This rotation placed the trifluoromethyl moiety in a tight hydrophobic pocket (comprising Val121, Val143, Leu198, Thr199, and Trp209) of HCA II with which the bulky ring of arylsulfonamides could not interact and created new hydrogen bonds and van der Waals contacts for the sulfonamide oxygens. These contacts, particularly the hydrophobic contacts of the trifluoromethyl group, could explain the much higher than expected affinity of trifluoromethanesulfonamide for HCA II.

Some ligands lie below the solid line and, thus, bind with affinities lower than expected based on the Brønsted plot using benzenesulfonamide as the reference compound. These ligands might encounter steric repulsion with the active site of CA II (e.g., the series of *ortho*- and *meta*-substituted benzenesulfonamides with alkyl chains, shown as open symbols)^{389,586} or might not be able to interact hydrophobically with CA II (e.g., methanesulfonamide, **189**). The observation that methanesulfonamide binds with an affinity that is ~10³-fold lower than benzenesulfonamide, even though both have similar values of p*K*_a (10.1–10.5), suggests that the phenyl ring makes a significant (~4 kcal mol⁻¹) contribution to affinity.

As mentioned previously, Krishnamurthy et al. constructed a QSAR between the affinity (*K*_d^{ArSO₂NH⁻}) of fluorinated benzenesulfonamides (**207–212**) for BCA II and p*K*_a and log *P* of the ligands (eq 22; Figure 16A).¹⁸² Assuming that the two hydrogen bonds between the enzyme and ligand were equal to one another in energy (Figure 13B), their analysis allows the partitioning of affinity to the structural interactions of the Zn^{II}–N bond, the hydrogen-bond network, and the hydrophobic contacts of the phenyl ring between the ligand and enzyme (Figure 18; section 10.2.4). Their results suggest that electrostatic contacts play a dominant role (~75% of the free energy of binding) in affinity with ~65% (~–8 kcal mol⁻¹) of the free energy being contributed by the Zn^{II}–N bond and ~10% (~–1 kcal mol⁻¹) by the hydrogen-bond network. Hydrophobic interactions between the phenyl ring and BCA II contribute the remaining ~25% (~–3.5 kcal mol⁻¹); this result is consistent with the fact that benzenesulfonamide has an affinity for HCA II ~10³-fold (~–4 kcal mol⁻¹) greater than methanesulfonamide does (see above). Given the small range in *K*_d^{ArSO₂NH⁻} for the data

obtained with the fluorinated benzenesulfonamides (Figure 16A), these conclusions cannot be quantitatively generalized to the binding of structurally complex arylsulfonamides to CA but should be qualitatively applicable (e.g., the Zn^{II}–N bond should be the dominant interaction between CA and arylsulfonamide).

10.3.5. What Value of p*K*_a for Arylsulfonamides Gives the Highest Affinity for CA?

The value of the p*K*_a of the arylsulfonamide has two effects on the affinity of the sulfonamide for CA, it (i) controls the fraction of sulfonamide in the active form (eqs 17 and 18) and (ii) controls the Lewis basicity of the sulfonamide anion (and, thus, the strength of the Zn^{II}–N bond and hydrogen-bond network). A lower p*K*_a would result in a greater fraction of the sulfonamide in the ionized form but would reduce the Lewis basicity of the anion (and the strength of the Zn^{II}–N bond, as well as affect the hydrogen-bond network).

Equation 23 shows the expected dependence of the logarithm of *K*_d^{obs} on the p*K*_a of the arylsulfonamide; this equation assumes a Brønsted relationship between log *K*_d^{ArSO₂NH⁻} and p*K*_a with a slope of –β and y-intercept of –*C* (the negative signs are used to make both constants positive).

$$\log K_d^{\text{obs}} = -(\beta \cdot \text{p}K_a + C) + \log(1 + 10^{\text{p}K_a - \text{pH}}) - \log \theta_{\text{CA-Zn}^{\text{II}}-\text{OH}_2^+} \quad (23)$$

The terms are as defined in eq 21. Equation 24a shows the analytical solution for the value of p*K*_a of the arylsulfonamide that results in the highest-affinity ligand (lowest value of *K*_d^{obs}) for the reaction shown in eq 18. In order to generate this equation, we set the derivative of eq 23 with respect to p*K*_a of the arylsulfonamide equal to zero and rearranged. Equation 24b shows an analogous analytical solution using the reaction in eq 17.

$$\text{p}K_a = \text{pH} + \log \frac{\beta}{1 - \beta} \quad (24a)$$

$$\text{p}K_a = \text{pH} - \log \frac{\beta}{1 - \beta} \quad (24b)$$

The variation of this optimal value of p*K*_a with β (between 0.1 and 0.9) is relatively modest (p*K*_a = pH of buffer ± 1 pH unit) for both equations.

Figure 19 shows a family of curves of eq 23 at different values of β. The key point is that, regardless of the value of β, a value of p*K*_a for the arylsulfonamide near the pH of the buffer (usually ~7.4) will give the highest-affinity arylsulfonamide (all other factors being equal). Others have reached this same general conclusion by examining rate and equilibria for other reactions in water.⁵⁹²

10.3.6. Conclusions

The value of the p*K*_a of the arylsulfonamide influences affinity in two ways, by varying (i) the fraction of the sulfonamide present in (or able to access) the reactive form and (ii) the Lewis basicity of the sulfonamide anion (and, thus, the strength of the Zn^{II}–N bond and the bonds of the hydrogen-bond network). Because these effects compete with one another (one increases the affinity with a change in p*K*_a, and the other decreases it), the highest-affinity arylsulfonamides will have a p*K*_a near the pH of the buffered medium.

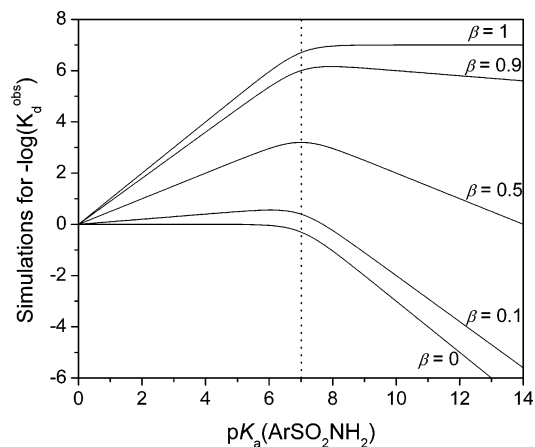


Figure 19. Variation of pK_a of the arylsulfonamide that will theoretically give the highest affinity ligand (lowest value of K_d^{obs}) to carbonic anhydrase II with β (eq 23). The curves were generated with a pH of the buffer of 7 (indicated by dotted vertical line).

Some changes in the structure of arylsulfonamides actually decrease the affinities of these sulfonamides for CA II relative to benzenesulfonamide (points below the solid line in Figure 17B). This effect suggests that steric repulsion between CA II and substituents on the aryl ring and/or the aryl ring itself can reduce affinity. A number of sulfonamides bind with affinities higher than expected based on a Brønsted relationship using benzenesulfonamide as the reference ligand (points above the solid line in Figure 17B). We believe that these ligands take advantage of contacts (in particular, hydrophobic contacts) with CA II that unsubstituted benzenesulfonamide cannot. The contacts can be either at the hydrophobic pocket in the active site of CA II or at a secondary site at the surface of the conical cleft of the enzyme (see sections 10.4 and 10.5).

The $\text{Zn}^{\text{II}}\text{--N}$ bond plays a dominant role ($\sim 65\%$ of the free energy) in the binding of benzenesulfonamide ligands (and, probably, also arylsulfonamide ligands) to CA II, with a smaller role played by the hydrogen-bond network ($\sim 10\%$) and hydrophobic contacts of the phenyl ring ($\sim 15\%$). Increasing the strength of hydrophobic contacts between the aryl ring of the arylsulfonamide and CA in ways that increase affinity, but that avoid steric repulsion and destabilization of the $\text{Zn}^{\text{II}}\text{--N}$ bond, could result in very high-affinity ligands to CA. Alternatively, the addition of hydrophobic elements to the benzenesulfonamide scaffold could accomplish this same objective (see section 10.4). For instance, we believe that the high-affinity ligand **109** (the outlier in Figure 17B) takes advantage of hydrophobic interactions from multivalent contacts involving a secondary site of the enzyme (see section 10.5.2).

10.4. Influence of the Sulfonamide Tail Group on the Binding of Arylsulfonamides to CA

10.4.1. General Approach

In this approach to increasing affinity of arylsulfonamides, the head region and the aryl ring are held constant, and the tail region is changed (Figure 11A). Most changes (within a homologous series with a common type of attachment to the aryl ring) have little influence on the value of pK_a of $p\text{-RC}_6\text{H}_4\text{SO}_2\text{NH}_2$; as a result, we believe that the binding of the ArSO_2NH^- head group and the phenyl ring is constant within each series. Thus, variations in K_d^{obs} provide direct

information about the interaction between the tail and the surface of CA outside of the region that binds the ArSO_2NH^- anion.

10.4.2. Interaction of Different Types of Tails with CA

10.4.2.1. Increasing the Length of Alkyl Tails Increased Affinity of Benzenesulfonamides for CA. King and Burgen, and Gao et al., examined the influence of the length of the tail for substituted benzenesulfonamides with alkyl tails on the observed dissociation constant (K_d^{obs}) for CA II.^{389,508} For the case of *ortho*- (**119–123**), *meta*- (**114–118**), and *para*-substituted (**6–10**, **30–35**, and **37–43**) benzenesulfonamides with alkyl tails, the affinity increased (K_d^{obs} decreased) as the length of the tail increased and reached a plateau when there were six methylene units in the tail (a length at which the tail should exceed the length of the conical cleft of CA II; see section 4.6) (Table 10). The increase in affinity with tail length is probably due to hydrophobic contacts between the tail and the “hydrophobic wall” of CA II (see section 10.5). The *ortho*- and *meta*-substituted benzenesulfonamides, however, interacted with HCA II with lower affinities than unsubstituted benzenesulfonamide (**1**) did (Figure 17). This result is probably due to steric constraints of the active site of HCA II that disfavor *ortho*- and *meta*-substitution on the phenyl ring and suggests that proper positioning of the alkyl tail is essential for high-affinity binding.⁵⁸⁶ Figure 17 shows all three series of alkyl tail-containing benzenesulfonamides as open symbols; each series lies roughly in a vertical line because of the similar values of pK_a of its members.

10.4.2.2. Benzenesulfonamides with Fluoroalkyl Tails. Gao et al. determined that benzenesulfonamides with fluoroalkyl tails (**22–27** and **45–48**) interacted with higher affinities with BCA II than benzenesulfonamides with alkyl tails (**16–21** and **37–44**) of the same length did (Table 10).⁵⁰⁸ They observed different slopes in linear fits to plots of $\log K_d^{\text{obs}}$ or $\log P$ (the partition coefficient between octanol and aqueous buffer) vs tail length (n) for the alkyl- and fluoroalkyl-containing benzenesulfonamides (Figure 20 parts A and B). Both series, however, had the same slopes in linear fits to plots of either $\log K_d^{\text{obs}}$ or $\log P$ vs the *molecular surface area* of the ligand (Figure 20 parts C and D); this result suggests that the higher affinities of sulfonamides with *fluoroalkyl* tails for BCA II than of those with *alkyl* tails can be explained by the fact that fluorine is larger than hydrogen, rather than by some intrinsic difference in hydrophobic interactions between the two.

Gao et al. proposed that the slight difference in y -intercepts of the plots (Figure 20 parts C and D) for sulfonamides with fluoroalkyl tails and with alkyl tails was due to the greater acidity of the proton of the carboxamide group adjacent to the tail (boxed in Figure 20) for the former than for the latter. A likely hypothesis is that this --CONH-- group hydrogen bonds to residues of the active site of BCA II; the effectiveness of this hydrogen-bond donation would be higher for sulfonamides with fluoroalkyl tails than for those with alkyl tails and may explain the slightly (~ 1 kcal mol^{-1}) more favorable free energy of binding of sulfonamides with fluoroalkyl tails than for those with alkyl tails.

10.4.2.3. Oligoethylene Glycol, Oligoglycine, and Oligosarcosine Tails: Values of K_d^{obs} Are Surprisingly Insensitive to the Length of the Tail. Jain et al. and Krishnamurthy et al. studied the binding of types of tails

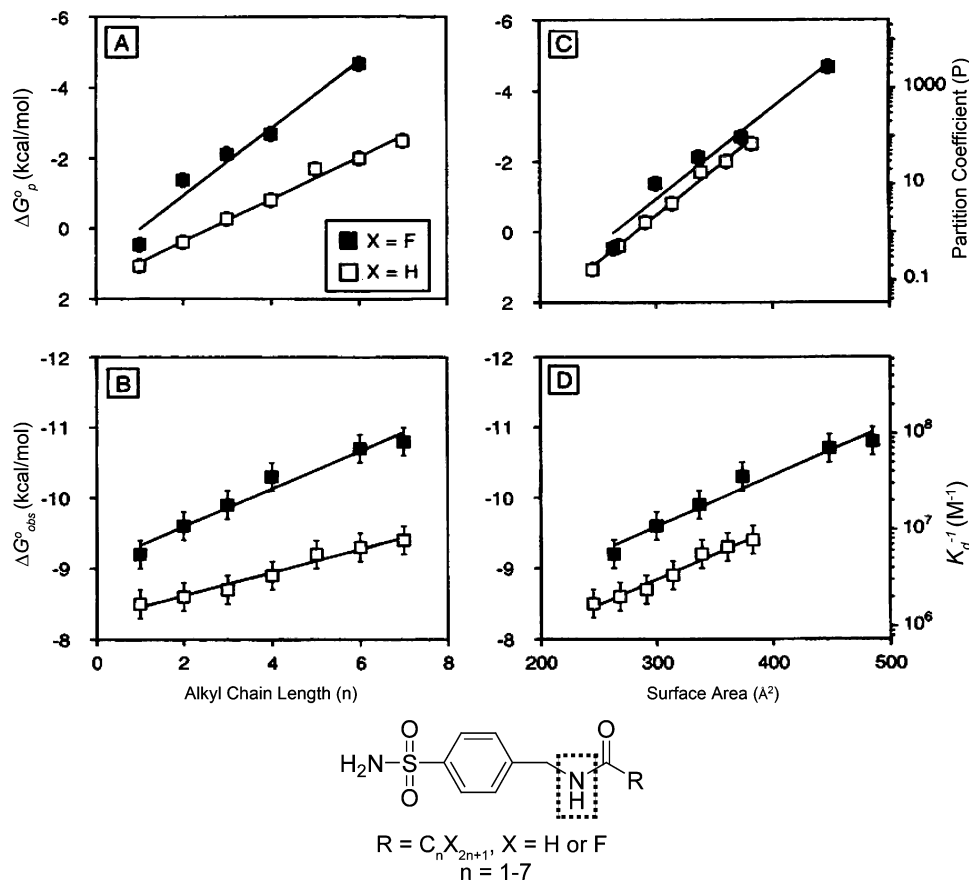


Figure 20. Variation of the observed free energy of binding to BCA II ($\Delta G^{\circ}_{\text{obs}}$) and the free energy of partitioning between octanol and water (ΔG°_p) of benzenesulfonamides containing alkyl and fluoroalkyl tails with the length of the tail (A and B) and with the molecular surface areas of the ligands (C and D). The plots show linear fits to the data. The differences in slopes between the alkyl and fluoroalkyl series in plots of ΔG°_p (A) or $\Delta G^{\circ}_{\text{obs}}$ (B) vs length of the tail were eliminated when these values were plotted vs molecular surface areas of the ligands (C and D). Gao et al. believe that the $-\text{NH}-$ of the carboxamide (enclosed in the dotted box) forms hydrogen bonds with residues of the active site of BCA II.⁵⁰⁸ Modified with permission from ref 508. Copyright 1995 American Chemical Society.

other than n -alkanes to CA II to explore the nature of the active site of the enzyme.^{377,415,593} Unlike benzenesulfonamides with alkyl and fluoroalkyl tails, *para*-substituted benzenesulfonamides with oligoethylene glycol (72–76), oligoglycine (63–68), and oligosarcosine (213–217) tails showed no variation of K_d^{obs} with the length of the tail (between one and five residues) for any of the series (Figure 21A), even though T_2 relaxation times from ^1H NMR and X-ray analysis of crystal structures of CA II–sulfonamide complexes demonstrated that these tails do interact with CA II.^{185,202,377} We discuss this surprising result further in section 10.6.3.

10.4.3. Conclusions

The systematic studies of benzenesulfonamides with alkyl and fluoroalkyl tails demonstrate that longer hydrophobic “tails” can increase the affinity of sulfonamides for CA II. These studies also suggest that fluoroalkyl tails and alkyl tails make the same contribution to hydrophobic binding to CA II when normalized for differences in molecular surface area.

The principle of increasing surface area to increase the affinity of proteins for ligands is not completely general, however. The results with benzenesulfonamides with oligoethylene glycol, oligoglycine, and oligosarcosine tails shows that, in certain cases, increasing the surface area of contact does not increase the affinity. Understanding the thermodynamic basis for these anomalous data requires a separate

examination of enthalpy and entropy of binding (see section 10.6).

10.5. Bivalent Approaches to CA Binding

10.5.1. General Approach: Addition of a Secondary Recognition Element to the Tail

Multivalency is the operation of multiple molecular recognition events or interactions between two entities (e.g., molecules, molecular aggregates, viruses, cells, and surfaces).^{416,594,595} It has been exploited extensively in the design of ligands for proteins.^{416,595} In principle, a multivalent ligand will benefit from two or more favorable interactions with the same translational and rotational entropic “cost” as a monovalent ligand with only one interaction.

Bivalency, the simplest form of multivalency, involves only two interactions between receptor and ligand. It has been used (incidentally or intentionally) in the design of *para*-substituted benzenesulfonamides to bind to CA: a secondary recognition element (SRE) is attached to the conserved arylsulfonamide primary recognition element (comprising the sulfonamide head group and phenyl ring) by a tail (Figure 11). The most successful bivalent arylsulfonamides have exploited contacts between the secondary recognition element and two hydrophobic patches in the conical cleft of CA II.^{284,377,507,508,596} As mentioned in section 10.2.3, the mode of binding of the head group and the phenyl ring (the primary recognition element) of the *p*-substituted

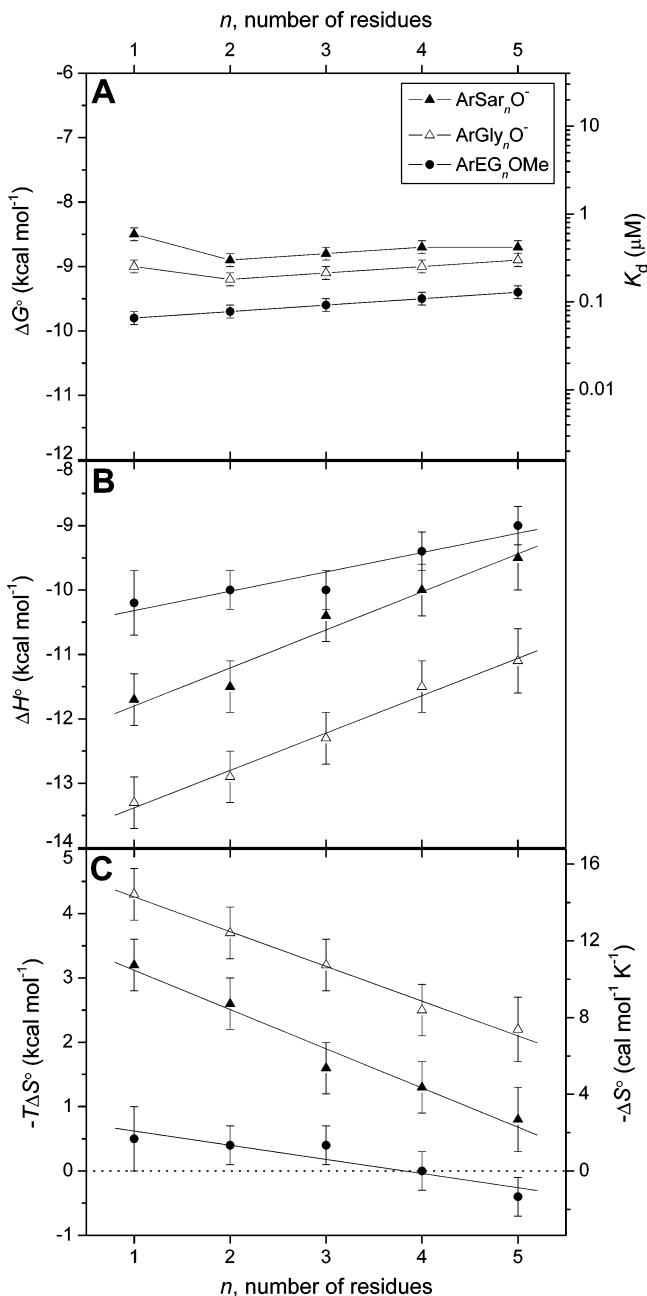


Figure 21. Variation in (A) observed free energy of binding and dissociation constant, (B) enthalpy of binding, and (C) entropy of binding with the number of residues in the chain for *para*-substituted benzenesulfonamides with oligoethylene glycol (ArEG_nOME, **72–76**), oligoglycine (ArGly_nO⁻, **63–67**), and oligosarcosine (ArSar_nO⁻, **213–217**) chains to BCA II. Linear fits to the data in (B) and (C) are shown. The observed fitting parameters (slope in kcal mol⁻¹ residue⁻¹, y-intercept in kcal mol⁻¹) are as follows: (for (B), in ΔH°) ArGly_nO⁻ (0.58 ± 0.04 , -14.0 ± 0.1), ArSar_nO⁻ (0.59 ± 0.07 , -12.4 ± 0.2), ArEG_nOME (0.30 ± 0.06 , -10.6 ± 0.2); (for (C), in $-T\Delta S^\circ$) ArGly_nO⁻ (-0.54 ± 0.03 , 4.8 ± 0.1), ArSar_nO⁻ (-0.61 ± 0.06 , 3.7 ± 0.2), ArEG_nOME (-0.22 ± 0.05 , 0.8 ± 0.2). Uncertainties were given by the linear least-squares fitting procedure. The horizontal dashed line in (C) separates favorable ($-T\Delta S^\circ < 0$) from unfavorable ($-T\Delta S^\circ > 0$) entropy of binding. Reproduced with permission from ref 415. Copyright 2006 American Chemical Society.

benzenesulfonamide is conserved with variation of the *para*-substituent; this consistent binding allows a direct evaluation of the influence of the secondary recognition element on affinity.

10.5.2. Hydrophobic Secondary Recognition Elements Close to the Phenyl Ring of the *para*-Substituted Benzenesulfonamide

10.5.2.1. Aromatic and Alkyl Moieties as Secondary Recognition Elements. Using *p*-substituted benzenesulfonamides of the form *p*-H₂NSO₂C₆H₄CONHR where R was a hydrophobic group (e.g., substituted benzenes (**52–54**), pyridine- and naphthalene-containing heterocycles (**59–62**), and nonaromatic rings (**49** and **50**)), Jain et al. demonstrated that the R group contributed to the affinity of arylsulfonamides (e.g., R = CH₃ (**5**), $K_d = 150$ nM; R = benzyl (**51**), $K_d = 1.1$ nM) for BCA II and HCA II and that affinity was independent of the exact structure of the hydrophobic group (e.g., for R = benzyl (**51**), cyclohexylmethyl (**49**), 1-adamantylmethyl (**50**), or 1-naphthylmethyl (**62**), $K_d \approx 1$ nM) (Table 10).²⁸⁴ This independence of affinity on the structure of the R group suggested that a hydrophobic secondary recognition element did not have to be carefully designed in order to contribute to the affinity. From an analysis of the X-ray crystal structure of the complex of HCA II with **51**, Jain et al. and Cappalonga Bunn et al. concluded that the R group makes contact with a hydrophobic pocket of HCA II defined by Phe131, Val135, Leu198, and Pro202 (see section 4.6).^{202,284}

Sigal and Whitesides examined the affinity of *para*-substituted benzenesulfonamides, with pendant amino acids (*p*-H₂NSO₂C₆H₄CONH-AA-OH) (**89–103**) as secondary recognition elements, for HCA II.⁵⁰⁷ They observed that hydrophobic amino acids increased the affinity of arylsulfonamides (Table 10) and that aliphatic amino acids contributed at least as much to affinity as aromatic ones (e.g., AA = Gly (**103**), $K_d = 310$ nM; AA = Ile (**101**) or Leu (**102**), $K_d = 9$ nM; AA = Phe (**103**), $K_d = 13$ nM). The investigators rationalized these results by concluding that, although the aromatic amino acids had greater hydrophobic surface areas than the aliphatic ones, this greater surface area of aromatic amino acids was partially compensated by their higher polarizability, which would stabilize these groups in polar solvents (that is, free in aqueous solution) and, thus, disfavor association with the enzyme.

10.5.2.2. Influence of Fluorination on the Secondary Recognition Element. Jain and co-workers examined the affinity of compounds of the form *p*-H₂NSO₂C₆H₄CONH-CH₂C₆H_nF_{5-n} (**55–58**), and the X-ray crystal structures of these ligands complexed with HCA II, to explore the nature of the interaction between the secondary phenyl ring of the ligand and Pro202 and Phe131 of CA II.^{180,249,515,516,597,598} Using HCA II and a mutant of HCA II where Phe131 was mutated to Val, the investigators claimed to dissect the interactions between the secondary recognition element and *wild-type* HCA II into (i) dipole–induced dipole interactions between the fluorinated ring of SRE and Pro202, (ii) dipole–quadrupole interactions between the fluorinated ring of SRE and Phe131, and (iii) quadrupole–quadrupole interactions between the fluorinated ring of SRE and Phe131.¹⁸⁰ The investigators generated a linear free energy relationship (with $R^2 = 0.83$) between affinity and these different multipole–multipole contributions for five of the ligands; their analysis suggested that the relative importance of the three terms varied within the series of ligands, with no single term being dominant for all of the ligands. While their correlation was impressive, the range in affinities of the arylsulfonamides for the two proteins (*wild-type* and mutant HCA II) was too narrow (variation in K_d^{obs} of ~ 20 -

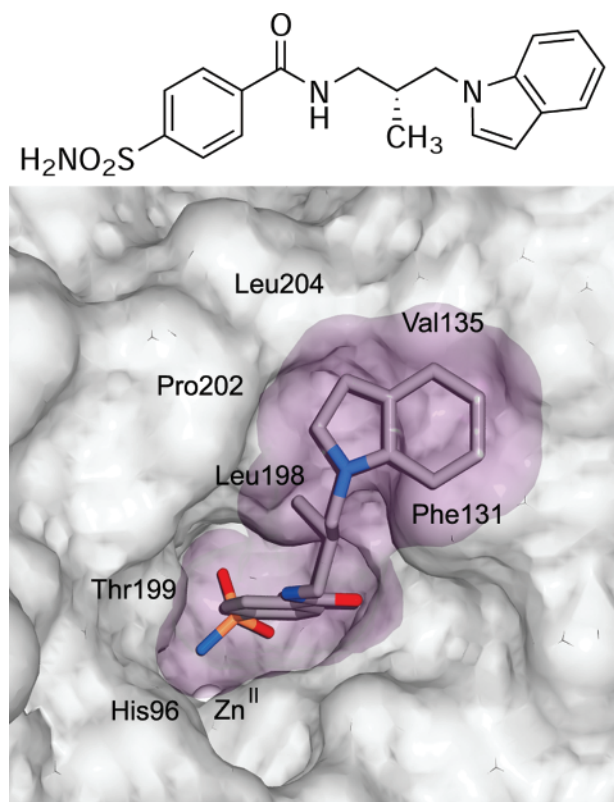


Figure 22. Structure of the active site of HCA II bound to compound **109** (shown as a chemical structure).¹⁸⁹ The van der Waals surface of the enzyme is opaque gray, and that of the ligand is translucent purple. Relevant residues are indicated, most notably Leu198 and Pro202 on the hydrophobic wall.

fold), and the number of ligands too small, to provide a real test of the underlying hypothesis.

10.5.2.3. Highest Affinity Ligand for HCA II Reported to Date. Grzybowski et al. exploited bivalency to design the highest affinity ligand (**109**) for HCA II reported to date ($K_d \approx 30$ pM).¹⁸⁹ This arylsulfonamide was designed by combinatorial small-molecule growth (CombiSMoG), a computational approach based on a knowledge-based potential (from analyses of reported X-ray crystal structures of HCA/ arylsulfonamide complexes) and a Monte Carlo ligand growth algorithm (see section 9.5). The X-ray crystal structure of **109** in complex with HCA II revealed that the indole moiety (a secondary recognition element) of the ligand made contacts with the hydrophobic pocket (Leu198, Pro202, Val135, and Phe131) of HCA II and that the *N*-methyl group fit into a tight pocket between Leu198 and Pro202 (Figure 22). This simulation successfully predicted the free energy and geometry of binding of **109** and of its enantiomer (**110**), which binds ~ 10 -fold less strongly (Table 10).

10.5.3. Hydrophobic Secondary Recognition Elements Separated from the Phenyl Ring of the Arylsulfonamide

10.5.3.1. Benzyl Moieties as Secondary Recognition Elements for the “Hydrophobic Wall” of CA. Jain et al. examined the binding of bivalent *para*-substituted benzenesulfonamides with benzyl moieties as secondary recognition elements and oligoglycine (**69–71**) or oligoethylene glycol (**77–82**) chains as tails.^{284,377} These ligands were engineered to allow the benzyl esters to interact with a second hydrophobic site of the enzyme, the “hydrophobic wall”, defined primarily by Leu198, Pro201, and Pro202 (and, to a lesser

extent, by Phe20). The affinities for HCA II of benzyl-ester-terminated benzenesulfonamides with tails of two (**69**) and three (**70**) Gly residues were the same ($K_d \sim 75$ nM), only ~ 2 fold higher than that for *p*-H₂NSO₂C₆H₄CONHCH₃ (**37**, $K_d = 150$ nM²⁸⁴) and ~ 4 -fold higher than the affinities for BCA II of benzenesulfonamides with Gly tails *without* benzyl esters (**64** and **65**). The affinity for BCA II of the benzenesulfonamide with four Gly residues (**71**, $K_d \approx 210$ nM) was ~ 3 -fold lower than those for **69** and **70**. The affinities of benzyl-ether-terminated benzenesulfonamides with tails of oligoethylene glycol (**77–82**) for BCA II decreased monotonically with increasing tail length, but only by a factor of 2 over the range of one (**77**) to six (**82**) residues. These affinities were only 4–5-fold higher than for *methyl*-ether-terminated benzenesulfonamides with oligoethylene glycol tails (**72–76**).

These results with oligoglycine and oligoethylene glycol tails suggest that the hydrophobic secondary recognition element must be close to the phenyl ring to exert a strong effect on affinity (e.g., for *p*-H₂NSO₂C₆H₄CONHCH₂Ph, $K_d \approx 1.1$ nM) and that the benzyl moieties well-separated from the phenyl ring of the substituted benzenesulfonamide were not interacting strongly with the hydrophobic wall of the enzyme. In line with these thermodynamic data, the crystal structure of the complex of HCA II with **70** revealed that the tail, and not the benzyl ester, interacted with Pro201 and Pro202; the benzyl ester could not be visualized in the structure due to disorder.^{202,284} Molecular dynamics simulations, however, have suggested a possible, transient interaction of the benzyl ester of **70** with Phe20 and Pro202 of HCA II.⁵⁹⁹

10.5.3.2. Hydrophobic Amino Acids as SREs. Boriack et al. examined the binding of arylsulfonamides of structure *p*-H₂NSO₂C₆H₄CONH(CH₂CH₂O)₂CH₂CH₂NHCO-AA-NH₃⁺ with amino acids (AAs) as secondary recognition elements and triethylene glycol as a tail (**83–85**).¹⁸⁵ They observed that *para*-substituted benzenesulfonamides containing nonpolar amino acids (AA = Gly (**84**), Phe (**85**), or Leu, $K_d \approx 15$ nM) bound with ~ 2 -fold higher affinity than the unsubstituted compound (**83**, $K_d \approx 43$ nM). X-ray crystal structures of complexes of the benzenesulfonamides with HCA II revealed that the oligoethylene glycol tail interacted with the hydrophobic wall of the enzyme and that, again, the secondary recognition elements (the pendant amino acids) were disordered and, thus, could not be visualized. This result, and the similar values of K_d for benzenesulfonamides with and without hydrophobic amino acids, are consistent with the results of Jain et al. presented above: hydrophobic secondary recognition elements make only a small contribution to affinity when separated from the phenyl ring of the benzenesulfonamide.

Sigal and Whitesides examined the affinity of *para*-substituted benzenesulfonamides containing hydrophobic amino acids separated from the phenyl ring by tails of zero (**96** and **98–102**), one, two, or three Gly residues.⁵⁰⁷ They observed that the increase in affinity contributed by the hydrophobic amino acid fell drastically as the tail length increased. For example, with Leu as the amino acid, the value of K_d increased from 9 nM for the benzenesulfonamides with zero Gly residues in the tail (**102**) to 130 nM with one Gly residue to 210 nM for the ligand with two or three Gly residues in the tail.

10.5.3.3. Unsuccessful Attempts to Design SREs to Interact with the Hydrophobic Pocket and Wall of CA. Attempts to design benzenesulfonamides that could interact

with both the hydrophobic pocket *and* hydrophobic wall of the enzyme have been largely unsuccessful.²⁸⁴ For example, **106** was designed to contain a phenyl substituent (phenylglycine, Phg, residue) to interact with the hydrophobic pocket and a benzyl ester to interact with the hydrophobic wall of HCA II; the affinity of this ligand, however, was the same as that of **51**, a substituted benzenesulfonamide with only a phenyl substituent. X-ray crystal structures demonstrated that the Phg residue of **106** interacted with the hydrophobic pocket of HCA II and that this interaction seemed to “steer” the benzyl ester away from the hydrophobic wall (the benzyl ester was not ordered enough to be located in the crystal structure).²⁸⁴

10.5.4. Hydrophilic or Charged Secondary Recognition Elements

A few studies have attempted to engineer contacts between hydrophilic or charged secondary recognition elements of substituted benzenesulfonamides and the hydrophilic half of the conical cleft of HCA II (see section 4.6).^{185,235,507} Sigal and Whitesides undertook the most rigorous study using amino acids as polar secondary recognition elements separated from the phenyl ring of the ligand by tails of zero (**89–95** and **97**), one, two, or three Gly residues.⁵⁰⁷ Their results demonstrated that charged or polar amino acids directly connected to the phenyl ring had either no effect on, or were deleterious to, affinity (e.g., Glu (**90**), $K_d = 530$ nM; Arg (**97**), $K_d = 220$ nM; Gln (**92**), $K_d = 140$; compared to Gly (**95**), $K_d = 310$ nM). The ligand with Thr as the secondary recognition element (**94**) demonstrated a ~ 6 -fold increase in affinity ($K_d = 53$ nM) over that with Gly (**95**); the investigators attributed this effect to hydrophobic contacts of Thr with HCA II instead of polar ones because the ligand with Ser (**93**, $K_d = 240$ nM) as the secondary recognition element had an affinity comparable to the ligand with Gly (**95**). This lack of effect of charged or polar secondary recognition elements persisted as these elements were spaced farther from the phenyl ring. The investigators attributed this lack of success to the fact that it is more difficult to engineer hydrogen bonds and ionic interactions than hydrophobic contacts;⁵⁰⁷ this idea is consistent with the observation that hydrogen bonds and ionic interactions are often geometrically demanding.^{4,30,397}

Boriack et al. also examined the affinity of polar or charged amino acids as secondary recognition elements, but their amino acids were linked to the benzenesulfonamide scaffold by triethylene glycol tails (**86–88**).¹⁸⁵ Consistent with the results of Sigal et al., ligands with polar (Ser (**86**), $K_d \approx 41$ nM) or charged (Glu (**87**), $K_d \approx 100$ nM; Lys (**88**), $K_d \approx 50$ nM) amino acids bound with affinities that were similar to, or slightly lower than, the control compound with no secondary recognition element (H (**83**), $K_d \approx 43$ nM).

10.5.5. Metal Ions as Secondary Recognition Elements

Two metal ions, Hg^{II} and Cu^{II}, have served as secondary recognition elements in the binding of benzenesulfonamides to HCA. The complex of HCA II with 3-acetoxymethyl-4-aminobenzenesulfonamide (**253**) is of historical importance. This inhibitor complex initially served as a heavy atom derivative of HCA II to aid in the determination of the crystal structure of the enzyme.^{159,600} That the Hg^{II} ion served as a (somewhat fortuitous) secondary recognition element was

not recognized until a pioneering study in which Eriksson et al. formed a complex between HCA II and **253**; they noticed that the Hg^{II} ion of **253** bound to His64 of HCA II.¹⁸⁶ Chakravarty and Kannan obtained similar results for the complex between **253** and HCA I.²¹¹ Hg^{II} has yet to be used as an explicit secondary recognition element to study the binding of ligands to CA.

Srivastava, Mallik, and co-workers examined the affinity of *para*-substituted benzenesulfonamides with Cu^{II} ions (coordinated by iminodiacetate moieties) serving as the secondary recognition elements (e.g., **218** and **219**) for HCA I and II and BCA II.^{181,596,601,602} For **218**, they observed a ~ 2 – 7 -fold higher affinity than for benzenesulfonamides with triethylene glycol tails (**83**, which contains a primary amine, and **74**, which contains a methyl ether), and for **219**, they observed an affinity comparable to that for a benzenesulfonamide with an ethyl tail (**38**).^{181,596,602} They believed that interactions between the Cu^{II} ion and a His of HCA were important because of the following: (i) the affinity of a metal-free version of **218** for HCA II was ~ 50 -fold lower than that of **218** and the same as that of benzenesulfonamide (**1**); (ii) the absorbance maximum of the Cu^{II} ion of **218** shifted to longer wavelength when titrated with HCA II; (iii) the affinity of **218** for HCA II that had been treated with diethyl pyrocarbonate, a reagent that reacts with accessible His residues,⁶⁰³ was ~ 15 -fold lower than that for HCA II.^{596,602}

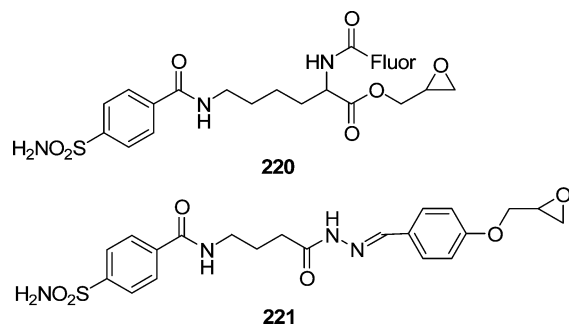
X-ray crystal structures of several complexes of Cu^{II}-containing ligands with HCA II revealed clear electron density of a Cu^{II} ion coordinated to the iminodiacetate (IDA) moiety of the ligand and to a His of the enzyme for only one of the ligands, **219**.¹⁸¹ In this complex, the ligand-bound Cu^{II} was chelated by His64, which lies inside the conical cleft of HCA II and serves as the proton shuttle for the enzyme (see section 4.6). Compound **219** also formed a complex with HCA I in which the ligand-bound Cu^{II} bound to another His residue in the conical cleft of the enzyme (His200). For the other complexes, no electron density for the IDA moiety, or for the putatively bound Cu^{II}, of the ligand bound at the active site was apparent, although free Cu^{II} ions that were not bound by a sulfonamide ligand were observed to be bound by one or more of the His residues of HCA II. Interestingly, they noted a 2:1 stoichiometry of ligand to HCA II in all of their complexes; the second ligand interacted with residues of the amino terminus of HCA II at the rim of the conical cleft.

While the idea of using a chelated Cu^{II} ion as a secondary recognition element to coordinate surface His residues of HCA is interesting, the increases in affinity observed so far have been modest (factors of < 10 in K_d^{obs}). Further, the approach has only been validated by X-ray crystallography for one of the Cu^{II}-containing ligands. A next generation of ligands that demonstrates high affinities (higher than ligands with hydrophobic SREs) and validation of metal ion coordination to surface His residues of CA by X-ray crystallography is necessary to prove the validity and utility of this approach.

10.5.6. Reactive Epoxides as Secondary “Recognition” Elements: Covalent Labeling of CA

Chen et al. and Takaoka et al. reported the use of *para*-substituted benzenesulfonamides with epoxides as secondary “recognition” elements (**220** and **221**).^{604,605} They demonstrated that their ligands selectively labeled one (or two

closely spaced) His residues of HCA II, and that the covalent reaction was directed by binding of the ligand to the active site of the enzyme: no labeling of HCA II was observed when a large excess of a high-affinity arylsulfonamide competitor was included in the reaction with the epoxide probe. Chen et al. demonstrated that their probe (**220**) labeled His64, a catalytically essential residue located in the conical cleft of HCA II (see section 4.6), and that it labeled HCA II selectively in the yeast proteome (when an extra, controlled amount of HCA II was added to the proteome).⁶⁰⁴ Using a probe (**221**) that lacked the fluorescein moiety (Fluor) of, and that was slightly longer than, **220**, Takaoka et al. were able to label a His residue at the amino terminus of HCA II (His3 or His4), outside of the conical cleft.⁶⁰⁵ They were able to regenerate the catalytic activity of the enzyme by removal of the sulfonamide moiety of the tethered molecule by reaction with an alkoxyamine.



10.5.7. Conclusions

Multivalency can enhance binding, but this approach has only made significant increases in affinity (>10-fold) with hydrophobic groups that are connected directly to the arylsulfonamide ring. This observation suggests that only the design of contacts to the hydrophobic pocket (Phe131, Val135, Leu198, and Pro202) near the active site of the enzyme has been effective; attempts to design contacts with residues of the “hydrophobic wall” (Leu198, Pro201, Pro202, and perhaps Phe20) of the enzyme have not yielded significant increases in affinity.

Although half of the conical cleft of CA contains hydrophilic or charged residues, the use of polar or charged secondary recognition elements has not resulted in increases in affinity (even when these elements are directly connected to the arylsulfonamide ring). This ineffectiveness could originate from hydrophilic or ionic interactions being intrinsically weaker than hydrophobic interactions or from the more stringent geometric requirements for these interactions than for hydrophobic interactions. The use of metals as secondary recognition elements to chelate His residues of CA is a promising idea but one that has, practically, only shown small effects so far (certainly smaller than for hydrophobic SREs). X-ray crystal structures have only validated coordination of a His residue of HCA—His64 of HCA II, His200 of HCA I (residues inside the conical cleft of HCA)—for one of the metal-containing ligands.

The active site-directed covalent labeling of His residues of HCA by epoxides as secondary recognition elements has been demonstrated. This approach has been successful in targeting HCA in an artificial mixture of proteins and could represent a means of converting weak interactions into strong ones.

10.6. Enthalpy and Entropy of Binding of Arylsulfonamides to CA

10.6.1. Overview and General Approach

Up to this point, we have only discussed the binding of arylsulfonamides to CA in terms of the free energy of binding (or K_d^{obs}). As we discussed in section 10.2.2, dissecting the free energy into its components of enthalpy and entropy will help us to understand the underlying physical principles of high-affinity binding. We believe that this understanding will ultimately facilitate the rational design of high-affinity ligands for proteins.

In this section, we survey the reported values of enthalpy and entropy of binding of arylsulfonamides to CA II. We adopt an organization similar to the one we used when discussing the free energy of binding: we explore the influence on the observed thermodynamics of binding of structural perturbations of the arylsulfonamide that affect the head group and the ring (sections 10.6.3–10.6.5) and the tail (section 10.6.6), separately. The observed values of enthalpy and entropy of binding depend on the experimental conditions: the pH, which determines the fractions of arylsulfonamide and CA II in the active forms (see section 10.3, Scheme 1), and the enthalpy of ionization of the buffer (since protons are taken up and released by the buffer). Thus, we only discuss the *observed* thermodynamic parameters for a series of arylsulfonamides reported under a given set of assay conditions (and often only those reported by one group of investigators).

To remove the dependence of the thermodynamic parameters on the assay conditions, in section 10.6.3 we calculate thermodynamic parameters for the binding of the arylsulfonamide anion to the $\text{CA-Zn}^{\text{II}}\text{-OH}_2^+$ form of the enzyme (eq 18). This analysis allows us to compare directly values obtained by different investigators, by different techniques, and under different experimental conditions. We also compare the thermodynamic parameters that have been determined by van't Hoff analysis and by microcalorimetry (section 10.6.4), when both sets of data are available.

10.6.2. Influence of Structural Perturbations of the Head and Ring Regions of the Arylsulfonamide on the Observed Enthalpy and Entropy of Binding

Taylor et al. were the first to determine the enthalpy and entropy of binding of a sulfonamide to CA; they measured the temperature-dependence of the affinity (K_d^{obs}) of *p*-nitrobenzenesulfonamide (**3**) for HCA II.⁴⁵⁸ Using van't Hoff analysis (eq 14), they concluded that binding was driven by enthalpy with only a small contribution of entropy (Table 13). Their van't Hoff plot showed slight curvature; this observation suggests that the change in heat capacity upon complexation was nonzero over this temperature range and brings into question the quantitative accuracy of their results (see section 10.2.2).

Table 13 lists all of the reported values of enthalpy ($\Delta H^{\circ}_{\text{obs}}$) and entropy ($-T\Delta S^{\circ}_{\text{obs}}$) for the binding of arylsulfonamides to HCA II and BCA II. We found no correlation between $\Delta H^{\circ}_{\text{obs}}$ or $-T\Delta S^{\circ}_{\text{obs}}$ and $\text{p}K_{\text{a}}$ (data not shown); this observation indicates that there are more contributions to these thermodynamic parameters than simply the formation of ArSO_2NH^- from ArSO_2NH_2 . We did, however, observe a reasonable correlation ($R^2 = 0.74$) between $\Delta H^{\circ}_{\text{obs}}$ and $-T\Delta S^{\circ}_{\text{obs}}$ (Figure 23A). We do not make too much of this linear plot, however. The range in $\Delta G^{\circ}_{\text{obs}}$ spanned by the

Table 13. Separated Values of Enthalpy and Entropy for the Association of Arylsulfonamides with CA II

Compound	CA II Variant	$\Delta G_{\text{obs}}^{\circ}$ (kcal mol ⁻¹)	$\Delta H_{\text{obs}}^{\circ}$ (kcal mol ⁻¹)	$-T\Delta S_{\text{obs}}^{\circ}$ (kcal mol ⁻¹)	$\Delta C_{p,\text{obs}}$ (cal mol ⁻¹ K ⁻¹)
1	HCA	-9.1 ^a	-10.9 ± 0.2 ^{b,c}	1.8	30 ± 20 ^{b,c}
1	BCA	-8.4 ± 0.05 ^{b,d}	-9.9 ± 0.05 ^{b,c}	1.5 ± 0.1	
1	BCA	-8.4 ± 0.05 ^{b,d}	-9.8 ± 0.05 ^{b,e}	1.4 ± 0.1	
1	BCA	-8.4 ± 0.05 ^{b,d}	-9.0 ± 0.5 ^{b,d}	0.7 ± 0.6	
3	HCA	-10.3 ^f	-9.5 ^{f,g}	-0.8	
4	BCA	-7.1 ± 0.2 ^{b,h}	-10.8 ± 0.12 ^{b,e}	3.7 ± 0.2	
4	BCA	-7.1 ± 0.2 ^{b,h}	-8.3 ± 3 ^{b,i}	1.2 ± 3.0	-52 ± 20 ^{b,h}
4	HCA	-6.6 ± 0.1 ^j	-7.7 ± 0.2 ^{g,j}	1.1 ± 0.2	
6	BCA	-9.7 ^a	-10.8 ^{b,e}	1.1	
29	BCA	-8.6 ± 0.13 ^{b,h}	-9.6 ± 1.5 ^{b,h,k}	1.0 ± 1.5	
29	BCA	-8.3 ± 0.3 ^l	-11.6 ± 0.4 ^{g,l}	3.3 ± 0.5	
29	BCA	-8.4 ± 0.2 ^{b,l}	-11.9 ± 0.4 ^{b,l}	3.5 ± 0.4	
29	BCA	-8.6 ± 0.02 ^{b,m}	-14.8 ± 0.5 ^{b,m}	6.2 ± 0.5	
37	BCA	-9.1 ± 0.03 ^{b,m}	-10.8 ± 0.4 ^{b,m}	1.7 ± 0.4	
63	BCA	-9.0 ± 0.02 ^{b,m}	-13.3 ± 0.4 ^{b,m}	4.3 ± 0.4	-24 ± 2 ^{b,m}
64	BCA	-9.1 ± 0.03 ^{b,m}	-12.9 ± 0.4 ^{b,m}	3.8 ± 0.4	
65	BCA	-9.1 ± 0.03 ^{b,m}	-12.3 ± 0.4 ^{b,m}	3.2 ± 0.4	-18 ± 10 ^{b,m}
66	BCA	-9.0 ± 0.02 ^{b,m}	-11.5 ± 0.4 ^{b,m}	2.5 ± 0.4	
67	BCA	-8.9 ± 0.04 ^{b,m}	-11.1 ± 0.5 ^{b,m}	2.2 ± 0.5	-20 ± 7 ^{b,m}
72	BCA	-9.8 ± 0.03 ^{b,m}	-10.2 ± 0.5 ^{b,m}	0.4 ± 0.5	-40 ± 8 ^{b,m}
73	BCA	-9.6 ± 0.03 ^{b,m}	-10.0 ± 0.3 ^{b,m}	0.4 ± 0.3	
74	BCA	-9.6 ± 0.06 ^{b,m}	-10.0 ± 0.3 ^{b,m}	0.4 ± 0.3	-47 ± 8 ^{b,m}
75	BCA	-9.4 ± 0.05 ^{b,m}	-9.4 ± 0.3 ^{b,m}	0.0 ± 0.3	
76	BCA	-9.4 ± 0.05 ^{b,m}	-9.0 ± 0.3 ^{b,m}	-0.4 ± 0.3	-40 ± 20 ^{b,m}
133	BCA	-8.8 ± 0.9 ^l	-5.7 ± 0.4 ^{g,l}	-3.1 ± 1.0	
133	BCA	-8.8 ± 0.9 ^{b,l}	-4.8 ± 0.4 ^{b,l}	-4.0 ± 1.0	
136	BCA	-11.1 ± 0.2 ^{b,h}	-5.2 ± 1.1 ^{b,h,k}	-5.8 ± 1.1	-155 ± 20 ^{b,h}
136	HCA	-10.7 ^{b,h}	-6.2 ^{b,h,k}	-4.5	-148 ^{b,h}
137	BCA	-10.4 ± 0.07 ^{b,h}	-10.2 ± 1.2 ^{b,h,k}	-0.2 ± 1.2	-107 ± 10 ^{b,h}
137	HCA	-11.2 ^{b,h}	-11.7 ^{b,h,k}	0.5	-64 ^{b,h}
138	BCA	-10.1 ± 0.07 ^{b,h}	-14.5 ^{b,c}	4.4	
138	BCA	-10.1 ± 0.07 ^{b,h}	-9.1 ± 1.6 ^{b,h,k}	-1.0 ± 1.6	-79 ± 20 ^{b,h}
138	HCA	-10.4 ^{b,h}	-10.4 ^{b,h,k}	0.0	-73 ^{b,h}
138	HCA	-10.4 ± 0.1 ^j	-10.7 ± 0.2 ^{g,j}	0.3 ± 0.2	
139	BCA	-11.4 ± 0.2 ^{j,n}	-14.4 ^{b,c}	3.0	
139	HCA	-11.4 ± 0.2 ^j	-15.0 ± 0.14 ^{b,c}	3.6 ± 0.2	-30 ± 20 ^{b,c}
139	HCA	-11.4 ± 0.2 ^j	-11.0 ± 0.4 ^{g,j}	-0.4 ± 0.4	
140	HCA	-11.9 ± 0.1 ^j	-8.6 ± 0.3 ^{g,j}	-3.3 ± 0.3	
157	HCA	-11.6 ± 0.1 ^j	-10.3 ± 0.4 ^{g,j}	-1.3 ± 0.4	
188	BCA	-10.7 ± 0.02 ^{b,h}	-8.9 ± 1.0 ^{b,h,k}	-1.8 ± 1.0	-35 ± 10 ^{b,h}
188	HCA	-10.9 ^{b,h}	-12.0 ^{b,h,k}	1.1	-48 ^{b,h}
188	HCA	-10.5 ± 0.1 ^j	-11.4 ± 0.2 ^{g,j}	0.9 ± 0.2	
207	BCA	-9.1 ± 0.06 ^{b,d}	-10.2 ± 0.2 ^{b,d}	1.1 ± 0.2	
208	BCA	-9.7 ± 0.07 ^{b,d}	-9.0 ± 0.2 ^{b,d}	-0.7 ± 0.2	
209	BCA	-8.5 ± 0.05 ^{b,d}	-7.8 ± 0.5 ^{b,d}	-0.7 ± 0.5	
210	BCA	-9.2 ± 0.05 ^{b,d}	-9.4 ± 0.4 ^{b,d}	0.2 ± 0.4	
211	BCA	-9.9 ± 0.14 ^{b,d}	-9.6 ± 0.3 ^{b,d}	-0.3 ± 0.3	
212	BCA	-10.4 ± 0.1 ^{b,d}	-8.9 ± 0.1 ^{b,d}	-1.4 ± 0.1	
213	BCA	-8.5 ± 0.03 ^{b,m}	-11.7 ± 0.4 ^{b,m}	3.2 ± 0.4	-43 ± 10 ^{b,m}
214	BCA	-8.9 ± 0.02 ^{b,m}	-11.5 ± 0.4 ^{b,m}	2.6 ± 0.4	
215	BCA	-8.8 ± 0.02 ^{b,m}	-10.4 ± 0.4 ^{b,m}	1.6 ± 0.4	-45 ± 16 ^{b,m}
216	BCA	-8.7 ± 0.03 ^{b,m}	-10.0 ± 0.4 ^{b,m}	1.3 ± 0.4	
217	BCA	-8.7 ± 0.03 ^{b,m}	-9.5 ± 0.3 ^{b,m}	0.8 ± 0.3	-49 ± 23 ^{b,m}
222	BCA	-6.1 ± 0.2 ^{b,h}	-2.4 ± 2.8 ^{b,h,k}	-3.7 ± 2.8	-50 ± 40 ^{b,h}

^a From references listed in Table 10. ^b Determined by calorimetry. ^c Measured in 50 mM Hepes buffer, pH 8.2.⁴⁰⁵ ^d Measured in 20 mM sodium phosphate buffer, pH 7.5.¹⁸² ^e Measured in 50 mM Tris buffer, pH 8.2.⁴⁰⁵ ^f Measured in 20 mM sodium phosphate buffer, pH 7.6.⁴⁵⁸ ^g Estimated by van't Hoff analysis. ^h Data reported at pH 7.0 and $T = 310 \text{ K}$ ⁴¹⁷ have been extrapolated to $T = 298 \text{ K}$. ⁱ Measured in 20 mM PIPES buffer, pH 7.0.⁴¹⁷ ^j Measured in 50 mM barbital buffer with "average" pH 7.5.⁶⁰⁸ ^k Extrapolated to a buffer enthalpy of ionization of zero.⁴¹⁷ ^l Measured in PBS (10 mM phosphate pH 7.4, 150 mM NaCl).⁴¹² ^m Measured in 20 mM sodium phosphate pH 7.5.⁴¹⁵ ⁿ Assumed to be equal to the value reported for HCA II.

ligands is much smaller than that in $\Delta H_{\text{obs}}^{\circ}$ or in $-T\Delta S_{\text{obs}}^{\circ}$; this fact requires a linear relationship between $\Delta H_{\text{obs}}^{\circ}$ and $-T\Delta S_{\text{obs}}^{\circ}$ (see section 10.2.2).^{574–576}

Consistent with the results of Taylor et al., the majority of arylsulfonamides bind to CA II with a small entropy of binding ($|T\Delta S_{\text{obs}}^{\circ}| < 2 \text{ kcal mol}^{-1}$) and lie between the two vertical dotted lines in Figure 23A. The few that bind with a change in entropy more favorable than these "limits" are relatively hydrophobic (e.g., ethoxzolamide, **140**; dansyl-

amide, **133**; and dichlorophenamide, **136**) and could be taking advantage of hydrophobic contacts with CA II. An interesting outlier is *p*-aminomethylbenzenesulfonamide (**222**); this sulfonamide binds with the lowest exothermicity ($\Delta H_{\text{obs}}^{\circ} = -2.4 \text{ kcal mol}^{-1}$) of all of the arylsulfonamides studied to date. This low exothermicity could be a result of electrostatic repulsion of the positive charge of the $-\text{CH}_2\text{NH}_3^+$ moiety of this sulfonamide by the positively charged active site of BCA II. Most of the arylsulfonamides that bind with very

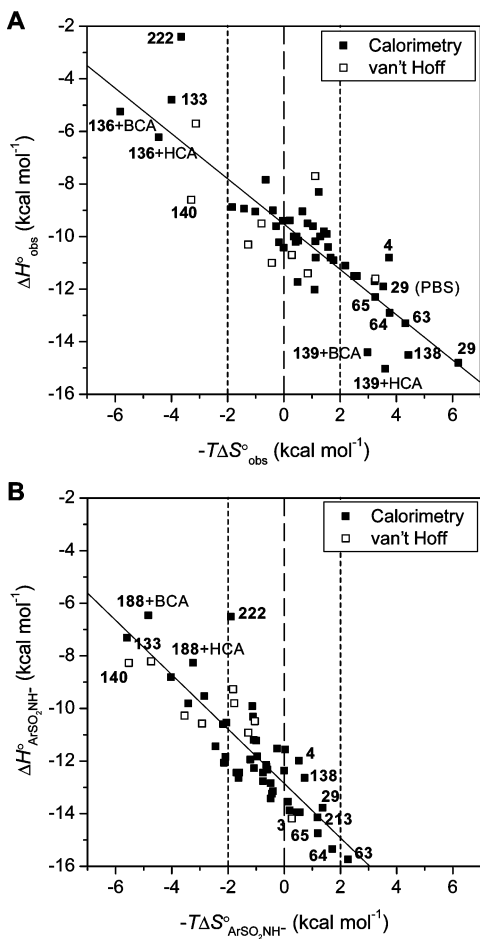


Figure 23. Variation of enthalpy with entropy for the association of arylsulfonamides with CA II. Plots for the (A) observed thermodynamic parameters and (B) those calculated for the association of the arylsulfonamide anion with CA $\text{--Zn}^{\text{II}}\text{--OH}_2^+$ (eq 18; Scheme 1) using eq 25 are shown. The data are listed in Tables 13 and 14. The fitting parameters and correlation coefficients (slope, y-intercept in kcal mol^{-1} , and R^2) are as follows: for (A) -0.86 ± 0.07 , -9.52 ± 0.17 , and 0.74 , and for (B) -1.03 ± 0.09 , -12.85 ± 0.18 , and 0.74 . Uncertainties are from the least-squares fitting procedure. The dashed lines separate favorable ($-T\Delta S^\circ < 0$) from unfavorable ($-T\Delta S^\circ > 0$) entropy of binding, and the dotted lines are placed to signify “moderate” entropy of binding with a magnitude of $T\Delta S^\circ \leq 2 \text{ kcal mol}^{-1}$.

unfavorable entropies ($-T\Delta S^\circ_{\text{obs}} > 2 \text{ kcal mol}^{-1}$) are negatively charged (e.g., carboxylates for **63**, **64**, **65**, and **29**); the unfavorable entropies could represent an entropic penalty for orienting the negative charges in the positively charged active site of BCA II.

The changes in heat capacity upon CA II–arylsulfonamide complexation (ΔC_p) were relatively modest for all arylsulfonamides that have been examined. These values are negative for all arylsulfonamides (except benzenesulfonamide, **1**); this observation suggests that hydrophobic (non-polar) surface area is buried upon complexation.⁵⁶⁶

10.6.3. Thermodynamics of Association of the Arylsulfonamide Anion (ArSO_2NH^-) with $\text{CA--Zn}^{\text{II}}\text{--OH}_2^+$

We wish to remove the dependence of the enthalpy ($\Delta H^\circ_{\text{obs}}$) and entropy ($-T\Delta S^\circ_{\text{obs}}$) of binding on the experimental conditions (e.g., pH and enthalpy of ionization of the buffer) and the physical properties (e.g., pK_a and enthalpy of ionization) of the arylsulfonamides themselves, in order to explore the *intrinsic* thermodynamics of association of

arylsulfonamides with CA II. For reasons that we have discussed in section 10.3.3, we have elected to use eq 18: the binding of the arylsulfonamide anion (ArSO_2NH^-) to the $\text{Zn}^{\text{II}}\text{--water}$ form of CA II ($\text{CA--Zn}^{\text{II}}\text{--OH}_2^+$). We calculate $\Delta G^\circ_{\text{ArSO}_2\text{NH}^-}$ from eq 21 and the well-known thermodynamic relation ($\Delta G^\circ = -RT \ln K_{\text{eq}} = RT \ln K_d$), $\Delta H^\circ_{\text{ArSO}_2\text{NH}^-}$ from eq 25, and $-T\Delta S^\circ_{\text{ArSO}_2\text{NH}^-}$ through subtraction of the two.

$$\Delta H^\circ_{\text{ArSO}_2\text{NH}^-} = \Delta H^\circ_{\text{obs}} + \theta_{\text{CA--Zn}^{\text{II}}\text{--OH}_2^+} (\Delta H^\circ_{\text{ion,CA--Zn}^{\text{II}}\text{--OH}_2^+} - \Delta H^\circ_{\text{ion,buffer}}) + \theta_{\text{ArSO}_2\text{NH}^-} (\Delta H^\circ_{\text{ion,buffer}} - \Delta H^\circ_{\text{ion,ArSO}_2\text{NH}_2}) \quad (25)$$

In eq 25, $\theta_{\text{CA--Zn}^{\text{II}}\text{--OH}_2^+}$ and $\theta_{\text{ArSO}_2\text{NH}^-}$ are defined in eqs 20a and 20b, $\Delta H^\circ_{\text{ion,buffer}}$ is the enthalpy of ionization of the buffer,⁶⁰⁶ $\Delta H^\circ_{\text{ion,ArSO}_2\text{NH}_2}$ is the enthalpy of ionization of the arylsulfonamide, and $\Delta H^\circ_{\text{ion,CA--Zn}^{\text{II}}\text{--OH}_2^+}$ is the enthalpy of ionization of the Zn^{II} -bound water of the enzyme (estimated to be $6.9 \text{ kcal mol}^{-1}$ from the temperature dependence of the esterase activity of BCA II; see section 8.3.2).⁶⁰⁷ Literature values of $\Delta H^\circ_{\text{ion,ArSO}_2\text{NH}_2}$ are available for some arylsulfonamides (Table 14). For those sulfonamides for which literature values were not available, we estimated them by interpolation from a linear plot of literature values of $\Delta H^\circ_{\text{ion,ArSO}_2\text{NH}_2}$ vs pK_a .

Table 14 lists the calculated thermodynamic data, and Figure 23B shows these data graphically. Similar to the results for the observed data, we observe no correlation between $\Delta H^\circ_{\text{ArSO}_2\text{NH}^-}$ or $-T\Delta S^\circ_{\text{ArSO}_2\text{NH}^-}$ and pK_a (data not shown). This result is compatible with the hypothesis that there are a number of structural interactions between the arylsulfonamide anion and CA II, each of which contributes to the enthalpy and entropy of binding. For the most part, values of $\Delta H^\circ_{\text{ArSO}_2\text{NH}^-}$ measured calorimetrically by different research groups differ by $<0.5 \text{ kcal mol}^{-1}$ (Table 14). There are a few exceptions: values of $\Delta H^\circ_{\text{ArSO}_2\text{NH}^-}$ for the binding of methazolamide (**138**) to BCA II differ by $\sim 2.5 \text{ kcal mol}^{-1}$ when measured by different investigators, and those for the binding of *p*-carboxybenzenesulfonamide (**29**) to BCA II differ by $\sim 3 \text{ kcal mol}^{-1}$ (Table 14). The different results for **138** could be due to the use of a low-sensitivity flow calorimeter by Binford et al.⁴⁰⁵ rather than a high-sensitivity isothermal titration calorimeter, as used by Matulis and Todd.⁴¹⁷ The situation is more complicated for **29**. The value of $\Delta H^\circ_{\text{ArSO}_2\text{NH}^-}$ for **29** reported by Day et al.⁴¹² is significantly less exothermic ($\Delta\Delta H^\circ_{\text{ArSO}_2\text{NH}^-} \approx 3 \text{ kcal mol}^{-1}$) than that reported by Krishnamurthy et al.⁴¹⁵ This difference could be due to the different experimental conditions: Day et al. used phosphate buffer containing sodium chloride (ionic strength $\approx 0.2 \text{ M}$), while Krishnamurthy et al. used phosphate buffer (ionic strength $\approx 0.05 \text{ M}$). The electrostatic interactions (and component thermodynamic parameters) between the carboxylate anion of the arylsulfonamide and BCA II would be expected to be sensitive to the ionic strength of the medium.

Enthalpy ($\Delta H^\circ_{\text{ArSO}_2\text{NH}^-}$) is a dominant factor in the binding of ArSO_2NH^- to $\text{CA--Zn}^{\text{II}}\text{--OH}_2^+$ (eq 18) (as $\Delta H^\circ_{\text{obs}}$ is in the *observed* binding of arylsulfonamides to CA II), but the entropy of binding ($-T\Delta S^\circ_{\text{ArSO}_2\text{NH}^-}$) is favorable for almost all of the sulfonamides for which data are reported (Figure 23B). This observation is consistent with our intuition: $-T\Delta S^\circ_{\text{ArSO}_2\text{NH}^-}$ should be slightly favorable (and near zero) for this reaction, because the number of water molecules

Table 14. Values of Enthalpy and Entropy for the Association of Arylsulfonamide Anion with CA–Zn^{II}–OH₂⁺

Compound	CA II Variant	p <i>K</i> _a	$\Delta H_{\text{ion,ArSO}_2\text{NH}_2}^{\circ}$ (kcal mol ⁻¹)	$\Delta G_{\text{ArSO}_2\text{NH}_2}^{\circ a}$ (kcal mol ⁻¹)	$\Delta H_{\text{ArSO}_2\text{NH}_2}^{\circ b}$ (kcal mol ⁻¹)	$-T\Delta S_{\text{ArSO}_2\text{NH}_2}^{\circ}$ (kcal mol ⁻¹)
1	HCA	10.1 ^{c,d}	9.1 ± 0.01 ^{d,e}	-13.5 ^c	-13.1 ^{e,f}	-0.4
1	BCA	10.1 ^{c,d}	9.1 ± 0.01 ^{d,e}	-12.8 ± 0.3 ^{e,g}	-12.1 ± 0.1 ^{e,f}	-0.6 ± 0.4
1	BCA	10.1 ^{c,d}	9.1 ± 0.01 ^{d,e}	-12.8 ± 0.3 ^{e,g}	-11.8 ± 0.1 ^{e,h}	-1.0 ± 0.4
1	BCA	10.1 ^{c,d}	9.1 ± 0.01 ^{d,e}	-12.9 ± 0.3 ^{e,g}	-12.3 ± 0.6 ^{e,g}	-0.6 ± 0.6
3	HCA	9.0 ^c	7.3 ⁱ	-13.9 ⁱ	-14.2 ^{j,k}	0.3
4	BCA	10.1 ^c	8.3 ⁱ	-11.5 ± 0.4 ^{e,l}	-12.0 ^{e,h}	0.5
4	BCA	10.1 ^c	8.3 ⁱ	-11.8 ± 0.3 ^{e,l}	-11.5 ^{e,l}	-0.3
4	HCA	10.1 ^c	8.3 ⁱ	-11.1 ± 0.3 ^m	-9.3 ^{k,m}	-1.8
6	BCA	10.2 ^c	8.3 ⁱ	-14.2 ^c	-12.1 ^{e,h}	-2.1
29	BCA	9.6 ⁿ	4.8 ± 0.7 ^{e,n}	-12.6 ± 0.3 ^{e,o}	-10.5 ± 1.7 ^{e,o}	-2.1 ± 1.7
29	BCA	9.6 ⁿ	4.8 ± 0.7 ^{e,n}	-12.2 ± 0.4 ^p	-10.9 ± 0.8 ^{k,p}	-1.3 ± 0.9
29	BCA	9.6 ⁿ	4.8 ± 0.7 ^{e,n}	-12.2 ± 0.3 ^{e,p}	-11.2 ± 0.8 ^{e,p}	-1.0 ± 0.9
29	BCA	9.6 ⁿ	4.8 ± 0.7 ^{e,n}	-12.4 ± 0.3 ^{e,q}	-13.8 ± 0.9 ^{e,q}	1.4 ± 0.9
37	BCA	10.3 ^c	8.4 ⁱ	-13.9 ± 0.3 ^{e,q}	-13.4 ^{e,q}	-0.5
63	BCA	10.1 ^r	8.3 ⁱ	-13.5 ± 0.3 ^{e,q}	-15.7 ^{e,q}	2.3
64	BCA	10.1 ^r	8.3 ⁱ	-13.6 ± 0.3 ^{e,q}	-15.3 ^{e,q}	1.7
65	BCA	10.1 ^r	8.3 ⁱ	-13.5 ± 0.3 ^{e,q}	-14.7 ^{e,q}	1.2
66	BCA	10.1 ^r	8.3 ⁱ	-13.5 ± 0.3 ^{e,q}	-13.9 ^{e,q}	0.4
67	BCA	10.1 ^r	8.3 ⁱ	-13.4 ± 0.3 ^{e,q}	-13.5 ^{e,q}	0.1
72	BCA	10.1 ^r	8.3 ⁱ	-14.3 ± 0.3 ^{e,q}	-12.6 ^{e,q}	-1.6
73	BCA	10.1 ^r	8.3 ⁱ	-14.1 ± 0.3 ^{e,q}	-12.4 ^{e,q}	-1.7
74	BCA	10.1 ^r	8.3 ⁱ	-14.0 ± 0.3 ^{e,q}	-12.4 ^{e,q}	-1.6
75	BCA	10.1 ^r	8.3 ⁱ	-13.9 ± 0.3 ^{e,q}	-11.8 ^{e,q}	-2.1
76	BCA	10.1 ^r	8.3 ⁱ	-13.9 ± 0.3 ^{e,q}	-11.4 ^{e,q}	-2.4
133	BCA	9.8 ^c	8.0 ⁱ	-12.9 ± 0.9 ^p	-8.2 ^{k,p}	-4.7
133	BCA	9.8 ^c	8.0 ⁱ	-12.9 ± 0.9 ^{e,p}	-7.3 ^{e,p}	-5.6
136	BCA	8.2 ⁿ	6.9 ± 0.4 ^{e,n}	-13.2 ± 0.3 ^{e,o}	-9.8 ± 1.2 ^{e,o}	-3.4 ± 1.2
136	HCA	8.2 ⁿ	6.9 ± 0.4 ^{e,n}	-12.8 ^{e,o}	-8.8 ^{e,o}	-4.0
137	BCA	7.3 ⁿ	5.4 ± 0.3 ^{e,n}	-11.5 ± 0.2 ^{e,o}	-11.6 ± 1.3 ^{e,o}	0.0 ± 1.3
137	HCA	7.3 ⁿ	5.4 ± 0.3 ^{e,n}	-12.4 ^{e,o}	-12.4 ^{e,o}	0.0
138	BCA	7.1 ⁿ	5.7 ± 0.2 ^{e,n}	-11.9 ± 0.2 ^{e,o}	-12.6 ± 0.1 ^{e,f}	0.7 ± 0.2
138	BCA	7.1 ⁿ	5.7 ± 0.2 ^{e,n}	-11.0 ± 0.2 ^{e,o}	-9.9 ± 1.7 ^{e,o}	-1.1 ± 1.7
138	HCA	7.1 ⁿ	5.7 ± 0.2 ^{e,n}	-11.4 ^{e,o}	-10.3 ^{e,o}	-1.1
138	HCA	7.1 ⁿ	5.7 ± 0.2 ^{e,n}	-11.6 ± 0.1 ^m	-9.8 ± 0.2 ^{k,m}	-1.8 ± 0.2
139	BCA	8.3 ^s	6.3 ± 0.1 ^s	-13.7 ± 0.3 ^o	-13.2 ^{e,f}	-0.4
139	HCA	8.3 ^s	6.3 ± 0.1 ^s	-13.7 ± 0.3 ^o	-13.9 ± 0.2 ^{e,f}	0.2 ± 0.4
139	HCA	8.3 ^s	6.3 ± 0.1 ^s	-13.5 ± 0.3 ^o	-10.6 ± 0.4 ^{k,m}	-2.9 ± 0.5
140	HCA	8.1 ^c	6.5 ⁱ	-13.8 ± 0.2 ^m	-8.3 ^{k,m}	-5.5
157	HCA	8.4 ^c	6.8 ⁱ	-13.8 ± 0.3 ^m	-10.3 ^{k,m}	-3.6
188	BCA	6.3 ⁿ	5.0 ± 0.3 ^{e,n}	-11.3 ± 0.1 ^{e,o}	-6.5 ± 1.0 ^{e,o}	-4.8 ± 1.0
188	HCA	6.3 ⁿ	5.0 ± 0.3 ^{e,n}	-11.5 ^{e,o}	-8.3 ^{e,o}	-3.3
188	HCA	6.3 ⁿ	5.0 ± 0.3 ^{e,n}	-11.5 ± 0.1 ^m	-10.5 ± 0.2 ^{k,m}	-1.1 ± 0.2
207	BCA	9.6 ^d	7.9 ± 0.03 ^{d,e}	-12.8 ± 0.3 ^{e,g}	-12.2 ± 0.2 ^{e,g}	-0.6 ± 0.4
208	BCA	9.7 ^d	8.5 ± 0.06 ^{d,e}	-13.6 ± 0.3 ^{e,g}	-11.6 ± 0.2 ^{e,g}	-2.0 ± 0.4
209	BCA	10.0 ^d	8.6 ± 0.03 ^{d,e}	-12.8 ± 0.3 ^{e,g}	-10.6 ± 0.5 ^{e,g}	-2.2 ± 0.6
210	BCA	9.1 ^d	7.8 ± 0.14 ^{d,e}	-12.3 ± 0.3 ^{e,g}	-11.2 ± 0.5 ^{e,g}	-1.1 ± 0.6
211	BCA	9.4 ^d	8.6 ± 0.04 ^{d,e}	-13.4 ± 0.3 ^{e,g}	-12.3 ± 0.3 ^{e,g}	-1.1 ± 0.5
212	BCA	8.2 ^d	7.6 ± 0.03 ^{d,e}	-12.4 ± 0.3 ^{e,g}	-9.5 ± 0.5 ^{e,g}	-2.9 ± 0.5
213	BCA	10.1 ^r	8.3 ⁱ	-13.0 ± 0.3 ^{e,q}	-14.1 ^{e,q}	1.2
214	BCA	10.1 ^r	8.3 ⁱ	-13.4 ± 0.3 ^{e,q}	-13.9 ^{e,q}	0.5
215	BCA	10.1 ^r	8.3 ⁱ	-13.3 ± 0.3 ^{e,q}	-12.8 ^{e,q}	-0.5
216	BCA	10.1 ^r	8.3 ⁱ	-13.2 ± 0.3 ^{e,q}	-12.4 ^{e,q}	-0.8
217	BCA	10.1 ^r	8.3 ⁱ	-13.1 ± 0.3 ^{e,q}	-11.9 ^{e,q}	-1.2
222	BCA	8.4 ⁿ	6.7 ± 2.0 ^{e,n}	-8.4 ± 0.3 ^{e,o}	-6.5 ± 3.4 ^{e,o}	-1.9 ± 3.4

^a Calculated using $\Delta G_{\text{obs}}^{\circ}$ from Table 10 and eq 21. ^b Calculated using values of $\Delta H_{\text{obs}}^{\circ}$ from Table 10 and eq 25. ^c From references listed in Table 10. ^d Measured in ref 182. ^e Determined by calorimetry. ^f Observed thermodynamic values measured in 50 mM Hepes buffer, pH 8.2.⁴⁰⁵ ^g Observed thermodynamic values measured in 20 mM phosphate buffer, pH 7.5.¹⁸² ^h Observed thermodynamic values measured in 50 mM Tris buffer, pH 8.2.⁴⁰⁵ ⁱ Estimated from a linear plot of $\Delta H_{\text{ion,ArSO}_2\text{NH}_2}^{\circ}$ vs p*K*_a for arylsulfonamides with experimental values of $\Delta H_{\text{ion,ArSO}_2\text{NH}_2}^{\circ}$. ^j Observed thermodynamic values.⁴⁵⁸ ^k Estimated by van't Hoff analysis. ^l Observed thermodynamic values measured in 20 mM PIPES buffer, pH 7.0.⁴¹⁷ ^m Observed thermodynamic values measured in 50 mM barbital buffer with "average" pH 7.5.⁶⁰⁸ ⁿ Measured in ref 417 and extrapolated to *T* = 298 K when necessary. ^o Observed thermodynamic values measured in 25 mM phosphate buffer, pH 7.0.⁴¹⁷ ^p Observed thermodynamic values measured in PBS (10 mM phosphate, pH 7.4, 150 mM NaCl).⁴¹² ^q Observed thermodynamic values measured in 20 mM sodium phosphate, pH 7.5.⁴¹⁵ ^r Assumed to be equal to the value for compound 38 (see Table 10). ^s Measured in ref 405.

surrounding the free arylsulfonamide anion should be slightly greater than the number surrounding the displaced water (from the Zn^{II} cofactor), while the *intrinsic* (translational and rotational) entropies of the arylsulfonamide anion and water are likely to be similar.⁵⁹⁴ This simple model assumes that the residual mobility and hydrophobic contacts of the arylsulfonamide anion when associated with CA II are the

same as those of the water when associated with CA II. Differences in either of these two will give values of entropy of binding ($-T\Delta S_{\text{ArSO}_2\text{NH}_2}^{\circ}$) that deviate significantly from zero.

Some arylsulfonamides bind with significantly favorable changes in entropy ($-T\Delta S_{\text{ArSO}_2\text{NH}_2}^{\circ} < -2$ kcal mol⁻¹; Figure 23B). Examining the structures of these ligands suggests that

they are able to take advantage of hydrophobic contacts with CA II, although we cannot rule out the explanation that these ligands have greater residual mobility in complexes with CA II than do the other arylsulfonamides. An interesting example is the structurally simple trifluoromethanesulfonamide (**188**), which binds with a very favorable $-T\Delta S^\circ_{\text{ArSO}_2\text{NH}^-}$. This observation is consistent with hydrophobic contacts of the trifluoromethyl moiety of the ligand with a hydrophobic pocket of HCA II revealed by X-ray crystallography (see section 10.3.4).²⁰¹ At the other extreme, there are some arylsulfonamides that bind with unfavorable $-T\Delta S^\circ_{\text{ArSO}_2\text{NH}^-}$. Most of these ligands are negatively charged, and their unfavorable entropies of binding could represent an entropic penalty for orienting their negative charges in the positively charged active site of CA II.

An interesting outlier in Figure 23B is *p*-aminomethylbenzenesulfonamide (**222**); this ligand binds with a lower exothermicity (less favorable $\Delta H^\circ_{\text{ArSO}_2\text{NH}^-}$) than anticipated and could suffer from electrostatic repulsion of its putative positive charge with the positively charged active site of BCA II (see section 10.6.2).

10.6.4. Comparison of $\Delta H^\circ_{\text{ArSO}_2\text{NH}^-}$ from Calorimetry and van't Hoff Analysis

As discussed in section 10.2.2, the two primary means of determining enthalpy and entropy of protein–ligand binding are calorimetry and van't Hoff analysis. This section uses the system of CA II and arylsulfonamides as a testing ground to compare the thermodynamic parameters obtained by both techniques.

There are only five arylsulfonamides (**139**, **138**, **188**, **133**, and **29**) for which values of enthalpy of binding have been reported by both calorimetry and van't Hoff analysis, and only two (**133** and **29**) for which these values have been reported under the same experimental conditions and by the same investigators (Table 14). There is no clear trend in the differences in values of $\Delta H^\circ_{\text{ArSO}_2\text{NH}^-}$ from the two types of experiments. For the binding of benzolamide (**139**) to HCA II, $\Delta H^\circ_{\text{ArSO}_2\text{NH}^-}$ from the calorimetric data of Binford et al. is ~ 3 kcal mol⁻¹ more exothermic than that from the van't Hoff data of Conroy and Maren (Table 14).^{405,608} While values of $\Delta H^\circ_{\text{ArSO}_2\text{NH}^-}$ for the binding of methazolamide (**138**) to HCA II measured by calorimetry by Matulis and Todd and van't Hoff analysis by Conroy and Maren showed good agreement ($\Delta\Delta H^\circ_{\text{ArSO}_2\text{NH}^-} \approx 0.5$ kcal mol⁻¹), the binding of trifluoromethanesulfonamide (**188**) to HCA II showed a significant discrepancy between values measured by the same two techniques (and in the direction opposite to that for **139**: $\Delta H^\circ_{\text{ArSO}_2\text{NH}^-}$ was ~ 2 kcal mol⁻¹ less exothermic from calorimetry than from van't Hoff analysis).^{417,608} In a study that allowed a direct comparison of the two techniques, Day et al. examined the thermodynamics of binding of dansylamide (DNSA, **133**) and *p*-carboxybenzenesulfonamide (**29**) to BCA II in solution using ITC and to BCA II immobilized in a thin layer of dextran on a gold surface using surface plasmon resonance spectroscopy (SPR; see sections 8.4.3 and 12) and van't Hoff analysis.⁴¹² They found that the values of enthalpy of binding determined by both techniques for both sulfonamides were within experimental error ($\Delta\Delta H^\circ_{\text{ArSO}_2\text{NH}^-} < 1$ kcal mol⁻¹; Tables 12 and 13).

Because only a limited number of cases can be compared directly, we cannot draw clear conclusions about the correlation between values of enthalpy of binding determined

by calorimetry and by van't Hoff analysis—that is, we do not know whether these values are within error of one another or whether there is a consistent discrepancy between the values measured by the two techniques. A controlled study of the thermodynamics of binding of a number of arylsulfonamides to CA determined by both techniques under the same experimental conditions would be necessary to examine this issue. Nevertheless, we believe that calorimetry is the superior technique for measuring enthalpy and entropy of binding because it measures directly the heat released (and, thus, the enthalpy) upon protein–ligand complexation, and it is not subject to the experimental artifacts (most of which are caused by the limited range in temperature that can be examined in biological systems) that often plague van't Hoff analyses (see section 10.2.2).

10.6.5. Influence of the Head Group: Fluorinated Benzenesulfonamides

Studies of the thermodynamics of binding of a heterogeneous set of arylsulfonamides (see sections 10.6.3 and 10.6.4) do not allow a direct estimate of the contributions of the head group or the aryl ring of the arylsulfonamide to the enthalpy and entropy of binding because of the heterogeneity of the interactions between each ligand and CA. This section highlights a well-controlled study by Krishnamurthy et al. that examines the thermodynamics of binding of a series of structurally similar ligands (fluorinated benzenesulfonamides, **207–212**) to BCA II.¹⁸²

As fluorination of the ring only slightly perturbs the size and shape of the ligands (and so they can be assumed to bind to the enzyme in a similar, conserved way), this study allowed the estimation of the magnitudes of the enthalpies (eq 26) and entropies (eq 27) of the different structural interactions between BCA II and benzenesulfonamide ligands. These equations were obtained from QSARs (Figure 16 parts B and C) between $\Delta H^\circ_{\text{ArSO}_2\text{NH}^-}$ or $-T\Delta S^\circ_{\text{ArSO}_2\text{NH}^-}$ and $\text{p}K_a$ and $\log P$ by assuming that the $\text{p}K_a$ -dependent term included both the $\text{Zn}^{\text{II}}\text{--N}$ bond ($\Delta H^\circ_{\text{Zn}^{\text{II}}\text{--N}}$ for its enthalpy of binding and $-T\Delta S^\circ_{\text{Zn}^{\text{II}}\text{--N}}$ for its entropy of binding) and the hydrogen-bond network ($\Delta H^\circ_{\text{H--bonds}}$ for its enthalpy of binding and $-T\Delta S^\circ_{\text{H--bonds}}$ for its entropy of binding), and the $\log P$ -dependent term consisted solely of the (mainly, hydrophobic) contacts between the phenyl ring and the enzyme ($\Delta H^\circ_{\text{ring}}$ for its enthalpy of binding from van der Waals contacts and $-T\Delta S^\circ_{\text{ring}}$ for its entropy of binding from the “hydrophobic effect”^{4,557–560}).

$$\Delta H^\circ_{\text{Zn}^{\text{II}}\text{--N}} + \Delta H^\circ_{\text{H--bonds}} = -1.58(\pm 0.47)\text{p}K_a + 3.9(\pm 5.0) \quad (26a)$$

$$\Delta H^\circ_{\text{ring}} = -0.21(\pm 0.82)\log P - 0.5(\pm 1.8) \quad (26b)$$

$$-T\Delta S^\circ_{\text{Zn}^{\text{II}}\text{--N}} - T\Delta S^\circ_{\text{H--bonds}} = 0.73(\pm 0.53)\text{p}K_a - 5.5(\pm 5.7) \quad (27a)$$

$$-T\Delta S^\circ_{\text{ring}} = -0.98(\pm 0.92)\log P - 2.2(\pm 2.0) \quad (27b)$$

Figure 18 shows the ranges in values of the component enthalpies and entropies for the structural interactions between BCA II and the benzenesulfonamide ligands. $\Delta H^\circ_{\text{ArSO}_2\text{NH}^-}$ is dominated by electrostatic interactions—the $\text{Zn}^{\text{II}}\text{--bond}$ and the hydrogen-bond network—and $-T\Delta S^\circ_{\text{ArSO}_2\text{NH}^-}$ is dominated by the hydrophobic contacts of the phenyl ring

with the enzyme. The slightly unfavorable contribution of electrostatic interactions to $-T\Delta S^\circ_{\text{ArSO}_2\text{NH}^-}$ probably reflects enthalpy/entropy compensation: more enthalpically favorable interactions have less mobility at the protein–ligand interface (resulting in less favorable entropy of binding) than less enthalpically favorable interactions (see section 10.2.2).

10.6.6. Influence of the Tail Group: Oligoethylene Glycol, Oligoglycine, and Oligosarcosine Tails

This section addresses the enthalpic and entropic contributions of the tail region of the arylsulfonamide to affinity (Figure 11A). Specifically, it summarizes current understanding of the thermodynamic basis for the insensitivity of K_d^{obs} to chain length (n) for benzenesulfonamides containing tails of oligoethylene glycol (72–76), oligoglycine (63–67), and oligosarcosine (213–217) (see section 10.4.2; Figure 21A). Because the values of pK_a of the sulfonamides are expected to be the same for all of these ligands, trends in the *observed* thermodynamic parameters ($\Delta H^\circ_{\text{obs}}$ and $-T\Delta S^\circ_{\text{obs}}$; Table 13) across the series are the same as trends in the thermodynamic parameters calculated for the binding of the sulfonamide anion to $\text{CA-Zn}^{\text{II}}-\text{OH}_2^+$ ($\Delta H^\circ_{\text{ArSO}_2\text{NH}^-}$ and $-T\Delta S^\circ_{\text{ArSO}_2\text{NH}^-}$; Table 14).

Whitesides, Christianson, and co-workers^{202,377} previously rationalized this insensitivity of K_d^{obs} by invoking enthalpy/entropy compensation: the interaction of the tail with CA II increased as the length of the tail increased (more favorable enthalpy of binding due to increasing number of van der Waals contacts), but this increase was *exactly* compensated by the increasing conformational cost of restriction of freely rotating bonds (more unfavorable entropy of binding).^{416,594,609} The investigators found it astonishing that enthalpy and entropy of binding would be perfectly compensating for three different classes of tails.

Using isothermal titration calorimetry (ITC), Krishnamurthy et al. demonstrated that, although the data were reproducible, this mechanistic hypothesis was completely incorrect.⁴¹⁵ They observed that the enthalpy of binding became *less* favorable, and the entropy of binding *less* unfavorable, as the length of the chain increased for arylsulfonamides with oligoethylene glycol, oligoglycine, and oligosarcosine tails, exactly *counter* to their expectations (Figure 21 parts B and C). In response to these data, the investigators proposed a different model in which the interface between the protein and the ligand became “looser” as the length of the tail of the sulfonamide increased; the looser interface would have greater entropic mobility and a less favorable enthalpy (due to fewer van der Waals contacts) than a “tighter” one (Figure 24). In their model, residues of the tail that are farther from the phenyl ring enthalpically destabilize the bound conformation of residues that are closer to the phenyl ring (Figure 24B). This effect results in the observed enthalpy/entropy compensation (Figure 24A).

10.6.7. Conclusions

Microcalorimetry makes it possible to obtain believable data describing the thermodynamics of binding. Some of the values of enthalpy for the binding of arylsulfonamides to CA II obtained by microcalorimetry differ significantly from those obtained using van't Hoff analysis (Tables 12 and 13). Such discrepancies have been reported previously in the literature for protein–ligand binding.^{578–580} While a rigorous comparison of thermodynamic values obtained from the two techniques is not possible because so few directly comparable

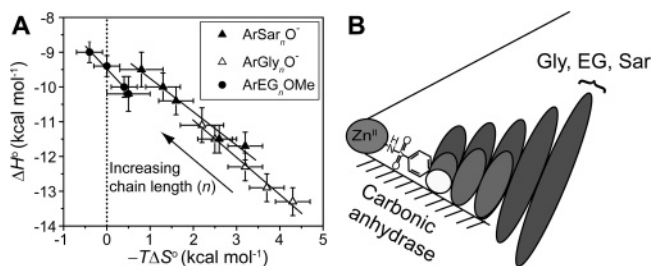


Figure 24. Association of *para*-substituted benzenesulfonamides with oligoethylene glycol (ArEG_nOMe, 72–76), oligoglycine (ArGly_nO⁻, 63–67), and oligosarcosine (ArSar_nO⁻, 213–217) tails with bovine carbonic anhydrase II. (A) Enthalpy/entropy compensation plot for the association. The solid lines are linear fits to the data sets and give values for the compensation (from the slopes) as follows: -0.96 ± 0.08 (ArSar_nO⁻), -1.07 ± 0.07 (ArGly_nO⁻), and -1.32 ± 0.09 (ArEG_nOMe); these observations demonstrate near-perfect compensation between enthalpy and entropy. The dotted vertical line separates favorable ($-T\Delta S^\circ < 0$) from unfavorable ($-T\Delta S^\circ > 0$) entropy of binding. (B) A schematic diagram for the association. This schematic diagram represents the catalytic cleft of the enzyme as a cone with the Zn^{II} cofactor at the apex. The bottom surface (shaded) of the cleft is the “hydrophobic wall” of the enzyme. Ellipses depict the residues of the ligand; the sizes of the ellipses are qualitatively proportional to the mobility of the individual residues. Benzenesulfonamide ligands with one (white), three (light gray), and five (dark gray) residues in the tail are shown. Modified with permission from ref 415. Copyright 2006 American Chemical Society.

data are available in the literature, we believe that calorimetry is the best technique for measuring the dissected thermodynamics for protein–ligand association for reasons discussed in section 10.2.2.

The *observed* binding of arylsulfonamides to CA II is strongly enthalpy ($\Delta H^\circ_{\text{obs}}$)-driven and generally opposed by a small-to-moderate (relative to the enthalpy) entropic ($-T\Delta S^\circ_{\text{obs}}$) term (Table 13; Figure 23A). When the observed data are used to calculate values of the changes in enthalpy and entropy for the reaction of the arylsulfonamide anion (ArSO₂NH⁻) with $\text{CA-Zn}^{\text{II}}-\text{OH}_2^+$ (eq 18), the entropic ($-T\Delta S^\circ_{\text{ArSO}_2\text{NH}^-}$) term is seen to be important (contributing up to 50% of the affinity), but $\Delta H^\circ_{\text{ArSO}_2\text{NH}^-}$ is still dominant for the association of most arylsulfonamide anions (Table 14; Figure 23B). The electrostatic interactions of the Zn^{II}–N bond and hydrogen-bond network are the dominant contributors to $\Delta H^\circ_{\text{ArSO}_2\text{NH}^-}$, while hydrophobic contacts between the ring and CA II are the dominant contributors to $-T\Delta S^\circ_{\text{ArSO}_2\text{NH}^-}$.

10.7. Overall Conclusions

10.7.1. Why Is CA a Good Model System for Rational Ligand Design?

The system of CA (especially HCA I, HCA II, and BCA II) and arylsulfonamides is a model in which it is possible to study separately the distinct components of binding of the arylsulfonamide: (i) the interaction of its head group with the enzyme (Zn^{II}–NH bond and –SO₂NH hydrogen-bond network), (ii) the interaction of its aryl ring with the hydrophobic pocket (active site) of CA, and (iii) the interaction of its tail and secondary recognition element with hydrophobic patches (adjacent to the active site) of CA (Figure 13B). This system of enzyme and ligand is well-suited for thermodynamic measurements because of the availability and ease of purification of CA (necessary for

techniques that require large amounts of material), as well as the straightforward synthesis of arylsulfonamides.

10.7.2. Lessons in Design of Arylsulfonamide Ligands for CA

Arylsulfonamides are the most effective ligands of CA. The hydrogen-bond network around the sulfonamide group, and the Zn^{II}–N bond, are both crucial components of the interaction. All high-affinity ligands for CA make use of the Zn^{II}–N bond; this observation highlights its importance in determining affinity. While the sulfonamide class of molecules has proven effective as high-affinity ligands for CA, the design of ligands with moieties that bind more tightly to Zn^{II} than sulfonamides do could result in the generation of even higher-affinity ligands.

Much of the extensive variation of the structure of arylsulfonamides has simply exemplified ways of varying the pK_a of the arylsulfonamide. The separation of the two effects of the pK_a of the arylsulfonamide on binding to CA—the fraction of sulfonamide present as the anion, ArSO₂NH[−], and the strength of the interaction of ArSO₂NH[−] with CA (the Zn^{II}–N bond and the hydrogen-bond network)—is essential for the rational design of high-affinity arylsulfonamides and for determining the importance of hydrophobic contacts between the arylsulfonamide and CA on affinity. Many arylsulfonamides have affinities higher than that expected from a Brønsted plot constructed using unsubstituted benzenesulfonamide (**1**) as a reference compound (Figure 17B); these arylsulfonamides are probably exploiting hydrophobic and/or multivalent contacts outside of the active site (contacts that benzenesulfonamide lacks) to increase affinity. Compound **109** exemplifies these design principles and is the highest-affinity sulfonamide known. At the lower end of affinity, certain sulfonamides (e.g., *ortho*-substituted alkyl series) bind more weakly than anticipated based on the Brønsted relationship, presumably because of unfavorable steric interactions between the aryl ring or substituents on the aryl ring and the cleft of CA. Understanding these high- and low-affinity deviations is crucial to furthering our ability to design high-affinity ligands rationally in this system.

A simple analysis (eqs 19 and 20) predicts a modest dependence of the pK_a (of the sulfonamide) that gives the highest-affinity binder to CA on β. The “best” pK_a for a ligand (with all other factors being equal) will be roughly the pH of the buffer (pK_a = pH ± 1 for β = 0.1–0.9) (eq 20; Figure 19).

The affinity between CA (at least CA II) and ligand is dominated (~65%) by the Zn^{II}–N bond with lesser contributions by the hydrogen-bond network (~10%) and hydrophobic contacts (~25%) of the ring (Figure 18). The Zn^{II}–N bond and the hydrogen-bond network primarily manifest themselves in the enthalpy of binding, with the contacts of the ring with CA appearing in the entropy of binding. In principle, high-affinity ligands can be designed by increasing the strength of the hydrophobic contacts (by increasing the size and hydrophobicity of the aryl ring) between the aryl ring of the ligand and CA. This approach, however, might suffer from undesired destabilization of the Zn^{II}–N bond or the hydrogen-bond network. A simpler approach has been the addition to the benzenesulfonamide scaffold of hydrophobic binding elements (either tails or secondary recognition elements) that interact with a surface of CA outside of its active site and that, thus, do not affect the binding of the sulfonamide head group or the phenyl ring.

Hydrophobic tails, which interact at a surface adjacent to the active site, lower the K_d^{obs} of arylsulfonamide ligands within a series of homologous compounds. Carefully controlled studies of *para*-substituted benzenesulfonamides with alkyl or fluoroalkyl tails have demonstrated that hydrophobic interactions are important in affinity. The use of a homologous series allows the clear separation of structural effects on affinity (e.g., here the values of pK_a of the arylsulfonamides were constant within each series).

Bivalent sulfonamides containing hydrophobic secondary recognition elements (SREs), which are able to interact with the “hydrophobic wall” of CA, bind with higher affinities than sulfonamides without these secondary elements. The exact structure of the hydrophobic SRE is not crucial to enhancing affinity. Sulfonamides containing hydrophilic or charged SREs are not of particularly high affinity (as compared to sulfonamides lacking SREs); these results reinforce the inference from many other studies that the engineering of electrostatic or ionic interactions is more challenging than the engineering of hydrophobic contacts.^{4,30,397} Results from studies involving the coordination of metal-containing SREs to surface His residues of HCA, while a promising idea, have been inconclusive.^{181,596,601,602}

Understanding enthalpy/entropy compensation with even relatively simple systems (e.g., sulfonamides with chains of oligoethylene glycol, oligoglycine, and oligosarcosine) is both very challenging and very instructive. We believe it will ultimately allow us to design high-affinity ligands by generating ligands with stabilizing enthalpic contacts but without the high entropic cost of binding that is typically associated with exothermic binders.

10.7.3. General Lessons in Rational Ligand Design

While the CA/arylsulfonamide system is simple (e.g., CA does not undergo gross conformational changes upon ligand binding, is a monomeric protein, and is not post-translationally modified with saccharides or phosphates), we still do not have a deep, predictive understanding of the binding of ligands to it (primarily because of our lack of understanding of entropy, central to such phenomena as the hydrophobic effect, enthalpy/entropy compensation, the structure of water, etc.). Our incomplete rationalization of this system suggests that there is still much work to be done on it—particularly in characterizing the thermodynamics of binding—to understand this system and to apply the lessons it has to teach to the design of ligands for other proteins.

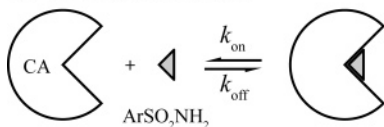
A few general themes have emerged from the study of this system:

(1) Measuring (or calculating from the observed affinity) the affinity of the species of the ligand and protein that actually interact is crucial in order to carry out meaningful studies of structure–activity relationships. Simply examining the observed affinities of a series of ligands will not allow the careful partitioning of affinity to different structural contributions (e.g., hydrophobic contacts of the aryl ring, Zn^{II}–N bond, and hydrogen-bond network) of the ligand.

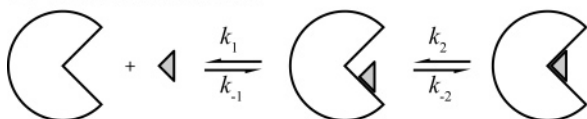
(2) Multivalent ligands—ligands that bind at both the primary (active) site and a secondary site removed from, but adjacent to, the active site—may be easier to design than ligands that bind just at the active site (even if there are multiple interactions at that site). This general statement will be particularly true when the active site is sterically congested.

Scheme 2. Two-State (A) and Three-State (B) Models for the Association of Arylsulfonamides with CA

A: Two-state model



B: Three-state model



(3) Exploiting hydrophobic contacts with proteins is one of the truly successful design principles for rational ligand design. These contacts have been successful at both the active site of the protein and at a secondary site removed from the active site.

(4) Electrostatic interactions might be intrinsically weaker and/or more challenging to engineer than hydrophobic interactions, possibly because the steric demands on hydrophobic bonding are less severe than those on electrostatic interactions.

11. Kinetics and Mechanism of Protein–Inhibitor Binding in Solution

11.1. Kinetics of Interaction of Arylsulfonamides with CA

11.1.1. Overview

The kinetics of association and dissociation of arylsulfonamides to CA (CA II, Table 15) are well-fit by either a two-state (Scheme 2A) or a three-state (Scheme 2B) model. In the two-state model, the arylsulfonamide associates with the enzyme and coordinates to the Zn^{II} cofactor in one step. In the three-state model, the arylsulfonamide first associates with the enzyme to form a hydrophobic, weakly bound, noncoordinated complex; the arylsulfonamide in this complex coordinates to the Zn^{II} cofactor in a second step.

In the remainder of section 11.1, we discuss the observed rate constants for association (k_{on}) and dissociation (k_{off}) using a two-state model. For this model, of course, $K_{\text{d}}^{\text{obs}} = k_{\text{off}}/k_{\text{on}}$. In section 11.2, we discuss the possible mechanisms for complexation of arylsulfonamides with CA that are consistent with the two- and three-state models. No deviation from pseudo-first-order kinetics has been observed for the association of arylsulfonamides with CA, so we can neither prove nor disprove that either a two- or three-state model is correct for describing the mechanism for complexation. Instead, we discuss the alternative mechanisms in light of the experimental results given in Section 11.1.

11.1.2. Influence of the Head Group and the Ring on the Kinetics of Binding

Taylor et al. demonstrated that, for a number of structurally unrelated arylsulfonamides, k_{on} had a 10-fold larger influence on $K_{\text{d}}^{\text{obs}}$ than did k_{off} (Figure 25).⁴⁵⁸ The largest value of k_{on} that they observed was $\sim 10^7 \text{ M}^{-1} \text{ s}^{-1}$ (Table 15), which is 2 orders of magnitude lower than the limit imposed by diffusion ($\sim 2 \times 10^9 \text{ M}^{-1} \text{ s}^{-1}$) for the collision of a small molecule (similar to benzenesulfonamide) with the surface

of a protein.⁶¹⁰ Alberty and Hammes showed that restricting the solid angle of approach for the collision of a small molecule with the surface of a protein would reduce the diffusion-controlled rate from this upper limit.⁶¹⁰ The conical cleft of CA restricts the solid angle of approach of the ligand (see section 4.6); thus, $2 \times 10^9 \text{ M}^{-1} \text{ s}^{-1}$ is an upper limit for the value of k_{on} . The rate of diffusion-controlled reactions should decrease slightly with increasing molecular weight of the substrate: the diffusion coefficient (D) is inversely proportional to the square root of the molecular weight (M): $D \approx M^{-1/2}$. The experimental data are not compatible with a simple, diffusion-controlled reaction: many large arylsulfonamides associate with CA with values of k_{on} greater than those for small ones; for example, k_{on} for **168** with HCA II is ~ 100 times larger than that for benzenesulfonamide (**1**) (Figure 26; see also section 11.2.3.2). Taylor et al. noted that k_{on} has a larger influence on K_{d} than does k_{off} , whereas k_{off} has a larger influence on K_{d} than does k_{on} for most metal–ligand associations.⁴⁵⁸ The fact that k_{on} is more important than k_{off} suggests a complicated reaction profile for the association of arylsulfonamides with the enzyme. We discuss these results and their impact on the mechanism in section 11.2.

Inorganic anions (e.g., CN^- , OCN^- , and SCN^-) have values of k_{on} near the diffusion limit for binding to Co^{II}–BCA II (Table 15). Using literature values for the diffusion coefficients in water ($1.5 \times 10^{-5} \text{ cm}^2 \text{ s}^{-1}$ for CN^- and $2.15 \times 10^{-5} \text{ cm}^2 \text{ s}^{-1}$ for SCN^-)⁶¹¹ and a solid angle of 2π (i.e., a hemisphere),⁶¹⁰ the diffusion-limited value of k_{on} is about $3 \times 10^9 \text{ M}^{-1} \text{ s}^{-1}$ for CN^- and $4 \times 10^9 \text{ M}^{-1} \text{ s}^{-1}$ for SCN^- . Prabhananda et al. have reported values of k_{on} of about $3 \times 10^9 \text{ M}^{-1} \text{ s}^{-1}$ for CN^- and $2 \times 10^9 \text{ M}^{-1} \text{ s}^{-1}$ for SCN^- (Table 15).²⁹¹ CN^- , SCN^- , NCO^- , and HCO_3^- do not displace the metal-bound water of CA II; rather, kinetic²⁹¹ and X-ray^{186,188} studies have demonstrated that the metal cofactor (Co^{II} or Zn^{II}) in 1:1 complexes of these anions with CA II has an expanded coordination sphere—the coordination expands to 5 (for CN^- with Co^{II}–BCA II and SCN^- with HCA II) or 6 (for HCO_3^- with Co^{II}–HCA II). The X-ray structures of HCA II with CN^- and NCO^- show that the water remains tetrahedrally coordinated to Zn^{II} and that the anion binds in the hydrophobic pocket of the enzyme (see section 4.6).²⁹⁴ Prabhananda et al. have reported a 2:1 complex between CN^- and Co^{II}–BCA II.²⁹¹ The complex forms by the association of BCA II–Co^{II}–CN with a second CN^- , which does displace the metal-bound water. The rate constant for this association is $5 \times 10^5 \text{ M}^{-1} \text{ s}^{-1}$, which is similar to the value of k_{on} for sulfonamides. These similar values for k_{on} suggest that the value of k_{on} for sulfonamides may depend on the rate at which the sulfonamide can displace the metal-bound water.

11.1.3. Which Are the Reactive Species of CA and Sulfonamide?

Taylor et al. further demonstrated that k_{on} (like $K_{\text{d}}^{\text{obs}}$; see section 10.3.2) is, in general, pH-dependent and gives a bell-shaped curve with pH bounded by two values of pK_{a} , while k_{off} is pH-independent over the range of pH 5–11 (Figure 27).³⁰² For the reasons presented in section 10.3.2 (Scheme 1; section 10.3.3) to rationalize the pH-dependence of $K_{\text{d}}^{\text{obs}}$,

Table 15. Kinetic Data for the Binding of Ligands to CA II

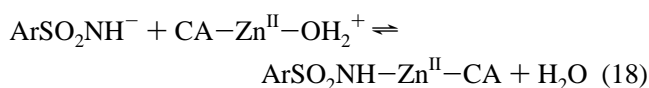
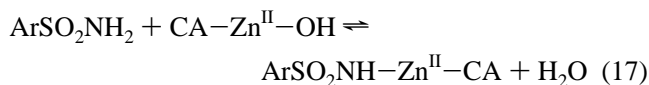
Compound	Structure	CA ^a	$k_{\text{on}} \times 10^{-5}$ (M ⁻¹ s ⁻¹)	k_{off} (s ⁻¹)	$K_{\text{d}}^{\text{obs}}$ (μM) ^b	pK _a	Tech ^c	Ref.
Type:								
1	R = H	H	8.8	0.18	0.20	10.1	SFF	389
2	R = Cl	H	5.1	0.062	0.12	--	SFF	458
3	R = NO ₂	H	7.4	0.048	0.065	--	SFF	458
6	R = CH ₃	H	11	0.092	0.084	10.2	SFF	389
7	R = CH ₂ CH ₃	H	33	0.097	0.029	10.4	SFF	389
8	R = (CH ₂) ₂ CH ₃	H	50	0.085	0.017	10.3	SFF	389
9	R = (CH ₂) ₃ CH ₃	H	100	0.050	0.0050	10.4	SFF	389
10	R = (CH ₂) ₄ CH ₃	H	250	0.034	0.0014	--	SFF	389
28	R = CH ₂ NHCO(CH ₂) ₄ CO-NHC[CH ₂ O(CH ₂) ₃ SCH ₂ COOH] ₃	B	0.15	0.0001 ^d	0.0067	--	ACE	392
29	R = CO ₂ H	H	2.7	0.073	0.27	--	SFF	458
29		B	0.48	0.037	0.77	--	SPR ^e	412
29		B	---	---	0.73	--	ITC	412
30	R = CO ₂ CH ₃	H	45	0.047	0.010	9.8	SFF	389
31	R = CO ₂ CH ₂ CH ₃	H	110	0.034	0.0030	9.7	SFF	389
32	R = CO ₂ (CH ₂) ₂ CH ₃	H	180	0.030	0.0017	9.8	SFF	389
33	R = CO ₂ (CH ₂) ₃ CH ₃	H	330	0.025	0.00076	9.7	SFF	389
34	R = CO ₂ (CH ₂) ₄ CH ₃	H	470	0.019	0.00040	10.1	SFF	389
35	R = CO ₂ (CH ₂) ₅ CH ₃	H	590	0.024	0.00041	--	SFF	389
37	R = CONHCH ₃	H	5.9	0.049	0.083	10.3	SFF	389
38	R = CONHCH ₂ CH ₃	H	8.6	0.026	0.030	10.1	SFF	389
39	R = CONH(CH ₂) ₂ CH ₃	H	11	0.0094	0.0085	10.1	SFF	389
41	R = CONH(CH ₂) ₃ CH ₃	H	18	0.0057	0.0032	10.1	SFF	389
41	R = CONH(CH ₂) ₄ CH ₃	H	26	0.0045	0.0017	10.2	SFF	389
42	R = CONH(CH ₂) ₅ CH ₃	H	38	0.0050	0.0013	--	SFF	389
43	R = CONH(CH ₂) ₆ CH ₃	H	43 ^f	0.0051	0.0012	--	SFF	389
63	R = CONHGlyOH	H	3.6 ^f	0.120	0.33	--	Comp	507
66	R = CONH(Gly) ₄ OH	H	2.5 ^f	0.090	0.36	--	Comp	507
223	R = CONHNle-OH ^g	H	22 ^f	0.011	0.0050	--	Comp	507
224	R = CONHCph-OH ^h	H	16 ^f	0.022	0.014	--	Comp	507
225	R = CONH(Gly) ₃ Nle-OH ^g	H	4.2 ^f	0.093	0.22	--	Comp	507
226	R = CONH(Gly) ₃ Cph-OH ^h	H	8.5 ^f	0.084	0.099	--	Comp	507
Type:								
114	R = CO ₂ CH ₃	H	8.7	0.61	0.70	9.8	SFF	389
115	R = CO ₂ CH ₂ CH ₃	H	17	1.0	0.59	9.6	SFF	389
116	R = CO ₂ (CH ₂) ₂ CH ₃	H	39	1.4	0.36	9.7	SFF	389
117	R = CO ₂ (CH ₂) ₃ CH ₃	H	89	1.0	0.11	9.6	SFF	389
118	R = CO ₂ (CH ₂) ₄ CH ₃	H	86	1.2	0.14	9.9	SFF	389
Type:								
119	R = CO ₂ CH ₃	H	0.13	0.49	38	9.3	SFF	389
120	R = CO ₂ CH ₂ CH ₃	H	0.18	0.28	16	9.5	SFF	389

Table 15 (Continued)

Compound	Structure	CA ^a	$k_{\text{on}} \times 10^{-5}$ (M ⁻¹ s ⁻¹)	k_{off} (s ⁻¹)	$K_{\text{d}}^{\text{obs}}$ (μM) ^b	pK _a	Tech ^c	Ref.
Type:								
121	R = CO ₂ (CH ₂) ₂ CH ₃	H	0.28	0.13	4.6	9.7	SFF	389
122	R = CO ₂ (CH ₂) ₃ CH ₃	H	0.63	0.11	1.7	9.8	SFF	389
123	R = CO ₂ (CH ₂) ₄ CH ₃	H	1.1	0.075	0.68	9.9	SFF	389
133		H	2.4	0.39	1.6	--	SFF	458
133		B	3.9	0.13	0.33	--	SPR ^e	412
133		B	3.8	0.16	0.42	--	SFF	412
133		B	---	---	0.36	--	ITC	412
135		H	6.6	0.14	0.21	--	SFF	458
137		H	48	0.068	0.014	--	SFF	458
166		H	5.8	0.075	0.13	--	SFF	458
168		H	110	0.033	0.0030	9.3	SFF	458
198	CN ⁻	Co	3.0×10^4	5.0×10^3	1.7	9.3 ^k	TJR	291
200	OCN ⁻	Co	1.0×10^3	1.0×10^4	100	3.9 ^k	TJR	291
201	SCN ⁻	Co	2.0×10^4	7.0×10^3	3.5	0.9 ^k	TJR	291
Type:								
275	R = (CH ₂) ₁₁ SH	B	0.35	0.0053	0.15	--	SPR ⁱ	620
275		B	0.042	0.0053	1.3	--	SPR ⁱ	620
276	R = CH ₃	B	--	--	0.05	--	Comp	467

^a Variant of CA: H = HCA II; B = BCA II; Co = Co^{II} variant of BCA II. ^b Calculated from k_{on} and k_{off} unless otherwise noted. ^c Technique: SFF = stopped-flow fluorescence; TJR = temperature-jump relaxation; ACE = affinity capillary electrophoresis; SPR = surface plasmon resonance spectroscopy; Comp = fluorescence competition. ^d Calculated from k_{on} and $K_{\text{d}}^{\text{obs}}$. ^e Surface plasmon resonance, with CA immobilized on a thin film of dextran. ^f Calculated from k_{off} and $K_{\text{d}}^{\text{obs}}$. ^g Nle = norleucine. ^h Cph = *p*-chlorophenylalanine. ⁱ Ligand is immobilized on a SAM at a fractional thiol coverage of 0.005 (a coverage that should allow a binding of CA equal to 15% of a total monolayer). ^j Ligand is immobilized on a SAM at a fractional thiol coverage of 0.02 (a coverage that should allow a binding of CA equal to 35% of a total monolayer). ^k pK_a of the conjugate acid.

only the schemes represented by eqs 17 and 18 are compatible with this experimental pH-dependence of k_{on} .



We discuss the two equations in the context of the experimental data in section 11.2.

11.1.4. Influence of the Tail on the Kinetics of Binding

King and Burgen examined the rate constants for association and dissociation of a homologous series of arylsulfon-

amides substituted at the *ortho*-, *meta*-, or *para*-positions with alkyl chains connected directly as esters or amides to the phenyl ring.³⁸⁹ For all of these series, $K_{\text{d}}^{\text{obs}}$ was again primarily influenced by k_{on} , rather than by k_{off} (Table 15). The lower affinities of the *meta*- (**114–118**) and *ortho*-substituted (**119–123**) ester series than of the *p*-substituted (**30–35**) ester series was primarily due to their lower values of k_{on} . For the *p*-substituted amide series (**37–43**), k_{off} played a larger role on $K_{\text{d}}^{\text{obs}}$ than in the other series; the investigators attributed this effect to the hydrogen bond between the carboxamide NH of the sulfonamide ligand and the residues of the active site of HCA II (such an interaction is not available for the *p*-substituted ester (**30–35**) or *p*-substituted alkyl series (**1** and **6–10**)).³⁸⁹ Boriack et al. and Cappalonga

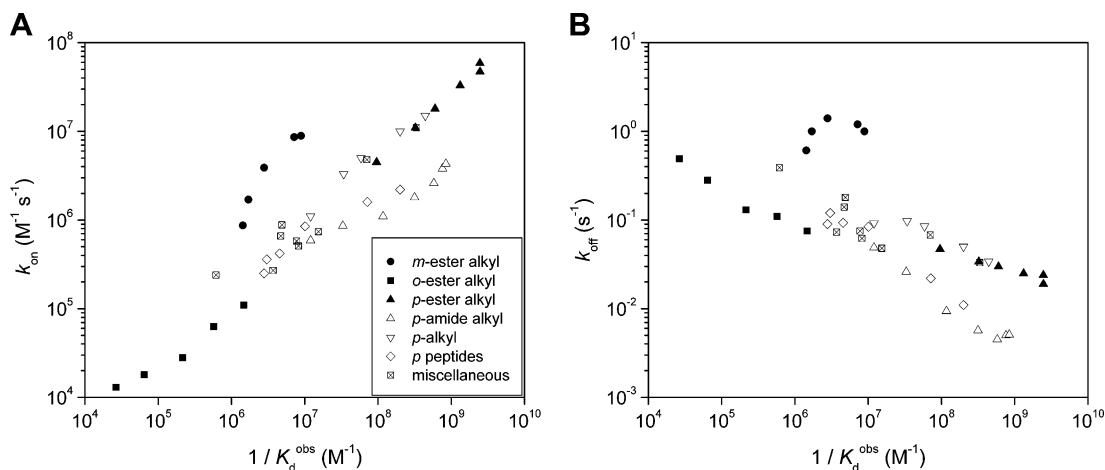


Figure 25. Variation of k_{on} (A) and k_{off} (B) with the (equilibrium) dissociation constant, $K_{\text{d}}^{\text{obs}}$, for several classes of arylsulfonamides. Structures for the different series are listed in Table 10 as follows: *m*-ester alkyl (114–118), *o*-ester alkyl (119–123), *p*-ester alkyl (30–35), *p*-amide alkyl (37–43), *p*-alkyl (7–10), *p*-peptides (63, 66, 223–226), and miscellaneous sulfonamides (1–3, 29, 133, 135, 137, 166, 168), and data listed in Table 15.

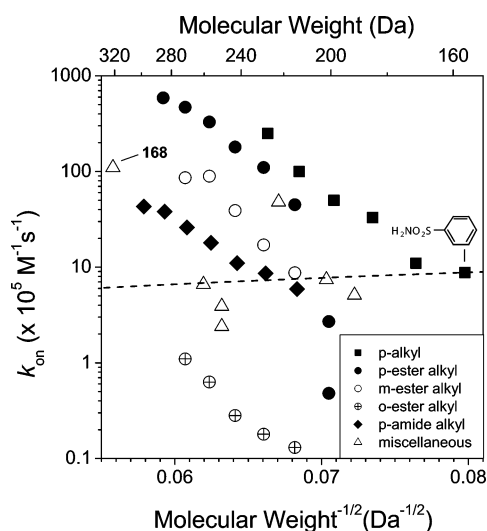


Figure 26. Variation of k_{on} with the molecular weight of several classes of arylsulfonamides. Structures for the different series are listed in Table 10 as follows: *p*-alkyl (1 and 6–10), *p*-ester alkyl (29–35), *m*-ester alkyl (114–118), *o*-ester alkyl (119–123), *p*-amide alkyl (37–43), and miscellaneous sulfonamides (2, 3, 29, 133, 135, 137, and 168), and data listed in Table 15. The slope of the dashed line represents the dependence of k_{on} on molecular weight that would be expected for a diffusion-controlled reaction, $k_{\text{on}} \approx (\text{molecular weight})^{-1/2}$. The line is drawn to pass through the value of k_{on} for benzenesulfonamide (1).

et al. observed by X-ray crystallography that there is actually a bridging water molecule between this carboxamide NH in compounds 70, 83, 84, and probably also 51 and 277, and the carbonyl oxygen of the backbone of Pro201 on HCA II.^{185,202}

A two-state model, based on diffusion-limited encounter and hydrophobic contacts between the tail of the arylsulfonamide and CA, predicts that k_{off} would decrease with the length of the chain. Such a model also predicts that k_{on} would decrease slightly with (or, at the least, be independent of) the length of the chain. Interestingly, King and Burgen noted that k_{on} increased with the length of the chain for all of the series (for the *p*-substituted alkyl series, the logarithm of k_{on} increased linearly with the length of the chain) with only a

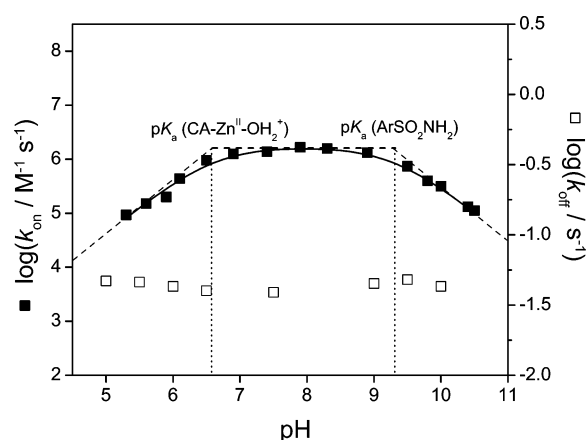


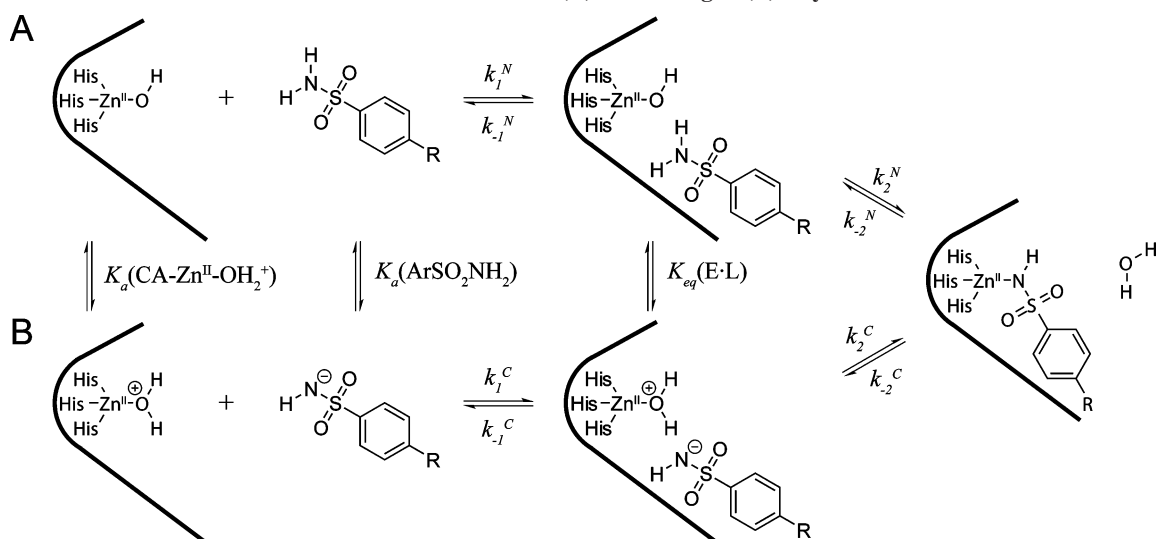
Figure 27. pH-dependence of the logarithms of rate constants for association (k_{on}) and for dissociation (k_{off}) of *p*-nitrobenzenesulfonamide (3) with human carbonic anhydrase II (HCA II). The open squares are experimental data for k_{off} and are pH-independent over the range examined. The black squares are experimental data for k_{on} , and the solid line is a simulation using eq 28 or 29 (see text) with a $\text{p}K_{\text{a}}$ of 6.6 for $\text{CA-Zn}^{\text{II}}\text{-OH}_2^+$ and a $\text{p}K_{\text{a}}$ of 9.3 for the arylsulfonamide. The dashed lines are tangents to the simulation at three regimes (slopes of 1, 0, and -1), and the dotted vertical lines show the values of $\text{p}K_{\text{a}}$. Data taken from Taylor et al.³⁰²

small variation in k_{off} with chain length.³⁸⁹ Taylor et al. noticed the same trend for k_{on} and k_{off} for a series of structurally unrelated compounds.⁴⁵⁸ The association reaction (described by k_{on}) of ligands with CA is, thus, not mass-transport limited for any but the fastest reactions (e.g., CN^- discussed in section 11.1.2).

11.1.5. Conclusions

The rate constant for association (k_{on}) of arylsulfonamides with CA (HCA I and II, at least) has a larger effect on the equilibrium affinity ($K_{\text{d}}^{\text{obs}}$) than does the rate constant for dissociation (k_{off}). This result contrasts with most metal–ligand complexations, in which the influence of k_{off} on $K_{\text{d}}^{\text{obs}}$ is larger than that of k_{on} . A two-state, diffusion-limited encounter model for association is incompatible with the observation that many large ligands (e.g., arylsulfonamides with long alkyl tails) have larger values of k_{on} than do small

Scheme 3. Three-State Models for the Association of Neutral (A) and Charged (B) Arylsulfonamides with CA



ligands (e.g., arylsulfonamides with short alkyl tails) (Figure 26 and section 11.2.3.2). A two-state model that is not diffusion-limited is still compatible with the data (see section 11.2). Values of k_{on} are sensitive to pH (while values of k_{off} are not, over the range pH 5–11); the pH-dependence of k_{on} is compatible with only two of the four possible two-state models for association: (i) the arylsulfonamide anion interacts with $\text{CA-Zn}^{\text{II}}\text{-OH}_2^+$ (eq 18) or (ii) the neutral arylsulfonamide interacts with $\text{CA-Zn}^{\text{II}}\text{-OH}$ (eq 17). Deciding between these two possibilities requires additional experimental data. In the next section, we describe a three-state model and compare it to the two-state model discussed in this section.

11.2. Mechanism of the Binding of Arylsulfonamides to CA

11.2.1. Overview

In this section, we discuss the experimental results presented in section 11.1 in light of two general mechanisms for association of arylsulfonamides with CA: a two-state model (Scheme 2A) and a three-state model containing an intermediate (Scheme 2B). There are two key questions that we seek to answer: (i) Which are the reactive species of CA and sulfonamide (eq 17 or 18)? (ii) Is there an intermediate in the association (Scheme 2B)? Scheme 3 shows two possible three-state models: Scheme 3A comprises a neutral set of reactive species (consistent with eq 17), and Scheme 3B comprises a charged set of reactive species that correspond to eq 18. The superscripts, N and C, of the microscopic rate constants in Scheme 3 denote the neutral and charged pathways.

11.2.2. Two-State Model for Binding (Assuming No Intermediate)

A two-state model for association (Scheme 2A) requires that the arylsulfonamide interacts directly with CA to form the final complex in a process that proceeds without a kinetically significant intermediate. The arylsulfonamide and CA must be in their reactive forms—either both are neutral or both are charged—for binding to occur. As mentioned in section 11.1.3, only the two-state models shown in eqs 17 and 18 are compatible with the pH-dependence of k_{on} (Figure 27). The observed rate constants can be used to calculate

the rate constants for the reactions shown in eqs 17 and 18 by using eqs 28 and 29, respectively,

$$k_{\text{on}}^{\text{ArSO}_2\text{NH}_2} = k_{\text{on}}(1 - \theta_{\text{ArSO}_2\text{NH}^-})(1 - \theta_{\text{CA-Zn}^{\text{II}}\text{-OH}_2^+}) \quad (28)$$

$$k_{\text{on}}^{\text{ArSO}_2\text{NH}^-} = k_{\text{on}}\theta_{\text{ArSO}_2\text{NH}^-}\theta_{\text{CA-Zn}^{\text{II}}\text{-OH}_2^+} \quad (29)$$

where $\theta_{\text{ArSO}_2\text{NH}^-}$ is the fraction of arylsulfonamide that is deprotonated and $\theta_{\text{CA-Zn}^{\text{II}}\text{-OH}_2^+}$ is the fraction of the Zn^{II} -coordinated water that is protonated (see eqs 20a and 20b in section 10.3.3).

Taylor et al. calculated a value of $k_{\text{on}}^{\text{ArSO}_2\text{NH}^-}$ for *p*-salicylazobenzenesulfonamide (**168**) of $\sim 10^{10} \text{ M}^{-1} \text{ s}^{-1}$ with HCA II.³⁰² Since this value is greater than that for the diffusion-limited encounter ($\sim 2 \times 10^9 \text{ M}^{-1} \text{ s}^{-1}$) of two neutral molecules in solution (see section 11.1.2), they concluded that the mechanism of eq 18 was not compatible with the data. They also showed that k_{on} for *p*-nitrobenzenesulfonamide (**3**) did not depend on ionic strength over the range of 0–1 M. From these results, they inferred that the reactive forms of the enzyme and/or arylsulfonamide were not charged, again arguing against the mechanism of eq 18. (An alternative explanation is that electrostatic effects are not important in determining k_{on} .) From this evidence, Taylor et al. concluded that the mechanism followed was that of eq 17.

Olander et al. have argued that eq 18 could still be a mechanistic possibility.^{612,613} Because the reactive forms of the arylsulfonamide and enzyme in eq 18 are both charged, Coulombic attraction might increase the rate of diffusion-limited encounter, and the value of $k_{\text{on}}^{\text{ArSO}_2\text{NH}^-}$ for **168** could be within this higher limit.⁶¹⁰ Taylor et al. demonstrated that the value of k_{on} was insensitive to ionic strength for **3**, which has no ionizable group other than the sulfonamide.³⁰² Olander et al. point out that the sulfonamide that violated the rate for neutral diffusion-limited encounter (**168**), however, contained a carboxylate group as well as the sulfonamide group.⁶¹² It is possible that the small charge on **3** (–1 using eq 18, 0 using eq 17) could explain its lack of dependence of k_{on} on ionic strength. Compound **168**, which has a greater charge than **3** (–2 using eq 18, –1 using eq 17), might exhibit a dependence of k_{on} on ionic strength; data for **168** have not been reported in the literature.

HCA II has only a small charge at neutral pH (Table 2, section 4.1);^{149,150} this fact argues against the mechanistic hypothesis of Olander et al. Theoretically, the possibility remains that some arylsulfonamides follow the mechanism in eq 17, while others follow the mechanism in eq 18. While a two-state model that follows either eq 17 or eq 18 may be possible, we believe that a three-state model better explains the data than any two-state model. We discuss the three-state model in the following section.

11.2.3. Three-State Model with an Intermediate (Pre-equilibrium)

11.2.3.1. Overview of the Model. Scheme 3 shows two possibilities for a three-state model (Scheme 2B) that differ only in the protonation states of the active forms of the arylsulfonamide and CA (eqs 17 and 18). We refer to Scheme 3A as the neutral pathway and Scheme 3B as the charged pathway. Other pathways are conceivable because the components of parts A and B of Scheme 3 are in equilibrium (with equilibrium constants denoted by $K_a(\text{CA}-\text{Zn}^{\text{II}}-\text{OH}_2^+)$, $K_a(\text{ArSO}_2\text{NH}_2)$, and $K_{\text{eq}}(\text{E}\cdot\text{L})$), but we will only consider the charged and neutral three-state possibilities here.

Using the steady-state approximation for the intermediate (E·L in Scheme 3), King and Burgen derived eq 30 for the observed rate constant for association (k_{on}).³⁸⁹ This derivation assumes that association goes to completion and is irreversible. This equation is written to be applicable for the mechanisms of either the charged or neutral pathway, so superscripts (N or C) for the microscopic rate constants are omitted. When most of the intermediates formed are nonproductive—that is, the intermediate falls apart more rapidly to reactants than it proceeds to products (a pre-equilibrium model)—eq 30 simplifies to eq 31 because $k_{-1} \gg k_2$ (K is the pre-equilibrium constant between the intermediate and the reactants and has units of M^{-1}).

$$k_{\text{on}} = \frac{k_1 k_2}{k_{-1} + k_2} \quad (30)$$

$$k_{\text{on}} = \frac{k_1 k_2}{k_{-1}} = K k_2 \quad (31)$$

Treating the observed rate constant for dissociation (k_{off}) in a similar manner affords eq 32 (here, assuming that the dissociation goes to completion and is irreversible).³⁸⁹ Assuming that $k_{-1} \gg k_2$ simplifies eq 32 to eq 33.

$$k_{\text{off}} = \frac{k_{-1} k_{-2}}{k_{-1} + k_2} \quad (32)$$

$$k_{\text{off}} = k_{-2} \quad (33)$$

Under the assumptions of the pre-equilibrium model, eqs 31 and 33 suggest that the observed rate constant for association (k_{on}) depends on the stability of the intermediate (relative to the reactants)—that is, on K —and the rate constant to form the final product from the intermediate (k_2), and that the rate constant for dissociation (k_{off}) depends only on the rate constant to form the intermediate from the final product (k_{-2}) (and not explicitly on the stability of the intermediate). Figure 28 illustrates these results graphically.

King and Burgen have argued that the first step in the mechanism—the association of arylsulfonamide and CA (specifically, HCA II) to form the intermediate—is pH-

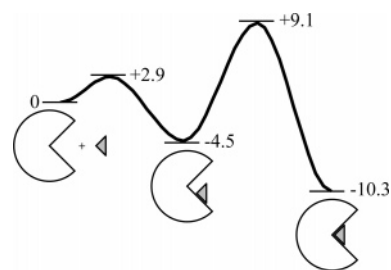


Figure 28. Possible free-energy diagram for the association of an arylsulfonamide with carbonic anhydrase. The values of energy shown for the different states are in kcal mol^{-1} and have been taken from experimental values for the association of *p*-nitrobenzenesulfonamide (**3**) with HCA II. Data taken from King and Burgen.³⁸⁹

independent (see section 11.2.3.2) but that the second step—the isomerization to form the final complex where the arylsulfonamide anion directly coordinates the Zn^{II} cofactor—is pH-dependent.³⁸⁹

11.2.3.2. Experimental Support for an Intermediate.

The observation that k_{on} has a stronger influence on $K_{\text{d}}^{\text{obs}}$ than does k_{off} provides support for the three-state model (Scheme 3). A two-state model would anticipate a greater influence of k_{off} than of k_{on} on $K_{\text{d}}^{\text{obs}}$ (see section 11.1.2). The observation that, in general, *para*-substituted benzenesulfonamides with longer alkyl chains have larger values of k_{on} than do those with shorter alkyl chains also provides support for the three-state model. A two-state model that depends on the diffusion-limited encounter of arylsulfonamide and CA would predict that k_{on} should slightly decrease with (or at least be independent of) the length of the alkyl chain (Figure 26). Furthermore, the values of k_{off} are mostly independent of the length of the alkyl chain of *para*-substituted benzenesulfonamides (Table 15). A two-state model, in which hydrophobic contacts between the tail and CA are important, would anticipate that values of k_{off} would decrease with increasing length of the alkyl chain (see section 11.1.4).

King and Burgen demonstrated that *apo*-HCA II, which lacks the essential Zn^{II} cofactor but has the same tertiary structure as *holo*-HCA II (HCA II with the Zn^{II} cofactor) (see sections 5 and 15.2.2), associated with *p*-substituted benzenesulfonamides with reasonable affinity: the affinities of arylsulfonamides for *apo*-HCA II ($K_{\text{d}}^{\text{apo}}$) were a factor of $\sim 3 \times 10^4$ -fold lower than those for *holo*-HCA II ($K_{\text{d}}^{\text{obs}}$), regardless of chain length.³⁸⁹ The logarithm of $K_{\text{d}}^{\text{apo}}$ decreased (affinity increased) linearly with the logarithm of the partition coefficients of the arylsulfonamide between octanol and water. The constant ratio of $K_{\text{d}}^{\text{apo}}$ to $K_{\text{d}}^{\text{obs}}$ and the correlation between $K_{\text{d}}^{\text{apo}}$ and the partition coefficient of the arylsulfonamide suggest that hydrophobicity influences affinity and that this contribution is independent of the presence of the Zn^{II} cofactor. The observation that *apo*-HCA II associates with reasonable affinity ($\sim \text{mM}$) to arylsulfonamides supports a three-state model, as the arylsulfonamide/*apo*-HCA II complex could resemble the intermediate.

The investigators also reported that *N*-(*p*-nitrophenylsulfonamido)acetamide ($\text{AcNHSO}_2\text{C}_6\text{H}_4\text{NO}_2$, NBSAc, the acetylated version of *p*-nitrobenzenesulfonamide (**3**)) associated with *holo*-HCA II with an affinity $\sim 10^4$ -fold lower than did **3** (NBSAc competes with arylsulfonamides for binding to *holo*-HCA II but does not coordinate the metal cofactor of HCA II).³⁸⁹ Further, King and Burgen demonstrated that the affinities of arylsulfonamides for *apo*-HCA II, and of NBSAc for *holo*-HCA II, were independent of pH over the range of

6–10 (unlike the case of **3**; Figure 14B and section 10.3.2). These results demonstrate that hydrophobic contacts between the arylsulfonamide and *apo*- and *holo*-HCA II are important to affinity, that the contribution of these contacts to affinity was the same for *apo*-HCA II and for *holo*-HCA II, and that these contacts were insensitive to pH. These observations provide support for the conjecture that the first step in the three-state model is pH-independent. Since the overall process for the association of sulfonamides with CA (at least for HCA I and II,³⁰² and likely for BCA II due to its high homology with HCA II; see Figures 3 and 4) is pH-dependent (Figure 27), the second step must be pH-dependent.

Banerjee et al. have observed evidence for an intermediate in the association of dansylamide (DNSA, **133**) with HCA I.⁶¹⁴ All traces from stopped-flow fluorescence for the interaction of DNSA with HCA I and HCA II were well-fit by monoexponential rate equations. For HCA I, but not for HCA II, the pseudo-first-order rate constants varied in a hyperbolic manner with the concentration of DNSA.⁶¹⁴ Equation 34a gives k_{obs} for a three-state model in which both association and dissociation of DNSA with CA are reversible.⁶¹⁵

$$k_{\text{obs}} = \frac{k_1 k_2 [\text{DNSA}] + (k_1 [\text{DNSA}] + k_{-1}) k_{-2}}{k_1 [\text{DNSA}] + k_{-1} + k_2} \quad (34a)$$

The hyperbolic dependence of k_{obs} on the concentration of DNSA is consistent with eq 34b, which follows from eq 34a when $k_1 [\text{DNSA}] + k_{-1} \gg k_2$ —that is, the first step (formation of the encounter complex) is fast relative to the second step (formation of the final complex with direct Zn^{II} –N coordination).

$$k_{\text{obs}} = \frac{k_2 [\text{DNSA}]}{k_{-1}/k_1 + [\text{DNSA}]} + k_{-2} \quad (34b)$$

The investigators did not observe evidence for an intermediate in the association of DNSA with HCA II; the pseudo-first-order rate constants increased linearly with the concentration of DNSA up to 80 μM . This result is consistent with a simple two-state model and two different three-state models. A three-state model with a rate-limiting second step ($k_1 [\text{DNSA}] + k_{-1} \gg k_2$) should follow eq 34b, but at low concentrations of DNSA (when $[\text{DNSA}] \ll k_{-1}/k_1$ in eq 34b), the hyperbolic dependence on $[\text{DNSA}]$ will appear to be linear ($k_{\text{obs}} = k_1 k_2 [\text{DNSA}]/k_{-1} + k_{-2}$).³⁰ Banerjee et al. argued that a three-state model in which the first step is slow and the second step is fast ($k_1 [\text{DNSA}] \ll k_2$, and $k_{-1} \ll k_2$) would follow eq 34c and also anticipate a linear dependence of k_{obs} on $[\text{DNSA}]$.⁶¹⁴

$$k_{\text{obs}} = k_1 [\text{DNSA}] + \frac{k_{-1} k_{-2}}{k_2 + k_{-2}} \quad (34c)$$

Figure 26 illustrates that k_{on} increases with increasing molecular weight. King and Burgen suggested that a larger alkyl group permits a ligand to form an intermediate complex with a wider range of angular variation, which in turn increases the probability of the sulfonamide entering the coordination sphere of the metal.³⁸⁹ Schlosshauer and Baker investigated the theoretical influence of orientational constraints on the rate constant for the association of two spherical species (“molecules”), each of which has an asymmetric, reactive patch on its surface.⁶¹⁶ They showed that the rate constant for association between two molecules

depends on the angular constraint, Φ_0 , with which the molecules must interact in order for association to occur; greater steric specificity corresponds to a smaller value for Φ_0 . Within a given series of arylsulfonamides, the molecular weight of the arylsulfonamides is proportional to the hydrophobic surface area (Figure 26). Given a three-state model, an increase in the hydrophobic surface area of the ligand should correspond to a *larger* value for Φ_0 : more surface area can interact (in more orientations) with the hydrophobic wall of CA to form the intermediate. A two-state model, however, predicts that an increase in the hydrophobic surface area of the ligand should *decrease* Φ_0 : a larger ligand must align more perfectly when binding to the active site of CA (to avoid having the hydrophobic tail sterically block the sulfonamide head group from interacting with the Zn^{II} cofactor) than a smaller ligand. Schlosshauer and Baker showed that the theoretical rate constant for association, k_{on} , increases with Φ_0 .⁶¹⁶ According to a three-state model, k_{on} should increase with the molecular weight (hydrophobic surface area) of a ligand, whereas a two-state model predicts that k_{on} should decrease with increasing molecular weight of the ligand. The data for the binding of arylsulfonamides with HCA II (Figure 26) are consistent with the three-state model.

Four observations support the presence of an intermediate in the mechanism of the binding of arylsulfonamides to CA: (i) k_{on} has a stronger influence on $K_{\text{d}}^{\text{obs}}$ than does k_{off} . (ii) k_{on} increases with the length of the alkyl chain of *para*-substituted benzenesulfonamides. (iii) Arylsulfonamides associate with *apo*-HCA II with reasonable affinity. (iv) The pseudo-first-order rate constant deviates from a linear dependence on the concentration of dansylamide (for HCA I). The reported experimental data, however, cannot distinguish between parts A and B of Scheme 3 (that is, we do not know which are the reactive forms in the intermediate that combine to form the final complex), because the limit imposed by diffusion (see section 11.2.2) can no longer serve as a differentiating criterion: proton-transfer could take place in the active site of the protein concomitant with Zn^{II} –N bond formation. Furthermore, we do not know which step is rate-limiting in the formation of the final CA–sulfonamide complex.

11.2.3.3. Must the Mechanism Involve an Intermediate?

No deviation from pseudo-first-order kinetics for the association of arylsulfonamides with HCA II has been observed. Such a deviation would be expected for the mechanisms proposed in Scheme 3 when the concentration of the intermediate is not negligible relative to those of reactant and final product (e.g., a high enough concentration of arylsulfonamide would make $k_1 [\text{arylsulfonamide}] \gg k_{-1}, k_2$); a non-negligible concentration of intermediate would result in a deviation from the steady-state approximation used for derivation of eqs 30–33 and a need to fit with a biexponential model. King and Burgen argued that the concentration of intermediate is negligible and its lifetime is too short (the intermediate—with free energy $\Delta G^\circ = -4.5 \text{ kcal mol}^{-1}$ from Figure 28—decays with a rate of $2.5 \times 10^3 \text{ s}^{-1}$) to detect by stopped-flow methods because of the moderate concentrations of enzyme and arylsulfonamide used for stopped-flow fluorescence. They demonstrated that, even with significant buildup of intermediate (~24% of total enzyme), kinetic constants obtained by using the steady-state approximation (eqs 30–32) would differ from full solutions (using a computer simulation that accounted for this amount of

intermediate) by <20%.³⁸⁹

The affinity of *apo*-HCA II for arylsulfonamides does not necessarily prove that there is a hydrophobically bound *intermediate* in the mechanism. In a two-state model, there could be hydrophobic interactions between CA and arylsulfonamide in the *transition state* (section 11.2.2). Such a transition state would have two distinct sets of interactions occurring (ArSO₂NH⁻ binding to the Zn^{II} cofactor and the aryl ring binding to a hydrophobic pocket).

The observation that the pseudo-first-order rate constants deviated from linearity for the association of DNSA with HCA I does not prove that *other* arylsulfonamides bind to CA in a three-state process. DNSA (**133**) is atypical of most arylsulfonamides: whereas most arylsulfonamides are more potent inhibitors for CA II than for CA I (see section 9.2.4),^{2,531} DNSA binds more tightly to HCA I than to HCA II.⁶¹⁴ The crystal structure of HCA II complexed with DNSA reveals that this sulfonamide binds in a different orientation than do other arylsulfonamides (e.g., benzenesulfonamide, **1**) because of its bulky aryl ring.^{203,614} Thus, the mechanism for the binding of DNSA to CA is probably different from the mechanism for the binding of most arylsulfonamides to CA. Finally, evidence that supports a three-state mechanism for the association of DNSA with HCA I does not necessarily imply the existence of a three-state mechanism for HCA II, although we believe this mechanism *is* the most common (or only) one.

We are, thus, in agreement with Banerjee, Olander, and King and Burgen, and believe that the three-state model involving an intermediate (Scheme 2B) is the most likely mechanism for the association of arylsulfonamides with CA.^{389,612,614} A two-state model (no intermediate; Scheme 2A), however, cannot be ruled out rigorously.

11.2.4. Conclusions

A three-state model, which involves an intermediate on the pathway of the binding of sulfonamides to CA, is *probable* but not *required*. The second step of the three-state model—the formation of the final complex from the intermediate—could involve the interaction of neutral (Scheme 3A) or charged (Scheme 3B) arylsulfonamide and CA. The rate-limiting steps for both association and dissociation likely involve the transition state for this step (with the possible exception of the binding of DNSA to HCA II). Given this pre-equilibrium model, if association goes to completion and is irreversible, then the rate constant for *association* depends on the stability of the intermediate, but that for *dissociation* does not.

We conclude (with the caveats characteristic of mechanistic work) that the mechanism of binding of arylsulfonamides to CA probably involves a hydrophobically bound intermediate and is not simply a two-state model. For sulfonamide–CA binding, k_{on} makes a larger impact on $K_{\text{d}}^{\text{obs}}$ than does k_{off} . Being able to design ligands with high values for k_{on} will allow us to design rationally ligands that bind tightly to CA (low $K_{\text{d}}^{\text{obs}}$).

Although CA is a relatively simple enzyme, its mechanism of association with arylsulfonamides is still astonishingly difficult to model. The mechanism of binding of ligands to proteins can be difficult to establish given the challenges of measuring transient, weakly populated intermediate states. To the extent that it remains difficult to understand fully the mechanisms of relatively “simple” enzymes like CA, it will remain even more difficult to understand the mechanisms

of more “complex” enzymes with perhaps more complex mechanisms. Perhaps surprisingly, the “mechanisms” of noncovalent processes remain less easily studied than those of covalent ones—processes that form and break bonds. Covalent processes can be relatively well-defined by kinetics and products (in favorable instances); there are, however, substantially fewer windows into noncovalent processes.

12. Protein–Ligand Interactions on Surfaces

12.1. Overview

Understanding molecular recognition at the interface between an aqueous solution and the surface of a solid is important for understanding the kinetics and thermodynamics of biochemical processes occurring at surfaces (e.g., signal transduction, viral adhesion, and the immune response). It is also important in interpreting results from such bioanalytical techniques as surface plasmon resonance (SPR; section 8.4.3) and quartz crystal microbalance (QCM). We only discuss SPR because it is the primary technique for studying protein–ligand binding at surfaces.^{617–619} CA has been a model protein for studying these interactions using SPR because its binding to ligands in solution is well-characterized, it has a well-defined binding site, and arylsulfonamides can be easily derivatized for immobilization on surfaces. We discuss differences in the thermodynamics of CA–sulfonamide binding in section 12.2 and in the kinetics of binding in section 12.3.

12.2. Comparison of Thermodynamic Values for Binding Measured at Surfaces and in Solution

Equilibrium dissociation constants ($K_{\text{d}}^{\text{obs}}$) for protein–ligand complexes measured by SPR are most commonly determined by using the relationship $K_{\text{d}}^{\text{obs}} = k_{\text{off}}/k_{\text{on}}$ and the values of the individual rate constants, but they can also be determined by measuring the change in refractive index at the surface as a function of the concentration of the free analyte, either protein or ligand (see section 8.4.3). Values of $K_{\text{d}}^{\text{obs}}$ determined by SPR for the binding of ligands to CA, where one of the components is immobilized on a surface, are generally similar in magnitude to those measured by calorimetric and spectroscopic techniques when both components are in solution (Table 15).^{412,465,467,483,620,621}

Day et al. measured the binding of DNSA (**133**) and **29** to BCA II in solution using isothermal titration calorimetry (ITC) and stopped-flow fluorescence (SFF) and to BCA II immobilized on a dextran-coated surface using SPR (Table 15).⁴¹² The values of $K_{\text{d}}^{\text{obs}}$ from SPR were the same as those measured by the solution-phase methods (differences of <10%) for both of the ligands. Mrksich et al.⁴⁶⁷ and Lahiri et al.⁶²⁰ examined the binding of BCA (isozymes I and II) to a SAM displaying **275** in a background of tri(ethylene glycol) thiols, chemical groups that reduce the nonspecific binding of proteins (see Figure 10 and section 8.4.3). They observed that binding in solution (using the control ligand **276**, which is structurally similar to **275**) was slightly tighter ($K_{\text{d}}^{\text{obs}}$ lower by ~3-fold; Table 15) than at the surface of the SAM.^{467,620} Mrksich et al. attributed this effect to either steric interactions between free BCA and surface-bound BCA (lateral steric effects; see Figure 10C and section 12.3.2)⁶²⁰ or to entropic repulsion between free BCA and the tri(ethylene glycol) tails of the SAM.⁴⁶⁷ Lateral steric effects

would not be expected to affect the results of Day et al. because ligand bound to surface-immobilized enzyme should not sterically interfere with the binding of free ligand.

12.3. Comparison of Kinetic Values for Binding Measured at Surfaces and in Solution

The situation with *rate constants*— k_{on} and k_{off} —is more complicated than with $K_{\text{d}}^{\text{obs}}$ because the individual rate constants can differ significantly when measured at surfaces and in solution, while values of $K_{\text{d}}^{\text{obs}}$ ($=k_{\text{off}}/k_{\text{on}}$) are often quite similar at surfaces and in solution (section 12.2). These differences may arise from several factors, including the following: (i) mass transport of analyte to the surface, (ii) rebinding of dissociated analyte molecules, (iii) lateral steric effects, (iv) nonspecific binding of molecules to the surface (using a mixed SAM that presents some oligo(ethylene glycol) groups can usually eliminate this problem), and (v) artifacts due to immobilization, which are not well-understood. We discuss the first three factors in more detail in the following sections.

12.3.1. Influence of Mass Transport and Rebinding on Kinetics of Binding

Immobilization of one binding partner on a surface reduces the translational and rotational freedom of that molecule and requires the other binding partner to diffuse through the interfacial fluid boundary layer—and possibly into a polymer (e.g., dextran)—to reach the surface (Figure 10B; section 8.4.3). If the rate of diffusion is not significantly greater than the rate of formation of the intermolecular complex, the effects of mass transport contribute to the observed rates of association and dissociation. Values of $K_{\text{d}}^{\text{obs}}$ are, however, not affected because the influence of mass transport on k_{on} and k_{off} is identical.^{465,620,621}

The effects of mass transport can be reduced or accounted for by several methods: (i) increasing the rate of flow of the analyte and, thus, reducing the thickness of the film of stationary fluid adjacent to the surface; (ii) reducing the molecular size, and thereby increasing the diffusion constant and the rate of diffusion, of the analyte; (iii) building a kinetic scheme that includes a mass-transport step; or (iv) using a surface that presents the target molecules oriented directly into solution (e.g., at the surface of a SAM or on a thin, highly cross-linked layer of dextran) rather than inside of a gel (e.g., a thick layer of dextran with a low density of cross-links).

The above strategies may allow the extraction of values for k_{on} and k_{off} from SPR that agree closely with values measured in solution. For example, Day et al. measured the kinetics of binding of **133** to BCA II in solution using stopped-flow fluorescence (SFF) and to BCA II immobilized on a surface using SPR (Table 15).⁴¹² Because of the fast rate constant of association of **133** with BCA II, they added a mass-transport step⁶²¹ to their reaction model. The estimated values of k_{on} and k_{off} from SPR were similar (difference of <30%) to those measured by SFF; this good agreement is likely due to (i) the reduction of the effects of mass transport by using a high flow rate (100 $\mu\text{L min}^{-1}$) and by immobilizing the protein to the surface (the ligand has a higher diffusion coefficient than the protein) and (ii) the inclusion of a mass-transport term in the kinetic scheme.

12.3.2. Lateral Steric Effects

Lahiri et al. observed that decreasing the fractional thiol coverage of arylsulfonamide **275** (relative to a “background”

tri(ethylene glycol) thiol; Figure 10) on a SAM from 0.02 to 0.005 (and, thus, decreasing the maximum amount of BCA II that could bind on the surface from 35% of a total monolayer to 15%) increased the value of k_{on} by a factor of 8, while the value of k_{off} remained constant (Table 15).⁶²⁰ To explain the data, they invoked the concept of lateral steric effects^{622–627}—an unfavorable steric repulsion between BCA II that is bound at the surface and BCA II that is free in solution (Figure 10C; section 8.4.3). Decreasing the fractional coverage of arylsulfonamide ligands on the surface should reduce the possibility of these unfavorable interactions between bound BCA II molecules and increase the observed value of k_{on} to its solution-phase value. Unfortunately, there are no solution-phase data in the literature for the kinetics of binding of **275**, or the structurally similar ligand **276**, to BCA II to which to compare their results.

12.4. Conclusions

SPR is a useful technique for determining what factors influence the kinetics and thermodynamics of binding that occurs at surfaces. In general, thermodynamic values ($K_{\text{d}}^{\text{obs}}$) obtained by SPR agree with those obtained by solution-phase measurements. Values for the rate constants, however, can differ between the two techniques. In order to obtain values for k_{on} and k_{off} from SPR that agree with those from solution, it is necessary to reduce the influences of mass transport and lateral steric effects. Both of these goals can be achieved by (i) using a low density of ligands on the surface, (ii) immobilizing the protein on the surface (rather than immobilizing the ligand), (iii) increasing the flow rate of the analyte, (iv) using a surface that exposes the target molecules directly into solution (e.g., at the surface of a SAM) rather than inside of a gel (e.g., a thick layer of dextran with a low density of cross-links), and (v) including a mass-transport step into the kinetic scheme, when necessary.

13. Protein–Ligand Interactions in the Gas Phase

13.1. Overview

Mass spectrometry (MS) has revolutionized the study of proteins in the gas phase.^{431–442,628–630} The system of CA and arylsulfonamides has been the subject of MS studies for three reasons: (i) CA has a tractable molecular weight; (ii) complexes between CA and arylsulfonamides are well-characterized structurally and thermodynamically (see sections 4 and 10); and (iii) CA is a particularly stable protein (see section 15). Section 8.3.7 describes the MS techniques used to study the binding of ligands to CA. This section discusses the experimental data from these studies. There are two main types of experiments that use MS, each of which has a different goal: (i) to determine the relative abundances of protein–ligand complexes (or ions released by dissociation of these complexes) in the gas phase, with the goal of estimating the relative affinities of the ligands for the protein in solution (section 13.2), and (ii) to determine the stabilities of protein–ligand complexes in the gas phase, with the goal of understanding the role of solvation in protein–ligand binding (section 13.3).

13.2. Using Mass Spectrometry to Estimate Solution-Phase Affinities

Using MS to estimate the relative affinities of ligands for CA in solution requires that the relative abundances of the

different protein–ligand complexes in the gas phase reflect those of the different complexes in the starting solution pool. Two factors are necessary to ensure that the relative abundances in the gas phase and in solution are equal: (i) ionization and vaporization procedures must generate intact noncovalent CA–ligand complexes in the gas phase and (ii) ionization efficiencies of complexes of different ligands with CA must be similar.

Cheng et al. examined the complexes of BCA II with *p*-substituted benzenesulfonamides with alkyl (**16–21** and **38–40**), fluoroalkyl (**22–27** and **45–47**), and dipeptidyl (ligands of structure $p\text{-H}_2\text{NSO}_2\text{C}_6\text{H}_4\text{CONH-AA-NHCH}_2\text{-CH}_2\text{CO}_2\text{H}$ where AA is an amino acid) tails (Table 10).⁴⁴³ The investigators equilibrated BCA II with the libraries of ligands and used ESI-FTICR-MS to generate and isolate ions of the BCA II–ligand complexes. The relative ion intensities of the different BCA II–ligand complexes in the mass spectra were related to the relative abundances of the different BCA II–ligand complexes in the gas phase and suggested the relative abundances of these complexes in solution, assuming that the ionization efficiencies of the different complexes were similar. Resolving the different protein–ligand complexes in the mass spectra was challenging when the ligands had similar masses. To address this issue, the investigators isolated and completely dissociated the desired protein–ligand complexes (corresponding to the unresolved peak) using collisional-induced dissociation (CID) with nitrogen gas molecules.⁴⁴³ The released ligands (in their -1 charge state) could be distinguished by their exact masses ($\Delta m \geq 0.025$ Da), and the relative ion intensities of the ligands allowed an estimate of the relative abundances of the different protein–ligand complexes in solution. The investigators observed a good correlation between the relative ion intensities of both the CID-released ligands and the protein–ligand complexes and values of K_d^{obs} measured in solution for the different ligands (Table 10).

Gao et al. expanded this ligand screening effort to compounds of the form $p\text{-H}_2\text{NSO}_2\text{C}_6\text{H}_4\text{CONH-AA}_1\text{-AA}_2\text{NHCH}_2\text{CH}_2\text{CO}_2\text{H}$, where AA₁ and AA₂ were either L-amino acids (library of 289 ligands) or D-amino acids (library of 256 ligands).⁴⁴⁴ Incubating BCA II with the two libraries and analyzing the BCA II–ligand complexes using ESI-FTICR-MS, they observed that the relative ion intensities of the CID-released ligands increased with increasing hydrophobicity of the ligands; this observation is in agreement with the results of a number of solution-phase studies (see section 10.4). They examined the solution-phase affinities of seven of the ligands (with a range in K_d^{obs} of ~ 30 -fold); these values of K_d^{obs} correlated closely with the relative ion intensities from the MS studies.

The results of Cheng et al. and Gao et al. suggest that ESI-FTICR-MS can be used to determine the relative abundances of different ligands complexed with CA (at least with BCA II) in *solution* and to estimate the relative solution-phase affinities of the ligands. Dissociating CA–ligand complexes with CID and analyzing the relative abundances of the released ligands allows the estimation of relative affinities of ligands with similar masses ($\Delta m \geq 0.025$ Da) in a high-throughput manner.

13.3. Using Mass Spectrometry to Understand the Stability of Protein–Ligand Complexes in the Gas Phase

The thermodynamics of stability of a protein–ligand complex in aqueous solution and in the gas phase (where there is no bulk water) *must* be fundamentally different, since, by definition, there is no hydrophobic effect in the gas phase and the energetics of electrostatic interactions are different between the two phases. Because of the absence of bulk water, a comparison of complex stabilities in solution and in the gas phase should reveal the role of water in these interactions; this approach has been used to understand the role of solvation in many organic reactions.^{631–633}

Whitesides, Smith, and co-workers used sustained off-resonance irradiation (SORI) coupled to ESI-FTICR-MS to study the stability of complexes of HCA II, BCA II, and *apo*-BCA II (BCA II lacking the Zn^{II} cofactor; see section 5) with different ligands in the gas phase.^{445,446} Gas-phase complex stability was estimated by the intensity of radiation (E_{50}) required to dissociate half of the CA II–ligand complex ions to unbound CA II ions; E_{50} increases with increasing stability of the complex.

Wu et al. reported values of E_{50} for complexes of BCA II with eight *p*-substituted benzenesulfonamides with short peptide tails.⁴⁴⁵ They did not observe a clear correlation between E_{50} and the hydrophobicity of the amino acid closest to the phenyl ring of the ligand, while they did observe such a correlation for the thermodynamic (K_d^{obs}) and kinetic stability (k_{off}) of the BCA II–ligand complexes in solution.⁴⁴⁵ Instead, they observed a linear correlation between E_{50} and the polar surface area of the ligands. Their results suggest that the stability of BCA II–ligand complexes in the gas phase is dominated by electrostatic interactions.⁴⁴⁵

Gao et al. studied the binding of $p\text{-H}_2\text{NSO}_2\text{C}_6\text{H}_4\text{CONH-Gly-Phe-CO}_2\text{H}$ to BCA II and *apo*-BCA II.⁴⁴⁶ While the ligand did bind to *apo*-BCA II (when *apo*-BCA II was treated with an excess of the ligand), the value of E_{50} for this complex was much lower (by 0.4 ± 0.1 V) than that for the BCA II–ligand complex. This result suggests that the Zn^{II} cofactor is bound to BCA II in the gas phase and contributes to the gas-phase stability of BCA II–ligand complexes. Gao et al. also examined the gas-phase stabilities of complexes of HCA II with *o*-nitrobenzenesulfonamide (*o*-NBS) and with *p*-nitrobenzenesulfonamide (**3**); they observed that the HCA II–**3** complex was significantly more stable ($\Delta E_{50} = 0.8 \pm 0.1$ V) than the HCA II–*o*-NBS complex.⁴⁴⁶ This observation is in agreement with the results of solution-phase studies of these ligands³⁸⁹ and with the general principle that *o*-substituted benzenesulfonamides have lower affinities for HCA II than their *p*-substituted analogues (a fact that has been rationalized by invoking steric repulsion between the *ortho*-position on the phenyl ring and the active site of HCA II; see section 10.4.2). Their results suggest that the steric environment in the binding pocket of HCA II is, at least to some extent, retained in the gas phase.

13.4. Conclusions

Mass spectrometry seems effective for screening CA–ligand interactions (and determining relative affinities) when care is taken to ensure that the relative abundances of different CA–ligand complex ions in the gas phase reflect those of the complexes in the starting solution pool.^{443,444} Thus, MS could be useful in estimating, or at least rank

ordering, the relative solution-phase affinities (values of K_d^{obs}) of ligands for proteins in general in a high-throughput manner.^{431,432}

While the structure of CA seems to be, at least, partially retained in the gas phase, the important thermodynamic forces for the stability of CA–ligand complexes seem to be very different in the gas phase than in solution. In gas-phase stability, electrostatic interactions (e.g., hydrogen bonding, van der Waals forces, etc.) between CA and ligand appear to be dominant, while in solution, the hydrophobic effect can make a very large contribution to stability; this result is consistent with reports for other protein–ligand systems.^{433,434,628,629} Thus, the results from the system of CA and arylsulfonamides serve to underscore the need for caution when attempting to extrapolate from stabilities in the gas phase to those in solution.

IV. Using CA as a Model Protein for Biophysical Studies

Our current understanding of the noncovalent interactions that determine the structure and properties of proteins is far from complete. We are able to list these interactions—electrostatic, hydrophobic, van der Waals, and hydrogen bonding—under labels that are perhaps artificially separated, but we are unable to assign qualitatively and quantitatively the importance of these interactions in protein folding, stability, aggregation, and ligand binding (see section 10). The following two sections describe the use of CA as a model protein in biophysical studies aimed at probing noncovalent interactions in proteins. Section 14 summarizes a series of studies, conducted mainly on CA, that examine the role of charge and electrostatic interactions in proteins using capillary electrophoresis (CE) and protein charge ladders—chemically modified derivatives of a protein. Section 15 reviews the body of work on folding of CA, its stability to various denaturants, and aggregation.

CA is a particularly suitable model for biophysical studies because its structure is well-defined and easily probed. It is particularly (and exceptionally) stable. Its folding pathway explicitly possesses features that are believed to be general features of protein folding—hydrophobic collapse and a molten-globule intermediate. The absence of intramolecular disulfide bonds in the native protein allows the study of aggregation without additional complications from intermolecular disulfide formation. A multitude of ligand binding and catalytic assays can serve as probes for the correctly folded active site (see section 8). The following sections describe in greater detail the features of CA that make it an attractive candidate for biophysical studies. They also present the results that are peculiar to CA.

14. Protein Charge Ladders as a Tool to Probe Electrostatic Interactions in Proteins

One of the general characteristics of a protein is the presence of multiple charged groups on its surface, in its active site, and in its interior. Our current understanding of the interactions between these groups and their effect on the stability and functionality of a protein is incomplete.³⁹⁷ Since the charge of a molecule is directly related to its electrophoretic mobility—a property easily measured by capillary electrophoresis (CE)³⁹⁵—CE is an excellent tool for probing the effects arising from electrostatic charges on a protein.

Whitesides and co-workers developed the idea of “protein charge ladders” to probe the effects and interactions of charged residues on the *surface* of a protein.³⁹⁷ In conjunction with CE and affinity capillary electrophoresis (ACE, see section 8.4.2), charge ladders are able to provide quantitative information on these electrostatic effects. Protein charge ladders and ACE were developed using CA as the model protein. A recent review on protein charge ladders summarizes the work done on this subject in detail,³⁹⁷ while the section below provides a brief overview of the studies conducted with CA.

14.1. Protein Charge Ladders

A protein charge ladder is a collection of derivatives of a protein that vary in the number of charged groups on their surface but share similar values of hydrodynamic drag.⁶³⁴ A charge ladder is most commonly formed by acetylating the ϵ -NH₂ groups of Lys residues (which exist as ϵ -NH₃⁺ at physiological pH), thereby removing approximately one positive charge with each acetylation (Figure 29A). (The N-terminal α -NH₂ group may also be modified, but the N-terminus of native, blood CA is acetylated post-translationally *in vivo*.) It is also possible to construct a charge ladder by modifying other charged groups (e.g., Glu, Asp, Arg) on a protein.^{397,635}

CE separates the members of a charge ladder into distinct peaks, or rungs, based on charge (Figure 29B) provided that the electrophoretic mobilities of the rungs are sufficiently different. The combination of protein charge ladders and CE provides a set of internally consistent data useful for quantifying certain electrostatic properties of proteins. These properties include (i) net charge of proteins,⁶³⁴ (ii) electrostatic contribution to binding of ligands to proteins,³⁹⁶ (iii) electrostatic contribution to protein folding,⁶³⁶ (iv) effects of charge on ion binding,⁶³⁷ and (v) effects of charge in ultrafiltration systems.⁶³⁸ In addition, protein charge ladders assist in understanding the characteristics of the networks of charges present in macromolecules as well as related phenomena (e.g., charge compensation).^{639,640}

CA II (bovine or human) has been a model system in the development and evaluation of the properties of protein charge ladders because (i) it is negatively charged in standard electrophoresis buffers (e.g., tris-Gly, pH 8.4) and does not substantially adsorb to the walls of a fused silica capillary; (ii) it is stable ($T_m = 65$ °C); (iii) a change of a unit of charge on the enzyme produces a change in the value of electrophoretic mobility that is sufficient to be easily resolved by CE; and (iv) its binding pocket is not significantly altered upon acetylation of Lys residues, thus allowing studies of the effects of charge on ligand binding. Below we review some of the interesting results—both CA-specific and general proof-of-principle—obtained using CA as the model protein for studies using protein charge ladders.

14.2. Determination of Net Charge (Z_0), Change in Charge (ΔZ) Upon Acetylation, and Hydrodynamic Radius of a Protein

The net charge of a protein is a fundamental physical parameter whose significance for structure or function (especially *in vivo*) is not well-understood.^{641–643} Estimating the value of net charge of a protein from standard values of pK_a of ionizable residues does not give accurate numbers; the values of pK_a depend strongly on the specific location

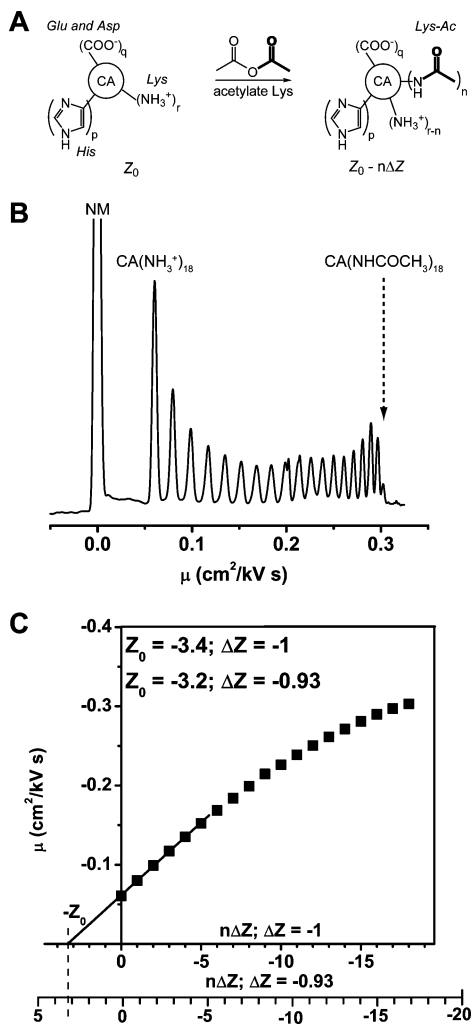


Figure 29. (A) Diagram summarizing the formation of a protein charge ladder. A protein contains multiple ionizable residues (only Lys, Asp or Glu, and His shown here), the charge state of which depends on the value of pH of the solution and the pK_a of the residue. Acetic anhydride reacts with the α -NH₃⁺ groups of lysine residue. The resulting mixture contains protein derivatives with different numbers and positions of acetylated lysine residues. (B) CE electropherogram showing the separation of the rungs of the charge ladder of BCA II, plotted on mobility (μ) scale. The peak labeled NM corresponds to the electrically neutral molecule (*p*-methoxybenzylalcohol) used to monitor electroosmotic flow. Native BCA II (CA(NH₃⁺)₁₈) and the last rung of the ladder (CA(NHCOCH₃)₁₈) are also labeled on the plot. The separation was done in tris-Gly, pH 8.4 buffer in a capillary measuring 47 cm in total length and 40 cm to the detector. (C) Plot of mobility (μ) of each rung versus the number of modified residues. Two x -axes are shown with calibration of $\Delta Z = -1$ and $\Delta Z = -0.93$. Linear regression line through the first six points provides the charge on the native protein at the intersection with the abscissa. The charge Z_0 of the native BCA II is estimated to be -3.4 if $\Delta Z = -1$ and -3.2 if $\Delta Z = -0.93$. Modified with permission from ref 640. Copyright 2003 American Chemical Society.

of the residue, the net charge of the protein, and the medium for “standard” values to be useful.³⁹⁷ Experimentally, the charge of a protein has been difficult to determine.^{397,644}

A simple experiment that consists of generating a protein charge ladder and analyzing it by CE provides a good estimate of the value of charge of the native protein under the conditions of the experiment.^{635,645,646} When the mobility of each rung is plotted against the change in charge ($n\Delta Z$) due to acetylation (where n is the number of acetylated groups and ΔZ is the change in charge of a Lys residue on

acetylation), a linear relationship is observed for the first five or six rungs. The intercept of the linear regression line through those points with the abscissa gives an estimate of the value of charge (Z_0) of the native protein (Figure 29C).

In order to get an absolute value of Z_0 , it is, however, necessary to know the value of ΔZ . At pH 8.4, the Lys ϵ -NH₃⁺ residues ($pK_a = 10.2$) are fully (>99%) protonated. Upon acetylation, one positive charge is formally removed from the amino group ($-\text{NH}_3^+ \rightarrow -\text{NHCOCH}_3$). The situation is, however, complicated by the fact that a protein contains a network of charges that “communicate” with each other electrostatically; this network is capable of responding to a change in charge of one of its groups with subtle changes in the charge state of other groups (especially HisH⁺) in a way that partially compensates for this change, a process called “charge regulation”.^{637,640} As a result, the value of $|\Delta Z|$ upon acetylation is <1 . Compensation of charge may occur by at least four mechanisms: (i) changes in the local proton concentration near the surface of a protein (i.e., the effective local value of pH decreases in response to removal of a positive charge), (ii) perturbation of ionization constants of other residues (i.e., the pK_a value of a neighboring ionizable residue increases in response to removal of a positive charge for a Lys group), (iii) altered affinity toward buffer ions that would differentially screen the increasing charge, or (iv) changes in the conformation of the protein that alter the values of pK_a of charged groups. The first two of these mechanisms are mathematically equivalent and can be represented by adapting the model of Linderström-Lang for cooperative proton binding⁶⁴⁷ to the current system.⁶³⁷ Gitlin et al.⁶⁴⁰ estimated $\Delta Z = 0.93 \pm 0.02$ for BCA II in tris-Gly buffer (25 mM tris, 192 mM Gly), pH 8.4 at 25 °C; the value is in close agreement to that estimated by Menon and Zydny.⁶³⁷ In general, the value of ΔZ is determined by the protein and its three-dimensional structure and by its environment. A related, but more detailed, study on charge regulation conducted on lysozyme⁶⁴⁸—a protein that is better suited for this study than CA because its ionization constants are better characterized experimentally than those of CA⁶⁴⁹—has confirmed that $|\Delta Z|$ is ~ 0.9 when the buffer pH is 8.4. With the approximation of $\Delta Z = -0.93$ upon acetylation, the charge (Z_0) for BCA II is -3.2 in tris-Gly buffer, pH 8.4.⁶⁴⁰ (Some of the early work on charge ladders used the value of $\Delta Z = -1$ in estimating charge and other parameters.)

The plot of mobility versus the number of modified residues can also be fit to the model of Henry for the electrophoretic mobility for colloids⁶⁵⁰ in order to determine the hydrodynamic radius of a protein.⁶⁴⁵ The values of hydrodynamic radius, determined by this method, are 2.6 nm for BCA II and 2.7 nm for HCA II. The investigators used the value of $\Delta Z = -1$ in this analysis; the analysis, however, remains fundamentally the same if a different value of ΔZ is used. Being able to predict hydrodynamic properties of proteins may prove important in the design of new techniques for the separation of proteins.

14.3. Probing Long-Range Electrostatic Contributions to the Binding of Charged Sulfonamides Using Charge Ladders and ACE

ACE of a protein charge ladder can determine simultaneously the affinities of the protein derivatives comprising each rung of the ladder for a common ligand.³⁹⁶ Plotting the free energies of binding of a protein to a ligand as a function

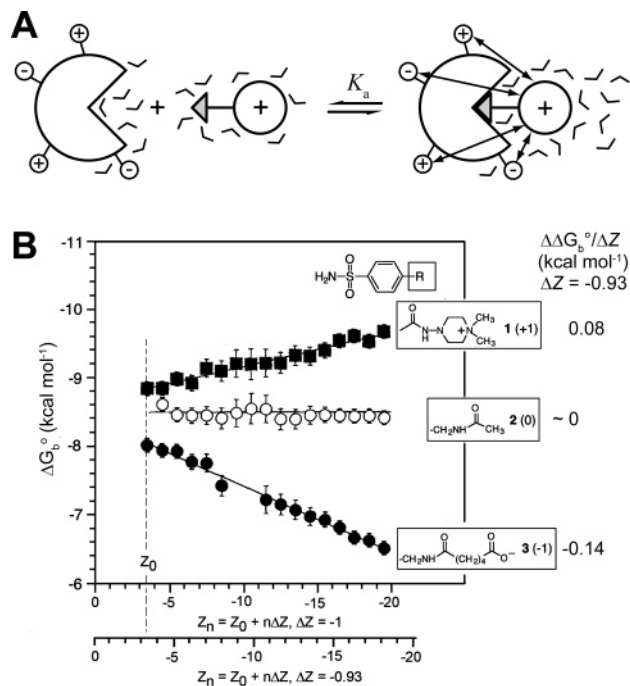


Figure 30. (A) Diagram illustrating the long-ranged electrostatic interactions of charged ligand with charges on the surface of the protein upon binding. (B) Dependence of the free energy of binding of negative, neutral, and positive ligands on the charge of a rung of a charge ladder of BCA II. Electrostatic contribution to the free energy of ligand binding is found to be 0 for a neutral ligand, 0.08 kcal mol⁻¹ per unit charge for a positively charged ligand, and -0.14 kcal mol⁻¹ for a negatively charged ligand with $\Delta Z = -0.93$. Modified with permission from ref 396. Copyright 1996 American Association for the Advancement of Science; www.sciencemag.org.

of the charge Z_n (where $Z_n = Z_0 + n\Delta Z$) of each rung of the ladder allows the study the effects of charge of the protein on binding and the estimation of electrostatics to the free energy of binding. Experiments conducted using the charge ladder of BCA II and three types of ligands—positively charged, neutral, and negatively charged (Figure 30)—demonstrated this technique.³⁹⁶ The affinity of the rungs of the charge ladder toward an electrically neutral ligand was essentially insensitive to the charge of the BCA II derivative. In the case of charged ligands, however, the free energy of binding (ΔG_b°) varied linearly with the charge of the protein derivative: ΔG_b° decreased (became more favorable) with increasing negative charge on BCA II ($\Delta\Delta G_b^\circ/\Delta Z = +0.08$ kcal mol⁻¹) for a positively charged ligand, and ΔG_b° increased (became less favorable) with increasing negative charge on BCA II for a negatively charged ligand ($\Delta\Delta G_b^\circ/\Delta Z = -0.14$ kcal mol⁻¹), with $\Delta Z = -0.93$.⁶⁵¹ The observation of invariable affinity of the rungs of the charge ladder for a neutral sulfonamide and additional studies by CD⁶⁵² implied that the active-site structure of BCA II was not disrupted by acetylation of the Lys residues. The dependence of the free energy of binding of charged sulfonamides on the net charge of BCA II thus demonstrates that long-range electrostatic interactions, arising from charged residues outside of the active site, can influence the affinity of ligands for proteins. Although the values of $\Delta\Delta G_b^\circ/\Delta Z$ are small ($\ll kT \approx 0.6$ kcal mol⁻¹), they can be detected and accurately measured because of the large number of derivatives studied simultaneously. Similar trends hold for the affinities of charged and neutral sulfonamides for HCA II charge ladders as well.⁶⁵³

Caravella et al. performed continuum electrostatic calculations to examine the contributions of individual Lys residues to the binding of sulfonamide ligands and to test whether the simulations can reproduce the results from the experiments with charge ladders.⁶⁵³ The simulations showed that many patterns of acetylations are compatible with the average (since each rung is a collection of regioisomers) affinities measured for each rung. The work also showed that the electrostatic free energy of binding of sulfonamides to CA (at least HCA II) consists of two contributions of similar magnitude. The first contribution is the direct Coulombic interaction between the charged or polar groups of the protein and the charged or polar groups in the binding pocket (either sulfonamide or hydroxide ion). The second contribution arises from the change in the shape of the regions of low and high dielectric constants that occurs when the ligand binds and water is displaced from the binding site. Most continuum electrostatic calculations account only for the direct Coulombic interaction; variable shape of the dielectric cavity can, however, also be energetically significant.⁶⁵³

14.4. Charge Ladders in the Gas Phase: Mass Spectrometry

An interesting but difficult-to-interpret complement to the work on CA charge ladders in solution is the study of charge ladders of CA in the gas phase.⁶⁵⁴ The origin of the distribution of charge states of proteins studied by ESI-MS is largely unknown and is the subject of two limiting hypotheses based on a correlation between (i) the net charge of the native protein in solution and the most abundant charge states formed on ionization⁶⁵⁵ or (ii) the number of basic residues (e.g., Lys, His, Arg) in the protein and the state with the largest net charge produced by ESI.⁶⁵⁶ Protein charge ladders formed in solution and separated by CE provide an excellent system with which to test these two hypotheses, because the number of unmodified Lys residues, and thus the net charge of species making up the rungs, change systematically, while the conformations of the proteins in solution apparently remain the same. Charge ladders of BCA II, along with those of hen eggwhite lysozyme and bovine pancreatic trypsin inhibitor, were used to test these hypotheses.⁶⁵⁴ The results indicated that neither the total charge nor the number of available amino groups correlated well with the distribution of ions generated by ESI. Instead, the results suggest a correlation between the molecular surface area of the native protein and the highest charge states produced—that is, greater molecular surface areas resulted in higher charge states. Thus, the distribution of charge states probably depends on structural factors such as the distances between the charged groups on the surface of a protein and the magnitude of the Coulombic interactions of these charged groups in the gas phase.⁶⁵⁴ Understanding the *structure* of proteins in the gas phase is an effort that is still early in its development (see section 13.3). Progress in it will, we believe, require tools such as the charge ladder of CA.

14.5. Protein Hydrophobic Ladders and Interactions with Sodium Dodecyl Sulfate

Protein hydrophobic ladders (Figure 31A) are generated by acylating Lys residues using hydrophobic acyl groups (e.g., benzoyl and hexanoyl).⁶⁵⁷ Hydrophobic charge ladders allow the hydrophobicity of the *surface* of the protein to be changed systematically. Each rung of the ladder contains the

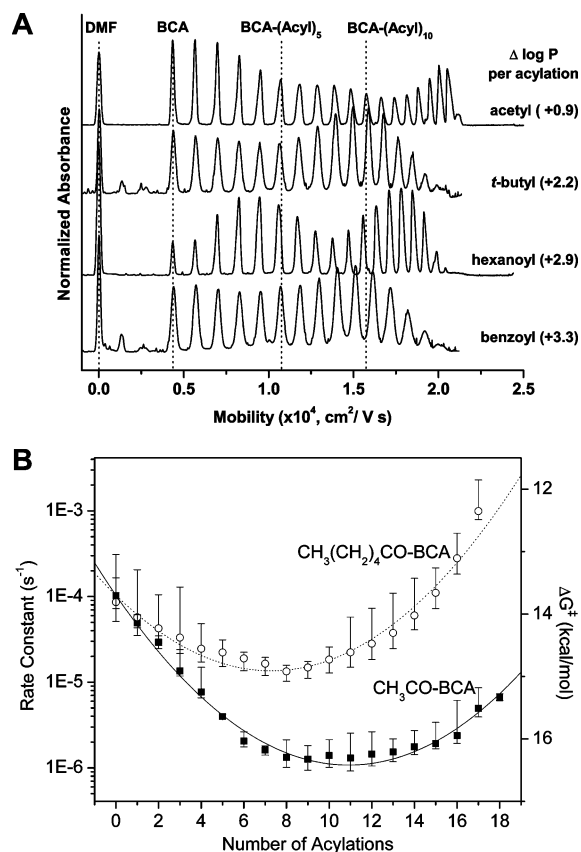


Figure 31. (A) Electropherograms of hydrophobic charge ladders of BCA II. The figure shows the increase in hydrophobicity parameter ($\log P$) for reactions from $-\text{NH}_3^+$ to respective $-\text{NH}-\text{Acyl}$ group. The dashed vertical lines mark the number of modifications and indicate that the mobilities of the early rungs of all ladders are indistinguishable, but the mobilities of the late rungs vary between the ladders, possibly due to the effects of increasing drag. Dimethylformamide (DMF) is used as an electrically neutral molecule to monitor the electroosmotic flow. (B) Rate constants and activation energies, calculated from transition-state theory, for denaturation of acetyl ($\text{CH}_3\text{CO}-\text{BCA}$, \blacksquare) and hexanoyl ($\text{CH}_2(\text{CH}_2)_4\text{CO}-\text{BCA}$, \circ) ladders of BCA II. The lines show the fit of the model, qualitatively described in the text. Adapted with permission from ref 657. Copyright 2006 The Biophysical Society.

derivatives of the protein with the same number of modified charges and the same number of hydrophobic groups added to its surface. The charge ladder in these experiments is a device for counting: the rung indicates the number of hydrophobic groups added, rather than (primarily) the change in charge. The additional hydrophobicity, added by the modifications, can be quantified by the change in hydrophobicity parameter, $\log P$.^{586,657,658} These ladders can be used to separate the effects of hydrophobicity and charge on denaturation and folding, transport, precipitation, and two-phase partitioning of proteins.

In a recent study, Gudiksen et al. used two ladders of BCA II—acetyl and hexanoyl—to study the effects of charge and hydrophobicity on the kinetics of denaturation of proteins with the surfactant sodium dodecyl sulfate (SDS).⁶⁵⁷ By comparing the rates of denaturation of the rungs within each charge ladder and between the two charge ladders, the investigators could separate the effects of net charge and hydrophobicity on the interaction of BCA II with SDS. The investigators measured the rates of denaturation by monitoring the decreasing peak areas of each rung by CE (the SDS-denatured protein peak did not overlap with any rungs of the ladder). Figure 31B shows that the variation of the

logarithm of the rate constants for denaturation (proportional to the activation energy for denaturation, ΔG^\ddagger) vs the number of acylations resulted in a U-shaped plot. Interestingly, the native BCA II was not the most stable protein in these series of derivatives. In both ladders, the intermediate rungs were the most kinetically stable to SDS. The rungs of the hexanoyl ladder denatured faster than the corresponding rungs of the acetyl ladder by factors of $\sim 10^1-10^3$. The investigators developed a model that allowed them to quantify the electrostatic and hydrophobic components of the difference in activation energy, $\Delta\Delta G^\ddagger$, between the n th rung and the native protein. The model accounted for four competing interactions that influence the stability of a rung to denaturation with SDS: (i) intramolecular electrostatic interaction, destabilizing with each acylation as the net negative charge on the protein increased; (ii) intermolecular electrostatic interaction, stabilizing with each acylation as the repulsion between the negatively charged protein and negatively charged SDS increased; (iii) intramolecular hydrophobic interaction, destabilizing with each acylation, as the hydrophobic surface area that is exposed to solvent increased; and (iv) intermolecular hydrophobic interaction, destabilizing with each acylation, as the interaction between the additional hydrophobic groups on the protein and the hydrophobic tail of SDS increased. The model indicated that, for the acetyl ladder, the electrostatic contributions to $\Delta\Delta G^\ddagger$ were much larger than the hydrophobic contributions, while for the latter rungs of the hexanoyl ladder, the hydrophobic and electrostatic components were similar in magnitude. The study was one of the few to separate the effects of charge and hydrophobicity in interactions of proteins and surfactants. BCA II was an excellent model for this study because (i) both acetyl and hexanoyl ladders could be generated in full and resolved by CE, (ii) all acylated derivatives remained stable at room temperature in the absence of the denaturant, and (iii) the rates of denaturation were sufficiently slow that they could be measured by CE.

14.6. Perfunctionalized Proteins

The charge-modified derivatives of proteins clearly exhibit different behavior than the unmodified proteins in terms of stability to denaturants and affinity for ligands. To be able to explore further the effects of surface and charge modifications, a procedure for the perfunctionalization of proteins is necessary. The ability to make just a single derivative of a protein, instead of a multitude of derivatives in a charge ladder, would allow the use of analytical methods other than CE to study the properties of these derivatives.

Yang et al. reported conditions to perfunctionalize the amino groups of three proteins (ubiquitin, lysozyme, and BCA II) with five different modifying agents (acetate, triethylene glycol carboxylate, benzoate, glutarate, and fluoropropionate).⁶⁵⁹ Denaturing the protein prior to the reaction reduced the amount of reagent required for perfunctionalization, presumably because denaturation rendered all amino groups accessible to the reagents. It is, however, possible to perfunctionalize proteins in a folded state, if the groups of interest are solvent-accessible.

Whitesides and co-workers explored the effects of surface charges on the properties of BCA II by comparing it to its peracetylated derivative.^{652,660} Peracetylated BCA II is a highly charged derivative of BCA II and is more negatively charged than native BCA II by ~ 16 units of charge (peracetylated BCA II has a net charge of approximately -19

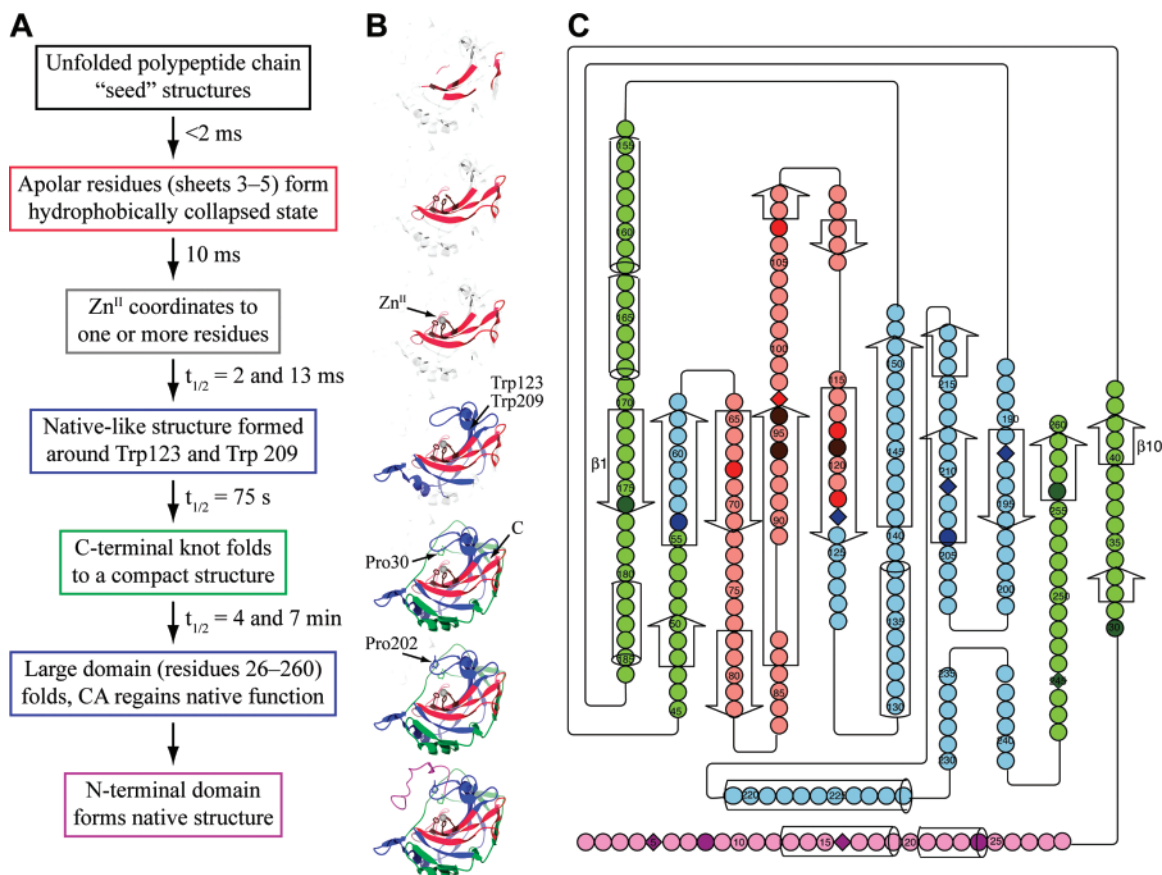


Figure 32. (A) Schematic of the pathway for the refolding of HCA II that has been denatured with GuHCl. (B) Three-dimensional representations of each intermediate in the refolding pathway outlined in (A). Unfolded sections of the enzyme are depicted as transparent ribbon structures superimposed on the already folded (colored) ribbon structures. The colors for each folded intermediate correspond to the colors used in part (C). (C) A two-dimensional representation of HCA I. The ten β -strands comprising the central β -sheet structure are numbered from left to right. Trp residues are displayed as diamonds. Darkly colored residues have been probed directly (see text) either by solvent accessibility, fluorescence quenching, or NMR. Lightly colored residues have not been probed directly, but their properties are inferred from neighboring residues. Red-colored residues retain structure at 8 M GuHCl. The brown residues are the His residues that chelate the Zn^{II} cofactor. The blue residues have structure in the molten-globule intermediate but are denatured at concentrations of GuHCl greater than 1.5 M. The green residues are required to have their native conformation before enzymatic activity is observed but are denatured in the molten-globule intermediate. The N-terminus is colored magenta; it folds after enzymatic activity is regained in the folding pathway. Adapted with permission from ref 693. Copyright 2003 American Chemical Society.

based on Debye–Hückel calculation).⁶⁵² Interestingly, peracetylated BCA II is stable at room temperature, can bind inhibitors, and possesses similar esterase activity to native BCA II.⁶⁵² It is, however, less stable to urea, guanidinium chloride, and heat than BCA II, but more kinetically stable to SDS,⁶⁶⁰ emphasizing the importance of electrostatic interactions in the stability of proteins. Gudiksen et al. utilized peracetylated BCA II in a study of the effects of surface charge on the ability of BCA II to fold into an active conformation; these results are discussed in section 15.3.4.⁶⁵²

14.7. Conclusions

CA II (bovine or human) has been the workhorse in the development of protein charge ladders. The absence of interactions of CA II with the capillary walls made the CE-based analysis of charge ladders of BCA II and HCA II particularly straightforward. The availability of multiple ligands (charged and uncharged) allowed for studies on the effects of net charge on the binding of ligands. These studies have raised, but not yet entirely settled, a number of issues in the understanding of electrostatic interactions in proteins. One observation is the presence of cooperative behavior in the ionization of residues upon acetylation.^{640,648} Another is the ability to modulate the binding affinities of charged

ligands by long-range electrostatic interactions, rather than by local modifications in the binding site.^{396,653} In addition, protein charge ladders provide a method to determine the net charge and hydrodynamic radius of proteins in one experiment;⁶⁴⁵ these properties may prove to be useful in predicting conditions a priori for the separation of proteins.

15. CA as a Model Protein for Studying the Denaturation and Renaturation of Proteins

15.1. Overview

Detailed studies of denaturation and folding of CA (HCA I, HCA II, and BCA II) have helped to understand its folding pathway, the relation between its structure and stability, and the general subject of protein folding (Figure 32). CA exhibits features typical of the folding of many proteins:^{661–673}

- (1) Denatured CA has residual structure, even at high concentrations of denaturants, that may template and direct the folding process.^{672,674–679}
- (2) CA forms a stable molten-globule intermediate in the folding pathway.^{665,678}
- (3) Proline isomerization is the rate-limiting step in the folding of CA.^{667,680–684}

(4) After denaturation with urea, guanidinium hydrochloride (GuHCl), heat, or SDS, CA renatures spontaneously after removal of the denaturant. The primary sequence thus contains all of the information needed for folding, and chaperones or post-translational modifications are not *required* for correct folding.^{673,685}

(5) CA interacts with chaperonins and, thus, provides a model system for studying the differences between assisted and unassisted folding.^{686–691}

(6) BCA II has no cysteines and cannot form disulfide bonds. Disulfide bonds can complicate the analysis of protein folding and contribute to aggregation.⁶⁹²

CA has three uncommon structural characteristics that are relevant to folding:

(1) A 10-stranded β -sheet spans the entire width of the protein (Figure 32C⁶⁹³). The details of folding pathways and intermediates for proteins composed predominantly of β -sheets have surfaced only in the last two decades, and CA (HCA II) has played a central role in these studies.⁶⁶¹

(2) CA has a very unusual C-terminal knot—that is, if CA were to be held at both ends and the ends were pulled, a knot would appear close to the C-terminus (Figure 2).^{152,694} Protein knots of this sort are known to occur in only four other proteins.^{695,696}

(3) CA has a strongly bound zinc ion, and the zinc-binding site could, in principle, nucleate or template folding.

Early work on denaturing different isoforms of CA demonstrated that HCA I is more stable than HCA II and that unfolding for all three isoforms (HCA I, HCA II, and BCA II) proceeds via intermediates in solutions of guanidinium chloride (GuHCl). In 1982, Henkens et al. identified and characterized a stable, partially folded intermediate,⁶⁷⁸ later identified as an inactive molten globule with native-like compactness, but with fluctuating tertiary structure.⁶⁶⁵ Multiple kinetic intermediates have been identified in the folding pathway of CA from GuHCl, with time scales of formation ranging from 2 ms to \sim 10 min. CA has since become a “classic protein”—that is, a model—for studies of denaturation by various denaturants and of folding of these denatured states. At this time, many of the intricate details of its denaturation by and folding pathway from guanidine chloride (GuHCl) and urea have been carefully elucidated,⁶⁶² while the details of unfolding and folding in the presence of other common denaturants (e.g., pH, heat, and sodium dodecyl sulfate) remain less clear. We first summarize the work on denaturation and folding of CA from GuHCl (Figure 32 parts A and B), then review the behavior of CA in other denaturants, and conclude with lessons on protein aggregation and its prevention, learned from the work with CA.

15.2. Pathway for Refolding of CA after Denaturation by Guanidine

15.2.1. Seeds for Protein Folding

The Levinthal paradox states that, if a protein randomly searches all possible conformations, it would not be able to fold properly within the age of the universe.^{697,698} To reduce the number of structures searched by the protein, Levinthal reasoned that one or more nucleation sites must exist that direct the folding and limit the number of structures sampled. Anfinsen, in his Nobel Prize acceptance speech, stated, “it seems reasonable to suggest that portions of a protein chain that can serve as nucleation sites for folding will be those

that can flicker in and out of the conformation that they occupy in the final protein.”⁶⁹⁹

The nucleation sites, now often called “seeds”, to which Anfinsen referred, may initiate folding by exchanging between random coil and ordered states. Seeds have been identified experimentally in many proteins.^{664,679,700} Not surprisingly, seeds typically comprise hydrophobic amino acids and retain their clustered state in the native protein. Seeds can stabilize long-range interactions that restrict the conformational space accessible to the protein, essentially decreasing the entropy of the unfolded state.⁶⁷⁹ Experiments with CA support the theory of seeds in protein folding and validate CA as a model for studying the influence of perturbations in the nucleation site on folding (Figure 32 parts A and B).

To confirm the presence of a seed in the denatured state of HCA II, Henkens and Oleksiak mutated Trp97 to Arg and denatured this mutant in 6.2 M GuHCl. They observed that the NMR resonances of five different His residues (presumably His94, 96, 107, 119, and 122) of the Trp97Arg mutant were shifted from those of denatured wild-type HCA II protein.⁶⁷⁷ The fact that a single mutation affects the conformation of multiple amino acid residues in an unfolded protein implies that residual structure is present in this region of the chain—the central β -strands.

In order to explore the structural features of denatured and intermediate states in folding, Carlsson et al. used site-directed mutagenesis to introduce labels into HCA II.⁷⁰¹ They made a Cys206Ser mutant of HCA II to remove the only native thiol group and introduced Cys residues into the hydrophobic core of HCA II by additional mutagenesis. By attaching spectroscopic probes (spin-labels or fluorescent labels) to these engineered Cys residues, or by measuring their chemical reactivity, Carlsson and co-workers studied solvent accessibility and local structure. Their work showed that many of the central β -strands (specifically β -strands 3 and 4) in the HCA II structure remained folded as the concentration of GuHCl was increased even up to the solubility limit of GuHCl (\sim 6 M).^{672,676}

The earliest event in the folding of CA involves the contraction of the hydrophobic core, β -strands 3–5 (Figure 32); this step can be followed by tryptophan (Trp) fluorescence. Trp fluorescence provides another sensitive probe of tertiary structure (section 8.3.1).⁷⁰² CA has six highly conserved Trp residues, and HCA II and BCA II have one additional Trp residue (Table 2). When HCA II that has been denatured with 6 M GuHCl is renatured by rapid dilution, its Trp fluorescence (believed to originate primarily from Trp97 in β -strand 4) increases rapidly in a burst lasting $<$ 2 ms and then plateaus at the fluorescence of the native protein.⁷⁰² Jonasson et al. believe that a hydrophobic collapse of the nonpolar residues surrounding Trp97, as the protein refolds, caused the observed increase in fluorescence. The rapid increase in fluorescence to a plateau does not require formation of a rigid hydrophobic structure but rather requires exclusion of water from near the center β -strands.⁶⁷⁵ The excluded water is a common feature of folding intermediates, especially of the molten globule.⁶⁷⁰ We discuss the details of the molten-globule intermediate in section 15.2.3.

These experiments suggest that the region of CA seeding the folding pathway is a cluster of hydrophobic amino acids located on the β -strands 3–5. This hydrophobic core of the protein adopts a native-like antiparallel β -sheet structure very rapidly and directs the rest of the folding pathway.

15.2.2. Metal Cofactor

An interesting question that can be addressed using CA is that of the role of metal cofactors in folding of proteins. The Zn^{II} ion in CA is coordinated to three His residues in β -strands 3 and 4 in the hydrophobic core of the protein (Figure 32; see section 4.6). The Zn^{II} ion influences the kinetics of folding after denaturation with GuHCl, although it does not affect the final conformational state of the folded protein.^{678,685,703} Yazgan and Henkens showed that folding is rapid (<10 min) in the presence of Zn^{II}; in its absence, or if it is added after the hydrophobic core has formed in the refolding process, folding required approximately twice as long to complete.⁶⁸⁵ Renaturation through a long-lived intermediate (a molten globule; see section 15.2.3) occurred in both the presence and absence of Zn^{II}.⁶⁸⁵ In addition to promoting folding to an intermediate state, the metal cofactor facilitates folding to the native enzyme.^{678,704}

Cobalt can replace Zn^{II} in the active site of CA without major structural changes or significant loss of activity (see section 5). Co^{II} can be observed directly by absorption (at 550 nm) or indirectly by fluorescence (it quenches the fluorescence of Trp residues of CA)⁷⁰² and, thus, can convey information on conformational changes occurring near the binding site of the metal ion during refolding (see section 8.3).

The absorption spectrum of the Co^{II} ion shows when the protein coordinates it during refolding. At concentrations of GuHCl greater than 1.5 M, Carlsson and co-workers could not observe absorbance by Co^{II}; this observation suggests that the compact metal-binding site is lost.^{704,705} Upon denaturing with GuHCl, the Zn^{II} ion may either remain loosely coordinated to the unfolded enzyme—possibly by remaining chelated to His 93 and 95—or bind the unfolded polypeptide during the early stages of protein folding. Gudiksen et al. have shown that denaturation of BCA II with sodium dodecyl sulfate (SDS) and subsequent renaturation in Zn^{II}-free buffer yields *apo*-BCA II.⁷⁰⁶ This result suggests that Zn^{II} is not bound to the denatured protein with high affinity and is not necessary for successful renaturation.

It is, however, possible to induce refolding of the molten-globule form of the apoenzyme simply by adding Zn^{II}. At 1.2 M GuHCl, Andersson et al. observed the apoenzyme in its molten-globule state, but upon addition of an equimolar (8.5 μ M) amount of ZnSO₄, the protein rapidly folded to its native state.⁷⁰⁴ Metal (Zn^{II} or Co^{II}) cofactor-induced refolding took place in three steps:

- (1) The metal ion bound to the molten globule. If Zn^{II} was added during the early stages of refolding the denatured Co^{II}–BCA II, most of the protein refolded into a Co^{II}–BCA II form—that is, Zn^{II} did not replace the Co^{II} ion.

- (2) The protein region surrounding the metal ion compacted, as measured by Trp quenching or visible absorption by Co^{II}. The absorption spectrum of the refolded protein was identical with that of the native protein; this observation demonstrates that Co^{II} has been bound tetrahedrally (as it is in the native structure).⁷⁰⁷

- (3) A functioning active center formed, as measured by enzyme activity. Although the high-affinity metal-binding site formed within 10 s of initiating folding, the *active* enzyme formed with a half-time of 9 min.

When Zn^{II} was used instead of Co^{II} during refolding, Andersson et al. observed similar rate constants for folding for the Zn^{II}-containing BCA II and the Co^{II}-containing BCA II. Zinc does not, however, have an observable absorbance,

nor does it quench tryptophan fluorescence. Therefore, the investigators could not measure binding of Zn^{II} directly; they could measure only the rate at which the activity returned.⁷⁰⁴

The Zn^{II} ion also affects the stability of the folded protein. The transition from the intermediate state to the unfolded state occurs at higher concentrations of GuHCl for the holoenzyme than for the apoenzyme; the holoenzyme is, thus, substantially more thermodynamically stable to denaturation than the apoenzyme.⁷⁰⁴ A curve of circular dichroism (CD; see section 8.3.6) ellipticity versus concentration of GuHCl can be analyzed to determine the concentration at which half of the enzyme is denatured (C_m). For the holoenzyme, C_m is ~ 1.7 M GuHCl; for the apoenzyme, C_m is ~ 1.0 M GuHCl.⁷⁰⁴ The relative stability of the enzyme toward unfolding has been reported by Henkens et al. to be as follows: Zn^{II}–BCA > Co^{II}–BCA > apoenzyme.⁶⁷⁸ This stability is apparent in both stages of unfolding—unfolding from the native state to the intermediate and from the intermediate to the fully denatured state.

Sulfonamide ligands, bound to the metal cofactor in the active site of the enzyme, can further stabilize the enzyme against denaturation.⁷⁰⁸ Almstedt et al. noticed an increase in the C_m for the unfolding of HCA II from its native state to the intermediate state in the presence of 10 μ M acetazolamide ($K_1 = 7.5$ nM); unfolding appeared to become a two-state process with a combined C_m of 1.42 M GuHCl for the unfolding from the native to the unfolded state (without acetazolamide, $C_m = 1.05$ M GuHCl for the unfolding from the native state to the intermediate and ~ 1.6 M GuHCl for the unfolding from the intermediate to the fully denatured state).

15.2.3. Molten Globule

Molten globules are common intermediate states in the protein folding process, both as stable equilibrium intermediates and as transient kinetic intermediates during the refolding process.^{709,671} Ohgushi and Wada coined the term “molten globule” in 1983.⁷⁰⁹ “Molten” refers to structural fluctuations, particularly by side chains; “globule” denotes the native-like structural compactness. The molten-globule state is characterized by four key features: (i) little or no tertiary structure, (ii) significant secondary structure, (iii) significantly more hydrophobic surface exposed to water than for the native state, and (iv) compactness (i.e., size) closer to the native state than to the unfolded state.⁷¹⁰ We discuss only aspects of the molten-globule intermediates relevant to the use of CA as a model protein for studies of folding. The importance of the molten globule in protein folding has been examined extensively elsewhere.⁷¹⁰(and references therein),711–715

BCA II forms a molten globule during refolding both in equilibrium denaturation⁶⁷⁸ and transiently during refolding (Figure 32 parts A and B).⁶⁶⁵ Henkens et al. and Dolgikh et al. observed a stable intermediate with all of the characteristics of a molten globule between concentrations of GuHCl of 1 and 2 M.^{665,678} Jagannadham and Balasubramanian identified a similar intermediate in refolding experiments with both HCA I and HCA II.⁷¹⁶ All four of the characteristics of a molten globule were observed in the refolding of CA.

15.2.3.1. Lack of Tertiary Structure.

The simplest measure of tertiary structure—enzyme activity—shows that the molten globule has no activity and, therefore, does not have native structure at the active site.⁶⁶⁵ Further evidence of the lack of tertiary structure comes from studies of absorbance and fluorescence of Trp residues. The lack of

absorbance at 292 nm for HCA II found by Mårtensson et al., and by Yazgan and Henkens, demonstrates that Trp residues are buried in the molten-globule structure.^{676,685} Henkens et al. found that the fluorescence depolarization for BCA was low in both the native and molten-globule states, a result that suggests that the Trp residues were relatively immobilized in both states.⁶⁷⁸ Furthermore, the emission wavelength of the molten-globule state was red-shifted (by 3 nm) as compared to the native state; this result reveals that Trp residues in the molten-globule state experience a less hydrophobic environment than in the native protein. Taken together, these results suggest that the environment surrounding Trp in the molten globule is compact (similar to the native state), but that the tertiary structure of the native state has not yet formed.

15.2.3.2. Significant Secondary Structure. CD is a commonly used technique for monitoring changes in the secondary and tertiary structures of proteins.⁷¹⁷ CD spectra of proteins are divided into two regions: the far-UV (190–250 nm) and the near-UV (250–300 nm). The far-UV region measures secondary structure; the near-UV region measures tertiary structure.⁷¹⁸ If a protein retains secondary structure without a well-defined, three-dimensional structure (as expected for a molten globule), the CD in the near-UV will be nearly zero, while the CD in the far-UV will have some features of the native protein.^{429,719}

The molten globule of HCA II has virtually no CD absorbance in the near-UV region.⁶⁷⁶ The absence of a near-UV CD spectrum suggests that, in the molten-globule state, the aromatic residues are in symmetric environments and, thus, do not contribute to the far-UV CD spectra. A standard analysis of secondary structure, therefore, can be used to study the molten-globule intermediate without complications arising from Trp residues. Borén et al. and Mårtensson et al. observed that the negative ellipticity measured in the far-UV was larger for the intermediate than for the native state of BCA II and HCA II, respectively; they interpreted this increase as being due to loss of interference from aromatic side chains in the symmetric environment of a molten globule.^{676,720} The large negative ellipticity indicates the presence of extensive β -structure in the molten globule. When the concentration of GuHCl increased, CA II denatured further, and the negative ellipticity decreased.^{676,720}

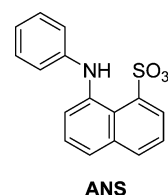
Jonasson et al. used site-directed mutagenesis to remove systematically Trp residues from the Cys206Ser mutant of HCA II in order to identify their individual contributions to fluorescence.⁶⁷⁵ They denatured the protein and observed refolding by monitoring the fluorescence of the Trp residues. They observed the return to native-like fluorescence intensity of Trp123, 192, 209 and 245 in two kinetic phases, with $t_{1/2} = 2$ and 13 s.⁶⁷⁵ All of these residues are on the edges of the hydrophobic core formed by β -sheets (5, 7, 8, and 9; Figure 32C) that penetrate the center of the enzyme, and the similar folding rates for these residues suggest the same rate-limiting step. This observation also implies that the native-like structure around these Trp residues occurs prior to the onset of enzymatic activity.

Although the spectral properties of Trp demonstrate that the fluorescence intensity and depolarization of the molten globule are native-like, the fluorescence wavelength and CD spectrum of the molten globule do not match those of the native protein. These results suggest that, in the molten-globule state, CA is compact and the Trp residues are immobilized but that the exact environment—the hydropho-

bicity in particular (as measured by fluorescence)—is different in the native and molten-globule states.

Freskgård et al. used site-directed mutagenesis of HCA II (in procedures similar to those described in section 15.2.1) to measure the solvent accessibility of Ser56 and Ile256, which are located in the outer β -strands (strands 1 and 10; Figure 32C).⁶⁹⁴ These residues have native-like structure in the molten-globule state at concentrations of GuHCl of 1–2 M, but they become fully exposed at higher concentrations of denaturant. Carlsson et al. found that Cys206 becomes inaccessible to labeling reagents within 0.1 s of renaturation; this finding indicates that β -strands 6 and 7 adopt a compact structure very early in the folding pathway.⁷⁰¹

15.2.3.3. Exposure of Hydrophobic Surface Area. ANS (1-anilinonaphthalene-8-sulfonate) binds tightly to hydrophobic cavities and surfaces but weakly to individual hydrophobic residues in a denatured polypeptide chain.⁷²¹



Fluorescence of ANS is a sensitive measure of the presence of hydrophobic surfaces and cavities (the quantum yield is 0.004 in water and increases to ~ 0.8 when bound to hydrophobic surfaces⁷²²). ANS binds strongly to BCA II in the molten-globule state with a fluorescence intensity that is much greater and more blue-shifted than when it is bound to the native or denatured protein.^{671,723} By measuring both the intensity of electron spin resonance (ESR) signals of spin labels and the transfer of energy from Trp residues to a dansyl label, Semisotnov et al. established that the rate of increase of ANS fluorescence was similar to the rate of molecular compaction.⁷²⁴ Their result indicates that hydrophobic patches are formed concomitantly with an increase in compactness upon renaturation.

15.2.3.4. Compactness of the Molten Globule. Hammarström et al. examined the compactness of the molten globule by studying pyrene excimer fluorescence.⁶⁷⁴ If two pyrenyl groups are separated by only a few angstroms, they can form a collective electronic excited-state dimer (an excimer) upon excitation.⁷²⁵ Hammarström et al. labeled positions 67 and 206 (in β -strands 3 and 7) of HCA II with pyrene groups. These residues are located on the edges of the β -sheet structure that spans the center of the enzyme (Figure 32). The intensity of excimer fluorescence increased with increasing concentration of GuHCl (from 0 to 0.17 M), because of the increased mobility of pyrene moieties on denaturation. The fluorescence reached a plateau between 1.7 and 3 M GuHCl and decreased above 3 M GuHCl; this observation suggests that, at concentrations of GuHCl below 3 M, the enzyme remained compact.

NMR also can be used to measure the compactness of proteins. Kutysenko and co-workers introduced a rigidity parameter (G) as a measure of residual structure and compactness of a denatured or partially denatured protein.^{726,727} G is defined as the ratio between the intensities of the spin diffusion spectrum and the normal ^1H NMR spectrum in a given spectral region of a protein. The values of G for HCA II indicate that the compactness of the molten globule ($G = 0.53$) is extremely close to that of the native

state ($G = 0.55$) and significantly more compact than the denatured state ($G < 0.1$).

One of the more controversial aspects of the current understanding of the molten-globule state, and thus of the pathway for folding of proteins, is the extent to which water molecules are excluded from the hydrophobic core of the protein.⁷²⁸ Size-exclusion fast performance liquid chromatography (FPLC) has been used to measure the size of the molten-globule state and thereby to estimate the volume of associated water molecules. Uversky found that BCA II, at a concentration of $1 \mu\text{g mL}^{-1}$, had a diameter of 5.0 nm in its native state, 5.2 nm in the molten-globule state, and 10 nm in the completely unfolded state (in 6 M GuHCl).⁷²⁹ The sizes measured for the native and unfolded states match those measured by dynamic light scattering.⁶⁷³ The similarity in sizes of the native and molten-globule states of BCA II suggests that the penetration of water into the molten globule is minimal.

Relaxation dispersion measurements of ^{17}O by NMR are commonly used to monitor directly the buried water molecules (internal hydration states) and water molecules transiently associated with the surface (external hydration states) of proteins and their molten-globule states. Using HCA II as a model, Denisov et al. found that the native and molten-globule states had only small differences (within experimental error) in the number of both tightly and weakly bound water molecules.⁷³⁰ Their results suggest that, for HCA II, there is very little change in hydration between the native and molten-globule states.

This work appears to conflict with earlier data from Gast and co-workers and Kataoka and co-workers obtained by light scattering and calorimetry;^{731–734} they observed a 30% increase in the volume and a change in heat capacity^{735,736} when α -lactalbumin and apomyoglobin were denatured. It is still unclear which proteins have hydration states that are more representative of proteins as a class and what conclusions (if any) can be drawn about universal aspects of hydration in molten globules. It is also possible that the molten globule is a distribution of states and that the different experimental techniques measure the average distribution of conformations in different ways.⁷²⁸ For example, the measurements of hydrodynamic radius may weight the larger states more heavily, while the NMR relaxation data may weight the compact states with more tightly bound water molecules more heavily.

Molten-globule intermediates have been identified along the pathways of folding for dozens of proteins.^{671,710} Many of these proteins belong to different structural types (α , $\alpha + \beta$, α/β) and have rates of refolding that differ by > 1 order of magnitude; these results suggest that the molten globule is a common intermediate in protein folding.⁶⁷¹ The main difference between the native and molten-globule states is the disruption of the tightly packed hydrophobic interactions of side-chain residues that bind the structural units together.⁶⁷⁰

15.2.4. C-terminal Folding, the C-terminal Knot, and Refolding of the Active Site

15.2.4.1. C-terminal Folding. The C-terminal domain of CA forms a knotted structure (Figure 2).^{695,696} Beta-strand 9 crosses over strand 10 such that, if the polypeptide chain were pulled at each end, a knot would remain in the protein. Using solvent accessibility studies like those described in section 15.2.1, Freskgård et al. probed the kinetics of active site refolding around Ile256, located close to the C-terminus

in β -strand 9 (Figure 32C).⁶⁹⁴ They denatured the protein with 5 M GuHCl and renatured it by dilution into tris- SO_4 buffer. They observed that Ile256 settled into the hydrophobic core of the protein with a half-time of 75 s. Since this time is much longer than the time it takes to form the molten globule, they concluded that not all of the β -structure was formed in the molten-globule intermediate. Many have attributed the long half-time of folding to slow isomerization about Pro residues;^{681–684,737} Ile256 is located close to Pro30 and, thus, should be affected directly by its dynamics. Since enzymatic activity is regained ~ 8 min after initiation of refolding (by dilution), additional folding from the molten-globule intermediate must occur to regain activity. β -Strand 9, which contains Ile256, presumably cannot adopt its final conformation before β -strand 10 reaches a native-like state. If β -strand 9 adopted its native structure early in the folding process, β -strand 10 would need to thread itself through a small tunnel in order to reach its native conformation (Figure 32 parts A and B).⁶⁹⁴

Carlsson et al. digested HCA I with carboxypeptidase to investigate the effects of C-terminal residues on the activity and stability of the enzyme.⁷³⁸ HCA I retained $\sim 90\%$ of its activity when up to three C-terminal residues were digested by carboxypeptidase; its stability to denaturation by GuHCl was, however, significantly reduced. The concentration of GuHCl at which the protein sample retained half of its activity (C_m) decreased from ~ 1.5 M for the native protein to ~ 0.6 M for the HCA I lacking three C-terminal residues. These observations indicate that the C-terminal sequence involved in the knot topology contains information that is vital for the stability, but not the activity, of the protein.

15.2.4.2. Recovery of Enzymatic Activity. The kinetics of the refolding of BCA II have also been studied using Neoprontosil, a ligand whose wavelength of maximum absorbance shifts from 545 to 485 nm when bound to the enzyme.⁶⁶⁸ Ko et al. found that Neoprontosil increased the midpoint of denaturation (C_m) of BCA II from 1.5 to 2.2 M GuHCl and so appeared to stabilize BCA II toward denaturation. When BCA II was renatured after denaturation with GuHCl, Neoprontosil bound to BCA II ($K_d < 10 \mu\text{M}$) in the molten-globule state. As BCA II renatured further, a conformational change of the protein perturbed the visible absorption and CD spectrum of Neoprontosil; this change was concomitant with the return of enzymatic activity (as measured by the hydrolysis of *p*-nitrophenyl acetate).

Using measurements of protein absorbance and tryptophan fluorescence, Semisotnov et al. found that BCA II achieved its native, functional structure in two kinetic phases, with $t_{1/2} = 2$ min and 10 min.⁷³⁹ In the shorter kinetic phase, the hydrophobic clusters desolvated, and a native-like hydrophobic core formed. Henkens et al. determined that this native-like hydrophobic core did not have enzymatic activity.⁶⁷⁸

15.2.4.3. Isomerization of Pro Residues. Isomerization of Pro residues has been proposed as the rate-limiting step in the majority of slow-refolding reactions of proteins, including those of CA;^{681–684,737} this characteristic makes CA a good model system for studying the kinetics of slow-folding proteins. Two of the Pro residues in CA II (Pro30 and Pro202) are in the *cis* conformation in the native state.¹⁸⁶ (BCA II has one more *trans*-Pro residue than does HCA II.)⁷³⁹ The native conformations of Pro peptide bonds should persist when CA is rapidly denatured because the rate of *cis*–*trans* isomerization in Pro residues ($t_{1/2} \approx 30 \text{ s}^{-1}$) is slow

compared to the rate of denaturation of CA.⁷⁴⁰ In double-jump experiments, the protein is denatured rapidly with GuHCl and then renatured by dilution to low concentrations of GuHCl with variable delay times. If *cis*–*trans* isomerization is rate-determining, the protein should refold much faster when renatured soon after denaturing (with a short delay time)—that is, before the Pro bonds have time to randomize their orientation—than with a long delay time (relative to the isomerization time of Pro bonds) before initiation of refolding. CA shows this dependence on delay time. With no delay between denaturing and renaturing, Semisotnov et al. observed the half-time for BCA II reactivation to be only 3 s.⁷³⁹ Prolonged incubation (~1 h) of the protein in the unfolded state, however, increased the half-time of reactivation to 10 min.⁷⁴¹ Double-jump experiments demonstrate that both slow stages in refolding—corresponding to C-terminal and active-site refolding—are Pro-dependent processes.⁷³⁹

Proline isomerase (PPIase) catalyzes the *cis*–*trans* isomerization of Pro residues in proteins and, thus, should increase the rate of refolding of CA if *cis*–*trans* isomerization is rate-limiting. Consistent with this hypothesis, Fransson et al. observed that incorporating PPIase in the refolding reaction mixture of GuHCl-denatured HCA II decreased the half-time of folding from 9 to 4 min and removed the effect of time delay in refolding.⁶⁶⁷ Further, the addition of Cyclosporin A, a specific inhibitor of PPIase,⁷⁴² completely abolished the observed PPIase-mediated acceleration of folding. If PPIase acted efficiently on all peptidyl-Pro bonds, the expected half-time of refolding would decrease to 1 min. Because the effect was smaller than expected, Fransson et al. speculated that PPIase could only act on Pro residues that were exposed during the refolding process.

Fransson et al. further proposed that each of the two *cis*-Pro residues in CA was responsible for one of the two slow stages of refolding: Pro30 for C-terminal folding and Pro202 for forming the native conformation of the active site.⁶⁶⁷ To test this idea, they made two HCA II mutants that would not allow the presence of *cis* conformations—Pro30Asn and Pro202Asn. The Pro30 mutant was unstable—that is, it did not fold to a stable conformation that could be studied—but the Pro202Asn mutant was stable. The Pro202Asn mutant refolded with a half-time of 9 min, which is the same (within error) as the half-time for refolding of wild-type HCA II. Addition of PPIase to this mutant decreased the rate of refolding to a half-time of 4 min. These results suggest that the *cis*-peptidyl-Pro202 bond does not limit the refolding rate and that another Pro residue must be responsible. Pro181 and Pro 30 are the least accessible of the invariant Pro residues,^{54,184,186} and they are, therefore, most likely to direct the slowest step in refolding.

Kern et al. studied folding of HCA II after a short (10 s) incubation in 5 M GuHCl and observed that only a fraction (~55%) of the protein refolded rapidly, while the rest refolded with kinetics similar to those observed for HCA II that had undergone prolonged denaturation.⁷⁴³ Since the denaturation interval of 10 s was not long enough to allow prolines to isomerize to non-native state, the investigators suggested that isomerization occurs during renaturation, allowing for the formation of the molten-globule state with correct and incorrect conformation of Pro. Addition of PPIase to the refolding solution decreased the fraction of protein that folded with rapid kinetics. These observations are consistent with the role of PPIase as a catalyst that isomerizes

Pro residues (both to and from their conformations in the native protein) in the folding process.⁶⁸⁰

15.2.5. N-terminal Folding

The final stage of folding of CA involves the N-terminus (Figure 32 parts A and B).⁷⁴⁴ Because two Trp residues are located at the N-terminus (Trp5 and Trp16; Figure 32C), intrinsic fluorescence can be used as a probe of N-terminal structure. Aronsson et al. observed that removal of the five N-terminal residues from HCA II destabilized the native state by 4–5 kcal mol⁻¹ relative to the intermediate state. Deleting an additional 23 residues, which constitute nearly one-tenth of the protein and an entire hydrophobic cluster, from the N-terminus (Figure 32C, purple residues) caused no further destabilization. In addition, the molten-globule intermediate was not measurably destabilized relative to the unfolded state; this result suggests that there are no net stabilizing tertiary interactions between the N-terminus and the rest of the molecule in the intermediate state. Removing residues 1–24 had no effect on the kinetics of reactivation activity of HCA II (as measured by esterase activity or DNSA binding) but did affect the kinetics of fluorescence increase. Trp fluorescence of denatured HCA II increased with time in a biphasic manner with half-times of 4 and 17 min (this fluorescence intensity was due to Trp5 and Trp16), while that for the HCA II mutant lacking 17 residues at the N-terminus had reached a plateau within 30 s (the non-N-terminal Trp were in their folded states);⁷⁴⁴ the difference suggests that the N-terminus folds in the last steps of folding and only after an enzymatically active native-like structure forms in the rest of the protein.

15.3. Denaturing CA with Other Denaturants

15.3.1. Urea

Bushmarina et al. did not observe a molten-globule intermediate during the unfolding of BCA II by urea, unlike experiments carried out in GuHCl (see section 15.2.3).⁶⁶³ Between 0 and ~5.5 M urea, the protein remains in its native state. A further increase in the concentration of denaturant (from 5.5 to 6.5 M) caused the protein to unfold completely, as detected by a decrease in fluorescence anisotropy. The investigators used binding of ANS to BCA II to measure the formation of the molten-globule state during denaturation and did not observe binding of ANS to BCA II at concentrations of urea between 0 and 8 M.

In agreement with Bushmarina et al., Borén et al. found that denaturation of HCA II with urea was an apparent two-state unfolding, with no intermediate in the pathway of denaturation (as monitored by tryptophan fluorescence).⁷⁴⁵ The midpoint of denaturation occurred at 4.4 M urea. The red-shift in the tryptophan fluorescence matched that of the protein denatured in GuHCl and demonstrated that the unfolded state of HCA II in urea was similar to that in GuHCl. They did find, in contrast to the results of Bushmarina et al. on BCA II, that a small amount of ANS bound to HCA II at 4.5 M urea. The binding of ANS suggests that some HCA II has the conformation of a molten globule at 4.5 M urea.

Borén et al. hypothesized that the difference in denaturation between urea and GuHCl was due to the ionic character of GuHCl. In the presence of 1.5 M NaCl, the denaturation of HCA II showed two transitions and a stable intermediate (from 3.0 to 6.4 M urea).⁷⁴⁵ The absorbance signal due to

the binding of ANS to this intermediate in the denaturation of HCA II with urea is similar to that due to the binding of ANS to the molten-globule intermediate formed in the denaturation of HCA II with GuHCl. The investigators proposed that the high ionic strength of solutions of NaCl helps to weaken ionic interactions in the native state of HCA II and to destabilize the protein to denaturation with urea. This need to disrupt stabilizing ionic interactions in the enzyme is, we presume, the basis for the difference in denaturation between urea and GuHCl.

15.3.2. Acid

15.3.2.1. Overview. Unfolding in acidic conditions is often claimed to occur because the folded protein has groups buried in neutral form that can be protonated at low pH. The protonation in acid may also cause unfavorable electrostatic interactions between all the positively charged groups or break hydrogen bonds and thus induce denaturation of the protein. The basic groups believed to be important in denaturation in acid are often histidine residues ($pK_a \approx 6.5$).⁷⁴⁶

Acid denaturation often results in denatured states that are less unfolded than those obtained with GuHCl; these states often possess large amounts of residual structure, especially in the presence of salt.^{747,748} Addition of GuHCl to the acid-denatured proteins can further denature them.⁷⁴⁹ Incomplete denaturation may be due to electrostatic repulsion that fails to overcome hydrophobic forces, salt bridges, and other favorable interactions. For this reason, CA denatured by acid seems to be quite sensitive to the concentrations of salts and buffers.⁷⁵⁰

15.3.2.2. Denaturation of CA with Acid has Two Transitions. When the pH of a BCA II solution is decreased from 8 to 2, BCA II denatures in two distinct transitions, the first occurring between pH 4.3 and 3.8 and the second occurring between pH 3.5 and 2.8. In the first transition, there is a decrease in the bands in the CD spectrum of BCA II that correspond to aromatic residues (297, 286, and 270 nm).⁷⁵¹ The decrease in these bands suggests an increased mobility of the individual aromatic residues and, presumably, an increase in protein size, as solvent molecules penetrate to the core of the protein. The CD band corresponding to α -helical structure, however, *increases* upon lowering the pH from 4.3 to 3.8. According to Beychock et al., HCA (isozymes I and II) below pH 4 has an α -helical content of 20%.^{719,752} This value for α -helical content is much higher than that of the protein at pH 7 (but the exact value is difficult to obtain because the CD spectrum of CA at pH 7 is complicated by the large number of aromatic residues that give a CD signal in the far UV).

15.3.2.3. First Transition. During the first transition in the acid denaturation, the intrinsic viscosity (η) of solutions of BCA II increases slightly (from 3.0 to 4.1 cm³/g).⁷⁵¹ This increase suggests an increased size of the denatured protein relative to the native protein. Nilsson and Lindskog demonstrated that, near pH 4, the expansion of BCA II occurs simultaneously with the protonation of seven buried His residues.⁷⁵³ Because the Zn^{II} cofactor is coordinated by three His residues, it is not surprising there is no measurable enzymatic activity at pH 3.7.

The presence of the Zn^{II} ion does not change the pathway for protein denaturation in acid, as measured by CD and UV absorbance spectroscopy, presumably because the Zn^{II} cofactor is removed early in the denaturation pathway (when

the His residues are protonated).⁷⁰³ Zn^{II} cofactor also has only a minor influence on the stability of the protein toward denaturation with acid: the pH of the midpoint of the denaturation is 4.1 for *holo*-BCA II and 4.5 for *apo*-BCA II.

15.3.2.4. Second Transition. In the second transition (pH 3.5 to 2.8), Wong and Hamlin observed a significant increase in the intrinsic viscosity (η) of the solution of BCA II; this increase suggests significant protein denaturation.⁷⁵¹ Measurements of viscosity clearly indicate that, unlike the enzyme denatured in GuHCl or urea ($\eta = 29.6$ cm³/g),⁶⁷³ the acid-denatured enzyme at pH 2 ($\eta = 8.4$ cm³/g) is not a random coil (expected value of $\eta = 29$ cm³/g). The value of intrinsic viscosity implies only a partial unfolding of the protein, to a different state than the nearly random coil that is formed in urea or GuHCl.

In the second transition, Flanagan and Hesketh found the rate constant for denaturation of HCA I to be second order with respect to hydrogen ion concentration; this result indicates that at least two groups are protonated.⁷⁵⁴ The rate of unfolding strongly depended on the ionic strength: increasing the ionic strength by an order of magnitude caused the rate of unfolding to increase by approximately the same amount. Because the observed kinetics so strongly depends on the ionic strength, it is reasonable to conclude that unfolding involves the breaking of ionic bonds. The stability of HCA I (and HCA II) also depended on the ionic strength of the buffer; increasing the ionic strength from 0.05 to 0.15 increased the midpoint of denaturation by 0.5 units of pH.^{755,756} An increase in ionic strength shields electrostatic charges and destabilizes ionic bonds; it is likely that the denaturation of CA by acid involves the disruption of specific electrostatic interactions.

Bushmarina et al. monitored the anisotropy of fluorescence as a measure of the mobility of Trp residues in acid-denatured BCA II.⁶⁶³ The rotational relaxation time, defined as the time it takes for the polarization anisotropy to decay to zero, reflects both the size of the molecule (larger molecules rotate more slowly than smaller molecules) and the motion of the fluorophores relative to the protein. Bushmarina et al. measured rotational relaxation times of 34 ns for native BCA II and 70 ns for the pH 3.6 intermediate; the relaxation time for a rigid sphere with a radius of 4 nm is 46 ns. The relaxation time of native BCA II is only slightly less than that of a sphere. The increased relaxation time of Trp residues in the pH 3.6 intermediate—nearly twice as long as for a sphere—suggests that the protein aggregates, and possibly dimerizes, at this pH.

In the second transition, the molecule of BCA II unfolds to expose buried aromatic residues.⁷⁵¹ The absorption spectrum of BCA II continues to red-shift as the pH is lowered from 3.5 to 2.8, with the midpoint of the second transition at a pH of 3. Wong and Hamlin also reported a decrease in the intensity of the CD signal at 222 nm over this range of pH. The authors attributed this decrease to a loss of α -helical structure, but because of the difficulty in assigning this band,⁷¹⁹ the loss may also reflect other structural changes.

15.3.2.5. Precipitation after Denaturation with Acid. When BCA II was allowed to renature by increasing the pH, Wong and Hamlin found that the protein precipitated at pH 4.2 and remained insoluble at pH 8.⁷⁵¹ Only ~25% of the enzymatic activity could be recovered when the protein was kept at pH 2.2 for 30 min and then returned to pH 7.

Measurements of UV-absorption of BCA II at 290 nm during the back-titration of the enzyme from pH 2.0 to 3.7 did not match those measured as the protein was denatured. Evidence suggests that CA aggregates and precipitates upon raising the pH after denaturation in acid.^{663,751,755,756} McCoy and Wong recovered ~85% of the enzymatic activity of BCA II after denaturation with acid if they added 6 M GuHCl to the protein at low pH and subsequently renatured by dialysis against buffer at pH 7 with no denaturant.⁷⁵⁷ It is clear that, because more of the protein aggregates than refolds, denaturing CA with acid is an irreversible process.

15.3.3. Heat

Relatively small changes in temperature can cause large changes in the conformation of a protein and lead to denaturation or intermolecular aggregation. These processes are usually highly cooperative; the temperature at which the protein undergoes major structural changes is its melting temperature.⁷⁴⁶

McCoy and Wong showed that BCA II precipitated out of water or tris buffer (0.09 M, pH 7.5) at 65 °C and remained as a precipitate, even upon further heating to 95 °C.⁷⁵⁷ Precipitation, which is probably due to the aggregation of the enzyme as hydrophobic patches are exposed, makes spectroscopic investigation under thermal denaturing conditions impossible. Therefore, studies of thermal denaturation require a technique that is effectively independent of the state of aggregation of the protein.

Bull and Breese developed a method that measures only changes in pH in an unbuffered solution of a protein as a function of temperature ($\Delta\text{pH}/\Delta T$) and is not affected by aggregation.⁷⁵⁸ The values of $\text{p}K_a$ for the side chains of amino acids in a native protein are often different from those of the free amino acids. On denaturation, amino acids become exposed to solvent, and the values of $\text{p}K_a$ of these residues change to values closer to those for the free amino acids. This change in values of $\text{p}K_a$ causes a net uptake or release of protons that can cause a measurable change of pH in an unbuffered solution. A plot of ΔpH versus ΔT typically has a sharp maximum at the melting temperature.

McCoy and Wong investigated the unfolding of BCA II from 25 to 85 °C.⁷⁵⁷ They observed that the pH of the solution slightly decreased from 25 to 55 °C. Near 60 °C, the pH increased abruptly, with a midpoint (and, therefore, a melting temperature, T_m) of 64.3 °C.⁷⁵⁷ The agreement between the melting temperature and the temperature at which BCA II precipitated suggests that precipitation is indeed due to the temperature-induced unfolding.

Almstedt et al. measured the value of T_m for HCA II by enzymatic activity (CO_2 hydration), Trp fluorescence, near-UV CD spectroscopy, and 1D-NMR.⁷⁰⁸ The melting temperature of HCA II was similar to that of BCA II (T_m of HCA II = 55–61 °C). Interestingly, whereas HCA II denatures in GuHCl from its native to its unfolded state by way of an intermediate (a molten globule), thermal denaturation of HCA II stops at this molten-globule state.^{676,708}

Lavecchia and Zugaro found the temperature at which the catalytic activity of BCA was lost to be very similar to the measured melting temperature.⁷⁵⁹ Changes in catalytic activity may reflect changes in the local structure of the active site, where a small change in conformation near the active site can cause complete loss of catalytic activity. The similarity in critical temperatures determined from studies of the loss of catalytic activity and of melting suggests that

the loss of activity is a consequence of conformational changes that affect the entire protein, rather than just the residues near the active site.

15.3.4. Sodium Dodecyl Sulfate (SDS)

Denaturation of proteins by surfactants is a complex subject in which the mechanism of unfolding and the structure of the final protein–surfactant complex are unknown. Interactions of CA with detergents have not been studied extensively, although in recent studies, Whitesides and co-workers^{652,657,706,760,761} used BCA II as a model protein to clarify the effects of electrostatic interactions in denaturation and renaturation of BCA II in SDS.

Some of the existing studies on denaturation and renaturation of CA by SDS are not consistent. In particular, McCoy and Wong⁷⁵⁷ and Whitesides and co-workers,^{652,706,760} reported significant differences in the yield of BCA II after refolding. Furthermore, because the two research groups used different techniques, it is unclear if the two studies are in agreement in other findings (e.g., Whitesides and co-workers did not observe the two different conformations observed by McCoy and Wong). Other studies of CA with surfactants or small hydrophobic molecules have focused on the effects of these molecules on the aggregation of CA and are reviewed in section 15.4.

Early studies of proteins denatured with SDS suggested that two distinct conformations exist in solutions containing low (0.025%) and high (0.1%) (w/v) concentrations of SDS (referred to as the low- and high-binding states, respectively),^{762,763} and that both are enzymatically inactive.⁷⁵⁷ CD studies indicated that both the high- and low-binding states have conformations that are different from either the native enzyme or the denatured state with GuHCl. The far-UV CD spectra of both the high- and low-binding states have a strong band with two minima at about 222 and 208 nm; this shape is typical for proteins with a large amount of α -helical structure^{764,765} and suggests that the SDS·BCA complex is stable and has more secondary structure than the state formed after denaturing with urea or GuHCl.

In the low-binding state (0.025% SDS), residual native-like character is still observed by near-UV CD spectroscopy.⁷⁵⁷ The near-UV CD spectrum of the high-binding state (0.1% SDS) is very similar to that of the acid-denatured state of BCA II. Both the high- and low-binding states have considerable (~30%) α -helical character, although the high Trp content in CA may affect this calculation.⁷¹⁹

Measurements of intrinsic viscosity show relatively low viscosity for solutions of the low-binding state ($\eta = 8.1 \text{ cm}^3 \text{ g}^{-1}$), and high viscosity for the high-binding state ($\eta = 18.1 \text{ cm}^3 \text{ g}^{-1}$).⁷⁵⁷ These measurements suggest that the high-binding state is more similar to a random coil ($\eta = 29 \text{ cm}^3 \text{ g}^{-1}$) than to the native enzyme ($\eta = 3.7 \text{ cm}^3 \text{ g}^{-1}$), but that the high-binding state is not fully unfolded. The low-binding state appears to retain some of the compact features of the folded enzyme.

Gudiksen et al. investigated the role of the Zn^{II} cofactor in the renaturation of BCA II that had been denatured with SDS.⁷⁰⁶ BCA II was treated with a high concentration of SDS (10 mM) and subsequently dialyzed in SDS-free buffer to renature the protein. Native and denatured forms of BCA II were characterized by capillary electrophoresis, which could resolve both states. By refolding BCA II in the presence of EDTA (to chelate any free Zn^{II}), they demonstrated that the Zn^{II} cofactor was not required for refolding

into a native-like conformation. When 10 μM ZnSO_4 was added, the refolded enzyme regained full sulfonamide-binding activity. They also demonstrated that the Zn^{II} cofactor does not remain bound to the denatured protein. The presence of the Zn^{II} cofactor did, however, increase both the total amount of refolded protein by ~ 2 -fold and the rate of refolding by ~ 8 -fold. These results are consistent with those of Yazgan and Henkens (section 15.2.2), which demonstrated that the presence of Zn^{II} increased the rate of refolding after denaturation with GuHCl .⁶⁸⁵ The rate of refolding in the absence of Zn^{II} after denaturation, however, was approximately one-half as fast for protein that had been denatured with SDS as for protein that had been denatured with GuHCl .

Whitesides and co-workers also investigated the role of surface charges in the refolding of BCA II denatured with SDS.^{652,657} All 18 Lys groups on BCA II were acetylated to give peracetylated protein (BCA II– Ac_{18} ; see section 14).⁶⁵⁹ BCA II– Ac_{18} was denatured with SDS and then dialyzed in the presence of Zn^{II} to refold the protein. On dialysis, BCA II– Ac_{18} refolded to its starting, active conformation; refolding was evaluated by measuring its affinity to DNSA, CD spectrum, and the rate of enzymatic hydrolysis of *p*-nitrophenyl acetate. Interestingly, BCA II and BCA II– Ac_{18} refolded with similar rates (within a factor of 2) and yield from the SDS-denatured state. This study demonstrates that modifying the charge on the surface of BCA II does not affect the ability of the protein to refold. This work suggests that large changes in the charge on the surface of a protein—at least for BCA II—do not preclude its folding into the native structure and that folding is driven by hydrophobic collapse rather than by the exclusion of charges from the interior of the protein.

Gitlin et al. investigated the role of surface charges in determining the relative stability of BCA II to BCA II– Ac_{18} and found that BCA II– Ac_{18} was *more* stable to denaturation with SDS than native BCA II.⁷⁶⁰ They were unable to determine if the difference was simply kinetic or represented a difference in thermodynamic stability between the two proteins due to aggregation of BCA II in intermediate concentrations of SDS (that prevented the measurement of rates of folding and unfolding).

15.4. Recovery of Enzymatic Activity after Refolding

15.4.1. CA as a Model for Studying Aggregation

Preventing protein aggregation is a major problem in biotechnology, medicine, and proteomics. The deposition of protein aggregates is also associated with a number of human diseases, including Huntington's, Alzheimer's, and Parkinson's diseases.^{766–774} Proteins in their molten-globule form are considered to be particularly prone to aggregation,⁷⁷⁵ and crossed β -sheets (intermolecular β -sheets that are perpendicular to the fiber axis) are a common structural feature of such aggregates.^{776,777} The presence of a molten-globule intermediate, and the large number of β -strands, make CA an excellent model system for studying the aggregation of proteins. Protein aggregation was once regarded as a nonspecific process, but recent studies suggest that aggregation may be due to specific interactions between partially folded intermediates.^{641,776,778–780}

Intermolecular aggregation of CA is the main barrier to obtaining catalytically active, refolded protein after denaturation or after some types of purification. When BCA II

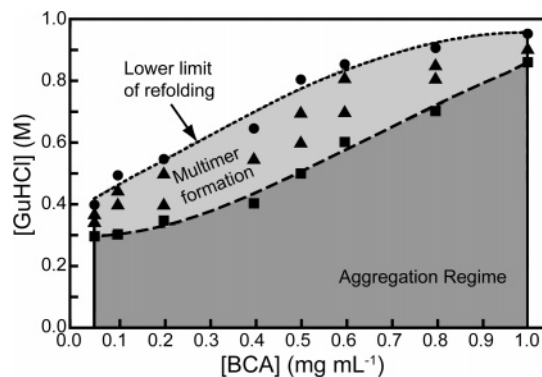


Figure 33. Regimes of refolding and aggregation of BCA II. Each datum represents rapid dilution of BCA II in 5 M GuHCl to a given final protein and GuHCl concentration. Conditions in the aggregation regime result in the immediate formation of micron-sized particulates. The upper boundary of the aggregation regime is defined by (■). Conditions in the multimer regime (▲) yielded measurable dimeric and trimeric species by CD before aggregation. The lower limit of refolding (●) is the regime where multimers form but do not proceed to form micron-sized particles. Adapted with permission from ref 781. Copyright 1990 American Chemical Society.

is renatured by increasing the pH from ~ 3 to 7, by cooling the protein to room temperature, or by removing detergent by dialysis, the majority of protein does not reform an active state in contrast to the high recovery for the renaturation of CA that had been denatured with GuHCl or urea, where activity could be regained nearly quantitatively (see sections 15.2 and 15.3.1). McCoy and Wong found that the refolding yield of acid-denatured or thermally denatured BCA II approached 99% when the denatured protein was treated with 6 M GuHCl and then dialyzed to remove the denaturant.⁷⁵⁷ McCoy and Wong renatured BCA II that had been denatured with 0.025% (w/v, 0.88 mM) SDS by dialysis and observed that $< 2\%$ of the activity was regained (as assayed by esterase hydrolysis).⁷⁵⁷ Gudiksen et al. demonstrated that BCA II could be renatured from 10 mM SDS by dialysis against tris-Glyc buffer (25 mM tris, 192 mM glycine), pH 8.4 in $\sim 80\%$ yield.⁷⁰⁶ The apparent discrepancy between the results of Gudiksen et al. and McCoy and Wong could be due to a difference in the experimental conditions used for renaturation: Gudiksen et al. used a lower concentration of protein than did McCoy and Wong, as well as a buffer of lower ionic strength, of different pH, and with additional Zn^{II} added. The difference in yield of refolded protein is possibly due to an increase in aggregation of the denatured protein under the conditions of McCoy and Wong relative to those of Gudiksen et al.

Cleland and Wang proposed that aggregation of CA (at least, that of BCA II) occurs primarily between molten-globule states and that denaturation with high concentrations of GuHCl breaks apart these aggregates and allows them to fold properly.⁷⁸¹ Experiments that measure the amount of properly refolded protein as a function of concentration of GuHCl support this hypothesis (Figure 33). A sample of BCA II denatured in 5 M GuHCl was renatured by diluting to a lower concentration of GuHCl . This study showed that, after dilution to a relatively low GuHCl concentration (0–1 M), a folding intermediate—presumably a molten globule—with a diameter slightly larger than that of the native BCA II formed within the dead time of the spectrometer.⁷⁸¹ At those concentrations of GuHCl , this molten globule aggregated either to micron-sized particles or remained as smaller

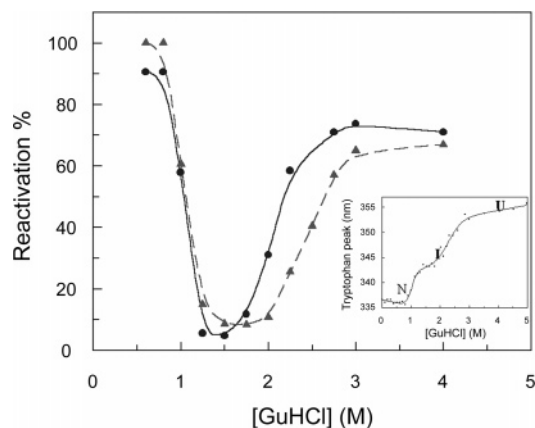


Figure 34. Yields of HCA II on refolding after denaturation with GuHCl. Reactivation of the enzyme was performed after incubation of protein for 24 h in the concentrations of GuHCl indicated on the *x*-axis. Refolding was induced by dilution of denatured enzyme to 0.3 M GuHCl in 0.1 M tris- H_2SO_4 , pH 7.5, and a final protein concentration of 0.85 μM . The enzyme activity was recorded after 2 h of refolding. The concentration of HCA II in the denaturation solution was 11 μM (●) and 22 μM (▲). The reactivation yields form a troughlike shape, implying that the amount of protein that can be reactivated decreases in parallel with the increase in concentration of molten globule. Inset: The curve showing unfolding of HCA II as measured by tryptophan fluorescence. The excitation wavelength was 295 nm, and the emission was recorded in the interval 310–450 nm using 5 nm slits for both excitation and emission light. The native protein (N) is observed from 0 to 1 M GuHCl, the molten-globule intermediate (I) is observed from ~1.5 to 2.5 M GuHCl, and the unfolded protein (U) is observed above 3 M GuHCl. Reproduced with permission from ref 783. Copyright 1999 American Society for Biochemistry and Molecular Biology.

aggregates (dimers and trimers), depending on the concentration of the protein (Figure 33). This study showed that high concentrations of GuHCl may keep hydrophobic clusters that are exposed to solution from aggregating.

Studies of refolding of BCA II by Wetlaufer and Xie⁷⁸² found that, in contrast to the results of Cleland and Wang,⁷⁸¹ the particle size and turbidity of the solution decreased over time after the solution of GuHCl-denatured BCA II was diluted below 1 M; this decrease in turbidity indicated that aggregates were dissociating and presumably refolding. In addition, Wetlaufer and Xie showed that ~60% of the original protein could be recovered in an active form within 150 min, even at protein concentrations as high as 4 mg mL^{-1} . They attributed the difference between the two studies to the presence of EDTA in the experiments of Cleland and Wang; the protein studied by them was, therefore, not *holo*-BCA II but rather a mixture of *holo*- and *apo*-BCA II. Gudiksen et al. have demonstrated that the recovery of protein was lower for *apo*-BCA II (35%) than for *holo*-BCA II (80%) when the protein was renatured after denaturation with SDS.⁷⁰⁶

Carlsson and co-workers examined the dependence of aggregation on the concentration of GuHCl used for denaturation.^{783,784} HCA II was treated for 24 h in concentrations of GuHCl ranging from 0.75 to 5 M. Refolding was induced by dilution of the denatured protein to 0.2 M GuHCl in 0.1 M tris buffer, pH 7.5, with a final protein concentration of 0.85 μM . Under these conditions, the native protein is the thermodynamically stable product. A plot of the percentage of active protein recovered versus the concentration of GuHCl used in the denaturation forms a troughlike curve (Figure 34). Yields of reactivation mirror the two stages of

unfolding (Figure 34 inset): (i) native protein to molten-globule intermediate and (ii) molten-globule intermediate to denatured chain. The width of the trough depends on the concentration of protein and indicates that aggregation is the cause of the low recoveries of active enzyme upon refolding.^{783,784} This observation suggests that the amount of protein active after refolding is lowest when starting from the molten globule.

Hammarström et al. used pyrene labels on Cys mutants of HCA II to probe the structure of the aggregated state after denaturation in GuHCl.⁷⁸³ Their method is very similar to that described in section 15.2.3; the major difference was that they used mutants labeled with only one pyrene. Consequently, only aggregated proteins showed excimer formation. They mapped the residues that were directly in contact in the aggregates using 20 different mutants. Only mutants with pyrenes in positions 97, 118, 123, 142, 150, and 206 showed excimer formation. These results demonstrate that the interactions of the aggregated species are highly specific and involve β -strands 4–7. They did not observe excimers in the unfolded or native states of HCA II, thus indicating that the native and denatured states do not form aggregates.

15.4.2. Preventing Aggregation

Because CA is a good model for studying the aggregation of proteins, it is also an excellent system for studying general methods of preventing aggregation of proteins. Karlsson et al. suppressed the aggregation of HCA II by stabilizing the native structure with an engineered disulfide bond.⁷⁸⁵ The Ala23Cys/Leu203Cys double mutant had an apparent two-state unfolding pathway, with no evidence of a molten-globule intermediate. This double mutant had a higher yield of refolded protein (95%) than did wild-type HCA II (75%), probably due to its reduced tendency to aggregate. In addition, the plot of the percentage of active protein recovered versus the concentration of GuHCl used in the denaturation—a plot similar in content to Figure 34—was relatively flat and did not display the pronounced minimum displayed by wild-type HCA II. These results demonstrate that stabilization of the native state of CA helps to avoid the aggregation trap (that is, the molten globule) in the folding landscape and allows CA to refold in high yield.

Wetlaufer and Xie used a variety of surfactants as passivating agents to suppress aggregation after denaturation by GuHCl.⁷⁸² The surfactant CHAPS, at concentrations above its critical micelle concentration (cmc), increased the yield of active, refolded protein from 37% to 81%; pentanol, hexanol, and cyclohexanol also increased the amount of active protein formed on refolding to >70%. The alcohols increased the recovery of BCA II when used at low concentrations (e.g., 1 hexanol molecule per 2–3 molecules of BCA II). These additives suppressed the initial formation of aggregates but were unable to dissolve preformed aggregates. Other additives, such as polyethylene glycol (PEG)⁷⁸⁶ and ANS,⁷⁸⁷ also prevented aggregation, presumably by associating weakly with hydrophobic patches of the intermediate in folding.⁷⁸⁷

Cleland and Randolph claimed that PEG inhibits aggregation by binding to the molten-globule intermediate based on experiments using a PEG-immobilized hydrophobic interaction column (HIC).⁷⁸⁸ The amount of BCA II bound to the column as a function of the concentration of GuHCl revealed a maximum at 2 M GuHCl. The peak in the binding curve

suggests that only the molten globule, and not native or denatured BCA II, binds to PEG.

Cleland et al. found that the maximum enhancement (a factor of 3) in the yield of refolded protein (as measured by enzymatic activity) occurred at a molar ratio ([PEG]/[BCA]) between 2 and 3.⁴²³ The best concentration of PEG for preventing aggregation of BCA II after denaturation with GuHCl depended on its molecular weight, but only PEG with a molecular weight between 1000 and 8000 effectively inhibited aggregation. Although PEG did not increase the rate of refolding, it prevented self-association and irreversible aggregation of BCA II (presumably by binding to the molten globule).

The role of additives other than PEG in preventing aggregation is much less clear, and it is currently impossible to predict whether a given additive will effectively reduce aggregation. Sharma and Sharma showed that cyclodextrins can prevent aggregation of BCA II;⁷⁸⁹ the cyclodextrins presumably have reversible, noncovalent interactions with some hydrophobic regions of the protein (aromatic side chains are plausible candidate sites) and thereby prevent intermolecular interactions. Karupiah and Sharma showed that cyclodextrin increased the yield of active BCA II after denaturation with GuHCl by nearly a factor of 3.⁷⁹⁰ The interactions of cyclodextrins with BCA II depended on the size of the cyclodextrins and on the substituents attached to the macrocycle.⁷⁸⁹ They found that, in general, the best aids for folding were neutral or cationic cyclodextrins with small cavities.

The “detergent-stripping method”, which is another method of preventing the aggregation of proteins, uses a detergent and a cyclodextrin in sequence.^{791,792} When BCA II was denatured by heat or GuHCl in the presence of detergent (e.g., SDS, cetyltrimethylammonium bromide (CTAB), or sodium tetradecyl sulfate (STS)), the detergent formed a complex with the denatured protein and prevented aggregation. These detergents prevented aggregation well below their values of cmc; this observation demonstrates that the protein was not simply dissolved in micelles but rather that it formed a detergent–protein complex. BCA II was unable to refold from the detergent-complexed state, but cyclodextrin could induce folding by stripping the detergent away from the protein. In this experiment, >80% of the protein could be recovered in an active form at protein concentrations of 0.03 mg/mL. A more water-soluble and less expensive, linear dextran could be used in place of cyclodextrin to remove detergent from HCA I.⁷⁹³

15.4.3. Chaperonin-Assisted Folding of CA

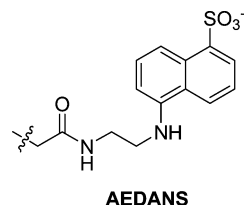
15.4.3.1. Overview. In living cells, a class of proteins known as “chaperonins” decreases the rate of aggregation of some unfolded proteins by encapsulating the protein while it folds;^{794,795} this process is believed to prevent the contact of hydrophobic patches on different proteins.⁷⁹⁶ Chaperonins may also catalyze the rate of folding for some proteins.^{797–799} The best studied of the chaperonins is the GroEL/ES complex from *E. coli*.⁸⁰⁰

15.4.3.2. Interaction of GroEL and GroEL/ES with CA. To determine if GroEL/ES interacted with HCA II in an unfolded or misfolded state, Persson et al. denatured HCA II with 5 M GuHCl and renatured the protein by dilution to 0.2 M GuHCl both in the presence and in the absence of GroEL/ES.⁶⁸⁸ The presence of GroEL/ES during refolding of HCA II after denaturation with GuHCl increased the yield

of active enzyme from ~70% to 100%. The time-course for reactivation was lengthened slightly ($t_{1/2} = 15$ min) when only GroEL was present, as compared to the time-course in the absence of chaperone ($t_{1/2} = 9$ min).⁶⁸⁸ If ATP was added in addition to the GroEL/ES complex when the protein was diluted to initiate refolding, the rate of folding matched that of unassisted folding, and the yield of folded protein was quantitative. Although HCA II interacted weakly with GroEL at room temperature, at elevated temperature, and at low concentrations of GuHCl, the amount of HCA II bound to GroEL increased significantly, presumably because GroEL bound only to the molten-globule intermediate.⁶⁸⁹

Landry and Gierasch proposed that the recognition motif for GroEL is a helical segment located at or near the N-terminus of the substrate.⁸⁰¹ Because CA contains two helical segments at the N-terminus (Figure 32), it is an ideal system for studying this hypothesis. Persson et al. found, however, that GroEL/ES was equally efficient at folding native HCA II and truncated mutants that were missing the helical segments.⁶⁸⁸ In the absence of chaperonin, truncated mutants of HCA II were no more likely to aggregate than was the native enzyme. They used EPR spectroscopy to study Cys mutants of HCA II with spin-labels attached to selected residues.⁶⁹¹ Spin-labels linked to interior portions of HCA II (residues 97, 123, and 206) were found to be immobile in the absence of GroEL. Upon binding to GroEL, however, isotopic line features appeared that indicated increased mobility. Increased mobility is of particular interest because this core of the protein (β -strands 2–6) does not denature at high concentrations of GuHCl and, thus, is identified as the site of specific interaction in studies of aggregation. These spin-labels are, however, more hindered than the peripheral spin-labels; this finding suggests that the hydrophobic core still exists but is loosened inside the GroEL cavity. Spin-labels linked to peripheral positions of HCA II, located on residues 16, 56, 176, and 245, showed substantial mobility in the absence of GroEL, but these labels were immobilized to varying degrees during interaction with the chaperone. Immobilization suggests that the periphery of the protein was constrained upon binding GroEL. These studies provide further evidence that, in addition to their ability to sequester proteins and prevent their aggregation, chaperone proteins loosen tightly folded hydrophobic regions that may be misfolded and aid in their refolding.

Using fluorescence resonance energy transfer (FRET), Hammarström et al. provided further evidence that the hydrophobic core of HCA II loosens upon interaction with GroEL.⁶⁸⁷ The investigators used the energy transfer from Trp residues to a Cys-bound fluorescent label (AEDANS) as a measure of the compactness of the protein. They showed that the volume of the molten globule was ~2.2-fold larger than the volume of the native enzyme. When bound to GroEL, the volume of HCA II increased further (~3–4-fold larger than the native enzyme); these measurements suggest that the molecule of HCA II is stretched inside the cavity of GroEL.



Hammarström et al. labeled two mutants of HCA II, Lys118Cys and Ile146Cys, with AEDANS in order to introduce a fluorescent probe in the central core of HCA II.⁶⁸⁷ They observed that the fluorescence emission spectrum was red-shifted in the presence of GroEL. This shift indicated that a more hydrophilic environment around these residues resulted from interaction with GroEL than in the isolated molten-globule state. The shift was quite large for this probe (10–15 nm) and suggested that GroEL extensively restructured the hydrophobic core.

The investigators also observed that GroEL underwent a large conformational change when bound to HCA II.⁶⁸⁶ At 50 °C, they observed that the fluorescence anisotropy of fluorescein-labeled GroEL increased in the presence of HCA II; this result suggests that a conformational change of GroEL accompanies its binding to HCA II. They also determined that the buried Cys residues of GroEL became accessible to solvent in the presence of HCA II, as measured by their rate of carboxymethylation. They suggested that the opening of the chaperonin caused the protein to be stretched and pulled apart.

15.4.3.3. Model for GroEL/GroES-Mediated Folding.

Despite a detailed understanding of the enzymology of the GroEL/GroES system, the underlying principles of chaperone-mediated protein folding remain a subject of debate.^{796,802–804} Several mechanisms have been proposed. The Anfinsen cage model states that GroEL and GroES provide a passive box in which folding can proceed unimpeded by intermolecular interactions; in essence, the GroEL/GroES complex behaves as a box of infinite dilution.^{805–807} The iterative annealing model asserts that GroEL binds to partially folded, but not yet aggregated, proteins and actively unfolds these intermediates. Upon release into solution, the protein is then allowed another chance to fold properly.^{808,809} The dynamic Anfinsen cage (DAC) model is somewhat of a compromise and suggests a dynamic interaction between GroEL and protein that leads to partial unfolding.⁸⁰⁴ The hydrophobic walls of GroEL bind to exposed hydrophobic surfaces of the misfolded or partially folded protein substrates. The binding of ATP to GroEL causes large conformational changes that “pull” on the hydrophobic surfaces of the protein substrate.⁸¹⁰ Cserrmely has suggested that chaperones work by loosening a core, hydrophobic portion of the protein, but not by unfolding the polypeptide chain.⁸¹¹ Loosening by this mechanism would allow water molecules to enter the hydrophobic core of the protein and cause a multidirectional expansion. The percolation of water into the core is a key step in chaperone activity.

Experiments investigating the interaction between HCA II and GroEL provide evidence for the chaperone percolation model, although the mechanism may differ for other proteins.⁷⁹⁶ The observed hydrophobic core of HCA II loosens, and an increase in hydrophilicity around these central residues strongly suggests the presence of water molecules in the hydrophobic core.⁶⁸⁷ The predicted, multidirectional expansion is observed by the 3–4-fold increase in the size of HCA II when GroEL binds and by the increase in size and flexibility of the GroEL molecule itself. With respect to these types of studies, CA is an ideal protein for testing specific predictions. In the presence or absence of GroEL, CA (at least HCA II) can fold; the ability to compare assisted and unassisted folding simplifies the analysis of changes in the folding pathway induced by the interactions with GroEL.

15.5. Conclusions from Studies on the Folding and Unfolding of CA

These studies demonstrate that CA is an excellent model for extracting general principles of protein folding. Its advantages are its availability, the ease with which it can be overexpressed in bacteria, the concomitant ability to make site-directed mutations, and the many aspects of its folding pathway that are prototypical in the folding of proteins. In addition to CA-specific information, studies of CA have led to a number of conclusions about protein folding:

(1) Proteins are not always random coils at high concentrations of denaturants. There may be residual structure in denatured states that act to seed the folding process.

(2) Molten globules can be stable intermediates, and investigation of the properties of these intermediates (i.e., the degree of hydration in the hydrophobic core) helps to understand the steps in protein folding.

(3) Proline isomerization can be the rate-limiting step in protein folding; the conformation of the chain may change both the rate at which the Pro bonds isomerize and the accessibility of protein residues to solvent and to proline isomerase.

(4) The pathways of unfolding, folding, and yield of correctly folded protein are dependent on the denaturant.

(5) Various classes of additives—small hydrophobic molecules, surfactants, cyclodextrins, and PEG polymers—can prevent the aggregation of proteins during refolding.

(6) Because CA folds in both the presence and absence of chaperones, the effects of chaperone proteins on protein folding can be deduced more easily with CA than with proteins in which folding is not possible in the absence of chaperones.

The pathway by which CA folds from GuHCl has been described carefully and specifically (Figure 32 parts A and B). The folding proceeds through five intermediates, with the isomerization of Pro residues being the rate-limiting step. Knowing the details of the interactions that cause CA to fold makes it an exceptionally useful model in understanding many of the more complicated aspects of protein folding. Specifically, CA has provided invaluable insight into controversial aspects of protein folding such as the hydration of the molten-globule state, the details of the process by which proteins aggregate, and the mechanism of the interaction of misfolded and unfolded proteins with GroEL.

V. Why is CA a Good Model?

16. Conclusions

In this section, we briefly summarize why CA is an attractive model protein for a variety of biochemical and biophysical studies and compare and contrast it with other model proteins. We also examine the key conclusions from the individual sections of this review in the context of what makes CA a model protein for biophysical studies. More detailed conclusions can be found at the end of the individual sections.

16.1. What Are the Strengths and Weaknesses of CA as a Model Protein?

CA is one of the best proteins now available for studies requiring a model enzyme or a receptor for a small molecule ligand. The advantages and disadvantages of using CA, rather

Table 16. Well-Defined Proteins Often Used as Model Enzymes or Small-Molecule Receptors

Protein	EC	Source	<i>M</i> (kDa)	Subunits	Cost ^a	Disulfide content	Cofactors	% α -helix	% β -strand	PDB (X-ray)	pI	Charge ladders?
insulin		bovine	5.7	2	\$	3		37.3	0	1APH	5.3	yes
protein G		recombinant	6.1	1	\$\$\$\$	0		25.0	42.8	1PGA	4.8	N/D
ubiquitin		human, bovine	8.6	1	\$\$	0		15.8	30.3	1TBE	6.56	yes
cytochrome C		equine heart	11.6	1	\$	0	heme	40.0	0	1WEJ	10.0	yes
ribonuclease A	3.1.27.5	bovine pancreas	13.6	1	\$\$	4		17.7	31.4	1XPS	9.8	yes
α -lactalbumin		bovine milk	14.1	1	\$	4	Ca ^{II} , Zn ^{II}	30.8	8.1	1F6S	4.8	yes
lysozyme	3.2.1.17	egg white	14.2	1	\$	4		30.2	6.2	193L	10.9	yes
calmodulin		bovine brain	16.6	1	\$\$\$	0	Ca ^{II}	50.0	2.7	1CM4	4.0	yes
myoglobin		equine heart	16.9	1	\$	0	heme	73.8	0	1WLA	6.8	yes
HIV protease	3.4.23.16	HIV	21.4	2	\$\$\$\$	0		4.0	46.4	1A30		N/D
trypsin	3.4.21.4	porcine pancreas	23.4	1	\$	6		7.1	30.0	1AVW		N/D
triosephosphate isomerase	5.3.1.1	yeast	26.6	1	\$\$\$	0	NAD	38.0	16.1	1YPI		N/D
carbonic anhydrase	4.2.1.1	bovine	29.3	1	\$	0	Zn ^{II}	7.6	25.7	1G6V	5.9	yes
carbonic anhydrase	4.2.1.1	human	29.3	1	\$\$\$	0	Zn ^{II}	9.2	27.4	1A42	7.6	yes
peroxidase	1.11.1.7	horseradish	33.7	1	\$\$	4	heme	44.7	1.9	1ATJ	7.2	yes
superoxide dismutase	1.15.1.1	human	32.5	2	\$\$\$\$	2	Zn ^{II} , Cu ^{II}			1HL5	5.0	yes
albumin		human serum	66.4	1	\$	17		68.7	0	1AO6	5.67	N/D
alcohol dehydrogenase	1.1.1.1	equine liver	79.5	2	\$	0	Zn ^{II}	23.9	22.1	1HLD	6.8	N/D
alkaline phosphatase	3.1.3.1	bacteria	94.0	2	\$\$	4	Zn ^{II}	28.3	17.7	1ALK	6.0	no
IgG		mouse	145	4	\$\$\$	17		4.2	44.7	1IGT		N/D
catalase	1.11.1.6	bovine	230	4	\$\$	0	heme, NADP	28.0	14.4	4BLC		N/D
β -galactosidase	3.2.1.23	bacteria	465	4	\$\$	0		10.5	35.3	1HN1	5.0	no

^a Cost structure: "\$" is below \$0.50 per mg protein; "\$\$" is between \$0.50 and \$10 per mg; "\$\$\$" is between \$10 and \$30 per mg; "\$\$\$\$" is above \$30 per mg protein.

than other particularly well-defined proteins, as a model for drug design and biophysics are best addressed by considering the criteria listed in Table 16. There are eleven main advantages of using CA (specifically HCA I, HCA II, and BCA II) as a model enzyme/receptor:

(1) It is monomeric, single-chain, stable, and intermediate in molecular weight.

(2) It is commercially available and inexpensive.

(3) It can be easily mutated and purified in high yield from *E. coli*.

(4) It contains no disulfide bonds.

(5) Its structure has been well-defined biophysically.

(6) It catalyzes a simple reaction in vivo—the hydration of carbon dioxide to bicarbonate.

(7) It has a number of straightforward assays to examine the binding of ligands.

(8) Its structure does not change drastically when it binds ligands.

(9) Its ligands are easy to synthesize (and, thus, it is easy to test different physical-organic models for protein–ligand binding).

(10) It has many metallovariants, many of which adopt similar tertiary structures as the wild-type enzyme.

(11) It readily forms charge ladders, and its analysis—both as native enzyme and in charge ladders—by CE is straightforward.

These advantages make CA particularly well-suited for biophysical studies that seek to understand (i) the binding of ligands to proteins (e.g., screening efforts, rational approaches to ligand design, and mechanistic hypotheses), (ii) how binding at the surface of a solid and in the gas phase compare to that in solution, (iii) the role of electrostatics in protein stability and protein–ligand binding, and (iv) the pathways of folding and unfolding of proteins. We discuss each of these studies in turn below.

Although the list of positive criteria is long, CA has three primary disadvantages in its use as a model protein:

(1) It contains a nonrepresentative binding site comprising a deep conical cleft, ~ 15 Å deep, with the binding of ligands occurring at the bottom of this cleft. It is, therefore, difficult to compare the binding of ligands and reactants to CA directly to similar studies of other enzymes with shallower binding pockets.

(2) It has an essential Zn^{II} cofactor. Much of the energy of binding of ligands to CA originates from the interaction of ligands with this cofactor. The presence of the Zn^{II} cofactor also complicates computational approaches to ligand discovery.

(3) It is composed primarily of β -sheets. Thus, its folding and unfolding pathways are unlikely to be representative of proteins with more α -helical content. Proteins with extensive β -sheet structure also tend to be prone to aggregation, which may compete with folding.

We believe that the advantages of CA far outweigh these disadvantages and make CA an excellent protein for biophysical studies.

16.2. What Are the Advantages of Using CA to Understand the Thermodynamics and Kinetics of Binding of Ligands to Proteins?

The ligands with the highest affinity for CA are the arylsulfonamides: the SO₂NH group of this class of molecules resembles the transition state for the physiological reaction catalyzed by CA (the interconversion of carbon dioxide and bicarbonate). This observation, thus, underscores the general principle that high-affinity ligands for enzymes are often transition-state analogs. The essential feature that has enabled the system of CA and arylsulfonamides to be used as a model for understanding protein–ligand binding is the fact that the different structural interactions between

CA and arylsulfonamide can, to a first-order approximation, be examined independently. Rigorous studies based on such an independent assessment of structural interactions have demonstrated that the pK_a of the arylsulfonamide, the hydrophobicity of the aryl ring, and the hydrophobic surface area of the ligand are important factors governing affinity. These studies have also revealed that multivalency is an effective design principle to generate high-affinity ligands by appending secondary components to a low-affinity ligand (at least in the case of hydrophobic secondary components). Moreover, such studies have suggested that ionic or electrostatic interactions between ligand and protein are much more challenging to engineer than are hydrophobic contacts. Finally, these studies have revealed that the phenomenon of enthalpy/entropy compensation is ubiquitous in protein–ligand binding and needs to be understood to be able to design high-affinity ligands for proteins.

The most likely model for the association of CA and arylsulfonamides involves three states: unbound CA and ligand, a hydrophobically bound intermediate, and a fully associated CA–ligand complex. This system thus reveals that the model of association of even a “simple” protein and ligand can be surprisingly complicated and suggests that simple two-state models for association could be very rare.

16.3. What Are the Advantages of Using CA to Compare Binding in Solution to That at Solid Surfaces or in the Gas Phase?

Oligoethylene glycol groups on the surfaces of solids prevent the nonspecific binding of CA to these surfaces, and thus, the thermodynamics and kinetics of binding of CA and arylsulfonamides can be studied rigorously at these surfaces. Values of the rate constants of association and dissociation (k_{on} and k_{off}) measured at the surfaces of solids are similar to those measured in solution when care is taken to reduce the influences of mass transport and lateral steric effects. The system of CA/arylsulfonamides, thus, suggests that protein–ligand binding at solid surfaces is not intrinsically different from that in solution and can, in principle, be used in high-throughput assays to find high-affinity ligands for proteins.

The tertiary structure of CA is at least partially retained in the gas phase. This stability allows the comparison of binding in the gas phase and in solution. Binding in the gas phase is driven primarily by electrostatic contacts, whereas binding in solution can be dominated by the “hydrophobic effect.” Thus, it may not be possible to infer stability in solution from measurements made in the gas phase.

16.4. What Are the Advantages of Using CA to Understand the Role of Electrostatics in Protein Stability and Protein–Ligand Binding?

CA does not adsorb to the walls of a glass capillary (used in CE) and can be modified with acylating agents that change the surface charge of the protein (and generate charged derivatives called charge ladders) in a controlled manner. These facts have allowed CA to be used as a model protein in biophysical studies of the importance of electrostatics in protein stability. These studies revealed that the ionization of residues upon acetylation involves cooperative behavior. They also demonstrated that the positive charges on all of the Lys groups of CA can be removed without significantly changing either the conformation of CA at 25 °C or its ability

to bind sulfonamides. The affinities of charged ligands, however, can be influenced by long-range electrostatic interactions (rather than by local modifications in the binding site). Electrostatic interactions can also influence the kinetics of denaturation of proteins by sodium dodecyl sulfate: removal of several positive charges from CA by acylation resulted in rates of denaturation that were slower by factors of $\sim 10^2$ than the native enzyme.

16.5. What Are the Advantages of Using CA to Understand How Proteins Fold and Unfold?

In addition to the advantages described in section 16.1, there are three reasons for using CA as a model in studying the denaturation of proteins:

- (1) Its folding pathway has many aspects that are prototypical in the folding of proteins.
- (2) It can fold with or without chaperonins (and, thus, allows the assessment of the influence of chaperonins on folding).
- (3) Its tendency to aggregate allows the investigation of the structural features responsible for aggregation and of additives that block aggregation.

Studies of CA suggest that folding for some proteins is initiated by hydrophobic interactions between “seed” residues, proceeds through a molten-globule intermediate, and is limited in rate by isomerization of proline residues. The Zn^{II} cofactor of CA is not necessary for its folding into its native structure. Aggregation of misfolded proteins of CA involves specific residues and can be corrected by chaperone proteins or minimized by the addition of surfactants and other small molecules. Surface charge also has little influence on the ability of CA, denatured in SDS, to refold into its native state, but does influence its stability to SDS and other denaturants. In these studies, CA provides a model for proteins that fold and unfold through a molten-globule intermediate and for proteins that comprise mostly β -sheets and are prone to aggregate during refolding.

16.6. Coda

Three-quarters of a century after its discovery in 1932 by Meldrum and Roughton,⁸¹² CA remains a protein of active research interest for medical, biophysical, and physical-organic studies. In the short section that follows, we briefly summarize articles that appeared in the interval between the time we initially submitted the review (December 2006) and the time of submission of the completed version of the review (December 2007). This section only provides references with a brief indication of content and does not place this work in the context of the individual sections.

Recent medical studies have investigated the expression of CA,^{813,814} the role of CA in membrane transport processes,^{815,816} and its role in a variety of diseases,⁸¹⁷ such as retinitis pigmentosa,⁸¹⁸ diabetes mellitus type II,⁸¹⁹ atopic dermatitis,⁸²⁰ brain cancer,⁸²¹ and colorectal cancer.⁸²²

Many recent biophysical studies have investigated the inhibition^{3,28,128,182,225,227,232,234–238,376,593,823–850} and activation^{226,851–853} of CA. The majority of these studies aimed to design isozyme-specific inhibitors and activators. Several others have developed QSARs for inhibitors^{854–865} and activators⁸⁶⁶ of various isozymes of CA. The interaction of CA with surfaces has also been investigated for delivering inhibitors to CA via nanoparticles⁸⁶⁷ and for disrupting the self-assembly of ion channels.⁸⁶⁸

The latest research on the structure and function of CA has focused on analyzing the proton shuttle,^{54,266–268,869–873} the binding of zinc to CA,⁸⁷⁴ and the pK_a of the zinc-bound water.³⁰⁵ In addition, several groups have further examined the denaturation, aggregation, and folding of CA.^{875–878}

Our hope is that this review will be useful to investigators who are looking for a way to navigate this still very dynamic field.

17. Acknowledgments

We thank Dr. Valentine I. Vullev for initial contributions to this review. Dr. John J. Baldwin (Vitae Pharmaceuticals) also commented helpfully on an early version of the review. Research using CA in our group has been supported by the NIH (GM51559 and GM30367). V.M.K. and I.G. acknowledge support from NDSEG and NSF predoctoral fellowships, respectively. A.R.U. and D.B.W. acknowledge support from the NIH for postdoctoral fellowships (AI057076 and GM067445, respectively).

18. References

- Stams, T.; Christianson, D. W. In *The Carbonic Anhydrases: New Horizons*; Chegwidden, W. R., Carter, N. D., Edwards, Y. H., Eds.; Birkhäuser Verlag: Basel, Switzerland, 2000; Vol. 90.
- Supuran, C. T.; Scozzafava, A.; Casini, A. *Med. Res. Rev.* **2003**, *23*, 146.
- Nishimori, I.; Minakuchi, T.; Kohsaki, T.; Onishi, S.; Takeuchi, H.; Vullo, D.; Scozzafava, A.; Supuran, C. T. *Bioorg. Med. Chem. Lett.* **2007**, *17*, 3585.
- Dill, K. A.; Bromberg, S. *Molecular Driving Forces: Statistical Thermodynamics in Chemistry & Biology*; Garland Science: New York, 2003.
- Whitesides, G. M.; Krishnamurthy, V. M. *Q. Rev. Biophys.* **2005**, *38*, 385.
- Deutsch, H. F. *Int. J. Biochem.* **1987**, *19*, 101.
- Henry, R. P. *Ann. Rev. Physiol.* **1996**, *58*, 523.
- Henry, R. P.; Swenson, E. R. *Resp. Physiol.* **2000**, *121*, 1.
- Gupta, S. P. *Prog. Drug Res.* **2003**, *60*, 171.
- Chegwidden, W. R.; Dogsdon, S. J.; Spencer, I. M. In *The Carbonic Anhydrases: New Horizons*; Chegwidden, W. R., Carter, N. D., Edwards, Y. H., Eds.; Birkhäuser Verlag: Basel, Switzerland, 2000; Vol. 90.
- Dodgson, S. J.; Tashian, R. E.; Gros, G.; Carter, N. D. *The Carbonic Anhydrases: Cellular Physiology and Molecular Genetics*; Plenum Press: New York, 1991.
- Tashian, R. E.; Hewitt-Emmett, D. *Ann. N. Y. Acad. Sci.* **1984**, *429*, 640.
- Wistrand, P. J. In *The Carbonic Anhydrases: New Horizons*; Chegwidden, W. R., Carter, N. D., Edwards, Y. H., Eds.; Birkhäuser Verlag: Basel, Switzerland, 2000; Vol. 90.
- Lindskog, S.; Silverman, D. N. In *The Carbonic Anhydrases: New Horizons*; Chegwidden, W. R., Carter, N. D., Edwards, Y. H., Eds.; Birkhäuser Verlag: Basel, Switzerland, 2000; Vol. 90.
- Carbonic Anhydrase: Its Inhibitors and Activators*; Supuran, C. T., Scozzafava, A., Conway, J., Eds.; CRC Press: Boca Raton, FL, 2004; Vol. 1.
- Snider, M. G.; Temple, B. S.; Wolfenden, R. *J. Phys. Org. Chem.* **2004**, *17*, 586.
- Khalifah, R. G. *J. Biol. Chem.* **1971**, *246*, 2561.
- Jewell, D. A.; Tu, C.; Paranawithana, S. R.; Tanhauser, S. M.; LoGrasso, P. V.; Laipis, P. J.; Silverman, D. N. *Biochemistry* **1991**, *30*, 1484.
- Ren, X.; Jonsson, B. H.; Millqvist, E.; Lindskog, S. *Biochim. Biophys. Acta* **1988**, *953*, 79.
- Baird, T. T., Jr.; Waheed, A.; Okuyama, T.; Sly, W. S.; Fierke, C. A. *Biochemistry* **1997**, *36*, 2669.
- Hurt, J. D.; Tu, C.; Laipis, P. J.; Silverman, D. N. *J. Biol. Chem.* **1997**, *272*, 13512.
- Heck, R. W.; Tanhauser, S. M.; Manda, R.; Tu, C.; Laipis, P. J.; Silverman, D. N. *J. Biol. Chem.* **1994**, *269*, 24742.
- Feldstein, J. B.; Silverman, D. N. *J. Biol. Chem.* **1984**, *259*, 5447.
- Earnhardt, J. N.; Qian, M.; Tu, C.; Lakkis, M. M.; Bergenhem, N. C. H.; Laipis, P. J.; Tashian, R. E.; Silverman, D. N. *Biochemistry* **1998**, *37*, 10837.
- Chegwidden, W. R.; Carter, N. D. In *The Carbonic Anhydrases: New Horizons*; Chegwidden, W. R., Carter, N. D., Edwards, Y. H., Eds.; Birkhäuser Verlag: Basel, Switzerland, 2000; Vol. 90.
- Lehtonen, J.; Shen, B.; Vihinen, M.; Casini, A.; Scozzafava, A.; Supuran, C. T.; Parkkila, A.-K.; Saarnio, J.; Kivelä, A. J.; Waheed, A.; Sly, W. S.; Parkkila, S. *J. Biol. Chem.* **2004**, *279*, 2719.
- Nishimori, I.; Vullo, D.; Innocenti, A.; Scozzafava, A.; Mastrolorenzo, A.; Supuran, C. T. *J. Med. Chem.* **2005**, *48*, 7860.
- Nishimori, I.; Minakuchi, T.; Onishi, S.; Vullo, D.; Scozzafava, A.; Supuran, C. T. *J. Med. Chem.* **2007**, *50*, 381.
- Nishimori, I.; Vullo, D.; Innocenti, A.; Scozzafava, A.; Mastrolorenzo, A.; Supuran, C. T. *Bioorg. Med. Chem. Lett.* **2005**, *15*, 3828.
- Fersht, A. *Structure and Mechanism in Protein Science*, 3rd ed.; W. H. Freeman: New York, 1999.
- Rosenberry, T. L. *Adv. Enzymol. Relat. Areas Mol. Biol.* **1975**, *43*, 103.
- Rosenberry, T. L.; Bernhard, S. A. *Biochemistry* **1972**, *11*, 4308.
- Rosenberry, T. L.; Bernhard, S. A. *Biochemistry* **1971**, *10*, 4114.
- Switala, J.; Loewen, P. C. *Arch. Biochem. Biophys.* **2002**, *401*, 145.
- Ogura, Y. *Arch. Biochem. Biophys.* **1955**, *57*, 288.
- Leveque, V. J.-P.; Stroupe, M. E.; Lepock, J. R.; Cabelli, D. E.; Trainer, J. A.; Nick, H. S.; Silverman, D. N. *Biochemistry* **2000**, *39*, 7131.
- Pocker, Y.; Meany, J. E. *Biochemistry* **1967**, *6*, 239.
- Pocker, Y.; Dickerson, D. G. *Biochemistry* **1968**, *7*, 1995.
- Sheridan, R. P.; Deakyne, C. A.; Allen, L. C. *Adv. Exp. Med. Biol.* **1980**, *132*, 705.
- Pocker, Y.; Sarkanen, S. *Adv. Enzymol. Mol. Biol.* **1978**, *47*, 149.
- Kaiser, E.; Lo, K.-W. *J. Am. Chem. Soc.* **1969**, *91*, 4912.
- Chenevert, R.; Rhlid, R. B.; Letourneau, M.; Gagnon, R.; D'Astous, L. *Tetrahedron: Asymmetry* **1993**, *4*, 1137.
- Henkart, P.; Guidotti, G.; Edsall, J. T. *J. Biol. Chem.* **1968**, *243*, 2447.
- Whitney, P. L.; Fölsch, G.; Nyman, P. O.; Malmström, B. G. *J. Biol. Chem.* **1967**, *242*, 4206.
- Briganti, F.; Mangani, S.; Scozzafava, A.; Vernaglione, G.; Supuran, C. T. *J. Biol. Inorg. Chem.* **1999**, *4*, 528.
- Krebs, J. F.; Fierke, C. A. *J. Biol. Chem.* **1993**, *268*, 948.
- Liang, J. Y.; Lipscomb, W. N. *Proc. Natl. Acad. Sci. U.S.A.* **1990**, *87*, 3675.
- Silverman, D. N.; Lindskog, S. *Acc. Chem. Res.* **1988**, *21*, 30.
- Krebs, J. F.; Rana, F.; Dluhy, R. A.; Fierke, C. A. *Biochemistry* **1993**, *32*, 4496.
- An, H.; Tu, C.; Ren, K.; Laipis, P. J.; Silverman, D. N. *Biochim. Biophys. Acta* **2002**, *1599*, 21.
- Ren, X.; Tu, C.; Laipis, P. J.; Silverman, D. N. *Biochemistry* **1995**, *34*, 8492.
- Steiner, H.; Jonsson, B. H.; Lindskog, S. *Eur. J. Biochem.* **1975**, *59*, 253.
- Tu, C.; Silverman, D. N.; Forsman, C.; Jonsson, B. H.; Lindskog, S. *Biochemistry* **1989**, *28*, 7913.
- Fisher, S. Z.; Maupin, C. M.; Budayova-Spano, M.; Govindasamy, L.; Tu, C.; Agbandje-McKenna, M.; Silverman, D. N.; Voth, G. A.; McKenna, R. *Biochemistry* **2007**, *46*, 2930.
- Nair, S. K.; Ludwig, P. A.; Christianson, D. W. *J. Am. Chem. Soc.* **1994**, *116*, 3659.
- Loferer, M. K.; Tautermann, C. S.; Loeffler, H. H.; Liedli, K. R. *J. Am. Chem. Soc.* **2003**, *125*, 8921.
- Liang, J.-Y.; Lipscomb, W. N. *J. Am. Chem. Soc.* **1986**, *108*, 5051.
- Liang, J.-Y.; Lipscomb, W. N. *Biochemistry* **1987**, *26*, 5293.
- Tautermann, C. S.; Loferer, M. K.; Voegelé, A. F.; Liedli, K. R. *J. Phys. Chem. B* **2003**, *107*, 12013.
- Rossi, K. A.; Merz, K. M.; Smith, G. M.; Baldwin, J. J. *J. Med. Chem.* **1995**, *38*, 2061.
- Smedarchina, Z.; Siebrand, W.; Fernandez-Ramos, A.; Cui, Q. *J. Am. Chem. Soc.* **2003**, *125*, 243.
- Cui, Q.; Karplus, M. *J. Phys. Chem. B* **2003**, *107*, 1071.
- Mauksch, M.; Brauer, M.; Weston, J.; Anders, E. *ChemBioChem* **2001**, *2*, 190.
- Merz, K. M., Jr.; Hoffman, J. M.; Dewar, M. J. S. *J. Am. Chem. Soc.* **1989**, *111*, 5636.
- Maren, T. H. *Ann. Rev. Physiol.* **1988**, *50*, 695.
- Sanyal, G.; Maren, T. H. *J. Biol. Chem.* **1981**, *256*, 608.
- Swenson, E. R. In *The Carbonic Anhydrases: New Horizons*; Chegwidden, W. R., Carter, N. D., Edwards, Y. H., Eds.; Birkhäuser Verlag: Basel, Switzerland, 2000; Vol. 90.
- Stabenau, E. K.; Heming, T. *Comp. Biochem. Physiol., Part A: Mol. Integr. Physiol.* **2003**, *136A*, 271.
- Shah, G. N.; Ulmasov, B.; Waheed, A.; Becker, T.; Makani, S.; Svichar, N.; Chesler, M.; Sly, W. S. *Proc. Natl. Acad. Sci. U.S.A.* **2005**, *102*, 16771.

- (70) Maren, T. H. In *The Carbonic Anhydrases: New Horizons*; Chegwidden, W. R., Carter, N. D., Edwards, Y. H., Eds.; Birkhäuser Verlag: Basel, Switzerland, 2000; Vol. 90.
- (71) Mincione, F.; Menabuoni, L.; Supuran, C. T. In *Carbonic Anhydrase: Its Inhibitors and Activators*; Supuran, C. T., Scozzafava, A., Conway, J., Eds.; CRC Press: Boca Raton, FL, 2004.
- (72) Gay, C. V.; Weber, J. A. *Crit. Rev. Eukaryotic Gene Expression* **2000**, *10*, 213.
- (73) Hentunen, T. A.; Harkonen, P. L.; Vaananen, H. K. In *The Carbonic Anhydrases: New Horizons*; Chegwidden, W. R., Carter, N. D., Edwards, Y. H., Eds.; Birkhäuser Verlag: Basel, Switzerland, 2000; Vol. 90.
- (74) Sun, M.-K.; Alkon, D. L. *Trends Pharm. Sci.* **2002**, *23*, 83.
- (75) Cammer, W. B.; Brion, L. P. In *The Carbonic Anhydrases: New Horizons*; Chegwidden, W. R., Carter, N. D., Edwards, Y. H., Eds.; Birkhäuser Verlag: Basel, Switzerland, 2000; Vol. 90.
- (76) Bryant, B. P. In *The Carbonic Anhydrases: New Horizons*; Chegwidden, W. R., Carter, N. D., Edwards, Y. H., Eds.; Birkhäuser Verlag: Basel, Switzerland, 2000; Vol. 90.
- (77) Parkkila, S. In *The Carbonic Anhydrases: New Horizons*; Chegwidden, W. R., Carter, N. D., Edwards, Y. H., Eds.; Birkhäuser Verlag: Basel, Switzerland, 2000; Vol. 90.
- (78) Parkkila, S.; Parkkila, A.-K.; Lehtola, J.; Reinila, A.; Sodervik, H.-J.; Rannisto, M.; Rajaniemi, H. *Dig. Dis. Sci.* **1997**, *42*, 1013.
- (79) Kivela, A. J.; Kivela, J.; Saarnio, J.; Parkkila, S. *World J. Gastroenterol.* **2005**, *11*, 155.
- (80) Parkkila, S.; Parkkila, A.-K.; Kivela, J. In *Carbonic Anhydrase: Its Inhibitors and Activators*; Supuran, C. T., Scozzafava, A., Conway, J., Eds.; CRC Press: Boca Raton, FL, 2004.
- (81) Swenson, E. R. In *The Carbonic Anhydrases: Cellular Physiology and Molecular Genetics*; Carter, N. D., Dodgson, S. J., Gros, G., Tashian, R. E., Eds.; Plenum Press: New York, 1991.
- (82) Geers, C.; Gros, G. *Physiol. Rev.* **2000**, *80*, 681.
- (83) Wetzel, P.; Gros, G. In *The Carbonic Anhydrases: New Horizons*; Chegwidden, W. R., Carter, N. D., Edwards, Y. H., Eds.; Birkhäuser Verlag: Basel, Switzerland, 2000; Vol. 90.
- (84) Berg, J. T.; Ramanathan, S.; Gabrielli, M. G.; Swenson, E. R. *J. Histochem. Cytochem.* **2004**, *52*, 1101.
- (85) Breton, S.; Hammar, K.; Smith, P. J. S.; Brown, D. *Am. J. Physiol.* **1998**, *275*, C1134.
- (86) Raisanen, S. R.; Lehenkari, P.; Tasanen, M.; Rakkila, P.; Harkonen, P. L.; Vaananen, H. K. *FASEB J.* **1999**, *13*, 513.
- (87) Cabiscol, E.; Levine, R. L. *Proc. Natl. Acad. Sci. U.S.A.* **1996**, *93*, 4170.
- (88) Švastová, E.; Hulíková, A.; Rafajová, M.; Zat'ovičová, M.; Gibadulinová, A.; Casini, A.; Cecchi, A.; Scozzafava, A.; Supuran, C. T.; Pastorek, J.; Pastoreková, S. *FEBS Lett.* **2004**, *577*, 439.
- (89) Cammer, W. In *The Carbonic Anhydrases: Cellular Physiology and Molecular Genetics*; Carter, N. D., Dodgson, S. J., Gros, G., Tashian, R. E., Eds.; Plenum Press: New York, 1991.
- (90) Wistrand, P. J.; Schenholm, M.; Lönnnerholm, G. *Invest. Ophthalmol. Vision Sci.* **1986**, *27*, 419.
- (91) Alward, W. L. M. *N. Engl. J. Med.* **1998**, *339*, 1298.
- (92) Kaur, I. P.; Aggarwal, D. In *Trends in Glaucoma Research*; Reece, S. M., Ed.; Nova Science Publishers: Hauppauge, NY, 2005.
- (93) Stefansson, E.; Pedersen, D. B.; Jensen, P. K.; la Cour, M.; Kiilgaard, J. F.; Bang, K.; Eysteinson, T. *Prog. Retinal Eye Res.* **2005**, *24*, 307.
- (94) Moldow, B.; Sander, B.; Larsen, M.; Engler, C.; Li, B.; Rosenberg, T.; Lund-Andersen, H. *Graefes Arch. Clin. Exp. Ophthalmol.* **1998**, *236*, 881.
- (95) Wolfensberger, T. J. *Doc. Ophthalmol.* **1999**, *97*, 387.
- (96) Maren, T. H.; Conroy, C. W.; Wynns, G. C.; Godman, D. R. *J. Pharmacol. Exp. Ther.* **1997**, *280*, 98.
- (97) Sun, M. K.; Alkon, D. L. *J. Pharmacol. Exp. Ther.* **2001**, *297*, 961.
- (98) Staley, K. J.; Soldo, B. L.; Proctor, W. R. *Science* **1995**, *269*, 977.
- (99) Sills, G. J.; Leach, J. P.; Kilpatrick, W. S.; Fraser, C. M.; Thompson, G. G.; Brodie, M. J. *Epilepsia* **2000**, *41*, S30.
- (100) Shinnar, S.; Gammon, K.; Bergman, E. W., Jr.; Epstein, M.; Freeman, J. M. *J. Pediatr.* **1985**, *107*, 31.
- (101) Cowan, F.; Whitelaw, A. *Acta Paediatr. Scand.* **1991**, *80*, 22.
- (102) Tawil, R.; McDermott, M. P.; Brown, R., Jr.; Shapiro, B. C.; Ptacek, L. J.; McManis, P. G.; Dalakas, M. C.; Spector, S. A.; Mendell, J. R.; Hahn, A. F.; Griggs, R. C. *Ann. Neurol.* **2000**, *47*, 46.
- (103) Puscas, I.; Coltau, M.; Baican, M.; Pasca, R.; Domuta, G. *Res. Commun. Mol. Pathol. Pharmacol.* **1999**, *105*, 213.
- (104) Puscas, I.; Gilau, L.; Coltau, M.; Pasca, R.; Domuta, G.; Baican, M.; Hecht, A. *Clin. Pharmacol. Ther.* **2000**, *68*, 443.
- (105) Schwartz, W. B.; Relman, A. S.; Leaf, A. *Ann. Intern. Med.* **1955**, *42*, 79.
- (106) Barbarino, F.; Toganel, E.; Brilinschi, C. *Carbonic Anhydrase Modulation Physiol. Pathol. Processes Org. [Pap. Symp.]* **1994**, 492.
- (107) Puscas, I.; Coltau, M.; Chis, F.; Bologna, O. *Carbonic Anhydrase Modulation Physiol. Pathol. Processes Org. [Pap. Symp.]* **1994**, 519.
- (108) Puscas, I.; Coltau, M.; Maghiar, A.; Domuta, G. *Exp. Toxicol. Pathol.* **2000**, *52*, 431.
- (109) Rousselle, A. V.; Heymann, D. *Bone* **2002**, *30*, 533.
- (110) Lomri, A.; Baron, R. *Proc. Natl. Acad. Sci. U.S.A.* **1992**, *89*, 4688.
- (111) Borthwick, K. J.; Kandemir, N.; Topaloglu, R.; Kornak, U.; Bakkaloglu, A.; Yordam, N.; Ozen, S.; Mocan, H.; Shah, G. N.; Sly, W. S.; Karet, F. E. *J. Med. Genet.* **2003**, *40*, 115.
- (112) Kenny, A. D. *SAAS Bull. Biochem. Biotech.* **1991**, *4*, 6.
- (113) Dodgson, S. J.; Forster, R. E., II. *Arch. Biochem. Biophys.* **1986**, *251*, 198.
- (114) Dodgson, S. J.; Cherian, K. *Am. J. Physiol. Endocrinol. Metab.* **1989**, *257*, E791.
- (115) Dodgson, S. J.; Forster, R. E., II. *J. Appl. Physiol.* **1986**, *60*, 646.
- (116) Lynch, C.; Fox, H.; Hazen, S. A.; Stanley, B. A.; Dodgson, S.; LaNoue, K. F. *Biochem. J.* **1995**, *310*, 197.
- (117) Forwand, S. A.; Landowne, M.; Follansbee, J. N.; Hansen, J. E. *N. Engl. J. Med.* **1968**, *279*, 839.
- (118) Wright, A. D.; Bradwell, A. R.; Fletcher, R. F. *Aviat., Space Environ. Med.* **1983**, *54*, 619.
- (119) Wagenaar, M.; Je Vos, P.; Heijdra, Y. F.; Teppema, L. J.; Folgering, H. T. M. *Eur. Respir. J.* **2002**, *20*, 1130.
- (120) Wagenaar, M.; Vos, P.; Heijdra, Y.; Teppema, L.; Folgering, H. *Chest* **2003**, *123*, 1450.
- (121) Mastrolorenzo, A.; Scozzafava, A.; Supuran, C. T. *J. Enzyme Inhib.* **2000**, *15*, 517.
- (122) Puccetti, L.; Fasolis, G.; Cecchi, A.; Winum, J. Y.; Gamberi, A.; Montero, J. L.; Scozzafava, A.; Supuran, C. T. *Bioorg. Med. Chem. Lett.* **2005**, *15*, 2359.
- (123) Supuran, C. T. *Expert Opin. Invest. Drugs* **2003**, *12*, 283.
- (124) Özensoy, Ö.; Puccetti, L.; Fasolis, G.; Arslan, O.; Scozzafava, A.; Supuran, C. T. *Bioorg. Med. Chem. Lett.* **2005**, *15*, 4862.
- (125) Pastorekova, S.; Pastorek, J. In *Carbonic Anhydrase: Its Inhibitors and Activators*; Supuran, C. T., Scozzafava, A., Conway, J., Eds.; CRC Press: Boca Raton, FL, 2004.
- (126) Pastorekova, S.; Vullo, D.; Casini, A.; Scozzafava, A.; Pastorek, J.; Nishimori, I.; Supuran, C. T. *J. Enzyme Inhib. Med. Chem.* **2005**, *20*, 211.
- (127) Owa, T.; Yoshino, H.; Okauchi, T.; Yoshimatsu, K.; Ozawa, Y.; Sugi, N. H.; Nagasu, T.; Koyanagi, N.; Kitoh, K. *J. Med. Chem.* **1999**, *42*, 3789.
- (128) Leese, M. P.; Leblond, B.; Smith, A.; Newman, S. P.; Di Fiore, A.; De Simone, G.; Supuran, C. T.; Purohit, A.; Reed, M. J.; Potter, B. V. L. *J. Med. Chem.* **2006**, *49*, 7683.
- (129) Beasley, N. J.; Wykoff, C. C.; Watson, P. H.; Leek, R.; Turley, H.; Gatter, K.; Pastorek, J.; Cox, G. J.; Ratcliffe, P.; Harris, A. L. *Cancer Res.* **2001**, *61*, 5262.
- (130) Robertson, N.; Potter, C.; Harris, A. L. *Cancer Res.* **2004**, *64*, 6160.
- (131) Span, P. N.; Bussink, J.; Manders, P.; Beex, L. V.; Sweep, C. G. *Br. J. Cancer* **2003**, *89*, 271.
- (132) Griffiths, E. A.; Pritchard, S. A.; Welch, I. M.; Price, P. M.; West, C. M. *Eur. J. Cancer* **2005**, *41*, 2792.
- (133) Kim, J.-Y.; Shin, H.-J.; Kim, T.-H.; Cho, K.-H.; Shin, K.-H.; Kim, B.-K.; Roh, J.-W.; Lee, S.; Park, S.-Y.; Hwang, Y.-J.; Han, I.-O. *J. Cancer Res. Clin. Oncol.* **2006**, *132*, 302.
- (134) Proescholdt, M. A.; Mayer, C.; Kubitz, M.; Schubert, T.; Liao, S.-Y.; Stanbridge, E. J.; Ivanov, S.; Oldfield, E. H.; Brawanski, A.; Merrill, M. J. *Neuro-Oncology* **2005**, *7*, 465.
- (135) Said, J. *Biomarkers* **2005**, *10*, S83.
- (136) Parkkila, S.; Rajaniemi, H.; Parkkila, A.-K.; Kivela, J.; Waheed, A.; Pastorekova, S.; Pastorek, J.; Sly, W. S. *Proc. Natl. Acad. Sci. U.S.A.* **2000**, *97*, 2220.
- (137) Ozawa, Y.; Sugi, N. H.; Nagasu, T.; Owa, T.; Watanabe, T.; Koyanagi, N.; Yoshino, H.; Kitoh, K.; Yoshimatsu, K. *Eur. J. Cancer* **2001**, *37*, 2275.
- (138) Yokoi, A.; Kuromitsu, J.; Kawai, T.; Nagasu, T.; Sugi, N. H.; Yoshimatsu, K.; Yoshino, H.; Owa, T. *Mol. Cancer Ther.* **2002**, *1*, 275.
- (139) Hewett-Emmett, D.; Tashian, R. E. *Mol. Phylogenet. Evol.* **1996**, *5*, 50.
- (140) Hewett-Emmett, D. In *The Carbonic Anhydrases: New Horizons*; Chegwidden, W. R., Carter, N. D., Edwards, Y. H., Eds.; Birkhäuser Verlag: Basel, Switzerland, 2000; Vol. 90.
- (141) Lane, T. W.; Morel, F. M. M. *Plant Physiol.* **2000**, *123*, 345.
- (142) Tripp, B. C.; Smith, K.; Ferry, J. G. *J. Biol. Chem.* **2001**, *276*, 48615.
- (143) So, A. K.-C.; Espie, G. S.; Williams, E. B.; Shively, J. M.; Heinhorst, S.; Cannon, G. C. *J. Bacteriol.* **2004**, *186*, 623.
- (144) Sawaya, M. R.; Cannon, G. C.; Heinhorst, S.; Tanaka, S.; Williams, E. B.; Yeates, T. O.; Kerfeld, C. A. *J. Biol. Chem.* **2006**, *281*, 7546.
- (145) Parkkila, S. In *The Carbonic Anhydrases: New Horizons*; Chegwidden, W. R., Carter, N. D., Edwards, Y. H., Eds.; Birkhäuser Verlag: Basel, Switzerland, 2000; Vol. 90.

- (146) Hilvo, M.; Tolvanen, M.; Clark, A.; Shen, B.; Shah, G. N.; Waheed, A.; Ralmi, P.; Hanninen, M.; Hamalainen, J. M.; Vihinen, M.; Sly, W. S.; Parkkila, S. *Biochem. J.* **2005**, *392*, 83.
- (147) Saito, R.; Sato, T.; Ikai, A.; Tanaka, N. *Acta Crystallogr., Sect. D* **2004**, *D60*, 792.
- (148) Nyman, P. O.; Lindskog, S. *Biochim. Biophys. Acta* **1964**, *85*, 141.
- (149) Funakoshi, S.; Deutsch, H. F. *J. Biol. Chem.* **1969**, *244*, 3438.
- (150) Jonsson, M.; Pettersson, E. *Acta Chem. Scand.* **1968**, *22*, 712.
- (151) Murakami, H.; Marelich, G. P.; Grubb, J. H.; Kyle, J. W.; Sly, W. S. *Genomics* **1987**, *1*, 159.
- (152) Alam, M. T.; Yamada, T.; Carlsson, U.; Ikai, A. *FEBS Lett.* **2002**, *519*, 35.
- (153) Nair, S. K.; Calderone, T. L.; Christianson, D. W.; Fierke, C. A. *J. Biol. Chem.* **1991**, *266*, 17320.
- (154) Osborne, W. R. A.; Tashian, R. E. *Anal. Biochem.* **1975**, *64*, 297.
- (155) Khalifah, R. G.; Strader, D. J.; Bryant, S. H.; Gibson, S. M. *Biochemistry* **1977**, *16*, 2241.
- (156) Krebs, J. F.; Ippolito, J. A.; Christianson, D. W.; Fierke, C. A. *J. Biol. Chem.* **1993**, *268*, 27458.
- (157) Pocker, Y.; Stone, J. T. *Biochemistry* **1968**, *7*, 2936.
- (158) Alexander, R. S.; Nair, S. K.; Christianson, D. W. *Biochemistry* **1991**, *30*, 11064.
- (159) Tilander, B.; Strandberg, B.; Fridborg, K. *J. Mol. Biol.* **1965**, *12*, 740.
- (160) Bernstein, F. C.; Koetzle, T. F.; Williams, G. J.; Meyer, E. F., Jr.; Brice, M. D.; Rodgers, J. R.; Kennard, O.; Shimanouchi, T.; Tasumi, M. *J. Mol. Biol.* **1977**, *112*, 535.
- (161) Eriksson, A. E.; Liljas, A. *Proteins: Struct., Funct., Genet.* **1993**, *16*, 29.
- (162) Stams, T.; Chen, Y.; Boriack-Sjodin, P. A.; Hurt, J. D.; Liao, J.; May, J. A.; Dean, T.; Laipis, P.; Silverman, D. N.; Christianson, D. W. *Protein Sci.* **1998**, *7*, 556.
- (163) Boriack-Sjodin, P. A.; Heck, R. W.; Laipis, P. J.; Silverman, D. N.; Christianson, D. W. *Proc. Natl. Acad. Sci. U.S.A.* **1995**, *92*, 10949.
- (164) Jude, K. M.; Wright, S. K.; Tu, C.; Silverman, D. N.; Viola, R. E.; Christianson, D. W. *Biochemistry* **2002**, *41*, 2485.
- (165) Heck, R. W.; Boriack-Sjodin, P. A.; Qian, M.; Tu, C.; Christianson, D. W.; Laipis, P. J.; Silverman, D. N. *Biochemistry* **1996**, *35*, 11605.
- (166) Whittington, D. A.; Grubb, J. H.; Waheed, A.; Shah, G. N.; Sly, W. S.; Christianson, D. W. *J. Biol. Chem.* **2004**, *279*, 7223.
- (167) Mallis, R. J.; Poland, B. W.; Chatterjee, T. K.; Fisher, R. A.; Darmawan, S.; Honzatko, R. B.; Thomas, J. A. *FEBS Lett.* **2000**, *482*, 237.
- (168) Huang, S.; Xue, Y.; Sauer-Eriksson, E.; Chirica, L.; Lindskog, S.; Jonsson, B. H. *J. Mol. Biol.* **1998**, *283*, 301.
- (169) Premkumar, L.; Greenblatt, H. M.; Bageshwar, U. K.; Savchenko, T.; Gokhman, I.; Sussman, J. L.; Zamir, A. *Proc. Natl. Acad. Sci. U.S.A.* **2005**, *102*, 7493.
- (170) Mitsuhashi, S.; Mizushima, T.; Yamashita, E.; Yamamoto, M.; Kumasaka, T.; Moriyama, H.; Ueki, T.; Miyachi, S.; Tsukihara, T. *J. Biol. Chem.* **2000**, *275*, 5521.
- (171) Kimber, M. S.; Pai, E. F. *EMBO J.* **2000**, *19*, 1407.
- (172) Cronk, J. D.; Endrizzi, J. A.; Cronk, M. R.; O'Neill, J. W.; Zhang, K. Y. *J. Protein Sci.* **2001**, *10*, 911.
- (173) Cronk, J. D.; Rowlett, R. S.; Zhang, K. Y.; Tu, C.; Endrizzi, J. A.; Lee, J.; Gareiss, P. C.; Preiss, J. R. *Biochemistry* **2006**, *45*, 4351.
- (174) Suarez Covarrubias, A.; Bergfors, T.; Jones, T. A.; Hoegbom, M. *J. Biol. Chem.* **2006**, *281*, 4993.
- (175) Suarez Covarrubias, A.; Larsson Anna, M.; Hogbom, M.; Lindberg, J.; Bergfors, T.; Bjorkelid, C.; Mowbray Sherry, L.; Unge, T.; Jones, T. A. *J. Biol. Chem.* **2005**, *280*, 18782.
- (176) Strop, P.; Smith, K. S.; Iverson, T. M.; Ferry, J. G.; Rees, D. C. *J. Biol. Chem.* **2001**, *276*, 10299.
- (177) Kisker, C.; Schindelin, H.; Alber, B. E.; Ferry, J. G.; Rees, D. C. *EMBO J.* **1996**, *15*, 2323.
- (178) Iverson, T. M.; Alber, B. E.; Kisker, C.; Ferry, J. G.; Rees, D. C. *Biochemistry* **2000**, *39*, 9222.
- (179) Håkansson, K.; Briand, C.; Zaitsev, V.; Xue, Y.; Liljas, A. *Acta Crystallogr., Sect. D* **1994**, *D50*, 101.
- (180) Kim, C.-Y.; Chang, J. S.; Doyon, J. B.; Baird, T. T., Jr.; Fierke, C. A.; Jain, A.; Christianson, D. W. *J. Am. Chem. Soc.* **2000**, *122*, 12125.
- (181) Jude, K. M.; Banerjee, A. L.; Haldar, M. K.; Manokaran, S.; Roy, B.; Mallik, S.; Srivastava, D. K.; Christianson, D. W. *J. Am. Chem. Soc.* **2006**, *128*, 3011.
- (182) Krishnamurthy, V. M.; Bohall, B. R.; Kim, C.-Y.; Moustakas, D. T.; Christianson, D. W.; Whitesides, G. M. *Chem. Asian J.* **2007**, *2*, 94.
- (183) Fisher, Z.; Hernandez Prada, J. A.; Yu, C.; Duda, D.; Yashioka, C.; An, H.; Govindasamy, L.; Silverman, D. N.; McKenna, R. *Biochemistry* **2005**, *44*, 1097.
- (184) Håkansson, K.; Carlsson, M.; Svensson, L. A.; Liljas, A. *J. Mol. Biol.* **1992**, *227*, 1192.
- (185) Boriack, P. A.; Christianson, D. W.; Kingery-Wood, J.; Whitesides, G. M. *J. Med. Chem.* **1995**, *38*, 2286.
- (186) Eriksson, A. E.; Kylsten, P. M.; Jones, T. A.; Liljas, A. *Proteins: Struct., Funct., Genet.* **1988**, *4*, 283.
- (187) Håkansson, K.; Wehnert, A.; Liljas, A. *Acta Crystallogr., Sect. D* **1994**, *D50*, 93.
- (188) Håkansson, K.; Wehnert, A. *J. Mol. Biol.* **1992**, *228*, 1212.
- (189) Grzybowski, B. A.; Ishchenko, A. V.; Kim, C.-Y.; Topalov, G.; Chapman, R.; Christianson, D. W.; Whitesides, G. M.; Shakhnovich, E. I. *Proc. Natl. Acad. Sci. U.S.A.* **2002**, *99*, 1270.
- (190) Temperini, C.; Scozzafava, A.; Puccetti, L.; Supuran, C. T. *Bioorg. Med. Chem. Lett.* **2005**, *15*, 5136.
- (191) Temperini, C.; Scozzafava, A.; Supuran, C. T. *Bioorg. Med. Chem. Lett.* **2006**, *16*, 5152.
- (192) Temperini, C.; Scozzafava, A.; Vullo, D.; Supuran, C. T. *Chem.—Eur. J.* **2006**, *12*, 7057.
- (193) Temperini, C.; Scozzafava, A.; Vullo, D.; Supuran, C. T. *J. Med. Chem.* **2006**, *49*, 3019.
- (194) Briganti, F.; Mangani, S.; Orioli, P.; Scozzafava, A.; Vernaglione, G.; Supuran, C. T. *Biochemistry* **1997**, *36*, 10384.
- (195) Jonsson, B. M.; Håkansson, K.; Liljas, A. *FEBS Lett.* **1993**, *322*, 186.
- (196) Kumar, V.; Kannan, K. K.; Sathyamurthi, P. *Acta Crystallogr., Sect. D* **1994**, *D50*, 731.
- (197) Mangani, S.; Håkansson, K. *Eur. J. Biochem.* **1992**, *210*, 867.
- (198) Kumar, V.; Kannan, K. K. *J. Mol. Biol.* **1994**, *241*, 226.
- (199) Boriack-Sjodin, P. A.; Zeitlin, S.; Chen, H.-H.; Crenshaw, L.; Gross, S.; Dantarayana, A.; Delgado, P.; May, J. A.; Dean, T.; Christianson, D. W. *Protein Sci.* **1998**, *7*, 2483.
- (200) Scolnick, L. R.; Clements, A. M.; Liao, J.; Crenshaw, L.; Hellberg, M.; May, J.; Dean, T. R.; Christianson, D. W. *J. Am. Chem. Soc.* **1997**, *119*, 850.
- (201) Håkansson, K.; Liljas, A. *FEBS Lett.* **1994**, *350*, 319.
- (202) Cappelanga Bunn, A. M.; Alexander, R. S.; Christianson, D. W. *J. Am. Chem. Soc.* **1994**, *116*, 5063.
- (203) Nair, S. K.; Elbaum, D.; Christianson, D. W. *J. Biol. Chem.* **1996**, *271*, 1003.
- (204) Weber, A.; Casini, A.; Heine, A.; Kuhn, D.; Supuran, C. T.; Scozzafava, A.; Klebe, G. *J. Med. Chem.* **2004**, *47*, 550.
- (205) Di Fiore, A.; Pedone, C.; D'Ambrosio, K.; Scozzafava, A.; De Simone, G.; Supuran, C. T. *Bioorg. Med. Chem. Lett.* **2006**, *16*, 437.
- (206) Alterio, V.; Vitale, R. M.; Monti, S. M.; Pedone, C.; Scozzafava, A.; Cecchi, A.; De Simone, G.; Supuran, C. T. *J. Am. Chem. Soc.* **2006**, *128*, 8329.
- (207) Menchise, V.; De Simone, G.; Alterio, V.; Di Fiore, A.; Pedone, C.; Scozzafava, A.; Supuran, C. T. *J. Med. Chem.* **2005**, *48*, 5721.
- (208) Elbaum, D.; Nair, S. K.; Patchan, M. W.; Thompson, R. B.; Christianson, D. W. *J. Am. Chem. Soc.* **1996**, *118*, 8381.
- (209) De Simone, G.; Vitale, R. M.; Di Fiore, A.; Pedone, C.; Scozzafava, A.; Montero, J.-L.; Winum, J.-Y.; Supuran, C. T. *J. Med. Chem.* **2006**, *49*, 5544.
- (210) Whittington, D. A.; Waheed, A.; Ulmasov, B.; Shah, G. N.; Grubb, J. H.; Sly, W. S.; Christianson, D. W. *Proc. Natl. Acad. Sci. U.S.A.* **2001**, *98*, 9545.
- (211) Chakravarty, S.; Kannan, K. K. *J. Mol. Biol.* **1994**, *243*, 298.
- (212) Menchise, V.; De Simone, G.; Di Fiore, A.; Scozzafava, A.; Supuran, C. T. *Bioorg. Med. Chem. Lett.* **2006**, *16*, 6204.
- (213) Fisher, S. Z.; Govindasamy, L.; Boyle, N.; Agbandje-McKenna, M.; Silverman David, N.; Blackburn, G. M.; McKenna, R. *Acta Crystallogr., Sect. F* **2006**, *F62*, 618.
- (214) Smith, G. M.; Alexander, R. S.; Christianson, D. W.; McKeever, B. M.; Ponticello, G. S.; Springer, J. P.; Randall, W. C.; Baldwin, J. J.; Habecker, C. N. *Protein Sci.* **1994**, *3*, 118.
- (215) Kim, C.-Y.; Whittington, D. A.; Chang, J. S.; Liao, J.; May, J. A.; Christianson, D. W. *J. Med. Chem.* **2002**, *45*, 888.
- (216) Recacha, R.; Costanzo, M. J.; Maryanoff, B. E.; Chattopadhyay, D. *Biochem. J.* **2002**, *361*, 437.
- (217) Lloyd, M. D.; Pederick, R. L.; Natesh, R.; Woo, L. W. L.; Purohit, A.; Reed, M. J.; Acharya, K. R.; Potter, B. V. L. *Biochem. J.* **2005**, *385*, 715.
- (218) Lloyd, M. D.; Thiagarajan, N.; Ho, Y. T.; Woo, L. W. L.; Sutcliffe, O. B.; Purohit, A.; Reed, M. J.; Acharya, K. R.; Potter, B. V. L. *Biochemistry* **2005**, *44*, 6858.
- (219) Grüneberg, S.; Stubbs, M. T.; Klebe, G. *J. Med. Chem.* **2002**, *45*, 3588.
- (220) Temperini, C.; Innocenti, A.; Scozzafava, A.; Supuran, C. T. *Bioorg. Med. Chem. Lett.* **2006**, *16*, 4316.
- (221) Guerri, A.; Briganti, F.; Scozzafava, A.; Supuran, C. T.; Mangani, S. *Biochemistry* **2000**, *39*, 12391.
- (222) Mangani, S.; Liljas, A. *J. Mol. Biol.* **1993**, *232*, 9.
- (223) Kannan, K. K. *Biomol. Struct., Conform., Funct., Evol., Proc. Int. Symp.* **1981**, *1*, 165.

- (224) Stams, T.; Nair, S. K.; Okuyama, T.; Waheed, A.; Sly, W. S.; Christianson, D. W. *Proc. Natl. Acad. Sci. U.S.A.* **1996**, *93*, 13589.
- (225) Temperini, C.; Innocenti, A.; Guerri, A.; Scozzafava, A.; Rusconi, S.; Supuran, C. T. *Bioorg. Med. Chem. Lett.* **2007**, *17*, 2210.
- (226) Temperini, C.; Innocenti, A.; Scozzafava, A.; Mastrolorenzo, A.; Supuran, C. T. *Bioorg. Med. Chem. Lett.* **2007**, *17*, 628.
- (227) Temperini, C.; Winum, J.-Y.; Montero, J.-L.; Scozzafava, A.; Supuran, C. T. *Bioorg. Med. Chem. Lett.* **2007**, *17*, 2795.
- (228) Abbate, F.; Supuran, C. T.; Scozzafava, A.; Orioli, P.; Stubbs, M. T.; Klebe, G. J. *Med. Chem.* **2002**, *45*, 3583.
- (229) Abbate, J.; Casini, A.; Owa, T.; Scozzafava, A.; Supuran, C. T. *Bioorg. Med. Chem. Lett.* **2004**, *14*, 217.
- (230) Abbate, J.; Winum, J.-Y.; Potter, B. V. L.; Casini, A.; Montero, J.-L.; Scozzafava, A.; Supuran, C. T. *Bioorg. Med. Chem. Lett.* **2004**, *14*, 231.
- (231) De Simone, G.; Di Fiore, A.; Menchise, V.; Pedone, C.; Antel, J.; Casini, A.; Scozzafava, A.; Wurl, M.; Supuran, C. T. *Bioorg. Med. Chem. Lett.* **2005**, *15*, 2315.
- (232) Winum, J.-Y.; Temperini, C.; Cheikh, K. E.; Innocenti, A.; Vullo, D.; Ciattini, S.; Montero, J.-L.; Scozzafava, A.; Supuran, C. T. *J. Med. Chem.* **2006**, *49*, 7024.
- (233) Casini, A.; Antel, J.; Abbate, F.; Scozzafava, A.; David, S.; Waldeck, H.; Schafer, S.; Supuran, C. T. *Bioorg. Med. Chem. Lett.* **2003**, *13*, 841.
- (234) Srivastava, D. K.; Jude, K. M.; Banerjee, A. L.; Haldar, M.; Manokaran, S.; Kooren, J.; Mallik, S.; Christianson, D. W. *J. Am. Chem. Soc.* **2007**, *129*, 5528.
- (235) Di Fiore, A.; Scozzafava, A.; Winum, J.-Y.; Montero, J.-L.; Pedone, C.; Supuran, C. T.; De Simone, G. *Bioorg. Med. Chem. Lett.* **2007**, *17*, 1726.
- (236) Alterio, V.; De Simone, G.; Monti, S. M.; Scozzafava, A.; Supuran, C. T. *Bioorg. Med. Chem. Lett.* **2007**, *17*, 4201.
- (237) Köhler, K.; Hillebrecht, A.; Wischeler, J. S.; Innocenti, A.; Heine, A.; Supuran, C. T.; Klebe, G. *Angew. Chem., Int. Ed.* **2007**, *46*, 7697.
- (238) Temperini, C.; Innocenti, A.; Mastrolorenzo, A.; Scozzafava, A.; Supuran, C. T. *Bioorg. Med. Chem. Lett.* **2007**, *17*, 4866.
- (239) Kannan, K. K.; Ramanadham, M.; Jones, T. A. *Ann. N. Y. Acad. Sci.* **1984**, *429*, 49.
- (240) Eriksson, A. E.; Jones, T. A.; Liljas, A. *Proteins: Struct., Funct., Genet.* **1988**, *4*, 274.
- (241) Budayova-Spano, M.; Fisher, S. Z.; Dauvergne, M. T.; Agbandje-McKenna, M.; Silverman, D. N.; Myles, D. A. A.; McKenna, R. *Acta Crystallogr., Sect. F* **2006**, *F62*, 6.
- (242) Duda, D. M.; Tu, C.; Fisher, S. Z.; An, H.; Yoshioka, C.; Govindasamy, L.; Laipis, P. J.; Agbandje-McKenna, M.; Silverman, D. N.; McKenna, R. *Biochemistry* **2005**, *44*, 10046.
- (243) Ippolito, J. A.; Baird, T. T., Jr.; McGee, S. A.; Christianson, D. W.; Fierke, C. A. *Proc. Natl. Acad. Sci. U.S.A.* **1995**, *92*, 5017.
- (244) Ippolito, J. A.; Christianson, D. W. *Biochemistry* **1993**, *32*, 9901.
- (245) Ippolito, J. A.; Christianson, D. W. *Biochemistry* **1994**, *33*, 15241.
- (246) Kiefer, L. L.; Ippolito, J. A.; Fierke, C. A.; Christianson, D. W. *J. Am. Chem. Soc.* **1993**, *115*, 12581.
- (247) Xue, Y.; Liljas, A.; Jonsson, B. H.; Lindskog, S. *Proteins: Struct., Funct., Genet.* **1993**, *17*, 93.
- (248) Lesburg, C. A.; Christianson, D. W. *J. Am. Chem. Soc.* **1995**, *117*, 6838.
- (249) Kim, C.-Y.; Chandra, P. P.; Jain, A.; Christianson, D. W. *J. Am. Chem. Soc.* **2001**, *123*, 9620.
- (250) Alexander, R. S.; Kiefer, L. L.; Fierke, C. A.; Christianson, D. W. *Biochemistry* **1993**, *32*, 1510.
- (251) Cox, J. D.; Hunt, J. A.; Compher, K. M.; Fierke, C. A.; Christianson, D. W. *Biochemistry* **2000**, *39*, 13687.
- (252) Huang, C.-c.; Lesburg, C. A.; Kiefer, L. L.; Fierke, C. A.; Christianson, D. W. *Biochemistry* **1996**, *35*, 3439.
- (253) Nair, S. K.; Christianson, D. W. *Biochemistry* **1993**, *32*, 4506.
- (254) Nair, S. K.; Krebs, J. F.; Christianson, D. W.; Fierke, C. A. *Biochemistry* **1995**, *34*, 3981.
- (255) Tweedy, N. B.; Nair, S. K.; Paterno, S. A.; Fierke, C. A.; Christianson, D. W. *Biochemistry* **1993**, *32*, 10944.
- (256) Xue, Y.; Vidgren, J.; Svensson, L. A.; Liljas, A.; Jonsson, B. H.; Lindskog, S. *Proteins: Struct., Funct., Genet.* **1993**, *15*, 80.
- (257) Krebs, J. F.; Fierke, C. A.; Alexander, R. S.; Christianson, D. W. *Biochemistry* **1991**, *30*, 9153.
- (258) Huang, S.; Sjöblom, B.; Sauer-Eriksson, A. E.; Jonsson, B.-H. *Biochemistry* **2002**, *41*, 7628.
- (259) Lesburg, C. A.; Huang, C.-c.; Christianson, D. W.; Fierke, C. A. *Biochemistry* **1997**, *36*, 15780.
- (260) Duda, D.; Tu, C.; Qian, M.; Laipis, P.; Agbandje-McKenna, M.; Silverman, D. N.; McKenna, R. *Biochemistry* **2001**, *40*, 1741.
- (261) Duda, D. M.; Govindasamy, L.; Agbandje-McKenna, M.; Tu, C. K.; Silverman, D. N.; McKenna, R. *Acta Crystallogr., Sect. D* **2003**, *D59*, 93.
- (262) Tu, C.; Qian, M.; An, H.; Wadhwa Nina, R.; Duda, D.; Yoshioka, C.; Pathak, Y.; McKenna, R.; Laipis Philip, J.; Silverman David, N. *J. Biol. Chem.* **2002**, *277*, 38870.
- (263) Bhatt, D.; Tu, C.; Fisher, S. Z.; Prada, J. A. H.; McKenna, R.; Silverman, D. N. *Proteins: Struct., Funct., Bioinf.* **2005**, *61*, 239.
- (264) Scolnick, L. R.; Christianson, D. W. *Biochemistry* **1996**, *35*, 16429.
- (265) Ferraroni, M.; Tilli, S.; Briganti, F.; Chegwidan, W. R.; Supuran Claudiu, T.; Wiebauer Karin, E.; Tashian Richard, E.; Scozzafava, A. *Biochemistry* **2002**, *41*, 6237.
- (266) Fisher, S. Z.; Tu, C.; Bhatt, D.; Govindasamy, L.; Agbandje-McKenna, M.; McKenna, R.; Silverman, D. N. *Biochemistry* **2007**, *46*, 3803.
- (267) Bhatt, D.; Fisher, S. Z.; Tu, C.; McKenna, R.; Silverman, D. N. *Biophys. J.* **2007**, *92*, 562.
- (268) Elder, I.; Fisher, Z.; Laipis, P. J.; Tu, C.; McKenna, R.; Silverman, D. N. *Proteins: Struct., Funct., Bioinf.* **2007**, *68*, 337.
- (269) Kiefer, L. L.; Paternao, S. A.; Fierke, C. A. *J. Am. Chem. Soc.* **1995**, *117*, 6831.
- (270) Culf, A. S.; Gerig, J. T.; Williams, P. G. *J. Biomol. NMR* **1997**, *10*, 293.
- (271) Gerig, J. T.; Moses, J. M. *J. Chem. Soc., Chem. Commun.* **1987**, 482.
- (272) Jarvet, J.; Olivson, A.; Mets, U.; Pooga, M.; Aguraiuja, R.; Lippmaa, E. *Eur. J. Biochem.* **1989**, *186*, 287.
- (273) Veenstra, D. L.; Gerig, J. T. *Magn. Reson. Chem.* **1998**, *36*, S169.
- (274) Dugad, L. B.; Cooley, C. R.; Gerig, J. T. *Biochemistry* **1989**, *28*, 3955.
- (275) Dugad, L. B.; Gerig, J. T. *Biochemistry* **1988**, *27*, 4310.
- (276) Kanamori, K.; Roberts, J. D. *Biochemistry* **1983**, *22*, 2658.
- (277) Blackburn, G. M.; Mann, B. E.; Taylor, B. F.; Worrall, A. F. *Eur. J. Biochem.* **1985**, *153*, 553.
- (278) Luy, B. *Angew. Chem., Int. Ed.* **2007**, *46*, 4214.
- (279) Sprangers, R.; Kay, L. E. *Nature* **2007**, *445*, 618.
- (280) Venters, R. A.; Farmer, B. T., II; Fierke, C. A.; Spicer, L. D. *J. Mol. Biol.* **1996**, *264*, 1101.
- (281) Sethson, I.; Edlund, U.; Holak, T. A.; Ross, A.; Jonsson, B.-H. *J. Biomol. NMR* **1996**, *8*, 417.
- (282) Guex, N.; Peitsch, M. C. *Electrophoresis* **1997**, *18*, 2714.
- (283) Lindahl, M.; Vidgren, J.; Eriksson, E.; Habash, J.; Harrop, S.; Helliwell, J.; Liljas, A.; Lindskog, M.; Walker, N. In *Carbonic Anhydrase: From Biochemistry and Genetics to Physiology and Clinical Medicine*; Botrè, F., Gros, G., Storey, B. T., Eds.; VCH: New York, 1991.
- (284) Jain, A.; Whitesides, G. M.; Alexander, R. S.; Christianson, D. W. *J. Med. Chem.* **1994**, *37*, 2100.
- (285) Nair, S. K.; Christianson, D. W. *J. Am. Chem. Soc.* **1991**, *113*, 9455.
- (286) Kannan, K. K.; Liljas, A.; Waara, I.; Bergsten, P. C.; Lovgren, S.; Strandberg, B.; Bengtsson, U.; Carlbom, U.; Fridborg, K.; Jarup, L.; Petef, M. *Cold Spring Harbor Symp. Quant. Biol.* **1971**, *36*, 221.
- (287) Liljas, A.; Kannan, K. K.; Bergsten, P. C.; Waara, I.; Fridborg, K.; Strandberg, B.; Carlbom, U.; Jarup, L.; Lovgren, S.; Petef, M. *Nature New Biol.* **1972**, *235*, 131.
- (288) Lindahl, M.; Liljas, A.; Habash, J.; Harrop, S.; Helliwell, J. R. *Acta Crystallogr., Sect. B* **1992**, *B48*, 281.
- (289) Christianson, D. W.; Fierke, C. A. *Acc. Chem. Res.* **1996**, *29*, 331.
- (290) Lindskog, S. In *Zinc Enzymes*; Bertini, I., Luchinat, C., Maret, W., Zeppezauer, M., Eds.; Birkhäuser: Boston, MA, 1986.
- (291) Prabhananda, B. S.; Rittger, E.; Grell, E. *Biophys. Chem.* **1987**, *26*, 217.
- (292) Stein, P. J.; Merrill, S. P.; Henkens, R. W. *J. Am. Chem. Soc.* **1977**, *99*, 3194.
- (293) Williams, T. J.; Henkens, R. W. *Biochemistry* **1985**, *24*, 2459.
- (294) Lindahl, M.; Svensson, L. A.; Liljas, A. *Proteins: Struct., Funct., Genet.* **1993**, *15*, 177.
- (295) Vallee, B. L.; Auld, D. S. *Acc. Chem. Res.* **1993**, *26*, 543.
- (296) Kernohan, J. C. *Biochim. Biophys. Acta* **1964**, *81*, 346.
- (297) Coleman, J. E. *J. Biol. Chem.* **1967**, *242*, 5212.
- (298) Lipton, A. S.; Heck, R. W.; Ellis, P. D. *J. Am. Chem. Soc.* **2004**, *126*, 4735.
- (299) Kernohan, J. C. *Biochim. Biophys. Acta* **1965**, *96*, 304.
- (300) Lindskog, S. *J. Biol. Chem.* **1963**, *238*, 945.
- (301) Lindskog, S. *Biochemistry* **1966**, *5*, 2641.
- (302) Taylor, P. W.; King, R. W.; Burgen, A. S. V. *Biochemistry* **1970**, *9*, 3894.
- (303) Liang, Z.; Xue, Y.; Behravan, G.; Jonsson, B.-H.; Lindskog, S. *Eur. J. Biochem.* **1993**, *211*, 821.
- (304) Kiefer, L. L.; Fierke, C. A. *Biochemistry* **1994**, *33*, 15233.
- (305) Riccardi, D.; Cui, Q. *J. Phys. Chem. A* **2007**, *111*, 5703.
- (306) Rogers, J. I.; Mukherjee, J.; Khalifah, R. G. *Biochemistry* **1987**, *26*, 5672.
- (307) Lindskog, S.; Thorslund, A. *Eur. J. Biochem.* **1968**, *3*, 453.
- (308) Deerfield, D. W., II; Carter, C. W., Jr.; Pedersen, L. G. *Int. J. Quantum Chem.* **2001**, *83*, 150.

- (309) Hunt, J. B.; Rhee, M.-J.; Storm, C. B. *Anal. Biochem.* **1977**, *79*, 614.
- (310) Lindskog, S.; Malmström, B. G. *J. Biol. Chem.* **1962**, *237*, 1129.
- (311) Hunt, J. A.; Ahmed, M.; Fierke, C. A. *Biochemistry* **1999**, *38*, 9054.
- (312) Armstrong, J. M.; Myers, D. V.; Verpoorte, J. A.; Edsall, J. T. *J. Biol. Chem.* **1966**, *241*, 5137.
- (313) Hunt, J. B.; Neece, S. H.; Schachman, H. K.; Ginsburg, A. *J. Biol. Chem.* **1984**, *259*, 14793.
- (314) Lindskog, S.; Nyman, P. O. *Biochim. Biophys. Acta* **1964**, *85*, 462.
- (315) Demille, G. R.; Larlee, K.; Livesey, D. L.; Mailer, K. *Chem. Phys. Lett.* **1979**, *64*, 534.
- (316) Haydock, C. *Los Alamos National Laboratory, Preprint Archive, Physics*; 2003, 1 arXiv:physics/0302097.
- (317) McCall, K. A.; Fierke, C. A. *Anal. Biochem.* **2000**, *284*, 307.
- (318) Led, J. J.; Neesgaard, E. *Biochemistry* **1987**, *26*, 183.
- (319) Kannan, K. K.; Fridborg, K.; Bergstén, P. C.; Liljas, A.; Lövgren, S.; Petef, M.; Strandberg, B.; Waara, I.; Adler, L.; Falkbring, S. O.; Göthe, P. O.; Nyman, P. O. *J. Mol. Biol.* **1972**, *63*, 601.
- (320) Yachandra, V.; Powers, L.; Spiro, T. G. *J. Am. Chem. Soc.* **1983**, *105*, 6596.
- (321) Hunt, J. A.; Fierke, C. A. *J. Biol. Chem.* **1997**, *272*, 20364.
- (322) McCall, K. A.; Fierke, C. A. *Biochemistry* **2004**, *43*, 3979.
- (323) Fierke, C. A.; Thompson, R. B. *Biometals* **2001**, *14*, 205.
- (324) Thompson, R. B.; Maliwal, B. P.; Fierke, C. A. *Anal. Biochem.* **1999**, *267*, 185.
- (325) Thompson, R. B.; Zeng, H.-H.; Maliwal, B. P.; Fierke, C. A. *Proc. SPIE—Int. Soc. Opt. Eng.* **2001**, *4252*, 12.
- (326) Hunt, J. A.; Lesburg, C. A.; Christianson, D. W.; Thompson, R. B.; Fierke, C. A. In *The Carbonic Anhydrases: New Horizons*; Chegwiddden, W. R., Carter, N. D., Edwards, Y. H., Eds.; Birkhäuser Verlag: Basel, Switzerland, 2000; Vol. 90.
- (327) Zeng, H. H.; Thompson, R. B.; Maliwal, B. P.; Fones, G. R.; Moffett, J. W.; Fierke, C. A. *Anal. Chem.* **2003**, *75*, 6807.
- (328) Frederickson, C. J.; Giblin, L. J.; Krezel, A.; McAdoo, D. J.; Muelle, R. N.; Zeng, Y.; Balaji, R. V.; Masalha, R.; Thompson, R. B.; Fierke, C. A.; Sarvey, J. M.; de Valdenebro, M.; Prough, D. S.; Zornow, M. H. *Exp. Neurol.* **2006**, *198*, 285.
- (329) Thompson, R. B.; Peterson, D.; Mahoney, W.; Cramer, M.; Maliwal, B. P.; Suh, S. W.; Frederickson, C.; Fierke, C.; Herman, P. J. *Neurosci. Methods* **2002**, *118*, 63.
- (330) Thompson, R. B.; Whetsell, W. O., Jr.; Maliwal, B. P.; Fierke, C. A.; Frederickson, C. J. *J. Neurosci. Methods* **2000**, *96*, 35.
- (331) Kimura, E.; Shiota, T.; Koike, T.; Shiro, M.; Kodama, M. *J. Am. Chem. Soc.* **1990**, *112*, 5805.
- (332) Kiefer, L. L.; Krebs, J. F.; Paterno, S. A.; Fierke, C. A. *Biochemistry* **1993**, *32*, 9896.
- (333) Parkin, G. *Adv. Inorg. Chem.* **1995**, *42*.
- (334) Vahrenkamp, H. *Acc. Chem. Res.* **1999**, *32*, 589.
- (335) Kimura, E. *Acc. Chem. Res.* **2001**, *34*, 171.
- (336) Parkin, G. *Chem. Rev.* **2004**, *104*, 699.
- (337) Alsfasser, R.; Powell, A. K.; Vahrenkamp, H. *Angew. Chem., Int. Ed. Engl.* **1990**, *29*, 898.
- (338) Alsfasser, R.; Ruf, M.; Trofimenko, S.; Vahrenkamp, H. *Chem. Ber.* **1993**, *126*, 703.
- (339) Alsfasser, R.; Trofimenko, S.; Looney, A.; Parkin, G.; Vahrenkamp, H. *Inorg. Chem.* **1991**, *30*, 4098.
- (340) Looney, A.; Parkin, G.; Alsfasser, R.; Ruf, M.; Vahrenkamp, H. *Angew. Chem., Int. Ed. Engl.* **1992**, *31*, 92.
- (341) Looney, A.; Saleh, A.; Zhang, Y.; Parkin, G. *Inorg. Chem.* **1994**, *33*, 1158.
- (342) Rombach, M.; Maurer, C.; Weis, K.; Keller, E.; Vahrenkamp, H. *Chem.—Eur. J.* **1999**, *5*, 1013.
- (343) The value of pK_a was determined potentiometrically in water/methanol/dichloromethane using suitable electrodes and referencing procedures.
- (344) Ruf, M.; Vahrenkamp, H. *Chem. Ber.* **1996**, *129*, 1025.
- (345) Ruf, M.; Weis, K.; Vahrenkamp, H. *J. Chem. Soc., Chem. Commun.* **1994**, 135.
- (346) Looney, A.; Han, R.; McNeill, K.; Parkin, G. *J. Am. Chem. Soc.* **1993**, *115*, 4690.
- (347) Bergquist, C.; Fillebeen, T.; Morlok, M. M.; Parkin, G. *J. Am. Chem. Soc.* **2003**, *125*, 6189.
- (348) Bergquist, C.; Parkin, G. *J. Am. Chem. Soc.* **1999**, *121*, 6322.
- (349) Sprigings, T. G.; Hall, C. D. *J. Chem. Soc., Perkin Trans. 2* **2001**, 2063.
- (350) Koike, T.; Kimura, E.; Nakamura, I.; Hashimoto, Y.; Shiro, M. *J. Am. Chem. Soc.* **1992**, *114*, 7338.
- (351) Zhang, X. P.; Vaneldik, R.; Koike, T.; Kimura, E. *Inorg. Chem.* **1993**, *32*, 5749.
- (352) Wade, W. S.; Koh, J. S.; Han, N.; Hoekstra, D. M.; Lerner, R. A. *J. Am. Chem. Soc.* **1993**, *115*, 4449.
- (353) Roberts, V. A.; Iverson, B. L.; Iverson, S. A.; Benkovic, S. J.; Lerner, R. A.; Getzoff, E. D.; Tainer, J. A. *Proc. Natl. Acad. Sci. U.S.A.* **1990**, *87*, 6654.
- (354) Iverson, B. L.; Iverson, S. A.; Roberts, V. A.; Getzoff, E. D.; Tainer, J. A.; Benkovic, S. J.; Lerner, R. A. *Science* **1990**, *249*, 659.
- (355) Mueller, H. N.; Skerra, A. *Biochemistry* **1994**, *33*, 14126.
- (356) Verpoorte, J. A.; Mehta, S.; Edsall, J. T. *J. Biol. Chem.* **1967**, *242*, 4221.
- (357) Henry, R. P. In *The Carbonic Anhydrases: Cellular Physiology and Molecular Genetics*; Carter, N. D., Dodgson, S. J., Gros, G., Tashian, R. E. Eds.; Plenum Press: New York, 1991.
- (358) Klocke, R. A. *J. Appl. Physiol.* **1976**, *40*, 707.
- (359) Sirs, J. A. *Trans. Faraday Soc.* **1958**, *54*, 207.
- (360) Rossi-Bernardi, L.; Berger, R. L. *J. Biol. Chem.* **1968**, *243*, 1297.
- (361) Silverman, D. N. *Methods Enzymol.* **1982**, *87*, 732.
- (362) Karler, R.; Woodbury, D. M. *Anal. Biochem.* **1963**, *6*, 381.
- (363) Forster, R. E.; Constantine, H. P.; Craw, M. R.; Rotman, H. H.; Klocke, R. A.; Thyrum, D. *J. Biol. Chem.* **1968**, *243*, 3317.
- (364) Gibbons, B. H.; Edsall, J. T. *J. Biol. Chem.* **1964**, *239*, 2539.
- (365) Kernohan, J. C.; Roughton, F. W. *J. Physiol.* **1968**, *197*, 345.
- (366) Kernohan, J. C. *Biochem. J.* **1970**, *120*, 26P.
- (367) Finazzi Agrò, A.; Morpurgo, L.; Mondovi, B. *Biophys. Chem.* **1974**, *2*, 151.
- (368) Chen, R. F.; Kernohan, J. C. *J. Biol. Chem.* **1967**, *242*, 5813.
- (369) Mårtensson, L.-G.; Jonasson, P.; Freskgård, P.-O.; Svensson, M.; Carlsson, U.; Jonsson, B.-H. *Biochemistry* **1995**, *34*, 1011.
- (370) Galley, W. C.; Strambini, G. B. *Nature* **1976**, *261*, 521.
- (371) Galley, W. C.; Stryer, L. *Proc. Natl. Acad. Sci. U.S.A.* **1968**, *60*, 108.
- (372) Bazin, M.; Aubailly, M.; Santus, R. *Chem. Phys. Lett.* **1972**, *13*, 310.
- (373) Parkkila, A.-K.; Parkkila, S.; Serlo, W.; Reunanen, M.; Vierjoki, T.; Rajaniemi, H. *Clin. Chim. Acta* **1994**, *230*, 81.
- (374) Vuori, J.; Rasi, S.; Takala, T.; Vaananen, K. *Clin. Chem.* **1991**, *37*, 2087.
- (375) Viappiani, C. *Biophys. Chem.* **1994**, *50*, 293.
- (376) Banerjee, J.; Halder, M. K.; Manokaran, S.; Mallik, S.; Srivastava, D. K. *Chem. Commun.* **2007**, 2723.
- (377) Jain, A.; Huang, S. G.; Whitesides, G. M. *J. Am. Chem. Soc.* **1994**, *116*, 5057.
- (378) Ponticello, G. S.; Freedman, M. B.; Habecker, C. N.; Lyle, P. A.; Schwam, H.; Varga, S. L.; Christy, M. E.; Randall, W. C.; Baldwin, J. J. *J. Med. Chem.* **1987**, *30*, 591.
- (379) Thompson, R. B.; Maliwal, B. P. *Anal. Chem.* **1998**, *70*, 1749.
- (380) Enander, K.; Dolphin, G. T.; Andersson, L. K.; Liedberg, B.; Lundström, I.; Baltzer, L. *J. Org. Chem.* **2002**, *67*, 3120.
- (381) Enander, K.; Dolphin, G. T.; Baltzer, L. *J. Am. Chem. Soc.* **2004**, *126*, 4464.
- (382) Bozym, R. A.; Thompson, R. B.; Stoddard, A. K.; Fierke, C. A. *ACS Chem. Biol.* **2006**, *1*, 103.
- (383) Lespagnol, A.; Osteux, R.; Bar, D. *Bull. Soc. Chim. Biol.* **1961**, *43*, 789.
- (384) Nguyen, R.; Huc, I. *Angew. Chem., Int. Ed.* **2001**, *40*, 1774.
- (385) Kaim, J. T.; Brodsky, W. A. *Am. J. Physiol.* **1959**, *197*, 1097.
- (386) Philpot, F. J.; Philpot, J. S. L. *Biochem. J.* **1936**, *30*, 2191.
- (387) Brinkman, R. J. *Physiol.* **1933**, *80*, 170.
- (388) Wilson, J. M.; Tanko, Q.; Wendland, M. M.; Meany, J. E.; Nedved, J. F.; Pocker, Y. *Physiol. Chem. Phys. Med. NMR* **1998**, *30*, 149.
- (389) King, R. W.; Burgen, A. S. V. *Proc. R. Soc. London, B* **1976**, *193*, 107.
- (390) King, R. W.; Burgen, A. S. V. *Biochim. Biophys. Acta* **1970**, *207*, 278.
- (391) Chu, Y. H.; Avila, L. Z.; Biebuyck, H. A.; Whitesides, G. M. *J. Med. Chem.* **1992**, *35*, 2915.
- (392) Avila, L. Z.; Chu, Y.-H.; Blossley, E. C.; Whitesides, G. M. *J. Med. Chem.* **1993**, *36*, 126.
- (393) Gomez, F. A.; Avila, L. Z.; Chu, Y.-H.; Whitesides, G. M. *Anal. Chem.* **1994**, *66*, 1785.
- (394) Chu, Y.-H.; Avila, L. Z.; Gao, J.; Whitesides, G. M. *Acc. Chem. Res.* **1995**, *28*, 461.
- (395) Grossman, P. D. *Capillary Electrophoresis: Theory and Practice*; Academic Press, Inc: San Diego, CA, 1992.
- (396) Gao, J.; Mammen, M.; Whitesides, G. M. *Science* **1996**, *272*, 535.
- (397) Gitlin, I.; Carbeck, J. D.; Whitesides, G. M. *Angew. Chem., Int. Ed.* **2006**, *45*, 3022.
- (398) Colton, I. J.; Carbeck, J. D.; Rao, J.; Whitesides, G. M. *Electrophoresis* **1998**, *19*, 367.
- (399) Chu, Y.-H.; Chen, J. K.; Whitesides, G. M. *Anal. Chem.* **1993**, *65*, 1314.
- (400) Biltonen, R. L.; Langerman, N. *Methods Enzymol.* **1979**, *61*, 287.
- (401) Sturtevant, J. M. *Methods Enzymol.* **1972**, *26*, 227.
- (402) Talhout, R.; Villa, A.; Mark, A. E.; Engberts, J. B. F. N. *J. Am. Chem. Soc.* **2003**, *125*, 10570.
- (403) Williams, D. H.; Stephens, E.; O'Brien, D. P.; Zhou, M. *Angew. Chem., Int. Ed.* **2004**, *43*, 6596.
- (404) Henkens, R. W.; Watt, G. D.; Sturtevant, J. M. *Biochemistry* **1969**, *8*, 1874.

- (405) Binford, J. S.; Lindskog, S.; Wadsö, I. *Biochim. Biophys. Acta* **1974**, *341*, 345.
- (406) Jelesarov, I.; Bosshard, H. R. *J. Mol. Recognit.* **1999**, *12*, 3.
- (407) Bhakuni, V. *Arch. Biochem. Biophys.* **1998**, *357*, 274.
- (408) Wiseman, T.; Williston, S.; Brandts, J. F.; Lin, L.-N. *Anal. Biochem.* **1989**, *179*, 131.
- (409) Khalifah, R. G.; Zhang, F.; Parr, J. S.; Rowe, E. S. *Biochemistry* **1993**, *32*, 3058.
- (410) Pierce, M. M.; Raman, C. S.; Nall, B. T. *Methods* **1999**, *19*, 213.
- (411) DiTusa, C. A.; Christensen, T.; McCall, K. A.; Fierke, C. A.; Toone, E. J. *Biochemistry* **2001**, *40*, 5338.
- (412) Day, Y. S. N.; Baird, C. L.; Rich, R. L.; Myszka, D. G. *Protein Sci.* **2002**, *11*, 1017.
- (413) Franchi, M.; Vullo, D.; Gallori, E.; Antel, J.; Wurl, M.; Scozzafava, A.; Supuran, C. T. *Bioorg. Med. Chem. Lett.* **2003**, *13*, 2857.
- (414) Melkko, S.; Scheuermann, J.; Dumelin, C. E.; Neri, D. *Nature Biotechnol.* **2004**, *22*, 568.
- (415) Krishnamurthy, V. M.; Bohall, B. R.; Semetey, V.; Whitesides, G. M. *J. Am. Chem. Soc.* **2006**, *128*, 5802.
- (416) Krishnamurthy, V. M.; Estroff, L. A.; Whitesides, G. M. In *Fragment-based Approaches in Drug Discovery*; Erlanson, D., Jahnke, W., Eds.; Wiley-VCH: Weinheim, Germany, 2006; Vol. 34.
- (417) Matulis, D.; Todd, M. In *Bioanalytical Chemistry 2: Applications of Calorimetry in the Biological Sciences*, 2nd ed.; Ladbury, J. E., Doyle, M. L., Eds.; John Wiley & Sons: New York, 2004.
- (418) Jain, A.; Marzluff, E. M.; Jacobsen, J. R.; Whitesides, G. M.; Grabowski, J. J. *J. Chem. Soc., Chem. Commun.* **1989**, 1557.
- (419) Carey, P. R.; King, R. W. *Biochemistry* **1979**, *18*, 2834.
- (420) Moratal, J. M.; Martinez-Ferrer, M. J.; Jimenez, H. R.; Donaire, A.; Castells, J.; Salgado, J. *J. Inorg. Biochem.* **1992**, *45*, 231.
- (421) Moratal, J. M.; Martinez-Ferrer, M. J.; Donaire, A.; Castells, J.; Salgado, J.; Jimenez, H. R. *J. Chem. Soc., Dalton Trans.* **1991**, 3393.
- (422) Anelli, P. L.; Bertini, I.; Fragai, M.; Lattuada, L.; Luchinat, C.; Parigi, G. *Eur. J. Inorg. Chem.* **2000**, *2000*, 625.
- (423) Cleland, J. L.; Hedgpeeth, C.; Wang, D. I. C. *J. Biol. Chem.* **1992**, *267*, 13327.
- (424) Hower, J. F.; Henkens, R. W.; Chesnut, D. B. *J. Am. Chem. Soc.* **1971**, *93*, 6665.
- (425) Taylor, J. S.; Mushak, P.; Coleman, J. E. *Proc. Natl. Acad. Sci. U.S.A.* **1970**, *67*, 1410.
- (426) Bayley, P.; Anson, M. *Biochem. Biophys. Res. Commun.* **1975**, *62*, 717.
- (427) Gianazza, E.; Sirtori, C. R.; Castiglioni, S.; Eberini, I.; Chrambach, A.; Rondanini, A.; Vecchio, G. *Electrophoresis* **2000**, *21*, 1435.
- (428) Berova, N.; Nakanishi, K.; Woody, R. W. *Circular Dichroism*, 2nd ed.; Wiley-VCH: New York, 2000.
- (429) Freskgård, P.-O.; Mårtensson, L.-G.; Jonasson, P.; Jonsson, B.-H.; Carlsson, U. *Biochemistry* **1994**, *33*, 14281.
- (430) Coleman, J. E. *J. Am. Chem. Soc.* **1967**, *89*, 6757.
- (431) Hofstadler, S. A.; Sannes-Lowery, K. A. *Nat. Rev. Drug Discovery* **2006**, *5*, 585.
- (432) Deng, G. J.; Sanyal, G. *J. Pharm. Biomed. Anal.* **2006**, *40*, 528.
- (433) Nesatyy, V. J. *Int. J. Mass Spectrom.* **2002**, *221*, 147.
- (434) Daniel, J. M.; Friess, S. D.; Rajagopalan, S.; Wendt, S.; Zenobi, R. *Int. J. Mass Spectrom.* **2002**, *216*, 1.
- (435) Purcell, A. W.; Gorman, J. J. *Mol. Cell. Proteomics* **2004**, *3*, 193.
- (436) Naylor, S.; Kumar, R. *Adv. Protein Chem.* **2003**, *65*, 217.
- (437) Sickmann, A.; Mreyen, M.; Meyer, H. E. *Adv. Biochem. Eng. Biotechnol.* **2003**, *83*, 141.
- (438) Loo, J. A. *Adv. Protein Chem.* **2003**, *65*, 25.
- (439) Karas, M. *G.I.T. Lab. J., Eur.* **2003**, *7*, 259.
- (440) Aebersold, R.; Mann, M. *Nature* **2003**, *422*, 198.
- (441) Trauger, S. A.; Webb, W.; Siuzdak, G. *Spectroscopy* **2002**, *16*, 15.
- (442) Mann, M.; Hendrickson, R. C.; Pandey, A. *Annu. Rev. Biochem.* **2001**, *70*, 437.
- (443) Cheng, X.; Chen, R.; Bruce, J. E.; Schwartz, B. L.; Anderson, G. A.; Hofstadler, S. A.; Gale, D. C.; Smith, R. D.; Gao, J.; Sigal, G. B.; Mammen, M.; Whitesides, G. M. *J. Am. Chem. Soc.* **1995**, *117*, 8859.
- (444) Gao, J.; Cheng, X.; Chen, R.; Sigal, G. B.; Bruce, J. E.; Schwartz, B. L.; Hofstadler, S. A.; Anderson, G. A.; Smith, R. D.; Whitesides, G. M. *J. Med. Chem.* **1996**, *39*, 1949.
- (445) Wu, Q.; Gao, J.; Joseph-McCarthy, D.; Sigal, G. B.; Bruce, J. E.; Whitesides, G. M.; Smith, R. D. *J. Am. Chem. Soc.* **1997**, *119*, 1157.
- (446) Gao, J.; Wu, Q.; Carbeck, J.; Lei, Q. P.; Smith, R. D.; Whitesides, G. M. *Biophys. J.* **1999**, *76*, 3253.
- (447) Kiese, M. *Biochem. Z.* **1941**, *307*, 400.
- (448) Roughton, F. J. W.; Booth, V. H. *Biochem. J.* **1946**, *40*, 319.
- (449) Roughton, F. J. W.; Booth, V. H. *Biochem. J.* **1946**, *40*, 309.
- (450) Davis, R. P. *J. Am. Chem. Soc.* **1959**, *81*, 5674.
- (451) Davis, R. P. *J. Am. Chem. Soc.* **1958**, *80*, 5209.
- (452) DeVoe, H.; Kistiakowsky, G. B. *J. Am. Chem. Soc.* **1961**, *83*, 274.
- (453) Kernohan, J. C.; Forrest, W. W.; Roughton, W. F. *J. Biochim. Biophys. Acta* **1963**, *67*, 31.
- (454) Kernohan, J. C. *Biochim. Biophys. Acta* **1966**, *118*, 405.
- (455) Pocker, Y.; Stone, J. T. *J. Am. Chem. Soc.* **1965**, *87*, 5497.
- (456) Pocker, Y.; Stone, J. T. *Biochemistry* **1968**, *7*, 3021.
- (457) Pocker, Y.; Storm, D. R. *Biochemistry* **1968**, *7*, 1202.
- (458) Taylor, P. W.; King, R. W.; Burgen, A. S. V. *Biochemistry* **1970**, *9*, 2638.
- (459) Kretschmann, E.; Raether, H. Z. *Naturforsch., A: Astrophys. Phys. Phys. Chem.* **1968**, *23*, 2135.
- (460) Ramsden, J. J. *J. Mol. Recognit.* **1997**, *10*, 109.
- (461) Fagerstam, L. G.; Frostell-Karlsson, A.; Karlsson, R.; Persson, B.; Ronnberg, I. *J. Chromatogr.* **1992**, *597*, 397.
- (462) Chaiken, I.; Rose, S.; Karlsson, R. *Anal. Biochem.* **1991**, *201*, 197.
- (463) Stenberg, E.; Persson, B.; Roos, H.; Urbaniczky, C. *J. Colloid Interface Sci.* **1991**, *143*, 513.
- (464) McDonnell, J. M. *Curr. Opin. Chem. Biol.* **2001**, *5*, 572.
- (465) Myszka, D. G. *Curr. Opin. Biotechnol.* **1997**, *8*, 50.
- (466) Rich, R. L.; Myszka, D. G. *J. Mol. Recognit.* **2003**, *16*, 351.
- (467) Mrksich, M.; Grunwell, J. R.; Whitesides, G. M. *J. Am. Chem. Soc.* **1995**, *117*, 12009.
- (468) Mrksich, M.; Sigal, G. B.; Whitesides, G. M. *Langmuir* **1995**, *11*, 4383.
- (469) Sigal, G. B.; Bamdad, C.; Barberis, A.; Strominger, J.; Whitesides, G. M. *Anal. Chem.* **1996**, *68*, 490.
- (470) Bishop, A. R.; Nuzzo, R. G. *Curr. Opin. Colloid Interface Sci.* **1996**, *1*, 127.
- (471) Xia, Y. N.; Rogers, J. A.; Paul, K. E.; Whitesides, G. M. *Chem. Rev.* **1999**, *99*, 1823.
- (472) Love, J. C.; Wolfe, D. B.; Haasch, R.; Chabinc, M. L.; Paul, K. E.; Whitesides, G. M.; Nuzzo, R. G. *J. Am. Chem. Soc.* **2003**, *125*, 2597.
- (473) Jiang, X.; Bruzewicz, D. A.; Thant, M. M.; Whitesides, G. M. *Anal. Chem.* **2004**, *76*, 6116.
- (474) Lahiri, J.; Isaacs, L.; Tien, J.; Whitesides, G. M. *Anal. Chem.* **1999**, *71*, 777.
- (475) Bain, C. D.; Troughton, E. B.; Tao, Y.-T.; Evall, J.; Whitesides, G. M.; Nuzzo, R. G. *J. Am. Chem. Soc.* **1989**, *111*, 321.
- (476) Laibinis, P. E.; Bain, C. D.; Nuzzo, R. G.; Whitesides, G. M. *J. Phys. Chem.* **1995**, *99*, 7663.
- (477) Xia, Y. N.; Whitesides, G. M. *Angew. Chem., Int. Ed. Engl.* **1998**, *37*, 551.
- (478) Yan, L.; Marzolin, C.; Terfort, A.; Whitesides, G. M. *Langmuir* **1997**, *13*, 6704.
- (479) Lahiri, J.; Ostuni, E.; Whitesides, G. M. *Langmuir* **1999**, *15*, 2055.
- (480) Whitesides, G. M.; Ostuni, E.; Takayama, S.; Jiang, X. Y.; Ingber, D. E. *Annu. Rev. Biomed. Eng.* **2001**, *3*, 335.
- (481) Mrksich, M.; Whitesides, G. M. *Annu. Rev. Biophys. Biomol. Struct.* **1996**, *25*, 55.
- (482) Chapman, R. G.; Ostuni, E.; Takayama, S.; Holmlin, R. E.; Yan, L.; Whitesides, G. M. *J. Am. Chem. Soc.* **2000**, *122*, 8303.
- (483) Chapman, R. G.; Ostuni, E.; Yan, L.; Whitesides, G. M. *Langmuir* **2000**, *16*, 6927.
- (484) Ostuni, E.; Chapman, R. G.; Liang, M. N.; Meluleni, G.; Peir, G.; Ingber, D. E.; Whitesides, G. M. *Langmuir* **2001**, *17*, 6336.
- (485) Ostuni, E.; Chapman, R. G.; Holmlin, R. E.; Takayama, S.; Whitesides, G. M. *Langmuir* **2001**, *17*, 5605.
- (486) Qian, X. P.; Metallo, S. J.; Choi, I. S.; Wu, H. K.; Liang, M. N.; Whitesides, G. M. *Anal. Chem.* **2002**, *74*, 1805.
- (487) Mullett, W. M.; Lai, E. P. C.; Yeung, J. M. *Methods* **2000**, *22*, 77.
- (488) Houseman, B. T.; Mrksich, M. In *Host-Guest Chemistry - Mimetic Approaches to Study Carbohydrate Recognition*; Springer-Verlag: Berlin, 2002; Vol. 218/2001.
- (489) Cooper, M. A. *Anal. Bioanal. Chem.* **2003**, *377*, 834.
- (490) Shumaker-Parry, J. S.; Campbell, C. T. *Anal. Chem.* **2004**, *76*, 907.
- (491) Marx, K. A. *Biomacromolecules* **2003**, *4*, 1099.
- (492) Kato, M.; Mrksich, M. *J. Am. Chem. Soc.* **2004**, *126*, 6504.
- (493) Ostuni, E.; Grzybowski, B. A.; Mrksich, M.; Roberts, C. S.; Whitesides, G. M. *Langmuir* **2003**, *19*, 1861.
- (494) Scozzafava, A.; Supuran, C. T. *J. Med. Chem.* **2002**, *45*, 284.
- (495) Bajaj, S.; Sambi, S. S.; Madan, A. K. *QSAR Comb. Sci.* **2004**, *23*, 431.
- (496) Ilies, M.; Banciu, M. D.; Ilies, M. A.; Scozzafava, A.; Caproiu, M. T.; Supuran, C. T. *J. Med. Chem.* **2002**, *45*, 504.
- (497) Ilies, M.; Scozzafava, A.; Supuran, C. T. In *Carbonic Anhydrase: Its Inhibitors and Activators*; Supuran, C. T., Scozzafava, A., Conway, J., Eds.; CRC Press: Boca Raton, FL, 2004; Vol. 1.
- (498) Supuran, C. T.; Vullo, D.; Manole, G.; Casini, A.; Scozzafava, A. *Curr. Med. Chem.: Cardiovasc. Hematol. Agents* **2004**, *2*, 49.
- (499) Supuran, C. T.; Scozzafava, A. *Expert Opin. Ther. Patents* **2002**, *12*, 217.
- (500) Maren, T. H. *Annu. Rev. Pharmacol. Toxicol.* **1976**, *16*, 309.

- (501) Mansoor, U. F.; Zhang, X.-R.; Blackburn, G. M. In *The Carbonic Anhydrases: New Horizons*; Chegwidan, W. R., Carter, N. D., Edwards, Y. H., Eds.; Birkhäuser Verlag: Basel, Switzerland, 2000; Vol. 90.
- (502) Scozzafava, A.; Mastrolorenzo, A.; Supuran, C. T. *Expert Opin. Ther. Patents* **2006**, *16*, 1627.
- (503) Kakeya, N.; Aoki, M.; Kamada, A.; Yata, N. *Chem. Pharm. Bull.* **1969**, *17*, 1010.
- (504) Lo, Y. S.; Nolan, J. C.; Maren, T. H.; Welstead, W. J.; Gripshover, D. F.; Shamblee, D. A. *J. Med. Chem.* **1992**, *35*, 4790.
- (505) Scholz, T. H.; Sondey, J. M.; Randall, W. C.; Schwam, H.; Thompson, W. J.; Mallorga, P. J.; Sugrue, M. F.; Graham, S. L. *J. Med. Chem.* **1993**, *36*, 2134.
- (506) Burbaum, J. J.; Ohlmeyer, M. H.; Reader, J. C.; Henderson, I.; Dillard, L. W.; Li, G.; Randle, T. L.; Sigal, N. H.; Chelsky, D.; Baldwin, J. J. *Proc. Natl. Acad. Sci. U.S.A.* **1995**, *92*, 6027.
- (507) Sigal, G. B.; Whitesides, G. M. *Bioorg. Med. Chem. Lett.* **1996**, *6*, 559.
- (508) Gao, J.; Qiao, S.; Whitesides, G. M. *J. Med. Chem.* **1995**, *38*, 2292.
- (509) Hunt, C. A.; Mallorga, P. J.; Michelson, S. R.; Schwam, H.; Sondey, J. M.; Smith, R. L.; Sugrue, M. F.; Shepard, K. L. *J. Med. Chem.* **1994**, *37*, 240.
- (510) Winum, J.-Y.; Casini, A.; Mincione, F.; Starnotti, M.; Montero, J.-L.; Scozzafava, A.; Supuran, C. T. *Bioorg. Med. Chem. Lett.* **2004**, *14*, 225.
- (511) Casini, A.; Scozzafava, A.; Mincione, F.; Menabuoni, L.; Starnotti, M.; Supuran, C. T. *Bioorg. Med. Chem. Lett.* **2003**, *13*, 2867.
- (512) Graham, S. L.; Hoffman, J. M.; Gautheron, P.; Michelson, S. R.; Scholz, T. H.; Schwam, H.; Shepard, K. L.; Smith, A. M.; Smith, R. L.; Sondey, J. M. *J. Med. Chem.* **1990**, *33*, 749.
- (513) Prugh, J. D.; Hartman, G. D.; Mallorga, P. J.; McKeever, B. M.; Michelson, S. R.; Murcko, M. A.; Schwam, H.; Smith, R. L.; Sondey, J. M.; Springer, J. P. *J. Med. Chem.* **1991**, *34*, 1805.
- (514) Baldwin, J. J.; Ponticello, G. S.; Anderson, P. S.; Christy, M. E.; Murcko, M. A.; Randall, W. C.; Schwam, H.; Sugrue, M. F.; Gautheron, P.; et al. *J. Med. Chem.* **1989**, *32*, 2510.
- (515) Doyon, J. B.; Hansen, E. A. M.; Kim, C. Y.; Chang, J. S.; Christianson, D. W.; Madder, R. D.; Voet, J. G.; Baird, T. A.; Fierke, C. A.; Jain, A. *Org. Lett.* **2000**, *2*, 2557.
- (516) Doyon, J. B.; Hansen, E. A. M.; Kim, C.-Y.; Chang, J. S.; Christianson, D. W.; Madder, R. D.; Voet, J. G.; Baird, T. A.; Fierke, C. A.; Jain, A. *Org. Lett.* **2000**, *2*, 1189.
- (517) Hartman, G. D.; Halczenko, W.; Smith, R. L.; Sugrue, M. F.; Mallorga, P. J.; Michelson, S. R.; Randall, W. C.; Schwam, H.; Sondey, J. M. *J. Med. Chem.* **1992**, *35*, 3822.
- (518) Hartman, G. D.; Halczenko, W.; Prugh, J. D.; Smith, R. L.; Sugrue, M. F.; Mallorga, P. J.; Michelson, S. R.; Randall, W. C.; Schwam, H.; Sondey, J. M. *J. Med. Chem.* **1992**, *35*, 3027.
- (519) Briganti, F.; Pierattelli, A.; Scozzafava, A.; Supuran, C. T. *Eur. J. Med. Chem.* **1996**, *31*, 1001.
- (520) Fenesan, I.; Popescu, R.; Scozzafava, A.; Crucin, V.; Mateciuc, E.; Bauer, R.; Ilies, M. A.; Supuran, C. T. *J. Enzyme Inhib.* **2000**, *15*, 297.
- (521) Maren, T. H. *Mol. Pharmacol.* **1992**, *41*, 419.
- (522) Mincione, F.; Menabuoni, L.; Briganti, F.; Mincione, G.; Scozzafava, A.; Supuran, C. T. *J. Enzyme Inhib.* **1998**, *13*, 267.
- (523) Winum, J.-Y.; Vullo, D.; Casini, A.; Montero, J.-L.; Scozzafava, A.; Supuran, C. T. *J. Med. Chem.* **2003**, *46*, 2197.
- (524) Mann, T.; Keilin, D. *Nature* **1940**, *146*, 164.
- (525) Maren, T. H. *Invest. Ophthalmol. Vision Sci.* **1974**, *13*, 479.
- (526) Scozzafava, A.; Banciu, M. D.; Popescu, A.; Supuran, C. T. *J. Enzyme Inhib.* **2000**, *15*, 443.
- (527) Supuran, C. T.; Scozzafava, A. *Curr. Med. Chem.: Immunol. Endocrinol. Metab. Agents* **2001**, *1*, 61.
- (528) Maren, T. H.; Conroy, C. W. *J. Biol. Chem.* **1993**, *268*, 26233.
- (529) Jayaweera, G. D. S. A.; MacNeil, S. A.; Trager, S. F.; Blackburn, G. M. *Bioorg. Med. Chem. Lett.* **1991**, *1*, 407.
- (530) Antonaroli, S.; Bianco, A.; Brufani, M.; Cellai, L.; Lo Baido, G.; Potier, E.; Bonomi, L.; Perfetti, S.; Fiaschi, A. I.; Segre, G. *J. Med. Chem.* **1992**, *35*, 2697.
- (531) Maren, T. H.; Wynns, G. C.; Wistrand, P. J. *Mol. Pharmacol.* **1993**, *44*, 901.
- (532) Tinker, J. P.; Coulson, R.; Weiner, I. M. *J. Pharmacol. Exp. Ther.* **1981**, *218*, 600.
- (533) Lucci, M. S.; Tinker, J. P.; Weiner, I. M.; DuBose, T. D., Jr. *Am. J. Physiol.* **1983**, *245*, F443.
- (534) Vullo, D.; Innocenti, A.; Nishimori, I.; Pastorek, J.; Scozzafava, A.; Pastoreková, S.; Supuran, C. T. *Bioorg. Med. Chem. Lett.* **2005**, *15*, 963.
- (535) Supuran, C. T. *Expert Opin. Ther. Patents* **2003**, *13*, 1545.
- (536) Wilkinson, B. L.; Bornaghi, L. F.; Houston, T. A.; Innocenti, A.; Supuran, C. T.; Poulsen, S.-A. *J. Med. Chem.* **2006**, *49*, 6539.
- (537) Shah, G. N.; Hewett-Emmett, D.; Grubb, J. H.; Migas, M. C.; Fleming, R. E.; Waheed, A.; Sly, W. S. *Proc. Natl. Acad. Sci. U.S.A.* **2000**, *97*, 1677.
- (538) Montgomery, J. C.; Venta, P. J.; Eddy, R. L.; Fukushima, Y.-S.; Shows, T. B.; Tashian, R. E. *Genomics* **1991**, *11*, 835.
- (539) Opavský, R.; Pastoreková, S.; Zelník, V.; Gibadulinová, A.; Stanbridge, E. J.; Závada, J.; Kettmann, R.; Pastorek, J. *Genomics* **1996**, *33*, 480.
- (540) Aldred, P.; Fu, P.; Barrett, G.; Penschow, J. D.; Wright, R. D.; Coghlan, J. P.; Fernley, R. T. *Biochemistry* **1991**, *30*, 569.
- (541) Skaggs, L. A.; Bergenhem, N. C. H.; Venta, P. J.; Tashian, R. E. *Gene* **1993**, *126*, 291.
- (542) Krebs, H. A.; Sykes, W. O.; Bartley, W. C. *Biochem. J.* **1947**, *41*, 622.
- (543) Innocenti, A.; Casini, A.; Alcaro, M. C.; Papini, A. M.; Scozzafava, A.; Supuran, C. T. *J. Med. Chem.* **2004**, *47*, 5224.
- (544) Huc, I.; Lehn, J.-M. *Proc. Natl. Acad. Sci. U.S.A.* **1997**, *94*, 2106.
- (545) Kolb, H. C.; Finn, M. G.; Sharpless, K. B. *Angew. Chem., Int. Ed.* **2001**, *40*, 2004.
- (546) Mocharla, V. P.; Colasson, B.; Lee, L. V.; Roper, S.; Sharpless, K. B.; Wong, C.-H.; Kolb, H. C. *Angew. Chem., Int. Ed.* **2005**, *44*, 116.
- (547) Doyon, J. B.; Snyder, T. M.; Liu, D. R. *J. Am. Chem. Soc.* **2003**, *125*, 12372.
- (548) Anderson, A. C. *Chem. Biol.* **2003**, *10*, 787.
- (549) Brooijmans, N.; Kuntz, I. D. *Ann. Rev. Biophys. Biomol. Struct.* **2003**, *32*, 335.
- (550) Joseph-McCarthy, D. *Pharmacol. Ther.* **1999**, *84*, 179.
- (551) Kitchen, D. B.; Decornez, H.; Furr, J. R.; Bajorath, J. *Nat. Rev. Drug Discovery* **2004**, *3*, 935.
- (552) Krumrine, J.; Raubacher, F.; Brooijmans, N.; Kuntz, I. *Methods Biochem. Anal.* **2003**, *44*, 443.
- (553) Taylor, R. D.; Jewsbury, P. J.; Essex, J. W. *J. Comput.-Aided Mol. Des.* **2002**, *16*, 151.
- (554) Ishchenko, A. V.; Shakhnovich, E. I. *J. Med. Chem.* **2002**, *45*, 2770.
- (555) DeWitte, R. S.; Shakhnovich, E. I. *J. Am. Chem. Soc.* **1996**, *118*, 11733.
- (556) Grüneberg, S.; Wendt, B.; Klebe, G. *Angew. Chem., Int. Ed.* **2001**, *40*, 389.
- (557) Southall, N. T.; Dill, K. A.; Haymet, A. D. J. *J. Phys. Chem. B* **2002**, *106*, 521.
- (558) Chandler, D. *Nature* **2002**, *417*, 491.
- (559) Chandler, D. *Nature* **2005**, *437*, 640.
- (560) Lazaridis, T. *Acc. Chem. Res.* **2001**, *34*, 931.
- (561) Honig, B.; Nicholls, A. *Science* **1995**, *268*, 1144.
- (562) Beece, D.; Eisenstein, L.; Frauenfelder, H.; Good, D.; Marden, M. C.; Reinisch, L.; Reynolds, A. H.; Sorensen, L. B.; Yue, K. T. *Biochemistry* **1980**, *19*, 5147.
- (563) Carlson, H. A. *Curr. Opin. Chem. Biol.* **2002**, *6*, 447.
- (564) Vamvaca, K.; Vogeli, B.; Kast, P.; Pervushin, K.; Hilvert, D. *Proc. Natl. Acad. Sci. U.S.A.* **2004**, *101*, 12860.
- (565) Benkovic, S. J.; Hammes-Schiffer, S. *Science* **2003**, *301*, 1196.
- (566) Sturtevant, J. M. *Proc. Natl. Acad. Sci. U.S.A.* **1977**, *74*, 2236.
- (567) Jencks, W. P. *Proc. Natl. Acad. Sci. U.S.A.* **1981**, *78*, 4046.
- (568) Page, M. I.; Jencks, W. P. *Proc. Natl. Acad. Sci. U.S.A.* **1971**, *68*, 1678.
- (569) Gilli, P.; Gerretti, V.; Gilli, G.; Borea, P. A. *J. Phys. Chem.* **1994**, *98*, 1515.
- (570) Lundquist, J. J.; Toone, E. J. *Chem. Rev.* **2002**, *102*, 555.
- (571) Dunitz, J. D. *Chem. Biol.* **1995**, *2*, 709.
- (572) Searle, M. S.; Westwell, M. S.; Williams, D. H. *J. Chem. Soc., Perkin Trans. 2* **1995**, 141.
- (573) Ford, D. M. *J. Am. Chem. Soc.* **2005**, *127*, 16167.
- (574) Cornish-Bowden, A. *J. Biosci.* **2002**, *27*, 121.
- (575) Houk, K. N.; Leach, A. G.; Kim, S. P.; Zhang, X. Y. *Angew. Chem., Int. Ed.* **2003**, *42*, 4872.
- (576) Sharp, K. *Protein Sci.* **2001**, *10*, 661.
- (577) Weber, G. *J. Phys. Chem.* **1995**, *99*, 1052.
- (578) Naghibi, H.; Tamura, A.; Sturtevant, J. M. *Proc. Natl. Acad. Sci. U.S.A.* **1995**, *92*, 5597.
- (579) Liu, Y.; Sturtevant, J. M. *Protein Sci.* **1995**, *4*, 2559.
- (580) Liu, Y.; Sturtevant, J. M. *Biophys. Chem.* **1997**, *64*, 121.
- (581) Williams, D. H.; Maguire, A. J.; Tsuzuki, W.; Westwell, M. S. *Science* **1998**, *280*, 711.
- (582) Calderone, C. T.; Williams, D. H. *J. Am. Chem. Soc.* **2001**, *123*, 6262.
- (583) Kumar, K.; King, R. W.; Carey, P. R. *Biochemistry* **1976**, *15*, 2195.
- (584) Merz, K. M., Jr.; Murcko, M. A.; Kollman, P. A. *J. Am. Chem. Soc.* **1991**, *113*, 4484.
- (585) Liljas, A.; Håkansson, K.; Jonsson, B. H.; Xue, Y. F. *Eur. J. Biochem.* **1994**, *219*, 1.
- (586) Hansch, C.; McClarin, J.; Klein, T.; Langridge, R. *Mol. Pharmacol.* **1985**, *27*, 493.

- (587) Clare, B. W.; Supuran, C. T. In *Carbonic Anhydrase: Its Inhibitors and Activators*; Supuran, C. T., Scozzafava, A., Conway, J., Eds.; CRC Press: Boca Raton, FL, 2004.
- (588) Coleman, J. E. *Annu. Rev. Pharmacol. Toxicol.* **1975**, *15*, 221.
- (589) Maren, T. H.; Rayburn, C. S.; Liddell, N. E. *Science* **1976**, *191*, 469.
- (590) Tibell, L.; Forsman, C.; Simonsson, I.; Lindskog, S. *Biochim. Biophys. Acta* **1984**, *789*, 302.
- (591) Vullo, D.; Franchi, M.; Gallori, E.; Pastorek, J.; Scozzafava, A.; Pastorekova, S.; Supuran, C. T. *J. Enzyme Inhib. Med. Chem.* **2003**, *18*, 403.
- (592) Jencks, W. P. *Catalysis in Chemistry and Enzymology*; Dover Publications: Mineola, NY, 1987.
- (593) Krishnamurthy, V. M.; Semetey, V.; Bracher, P. J.; Shen, N.; Whitesides, G. M. *J. Am. Chem. Soc.* **2007**, *129*, 1312.
- (594) Mammen, M.; Choi, S.-K.; Whitesides, G. M. *Angew. Chem., Int. Ed.* **1998**, *37*, 2755.
- (595) Choi, S.-K. *Synthetic Multivalent Molecules: Concepts and Biomedical Applications*; John Wiley & Sons, Inc.: Hoboken, NY, 2004.
- (596) Roy, B. C.; Banerjee, A. L.; Swanson, M.; Jia, X. G.; Haldar, M. K.; Mallik, S.; Srivastava, D. K. *J. Am. Chem. Soc.* **2004**, *126*, 13206.
- (597) Maddar, R. D.; Kim, C. Y.; Chandra, P. P.; Doyon, J. B.; Baird, T. A.; Fierke, C. A.; Christianson, D. W.; Voet, J. G.; Jain, A. *J. Org. Chem.* **2002**, *67*, 582.
- (598) Doyon, J. B.; Jain, A. *Org. Lett.* **1999**, *1*, 183.
- (599) Chin, D. N.; Whitesides, G. M. *J. Am. Chem. Soc.* **1995**, *117*, 6153.
- (600) Fridborg, K.; Kannan, K. K.; Liljas, A.; Lundin, J.; Strandberg, B.; Strandberg, R.; Tilander, B.; Wiren, G. *J. Mol. Biol.* **1967**, *25*, 505.
- (601) Roy, B. C.; Hegge, R.; Rosendahl, T.; Jia, X.; Lareau, R.; Mallik, S.; Srivastava, D. K. *Chem. Commun.* **2003**, 2328.
- (602) Banerjee, A. L.; Swanson, M.; Roy, B. C.; Jia, X.; Haldar, M. K.; Mallik, S.; Srivastava, D. K. *J. Am. Chem. Soc.* **2004**, *126*, 10875.
- (603) Miles, E. W. *Methods Enzymol.* **1977**, *47*, 431.
- (604) Chen, G.; Heim, A.; Riether, D.; Yee, D.; Milgrom, Y.; Gawinowicz, M. A.; Sames, D. *J. Am. Chem. Soc.* **2003**, *125*, 8130.
- (605) Takaoka, Y.; Tsutsumi, H.; Kasagi, N.; Nakata, E.; Hamachi, I. *J. Am. Chem. Soc.* **2006**, *128*, 3273.
- (606) Goldberg, R. N.; Kishore, N.; Lennen, R. M. *J. Phys. Chem. Ref. Data* **2002**, *31*, 231.
- (607) Pocker, Y.; Stone, J. T. *Biochemistry* **1968**, *7*, 4139.
- (608) Conroy, C. W.; Maren, T. H. *Mol. Pharmacol.* **1995**, *48*, 486.
- (609) Mammen, M.; Shakhnovich, E. I.; Whitesides, G. M. *J. Org. Chem.* **1998**, *63*, 3168.
- (610) Alberty, R. A.; Hammes, G. G. *J. Phys. Chem.* **1958**, *62*, 154.
- (611) Shimizu, K.; Osteryoung, R. A. *Anal. Chem.* **1981**, *53*, 2350.
- (612) Olander, J.; Bosen, S. F.; Kaiser, E. T. *J. Am. Chem. Soc.* **1973**, *95*, 1616.
- (613) Olander, J.; Bosen, S. F.; Kaiser, E. T. *J. Am. Chem. Soc.* **1973**, *95*, 4473.
- (614) Banerjee, A. L.; Tobwala, S.; Ganguly, B.; Mallik, S.; Srivastava, D. K. *Biochemistry* **2005**, *44*, 3673.
- (615) Strickland, S.; Palmer, G.; Massey, V. *J. Biol. Chem.* **1975**, *250*, 4048.
- (616) Schlosshauer, M.; Baker, D. *J. Phys. Chem. B* **2002**, *106*, 12079.
- (617) Huber, W.; Mueller, F. *Curr. Pharm. Des.* **2006**, *12*, 3999.
- (618) Boozer, C.; Kim, G.; Cong, S. X.; Guan, H. W.; Londergan, T. *Curr. Opin. Biotechnol.* **2006**, *17*, 400.
- (619) Pattnaik, P. *Appl. Biochem. Biotechnol.* **2005**, *126*, 79.
- (620) Lahiri, J.; Isaacs, L.; Grzybowski, B.; Carbeck, J. D.; Whitesides, G. M. *Langmuir* **1999**, *15*, 7186.
- (621) Myszkla, D. G.; He, X.; Dembo, M.; Morton, T. A.; Goldstein, B. *Biophys. J.* **1998**, *75*, 583.
- (622) Su, X. L.; Sun, Y. *AIChE J.* **2006**, *52*, 2921.
- (623) Jones, M. N. *Curr. Opin. Colloid Interface Sci.* **1996**, *1*, 91.
- (624) Edwards, P. R.; Gill, A.; Pollardknight, D. V.; Hoare, M.; Buckle, P. E.; Lowe, P. A.; Leatherbarrow, R. *J. Anal. Biochem.* **1995**, *231*, 210.
- (625) Spinke, J.; Liley, M.; Schmitt, F. J.; Guder, H. J.; Angermaier, L.; Knoll, W. *J. Chem. Phys.* **1993**, *99*, 7012.
- (626) Tamm, L. K.; Bartoldus, I. *Biochemistry* **1988**, *27*, 7453.
- (627) Berg, O. G. *Makromol. Chem. Macromol. Symp.* **1988**, *17*, 161.
- (628) Nousiainen, M.; Derrick, P. J.; Lafitte, D.; Vainiotalo, P. *Biophys. J.* **2003**, *85*, 491.
- (629) Isabel Catalina, M.; de Mol, N. J.; Fischer, M. J. E.; Heck, A. J. R. *Phys. Chem. Chem. Phys.* **2004**, *6*, 2572.
- (630) Aebersold, R. *J. Am. Soc. Mass Spectrom.* **2003**, *14*, 685.
- (631) Regan, C. K.; Craig, S. L.; Brauman, J. I. *Science* **2002**, *295*, 2245.
- (632) Gronert, S. *Chem. Rev.* **2001**, *101*, 329.
- (633) Chabinc, M. L.; Craig, S. L.; Regan, C. K.; Brauman, J. I. *Science* **1998**, *279*, 1882.
- (634) Colton, I. J.; Anderson, J. R.; Gao, J.; Chapman, R. G.; Isaacs, L.; Whitesides, G. M. *J. Am. Chem. Soc.* **1997**, *119*, 12701.
- (635) Carbeck, J. D.; Colton, I. J.; Anderson, J. R.; Deutch, J. M.; Whitesides, G. M. *J. Am. Chem. Soc.* **1999**, *121*, 10671.
- (636) Negin, R. S.; Carbeck, J. D. *J. Am. Chem. Soc.* **2002**, *124*, 2911.
- (637) Menon, M. K.; Zydney, A. L. *Anal. Chem.* **2000**, *72*, 5714.
- (638) Menon, M. K.; Zydney, A. L. *J. Membr. Sci.* **2001**, *181*, 179.
- (639) Allison, S. A.; Carbeck, J. D.; Chen, C.; Burkes, F. J. *Phys. Chem. B* **2004**, *108*, 4516.
- (640) Gitlin, I.; Mayer, M.; Whitesides, G. M. *J. Phys. Chem. B* **2003**, *107*, 1466.
- (641) Chiti, F.; Stefani, M.; Taddei, N.; Ramponi, G.; Dobson, C. M. *Nature* **2003**, *424*, 805.
- (642) Shaw, K. L.; Grimsley, G. R.; Yakovlev, G. I.; Makarov, A. A.; Pace, C. N. *Protein Sci.* **2001**, *10*, 1206.
- (643) Ilinskaya, O. N.; Dreyer, F.; Mitkevich, V. A.; Shaw, K. L.; Pace, C. N.; Makarov, A. A. *Protein Sci.* **2002**, *11*, 2522.
- (644) Winzor, D. J. *Anal. Biochem.* **2004**, *325*, 1.
- (645) Carbeck, J. D.; Negin, R. S. *J. Am. Chem. Soc.* **2001**, *123*, 1252.
- (646) Gao, J.; Whitesides, G. M. *Anal. Chem.* **1997**, *69*, 575.
- (647) Linderström-Lang, K. U. *Compt. Rend. Trav. Lab. Carlsberg* **1924**, *15*, 1.
- (648) Sharma, U.; Negin, R. S.; Carbeck, J. D. *J. Phys. Chem. B* **2003**, *107*, 4653.
- (649) Kuramitsu, S.; Hamaguchi, K. *J. Biochem.* **1980**, *87*, 1215.
- (650) Hunter, R. J. *Foundations of Colloid Science*; Oxford University Press: New York, 1991.
- (651) Carbeck, J. D.; Colton, I. J.; Gao, J.; Whitesides, G. M. *Acc. Chem. Res.* **1998**, *31*, 343.
- (652) Gudiksen, K. L.; Gitlin, I.; Yang, J.; Urbach, A. R.; Moustakas, D. T.; Whitesides, G. M. *J. Am. Chem. Soc.* **2005**, *127*, 4707.
- (653) Caravella, J. A.; Carbeck, J. D.; Duffy, D. C.; Whitesides, G. M.; Tidor, B. *J. Am. Chem. Soc.* **1999**, *121*, 4340.
- (654) Carbeck, J. D.; Severs, J. C.; Gao, J.; Wu, Q.; Smith, R. D.; Whitesides, G. M. *J. Phys. Chem. B* **1998**, *102*, 10596.
- (655) Smith, R. D.; Loo, J. A.; Ogorzalek Loo, R. R.; Busman, M.; Udseth, H. R. *Mass Spectrom. Rev.* **1991**, *10*, 359.
- (656) Schnier, P. D.; Gross, D. S.; Williams, E. R. *J. Am. Chem. Soc.* **1995**, *117*, 6747.
- (657) Gudiksen, K. L.; Gitlin, I.; Moustakas, D. T.; Whitesides, G. M. *Biophys. J.* **2006**, *91*, 298.
- (658) Pliška, V.; Schmidt, M.; Fauchere, J. L. *J. Chromatogr.* **1981**, *216*, 79.
- (659) Yang, J.; Gitlin, I.; Krishnamurthy, V. M.; Vazquez, J. A.; Costello, C. E.; Whitesides, G. M. *J. Am. Chem. Soc.* **2003**, *125*, 12392.
- (660) Gitlin, I.; Gudiksen, K. L.; Whitesides, G. M. *ChemBioChem* **2006**, *7*, 1241.
- (661) Carlsson, U.; Jonsson, B.-H. *Curr. Opin. Struct. Biol.* **1995**, *5*, 482.
- (662) Carlsson, U.; Jonsson, B.-H. In *The Carbonic Anhydrases: New Horizons*; Chegwidden, W. R., Carter, N. D., Edwards, Y. H., Eds.; Birkhäuser Verlag: Basel, Switzerland, 2000; Vol. 90.
- (663) Bushmarina, N. A.; Kuznetsova, I. M.; Biktashev, A. G.; Turoverov, K. K.; Uversky, V. N. *ChemBioChem* **2001**, *2*, 813.
- (664) Dill, K. A.; Shortle, D. *Annu. Rev. Biochem.* **1991**, *60*, 795.
- (665) Dolgikh, D. A.; Kolomiets, A. P.; Bolotina, I. A.; Ptitsyn, O. B. *FEBS Lett.* **1984**, *165*, 88.
- (666) Edsall, J. T.; Mehta, S.; Myers, D. V.; Armstrong, J. M. *Biochem. Z.* **1966**, *345*, 9.
- (667) Franzson, C.; Freskgård, P. O.; Herbertsson, H.; Johansson, Å.; Jonasson, P.; Mårtensson, L.-G.; Svensson, M.; Jonsson, B. H.; Carlsson, U. *FEBS Lett.* **1992**, *296*, 90.
- (668) Ko, B. P. N.; Yazgan, A.; Yeagle, P. L.; Lottich, S. C.; Henkens, R. W. *Biochemistry* **1977**, *16*, 1720.
- (669) Montich, G. G. *Biochim. Biophys. Acta* **2000**, *1468*, 115.
- (670) Ptitsyn, O. B. In *Protein Folding*; Creighton, T. E., Ed.; 1992.
- (671) Ptitsyn, O. B.; Pain, R. H.; Semisotnov, G. V.; Zerovnik, E.; Razgulyaev, O. I. *FEBS Lett.* **1990**, *262*, 20.
- (672) Svensson, M.; Jonasson, P.; Freskgård, P.-O.; Jonsson, B.-H.; Lindgren, M.; Mårtensson, L.-G.; Gentile, M.; Borén, K.; Carlsson, U. *Biochemistry* **1995**, *34*, 8606.
- (673) Wong, K.-P.; Tanford, C. *J. Biol. Chem.* **1973**, *248*, 8518.
- (674) Hammarström, P.; Kalman, B.; Jonsson, B.-H.; Carlsson, U. *FEBS Lett.* **1997**, *420*, 63.
- (675) Jonasson, P.; Aronsson, G.; Carlsson, U.; Jonsson, B. H. *Biochemistry* **1997**, *36*, 5142.
- (676) Mårtensson, L.-G.; Jonsson, B. H.; Freskgård, P. O.; Kihlgren, A.; Svensson, M.; Carlsson, U. *Biochemistry* **1993**, *32*, 224.
- (677) Henkens, R. W.; Oleksiak, T. P. In *Carbonic Anhydrase: From Biochemistry and Genetics to Physiology and Clinical Medicine*; Botré, F., Gros, G., Storey, B. T., Eds.; VCH: New York, 1991.
- (678) Henkens, R. W.; Kitchell, B. B.; Lottich, S. C.; Stein, P. J.; Williams, T. J. *Biochemistry* **1982**, *21*, 5918.
- (679) Hammarström, P.; Carlsson, U. *Biochem. Biophys. Res. Commun.* **2000**, *276*, 393.
- (680) Freskgård, P. O.; Bergenhem, N.; Jonsson, B.-H.; Svensson, M.; Carlsson, U. *Science* **1992**, *258*, 466.
- (681) Levitt, M. *J. Mol. Biol.* **1981**, *145*, 251.

- (682) Baldwin, R. L. *Annu. Rev. Biochem.* **1975**, *44*, 453.
- (683) Lin, L. N.; Hasumi, H.; Brandts, J. F. *Biochim. Biophys. Acta* **1988**, *956*, 256.
- (684) Wetlaufer, D. B. *Biopolymers* **1985**, *24*, 251.
- (685) Yazgan, A.; Henkens, R. W. *Biochemistry* **1972**, *11*, 1314.
- (686) Hammarström, P.; Persson, M.; Owenius, R.; Lindgren, M.; Carlsson, U. *J. Biol. Chem.* **2000**, *275*, 22832.
- (687) Hammarström, P.; Persson, M.; Carlsson, U. *J. Biol. Chem.* **2001**, *276*, 21765.
- (688) Persson, M.; Aronsson, G.; Bergenheim, N.; Freskgård, P.-O.; Jonsson, B.-H.; Surin, B. P.; Spangfort, M. D.; Carlsson, U. *Biochim. Biophys. Acta* **1995**, *1247*, 195.
- (689) Persson, M.; Carlsson, U.; Bergenheim, N. C. H. *Biochim. Biophys. Acta* **1996**, *1298*, 191.
- (690) Persson, M.; Carlsson, U.; Bergenheim, N. *FEBS Lett.* **1997**, *411*, 43.
- (691) Persson, M.; Hammarström, P.; Lindgren, M.; Jonsson, B.-H.; Svensson, M.; Carlsson, U. *Biochemistry* **1999**, *38*, 432.
- (692) Yon, J. M. *J. Cell. Mol. Med.* **2002**, *6*, 307.
- (693) Kjellsson, A.; Sethson, I.; Jonsson, B.-H. *Biochemistry* **2003**, *42*, 363.
- (694) Freskgård, P. O.; Carlsson, U.; Mårtensson, L.-G.; Jonsson, B. H. *FEBS Lett.* **1991**, *289*, 117.
- (695) Takusagawa, F.; Kamitori, S. *J. Am. Chem. Soc.* **1996**, *118*, 8945.
- (696) Taylor, W. R. *Nature* **2000**, *406*, 916.
- (697) Two dihedrals determine the three-dimensional structure of the main chain of a protein, if the amide bond is held planar. If only local interactions are considered, these dihedrals have few preferred values that correspond to the local minima of the torsion energy around each rotation bond. For four atoms along a rotation bond, three values of angles in gauche ($\pm 60^\circ$) and trans (180°) correspond to rather stable local minima of the torsion energy, and thus, only 6 conformations need to be examined per amino acid, so that at least 6*N* conformations exist for a protein with *N* amino acids. With CA, $N = 259$ and there are 6^{259} ($\approx 10^{201}$) possible conformations. Considering an average rotation frequency around each bond of 10^{13} s⁻¹ (see Wetlaufer, D. B. *Proc. Natl. Acad. Sci. U.S.A.* **1973**, *70*, 697 and Levinthal, C. *J. Chim. Phys.-Chim. Biol.* **1968**, *65*, 44), it would take this protein about 10^{188} s ($\approx 10^{180}$) to sample all possible conformations; that is, a duration that is longer than the age of the universe (2×10^{10} years).
- (698) Levinthal, C. *J. Chim. Phys.-Chim. Biol.* **1968**, *65*, 44.
- (699) Anfinsen, C. B. *Science* **1973**, *181*, 223.
- (700) Baldwin, R. L. *Trends Biochem. Sci.* **1986**, *11*, 6.
- (701) Carlsson, U.; Aasa, R.; Henderson, L. E.; Jonsson, B. H.; Lindskog, S. *Eur. J. Biochem.* **1975**, *52*, 25.
- (702) Lakowicz, J. R. *Principles of Fluorescence Spectroscopy*, 2nd ed.; Kluwer Academic/Plenum: New York, 1999.
- (703) Wong, K.-P.; Hamlin, L. M. *Arch. Biochem. Biophys.* **1975**, *170*, 12.
- (704) Andersson, D.; Hammarström, P.; Carlsson, U. *Biochemistry* **2001**, *40*, 2653.
- (705) Bergenheim, N.; Carlsson, U. *Biochim. Biophys. Acta* **1989**, *998*, 277.
- (706) Gudiksen, K. L.; Urbach, A. R.; Gitlin, I.; Yang, J.; Vazquez, J. A.; Costello, C. E.; Whitesides, G. M. *Anal. Chem.* **2004**, *76*, 7151.
- (707) Bergenheim and Carlsson (Bergenheim, N.; Carlsson, U. *Biochim. Biophys. Acta* **1989**, *998*, 227) found that the rate of the increase in absorbance due to Co^{II} depended on the concentration of Co^{II} with a second-order rate constant of $140 \text{ M}^{-1}\text{s}^{-1}$.
- (708) Almstedt, K.; Lundqvist, M.; Carlsson, J.; Carlsson, M.; Persson, B.; Jonsson, B.-H.; Carlsson, U.; Hammarström, P. *J. Mol. Biol.* **2004**, *342*, 619.
- (709) Ohgushi, M.; Wada, A. *FEBS Lett.* **1983**, *164*, 21.
- (710) Fink, A. L. *Methods Mol. Biol.* **1995**, *40*, 343.
- (711) Khan, R. H.; Khan, F. *Biochemistry (Moscow)* **2002**, *67*, 520.
- (712) Kuwajima, K.; Arai, M. *Front. Mol. Biol.* **2000**, *32*, 138.
- (713) Kuwajima, K. *Proc. Indian Natl. Sci. Acad. A: Phys. Sci.* **2002**, *68*, 333.
- (714) Dobson, C. M.; Karplus, M. *Curr. Opin. Struct. Biol.* **1999**, *9*, 92.
- (715) Creighton, T. E. *Trends Biochem. Sci.* **1997**, *22*, 6.
- (716) Jagannadham, M. V.; Balasubramanian, D. *FEBS Lett.* **1985**, *188*, 326.
- (717) Sreerama, N.; Woody, R. W. In *Circular Dichroism: Principles and Applications*, second ed.; Berova, N., Nakanishi, K., Woody, R. W., Eds.; John Wiley and Sons: New York, 2000.
- (718) In the far-UV, the chromophore is the peptide bond in a regular, folded environment. Alpha-helix, beta-sheet, and random-coil structures each give rise to a characteristic shape and magnitude of CD. In the near-UV, the chromophore is primarily the side chains of amino acids, specifically aromatic side chains and disulfides; the CD signals produced by these groups are sensitive to the overall tertiary structure of the protein.
- (719) The analysis of CA using CD is not straightforward. Carlsson and co-workers (Borén, K.; Andersson, P.; Larsson, M.; Carlsson, U. *Biochim. Biophys. Acta* **1999**, *1430*, 111; Freskgård, P.-O.; Mårtensson, L.-G.; Jonasson, P.; Jonsson, B.-H.; Carlsson, U. *Biochemistry* **1994**, *33*, 14281) found that the aromatic residues contribute extensively to the far-UV region of the CD spectrum of native CA, so that the determination of secondary structure using the far-UV region is difficult. Furthermore, the CD signature in the far-UV also varies among the different isoforms of CA, although they have similar crystal structures (section 4.4).
- (720) Borén, K.; Andersson, P.; Larsson, M.; Carlsson, U. *Biochim. Biophys. Acta* **1999**, *1430*, 111.
- (721) Stryer, L. *J. Mol. Biol.* **1965**, *13*, 482.
- (722) Bismuto, E.; Gratton, E.; Lamb, D. C. *Biophys. J.* **2001**, *81*, 3510.
- (723) Semisotnov, G. V.; Rodionova, N. A.; Razgulyaev, O. I.; Uversky, V. N.; Gripas, A. F.; Gilmanshin, R. I. *Biopolymers* **1991**, *31*, 119.
- (724) Semisotnov, G. V.; Rodionova, N. A.; Kutysenko, V. P.; Ebert, B.; Blanck, J.; Ptitsyn, O. B. *FEBS Lett.* **1987**, *224*, 9.
- (725) Förster, T. *Angew. Chem., Int. Ed. Engl.* **1969**, *8*, 333.
- (726) Kutysenko, V. P.; Cortijo, M. *Protein Sci.* **2000**, *9*, 1540.
- (727) Kutysenko, V. P. *Mol. Biol. (Moscow)* **2001**, *35*, 80.
- (728) Shortle, D. *Nature Struct. Biol.* **1999**, *6*, 203.
- (729) Uversky, V. N. *Biochemistry* **1993**, *32*, 13288.
- (730) Denisov, V. P.; Jonsson, B.-H.; Halle, B. *Nature Struct. Biol.* **1999**, *6*, 253.
- (731) Gast, K.; Zirwer, D.; Welfle, H.; Bychkova, V. E.; Ptitsyn, O. B. *Int. J. Biol. Macromol.* **1986**, *8*, 231.
- (732) Gast, K.; Damaschun, H.; Misselwitz, R.; Mueller-Frohne, M.; Zirwer, D.; Damaschun, G. *Eur. Biophys. J.* **1994**, *23*, 297.
- (733) Kataoka, M.; Kuwajima, K.; Tokunaga, F.; Goto, Y. *Protein Sci.* **1997**, *6*, 422.
- (734) Kataoka, M.; Nishii, I.; Fujisawa, T.; Ueki, T.; Tokunaga, F.; Goto, Y. *J. Mol. Biol.* **1995**, *249*, 215.
- (735) Freire, E. *Annu. Rev. Biophys. Biomol. Struct.* **1995**, *24*, 141.
- (736) Fink, A. L. *Annu. Rev. Biophys. Biomol. Struct.* **1995**, *24*, 495.
- (737) Brandts, J. F.; Halvorson, H. R.; Brennan, M. *Biochemistry* **1975**, *14*, 4953.
- (738) Carlsson, U.; Henderson, L. E.; Nyman, P. O.; Samuelsson, T. *FEBS Lett.* **1974**, *48*, 167.
- (739) Semisotnov, G. V.; Uverskii, V. N.; Sokolovskii, I. V.; Gutin, A. M.; Razgulyaev, O. I.; Rodionova, N. A. *J. Mol. Biol.* **1990**, *213*, 561.
- (740) Fischer, G.; Heins, J.; Barth, A. *Biochim. Biophys. Acta* **1983**, *742*, 452.
- (741) For HCA II, the half-time of reactivation increases from 1 to 9 min as the time between denaturation and renaturation increases from 15 s to 1 h (see Fransson et al. *FEBS Lett.* **1992**, *296*, 90).
- (742) Takahashi, N.; Hayano, T.; Suzuki, M. *Nature* **1989**, *337*, 473.
- (743) Kern, G.; Kern, D.; Schmid, F. X.; Fischer, G. *J. Biol. Chem.* **1995**, *270*, 740.
- (744) Aronsson, G.; Mårtensson, L.-G.; Carlsson, U.; Jonsson, B. H. *Biochemistry* **1995**, *34*, 2153.
- (745) Borén, K.; Grankvist, H.; Hammarström, P.; Carlsson, U. *FEBS Lett.* **2004**, *566*, 95.
- (746) Creighton, T. E. *Proteins: Structures and Molecular Properties*, 2nd ed.; W. H. Freeman and Company: New York, 1993.
- (747) Brandts, J. F. *J. Am. Chem. Soc.* **1964**, *86*, 4291.
- (748) Brandts, J. F. *J. Am. Chem. Soc.* **1964**, *86*, 4302.
- (749) Aune, K. C.; Salahuddin, A.; Zarlengo, M. H.; Tanford, C. *J. Biol. Chem.* **1967**, *242*, 4486.
- (750) Fink, A. L.; Calciano, L. J.; Goto, Y.; Kurotsu, T.; Palleros, D. R. *Biochemistry* **1994**, *33*, 12504.
- (751) Wong, K.-P.; Hamlin, L. M. *Biochemistry* **1974**, *13*, 2678.
- (752) Beychok, S.; Armstrong, J. M.; Lindblow, C.; Edsall, J. T. *J. Biol. Chem.* **1966**, *241*, 5150.
- (753) Nilsson, A.; Lindskog, S. *Eur. J. Biochem.* **1967**, *2*, 309.
- (754) Flanagan, M. T.; Hesketh, T. R. *Eur. J. Biochem.* **1974**, *44*, 251.
- (755) Riddiford, L. M. *J. Biol. Chem.* **1965**, *240*, 168.
- (756) Riddiford, L. M.; Stellwagen, R. H.; Mehta, S.; Edsall, J. T. *J. Biol. Chem.* **1965**, *240*, 3305.
- (757) McCoy, L. F., Jr.; Wong, K.-P. *Biochemistry* **1981**, *20*, 3062.
- (758) Bull, H. B.; Breese, K. *Arch. Biochem. Biophys.* **1973**, *158*, 681.
- (759) Lavecchia, R.; Zugaro, M. *FEBS Lett.* **1991**, *292*, 162.
- (760) Gitlin, I.; Gudiksen, K. L.; Whitesides, G. M. *J. Phys. Chem. B* **2006**, *110*, 2372.
- (761) Gudiksen, K. L.; Gitlin, I.; Whitesides, G. M. *Proc. Natl. Acad. Sci. U.S.A.* **2006**, *103*, 7968.
- (762) Takagi, T.; Tsujii, K.; Shirahama, K. *J. Biochem.* **1975**, *77*, 939.
- (763) Reynolds, J. A.; Tanford, C. *J. Biol. Chem.* **1970**, *245*, 5161.
- (764) Greenfield, N. J.; Fasman, G. D. *Biochemistry* **1969**, *8*, 4108.
- (765) Greenfield, N. J.; Davidson, B.; Fasman, G. D. *Biochemistry* **1967**, *6*, 1630.
- (766) Iwatsubo, T. In *Frontiers of the Mechanisms of Memory and Dementia*; Kato, T., Ed.; Elsevier Science B. V.: Amsterdam, The Netherlands, 2000; Vol. 1200.

- (767) Wanker, E. E. *Biol. Chem.* **2000**, *381*, 937.
- (768) Merlini, G.; Bellotti, V.; Andreola, A.; Palladini, G.; Obici, L.; Casarini, S.; Perfetti, V. *Clin. Chem. Lab. Med.* **2001**, *39*, 1065.
- (769) Hetz, C.; Soto, C. *Cell. Mol. Life Sci.* **2003**, *60*, 133.
- (770) Perlmutter, D. H. *J. Clin. Invest.* **2002**, *110*, 1219.
- (771) Bates, G. *Lancet* **2003**, *361*, 1642.
- (772) Stolzing, A.; Grune, T. *NATO Sci. Ser., Ser. I: Life Behav. Sci.* **2003**, *344*, 170.
- (773) Soto, C. *FEBS Lett.* **2001**, *498*, 204.
- (774) Dumery, L.; Bourdel, F.; Soussan, Y.; Fialkowski, A.; Viale, S.; Nicolas, P.; Reboud-Ravaux, M. *Pathol. Biol.* **2001**, *49*, 72.
- (775) Ptitsyn, O. B. *Adv. Protein Chem.* **1995**, *47*, 83.
- (776) Fink, A. L. *Fold. Des.* **1998**, *3*, R9.
- (777) Kundu, B.; Guptasarma, P. *Biochem. Biophys. Res. Commun.* **2002**, *293*, 572.
- (778) Oberg, K.; Chrnyk, B. A.; Wetzel, R.; Fink, A. L. *Biochemistry* **1994**, *33*, 2628.
- (779) Aymard, P.; Nicolai, T.; Durand, D.; Clark, A. *Macromolecules* **1999**, *32*, 2542.
- (780) Bauer, R.; Carrotta, R.; Rischel, C.; Ogendal, L. *Biophys. J.* **2000**, *79*, 1030.
- (781) Cleland, J. L.; Wang, D. I. C. *Biochemistry* **1990**, *29*, 11072.
- (782) Wetlaufer, D. B.; Xie, Y. *Protein Sci.* **1995**, *4*, 1535.
- (783) Hammarström, P.; Persson, M.; Freskgård, P.-O.; Mårtensson, L.-G.; Andersson, D.; Jonsson, B.-H.; Carlsson, U. *J. Biol. Chem.* **1999**, *274*, 32897.
- (784) Hammarström, P.; Owenius, R.; Mårtensson, L.-G.; Carlsson, U.; Lindgren, M. *Biophys. J.* **2001**, *80*, 2867.
- (785) Carlsson, M.; Mårtensson, L.-G.; Olofsson, P.; Carlsson, U. *Biochemistry* **2004**, *43*, 6803.
- (786) Cleland, J. L.; Wang, D. I. C. *BioTechnology* **1990**, *8*, 1274.
- (787) Kundu, B.; Guptasarma, P. *Proteins: Struct., Funct., Genet.* **1999**, *37*, 321.
- (788) Cleland, J. L.; Randolph, T. W. *J. Biol. Chem.* **1992**, *267*, 3147.
- (789) Sharma, L.; Sharma, A. *Eur. J. Biochem.* **2001**, *268*, 2456.
- (790) Karupiah, N.; Sharma, A. *Biochem. Biophys. Res. Commun.* **1995**, *211*, 60.
- (791) Rozema, D.; Gellman, S. H. *J. Biol. Chem.* **1996**, *271*, 3478.
- (792) Rozema, D.; Gellman, S. H. *J. Am. Chem. Soc.* **1995**, *117*, 2373.
- (793) Sundari, C. S.; Raman, B.; Balasubramanian, D. *FEBS Lett.* **1999**, *443*, 215.
- (794) Gething, M. J.; Sambrook, J. *Nature* **1992**, *355*, 33.
- (795) Becker, J.; Craig, E. A. *Eur. J. Biochem.* **1994**, *219*, 11.
- (796) Brinker, A.; Pfeifer, G.; Kerner, M. J.; Naylor, D. J.; Hartl, F. U.; Hayer-Hartl, M. *Cell* **2001**, *107*, 223.
- (797) Zahn, R.; Perrett, S.; Fersht, A. R. *J. Mol. Biol.* **1996**, *261*, 43.
- (798) Zahn, R.; Perrett, S.; Stenberg, G.; Fersht, A. R. *Science* **1996**, *271*, 642.
- (799) Zahn, R.; Spitzfaden, C.; Ottiger, M.; Wuethrich, K.; Plueckthun, A. *Nature* **1994**, *368*, 261.
- (800) The crystal structure of GroEL (see Braig, et al. *Nature*, **1994**, *371*, 578) shows a large tetradecameric complex comprising two seven-membered rings stacked on top of each other (see Saibil, H.; Wood, S. *Curr. Opin. Struct. Biol.* **1993**, *3*, 207). The apical domains of the subunits expose hydrophobic binding surfaces toward the center of the ring and engage in multiple contacts with a nonnative substrate protein (see Farr et al. *Cell* **1997**, *89*, 927 and Fenton et al. *Nature* **1994**, *371*, 614). A second crystal structure shows GroEL bound to its co-chaperonin GroES (see Xu, Z.; Horwich, A. L.; Sigler, P. B. *Nature*, **1997**, *388*, 741). GroES is a 10 kDa subunit that binds as a heptamer to one of the seven-membered rings of GroEL; this process caps the central cavity and sequesters the misfolded protein in this cavity (see Langer, T.; Pfeifer, G.; Martin, J.; Baumeister, W.; Hartl, F. U. *EMBO J.* **1992**, *11*, 4757).
- (801) Landry, S. J.; Gierasch, L. M. *Trends Biochem. Sci.* **1991**, *16*, 159.
- (802) Ellis, R. J.; Hartl, F. U. *FASEB J.* **1996**, *10*, 20.
- (803) Coyle, J. E.; Jaeger, J.; Gross, M.; Robinson, C. V.; Radford, S. E. *Folding Des.* **1997**, *2*, R93.
- (804) Betancourt, M. R.; Thirumalai, D. *J. Mol. Biol.* **1999**, *287*, 627.
- (805) Agard, D. A. *Science* **1993**, *260*, 1903.
- (806) Ellis, R. J. *Curr. Biol.* **1994**, *4*, 633.
- (807) Wang, J. D.; Weissman, J. S. *Nature Struct. Biol.* **1999**, *6*, 597.
- (808) Todd, M. J.; Viitanen, P. V.; Lorimer, G. H. *Science* **1994**, *265*, 659.
- (809) Shtilerman, M.; Lorimer, G. H.; Englander, S. W. *Science* **1999**, *284*, 822.
- (810) Saibil, H. R.; Ranson, N. A. *Trends Biochem. Sci.* **2002**, *27*, 627.
- (811) Csermely, P. *Bioassays* **1999**, *21*, 959.
- (812) Brinkman, R.; Margaria, R.; Meldrum, N. U.; Roughton, F. J. W. *Proc. Physiol. Soc. J. Physiol.* **1932**, *75*, 3P.
- (813) Liu, C. G.; Xu, K. Q.; Xu, X.; Huang, J. J.; Xiao, J. C.; Zhang, J. P.; Song, H. P. *Clin. Exp. Pharmacol. Physiol.* **2007**, *34*, 998.
- (814) Takacova, M.; Barathova, M.; Hulikova, A.; Ohradnova, A.; Kopacek, J.; Parkkila, S.; Pastorek, J.; Pastorekova, S.; Zatovicova, M. *Int. J. Oncology* **2007**, *31*, 1103.
- (815) Morgan, P. E.; Pastorekova, S.; Stuart-Tilley, A. K.; Alper, S. L.; Casey, J. R. *Am. J. Physiol., Cell Physiol.* **2007**, *293*, C738.
- (816) Weise, A.; Becker, H. M.; Deitmer, J. W. *J. Gen. Physiol.* **2007**, *130*, 203.
- (817) Supuran, C. T. *Nat. Rev. Drug Discovery*, **2008**, *7*, 168.
- (818) Alvarez, B. V.; Vithana, E. N.; Yang, Z.; Koh, A. H.; Yeung, K.; Yong, V.; Shandro, H. J.; Chen, Y.; Kolatkar, P.; Palasingam, P.; Zhang, K.; Aung, T.; Casey, J. R. *Invest. Ophthalmol. Visual Sci.* **2007**, *48*, 3459.
- (819) Gambhir, K. K.; Ornasir, J.; Headings, V.; Bonar, A. *Biochem. Genet.* **2007**, *45*, 431.
- (820) Kamsteeg, M.; Zeeuwen, P.; de Jongh, G. J.; Rodijk-Olthuis, D.; Zeeuwen-Franssen, M. E. J.; van Erp, P. E. J.; Schalkwijk, J. *Invest. Dermatol.* **2007**, *127*, 1786.
- (821) Haapasalo, J.; Nordfors, K.; Jarvela, S.; Bragge, H.; Rantala, I.; Parkkila, A. K.; Haapasalo, H.; Parkkila, S. *Neuro-Oncology* **2007**, *9*, 308.
- (822) Niemela, A. M.; Hynninen, P.; Mecklin, J. P.; Kuopio, T.; Kokko, A.; Aaltonen, L.; Parkkila, A. K.; Pastorekova, S.; Pastorek, J.; Waheed, A.; Sly, W. S.; Orntoft, T. F.; Kruhoffer, M.; Haapasalo, H.; Parkkila, S.; Kivella, A. J. *Cancer Epidemiol., Biomarkers Prev.* **2007**, *16*, 1760.
- (823) Abdel-Hamid, M. K.; Abdel-Hafez, A. A.; El-Koussi, N. A.; Mahfouz, N. M.; Innocenti, A.; Supuran, C. T. *Bioorg. Med. Chem.* **2007**, *15*, 6975.
- (824) Colinas, P. A.; Bravo, R. D.; Vullo, D.; Scozzafava, A.; Supuran, C. T. *Bioorg. Med. Chem. Lett.* **2007**, *17*, 5086.
- (825) De Simone, G.; Supuran, C. T. *Curr. Top. Med. Chem.* **2007**, *7*, 879.
- (826) Dogne, J. M.; Thiry, A.; Pratico, D.; Masereel, B.; Supuran, C. T. *Curr. Top. Med. Chem.* **2007**, *7*, 885.
- (827) Dudutiene, V.; Baranauskienė, L.; Matulis, D. *Bioorg. Med. Chem. Lett.* **2007**, *17*, 3335.
- (828) Edwards, P. *Drug Discovery Today* **2007**, *12*, 497.
- (829) Hemmateenejad, B.; Miri, R.; Tabarad, M.; Jafarpour, M.; Shamsipur, M. *Drugs Future* **2007**, *32*, 86.
- (830) Hilvo, M.; Supuran, C. T.; Parkkila, S. *Curr. Top. Med. Chem.* **2007**, *7*, 893.
- (831) Innocenti, A.; Vullo, D.; Pastorek, J.; Scozzafava, A.; Pastorekova, S.; Nishimori, I.; Supuran, C. T. *Bioorg. Med. Chem. Lett.* **2007**, *17*, 1532.
- (832) Kumar, V.; Madan, A. K. *J. Math. Chem.* **2007**, *42*, 925.
- (833) Mincione, F.; Scozzafava, A.; Supuran, C. T. *Curr. Top. Med. Chem.* **2007**, *7*, 849.
- (834) Nishimori, I.; Innocenti, A.; Vullo, D.; Scozzafava, A.; Supuran, C. T. *Bioorg. Med. Chem.* **2007**, *15*, 6742.
- (835) Nishimori, I.; Innocenti, A.; Vullo, D.; Scozzafava, A.; Supuran, C. T. *Bioorg. Med. Chem. Lett.* **2007**, *17*, 1037.
- (836) Nuti, E.; Orlandini, E.; Nencetti, S.; Rossello, A.; Innocenti, A.; Scozzafava, A.; Supuran, C. T. *Bioorg. Med. Chem.* **2007**, *15*, 2298.
- (837) Pastorekova, S.; Kopacek, J.; Pastorek, J. *Curr. Top. Med. Chem.* **2007**, *7*, 865.
- (838) Riley, K. E.; Cui, G. L.; Merz, K. M. *J. Phys. Chem. B* **2007**, *111*, 5700.
- (839) Safarian, S.; Bagheri, F.; Moosavi-Movahedi, A. A.; Amanlou, M.; Sheibani, N. *Protein J.* **2007**, *26*, 371.
- (840) Salmon, A. J.; Williams, M. L.; Innocenti, A.; Vullo, D.; Supuran, C. T.; Poulsen, S. A. *Bioorg. Med. Chem. Lett.* **2007**, *17*, 5032.
- (841) Santos, M. A.; Marques, S.; Vullo, D.; Innocenti, A.; Scozzafava, A.; Supuran, C. T. *Bioorg. Med. Chem. Lett.* **2007**, *17*, 1538.
- (842) Smaine, F. Z.; Winum, J. Y.; Montero, J. L.; Regainia, Z.; Vullo, D.; Scozzafava, A.; Supuran, C. T. *Bioorg. Med. Chem. Lett.* **2007**, *17*, 5096.
- (843) Supuran, C. T. *Curr. Top. Med. Chem.* **2007**, *7*, 823.
- (844) Thiry, A.; Dogne, J.; Supuran, C. T.; Masereel, B. *Curr. Top. Med. Chem.* **2007**, *7*, 855.
- (845) Thiry, A.; Masereel, B.; Dogne, J. M.; Supuran, C. T.; Wouters, J.; Michaux, C. *Chem. Med. Chem.* **2007**, *2*, 1273.
- (846) Vitale, R. M.; Pedone, C.; Amodeo, P.; Antel, J.; Wurl, M.; Scozzafava, A.; Supuran, C. T.; De Simone, G. *Bioorg. Med. Chem.* **2007**, *15*, 4152.
- (847) Wilkinson, B. L.; Bornaghi, L. F.; Houston, T. A.; Innocenti, A.; Vullo, D.; Supuran, C. T.; Poulsen, S. A. *J. Med. Chem.* **2007**, *50*, 1651.
- (848) Wilkinson, B. L.; Bornaghi, L. F.; Houston, T. A.; Innocenti, A.; Vullo, D.; Supuran, C. T.; Poulsen, S. A. *Bioorg. Med. Chem. Lett.* **2007**, *17*, 987.
- (849) Winum, J. Y.; Scozzafava, A.; Montero, J. L.; Supuran, C. T. *Curr. Top. Med. Chem.* **2007**, *7*, 835.

- (850) Winum, J. Y.; Thiry, A.; El Cheikh, K.; Dogne, J. M.; Montero, J. L.; Vullo, D.; Scozzafava, A.; Masereel, B.; Supuran, C. T. *Bioorg. Med. Chem. Lett.* **2007**, *17*, 2685.
- (851) Nishimori, I.; Onishi, S.; Vullo, D.; Innocenti, A.; Scozzafava, A.; Supuran, C. T. *Bioorg. Med. Chem.* **2007**, *15*, 5351.
- (852) Vullo, D.; Innocenti, A.; Nishimori, I.; Scozzafava, A.; Kaila, K.; Supuran, C. T. *Bioorg. Med. Chem. Lett.* **2007**, *17*, 4107.
- (853) Vullo, D.; Nishimori, I.; Innocenti, A.; Scozzafava, A.; Supuran, C. T. *Bioorg. Med. Chem. Lett.* **2007**, *17*, 1336.
- (854) Clare, B. W.; Supuran, C. T. *Expert Opin. Drug Metab. Toxicol.* **2006**, *2*, 113.
- (855) Eroglu, E.; Turkmen, H.; Guler, S.; Palaz, S.; Oltulu, O. *Int. J. Mol. Sci.* **2007**, *8*, 145.
- (856) Huang, H. Q.; Pan, X. L.; Tan, N. H.; Zeng, G. Z.; Ji, C. J. *Eur. J. Med. Chem.* **2007**, *42*, 365.
- (857) Jalah-Heravi, M.; Kyani, A. *Eur. J. Med. Chem.* **2007**, *42*, 649.
- (858) Khadikar, P. V.; Clare, B. W.; Balaban, A. T.; Supuran, C. T.; Agarwal, V. K.; Singh, J.; Joshi, A. K.; Lakwani, M. *Rev. Roum. Chim.* **2006**, *51*, 703.
- (859) Kumar, S.; Singh, V.; Tiwari, M. *Med. Chem.* **2007**, *3*, 379.
- (860) Laszlo, T. *Rev. Chim.* **2007**, *58*, 191.
- (861) Singh, S.; Singh, J.; Ingle, M.; Mishra, R.; Khadikar, P. V. *ARKIVOC* **2006**, *xvi*, 1.
- (862) Singh, J.; Lakhwani, M.; Khadikar, P. V.; Balaban, A. T.; Clare, B. W.; Supuran, C. T. *Rev. Roum. Chim.* **2006**, *51*, 691.
- (863) Tarko, L.; Supuran, C. T. *Bioorg. Med. Chem.* **2007**, *15*, 5666.
- (864) Tuccinardi, T.; Nuti, E.; Ortore, G.; Supuran, C. T.; Rossello, A.; Martinelli, A. *J. Chem. Inf. Model.* **2007**, *47*, 515.
- (865) Henunateenejad, B.; Miri, R.; Jafarpour, M.; Tabarzad, M.; Shamsipur, M. *QSAR Comb. Sci.* **2007**, *26*, 1065.
- (866) Singh, J.; Shaik, B.; Singh, S.; Sikhima, S.; Agrawal, V. K.; Khadikar, P. V.; Supuran, C. T. *Bioorg. Med. Chem.* **2007**, *15*, 6501.
- (867) Patil, S.; Reshetnikov, S.; Haldar, M. K.; Seal, S.; Mallik, S. *J. Phys. Chem. C* **2007**, *111*, 8437.
- (868) Mayer, M.; Semetey, V.; Gitlin, I.; Yang, J.; Whitesides, G. M. *J. Am. Chem. Soc.* **2008**, *130*, 1453.
- (869) Maupin, C. M.; Voth, G. A. *Biochemistry* **2007**, *46*, 2938.
- (870) Miscione, G. P.; Stenta, M.; Spinelli, D.; Anders, E.; Bottoni, A. *Theor. Chem. Acc.* **2007**, *118*, 193.
- (871) Roy, A.; Taraphder, S. *J. Phys. Chem. B* **2007**, *111*, 10563.
- (872) Shimahara, H.; Yoshida, T.; Shibata, Y.; Shimizu, M.; Kyogoku, Y.; Sakiyama, F.; Nakazawa, T.; Tate, S.; Ohki, S.; Kato, T.; Moriyama, H.; Kishida, K.; Tano, Y.; Ohkubo, T.; Kobayashi, Y. *J. Biol. Chem.* **2007**, *282*, 9646.
- (873) Silverman, D. N.; McKenna, R. *Acc. Chem. Res.* **2007**, *40*, 669.
- (874) Caprita, R.; Caprita, A.; Ilia, G.; Ciucanu, I. *Rev. Chim.* **2006**, *57*, 1112.
- (875) Hollowell, H. N.; Younvanich, S. S.; McNevin, S. L.; Britt, B. M. *J. Biochem. Mol. Biol.* **2007**, *40*, 205.
- (876) Sarraf, N. S.; Saboury, A. A.; Nemati, T.; Karbassi, F. *Asian J. Chem.* **2007**, *19*, 531.
- (877) Yan, M.; Liu, Z. X.; Lu, D. N.; Liu, Z. *Biomacromolecules* **2007**, *8*, 560.
- (878) Yazdanparast, R.; Khodarahmi, R. *Int. J. Biol. Macromol.* **2007**, *40*, 319.

CR050262P